



Universität
Rostock



Traditio et Innovatio

Phenology of phytoplankton blooms and its response to environmental changes in the Baltic Sea

Kumulative Dissertation

zur Erlangung des akademischen Grades
Doctor rerum naturalium (Dr. rer. nat.)
der Mathematisch-Naturwissenschaftlichen Fakultät
der Universität Rostock

vorgelegt von

Oscar Dario Beltran Perez

geboren am 16.06.1989 in Medellín, Kolumbien

Rostock, Juni 2023



Dieses Werk ist lizenziert unter einer
Creative Commons Namensnennung 4.0 International Lizenz.

Anmerkung

Die vorliegende Promotionsarbeit wurde im Zeitraum von Oktober 2018 bis Juni 2023 am Leibniz-Institut für Ostseeforschung Warnemünde in der Sektion Meereschemie, Arbeitsgruppe Bio-physikalische Wechselwirkungen, unter der Betreuung von Prof. Dr. Joanna J. Waniek angefertigt. Gedruckt und/oder veröffentlicht mit Förderung durch den Deutschen Akademischen Austauschdienst.

Gutachter:

Prof. Dr. habil. Joanna J. Waniek, Leibniz-Institut für Ostseeforschung Warnemünde

PD Dr. Stefan Forster, Institut für Biowissenschaften (IfBi) der Universität Rostock

Ort und Datum der Einreichung: Rostock, den 15. Juni 2023

Ort und Datum der Dissertation: Rostock, den 10. November 2023

Eidesstattliche Erklärung

Ich versichere hiermit an Eides statt, dass ich die vorliegende Arbeit selbstständig angefertigt und ohne fremde Hilfe verfasst habe, keine außer den von mir angegebenen Hilfsmitteln und Quellen dazu verwendet habe und die den benutzten Werken inhaltlich und wörtlich entnommenen Stellen als solche kenntlich gemacht habe.

Oscar Dario Beltran Perez

Acknowledgments

I would like to express my deepest gratitude to several persons and organizations that have played a fundamental role in the successful completion of my PhD. Their support, encouragement, and contributions have been invaluable, and I am truly grateful.

First and foremost, I would like to thank my wife Isabel and my daughter Julieta for their unwavering support during these years of long working hours. They have been a constant source of motivation, and their love and encouragement have sustained me through the challenges of this journey.

I am immensely grateful to my supervisor, Joanna Waniek, for her exceptional guidance, unwavering support, and profound patience. Her expertise, dedication, and insightful feedback have been instrumental in shaping my research and fostering my growth as a scientist.

I would like to extend my sincere gratitude to the German Academic Exchange Service (DAAD) for the scholarship that enabled me to pursue my PhD in Germany. I would also like to thank the Leibniz Institute for Baltic Sea Research Warnemünde (IOW) for the financial support and resources provided, which were indispensable for the successful completion of my research and PhD.

My research was carried out with data from various institutions and monitoring programs, to which I would also like to express my gratitude, including HELCOM Baltic Sea Monitoring Program, Leibniz Institute for Baltic Sea Research Warnemünde (IOW), Deutscher Wetterdienst (DWD), Bundesamt für Seeschifffahrt und Hydrographie (BSH), Swedish Meteorological and Hydrological Institute (SMHI), European Centre for Medium-Range Weather Forecasts (ECMWF), National Oceanic and Atmospheric Administration (NOAA) and Copernicus Marine Service.

To all my co-authors, I extend my sincere appreciation for their valuable contributions to my research. Their collaboration and insights have enriched my work and broadened its scope. I would like to acknowledge the reviewers and editors of my manuscripts for their meticulous evaluation and constructive feedback. Their expert guidance and suggestions have significantly improved the quality of my research.

My heartfelt thanks go to Erika and Werner for their tremendous support in helping me adapt to a new country, their openness, warmth, and hospitality have made my transition smoother. I am very grateful for allowing me to get to know the German culture, traditions and all that Germany has to offer. Opening the doors of their home and family to me has been a truly enriching experience.

I am deeply grateful to my friends and colleagues, both those who have moved to other institutes, cities and countries and those who are still at the institute. Their unwavering support has made this journey more enjoyable. The daily interactions, discussions, and shared experiences have created a nurturing and inspiring environment. I am fortunate to have had such wonderful companions on this academic journey.

Finally, I would like to extend my sincere appreciation to all my colleagues in the Marine Chemistry department at IOW. The opportunity to get to know them closely, both personally and professionally, has been a privilege. Their collective knowledge, expertise, and enthusiasm have contributed to my growth as a scientist and enriched my experience at the institute.

To all of you, my sincere and heartfelt thanks!

Abstract

Changes in the occurrence of phytoplankton blooms affect the whole Baltic Sea ecosystem including the nutrient pool, biogeochemical cycles, sinking material and, of course, the food web. However, only a few phenological studies have been carried out, partly due to the lack of long-term in situ observations. Nowadays, the limitations to carry out studies of bloom phenology have been reduced by the advances in technology, the increased amount of in situ observations available, and advances in coupled physical-biological models, providing a better understanding of the ecosystem functioning. Cyanobacteria blooms regularly occur in the Baltic Sea, which has allowed their study through samples collected every year specifically from the Gotland Basin, eastern Baltic Sea.

Total biomass of the bloom-forming species *Nodularia spumigena*, *Aphanizomenon sp.* and *Dolichospermum spp.*, water column parameters, nutrients and weather conditions were used to define the phenology and Optimum Environmental Window for the occurrence of cyanobacteria blooms in the eastern Baltic Sea during the period 1990–2017. It was found that the timing of the onset of the bloom was driven by several environmental variables including sea surface temperature, air temperature, outgoing long-wave radiation, mixed layer depth, water column stability expressed as Brunt-Väisälä frequency, phosphate concentration and wind speed. The maximum cyanobacteria biomass was mainly controlled by the sensible and latent heat flux, suggesting that a minimal effect or balance between the other driving factors may be occurring leaving the bloom only controlled by these two components of the net heat flux. The decline of the bloom was driven by net heat flux components (incoming solar radiation, sensible heat flux, latent heat flux) and phosphate concentration. The overall effect of these explanatory variables on each stage of the bloom determines whether the bloom occurs earlier or lasts longer in the eastern Baltic Sea.

In addition, a physical-biological model was developed for a more detailed analysis of the inter-annual variability and phenology of cyanobacteria blooms and their changes associated with environmental conditions over the last 30 years. The model results showed a significant trend in the onset and length of cyanobacteria blooms in the eastern Baltic Sea. Cyanobacteria blooms occurred 9 days earlier and lasted 15 days longer over the period 1990-2019. No significant trend was observed for diatom blooms during the same study period with

respect to the onset, maximum abundance, decline or length of the bloom. The results suggested that warm periods affect diatom and cyanobacteria blooms differently. Overall, cyanobacteria blooms are more sensitive to environmental changes than diatom blooms and are therefore more vulnerable to changes caused by climate change in the Baltic Sea.

Sinking particles provide the major connection between processes in the upper part of the water column and the seafloor. Sediment trap samples collected at ca. 180 m depth between 1999 and 2020 were analyzed to determine this connection in the Gotland Basin, eastern Baltic Sea. The variables studied included total particle flux, particulate organic carbon and nitrogen, biogenic silica, C:N ratio and the isotopic composition of organic carbon and nitrogen. Based on the analysis, it was possible to determine the temporal variability of the particle flux and its components as well as its relationship with phytoplankton blooms and environmental changes. It was found that the highest particle flux occurred mostly in April, July and November, during and after the occurrence of phytoplankton blooms in the Gotland Basin. Furthermore, the highest total particle flux was observed during the summer season (June-August). The observed changes in the isotopic composition of the sinking particles indicated a shift in the phytoplankton community from silicon-rich species to nitrogen-fixing cyanobacteria over the year. Although no significant trend was observed in the data, the temporal changes in the particle flux and its components reflected the temporal changes in the phytoplankton community.

Overall, the difficulty of conducting phenological studies is due to the natural variability of phytoplankton blooms and the temporal and spatial constraints this imposes on phytoplankton bloom detection. However, using in situ observations, a coupled physical-biological model and sediment trap data, it was possible to determine how the phenology of cyanobacteria blooms is changing in the eastern Baltic Sea and how these changes are related to environmental conditions. Thus, the findings of this thesis provide new and valuable insights for our understanding of phytoplankton blooms and underscore the importance of continued monitoring to understand the potential impacts of environmental changes on this fragile ecosystem.

Zusammenfassung

Veränderungen im Auftreten von Phytoplanktonblüten wirken sich auf das gesamte Ökosystem der Ostsee aus, einschließlich des Nährstoffpools, der biogeochemischen Kreisläufe, des Sinkmaterials und natürlich des Nahrungsnetzes. Es wurden jedoch nur wenige phänologische Studien durchgeführt, was zum Teil darauf zurückzuführen ist, dass es keine langfristigen in-situ-Beobachtungen gibt. Heutzutage sind die Einschränkungen bei der Durchführung von Studien zur Phänologie der Blüte durch die Fortschritte in der Technologie, die größere Menge an verfügbaren in-situ-Daten und die Fortschritte bei gekoppelten physikalisch-biologischen Modellen geringer geworden, was ein besseres Verständnis der Funktionsweise des Ökosystems ermöglicht. Cyanobakterienblüten treten in der Ostsee regelmäßig auf, was ihre Untersuchung anhand von Proben ermöglicht hat, die jedes Jahr speziell im Gotland-Becken in der östlichen Ostsee gesammelt wurden.

Die Gesamtbiomasse der blütenbildenden Arten *Nodularia spumigena*, *Aphanizomenon sp.* und *Dolichospermum spp.*, Parameter der Wassersäule, Nährstoffe und Wetterbedingungen wurden verwendet, um die Phänologie und das Optimum Environmental Window für das Auftreten von Cyanobakterienblüten in der östlichen Ostsee im Zeitraum 1990-2017 zu bestimmen. Es zeigte sich, dass der Zeitpunkt des Ausbruchs der Blüte von mehreren Umweltparametern abhängt, darunter die Temperatur der Meeresoberfläche, die Lufttemperatur, die ausgehende langwellige Strahlung, die Tiefe der durchmischten Schicht, die Stabilität der Wassersäule, ausgedrückt als Brunt-Väisälä-Frequenz, die Phosphatkonzentration und die Windgeschwindigkeit. Die maximale Cyanobakterien-Biomasse wurde hauptsächlich durch den fühlbaren und latenten Wärmefluss gesteuert, was darauf hindeutet, dass eine minimale Auswirkung oder ein Gleichgewicht zwischen den anderen treibenden Faktoren besteht, so dass die Blüte nur durch diese beiden Komponenten des Nettowärmeflusses gesteuert wird. Der Rückgang der Blüte wurde durch die Komponenten des Nettowärmeflusses (eingehende Sonnenstrahlung, fühlbarer Wärmefluss, latenter Wärmefluss) und die Phosphatkonzentration gesteuert. Die Gesamtwirkung dieser erklärenden Parameter auf die einzelnen Stadien der Blüte bestimmt, ob die Blüte in der östlichen Ostsee früher einsetzt oder länger andauert.

Darüber hinaus wurde ein physikalisch-biologisches Modell entwickelt, um die interannuelle Variabilität und Phänologie der Cyanobakterienblüte und ihre Veränderungen in Verbindung mit den Umweltbedingungen der letzten 30 Jahre genauer zu analysieren. Die Modellergebnisse zeigten einen signifikanten Trend in Bezug auf das Auftreten und die Dauer von

Cyanobakterienblüten in der östlichen Ostsee. Cyanobakterienblüten traten im Zeitraum 1990-2019 9 Tage früher auf und dauerten 15 Tage länger. Bei den Kieselalgenblüten wurde im gleichen Untersuchungszeitraum kein signifikanter Trend hinsichtlich des Beginns, der maximalen Abundanz, des Rückgangs oder der Dauer der Blüte festgestellt. Die Ergebnisse deuten darauf hin, dass Warmzeiten sich unterschiedlich auf Kieselalgen- und Cyanobakterienblüten auswirken. Insgesamt reagieren Cyanobakterienblüten empfindlicher auf Umweltveränderungen als Kieselalgenblüten und sind daher anfälliger für durch den Klimawandel verursachte Veränderungen in der Ostsee.

Absinkende Partikel sind die wichtigste Verbindung zwischen den Prozessen im oberen Teil der Wassersäule und dem Meeresboden. Sinkstofffallenproben, die zwischen 1999 und 2020 in ca. 180 m Tiefe zwischen 1999 und 2020 gesammelt wurden, wurden analysiert, um diese Verbindung im Gotland-Becken in der östlichen Ostsee zu bestimmen. Zu den untersuchten Parametern gehörten der Gesamtpartikelfluss, partikulärer organischer Kohlenstoff und Stickstoff, biogene Kieselsäure, das C:N-Verhältnis und die Isotopenzusammensetzung von organischem Kohlenstoff und Stickstoff. Anhand der Analyse konnte die zeitliche Variabilität des Partikelflusses und seiner Komponenten sowie seine Beziehung zu Phytoplanktonblüten und Umweltveränderungen bestimmt werden. Es wurde festgestellt, dass der höchste Partikelfluss vor allem im April, Juli und November auftrat, also während und nach dem Auftreten von Phytoplanktonblüten im Gotland-Becken. Außerdem wurde der höchste Beitrag zum Gesamtpartikelfluss in der Sommersaison (Juni-August) beobachtet. Die beobachteten Veränderungen in der Isotopenzusammensetzung der sinkenden Partikel deuten auf eine Verschiebung in der Phytoplanktongemeinschaft von siliziumreichen Arten zu stickstofffixierenden Cyanobakterien im Laufe des Jahres hin. Obwohl in den Daten kein signifikanter Trend zu erkennen war, spiegelten die zeitlichen Veränderungen des Partikelflusses und seiner Komponenten die zeitlichen Veränderungen in der Phytoplanktongemeinschaft.

Die Schwierigkeit bei der Durchführung phänologischer Studien liegt in der natürlichen Variabilität der Phytoplanktonblüte und den damit verbundenen zeitlichen und räumlichen Einschränkungen bei der Erkennung von Phytoplanktonblüten. Mit Hilfe von in-situ-Daten, einem gekoppelten physikalisch-biologischen Modell und Daten aus Sinkstofffallen konnte jedoch ermittelt werden, wie sich die Phänologie der Cyanobakterienblüte in der östlichen Ostsee verändert und wie diese Veränderungen mit Umweltparametern zusammenhängen. Die Ergebnisse dieser Studie liefern somit neue und wertvolle Erkenntnisse für unser Verständnis der Phytoplanktonblüte und unterstreichen die Bedeutung einer kontinuierlichen Überwachung, um die möglichen Auswirkungen von Umweltveränderungen auf dieses empfindliche Ökosystem zu verstehen.

Contents

Abstract	vi
Zusammenfassung	viii
List of figures	xii
List of tables	xiv
List of abbreviations	xv
1 Introduction	1
1.1 Harmful algal blooms	1
1.2 Phytoplankton blooms	2
1.3 Phytoplankton blooms in the Baltic Sea	5
1.4 Phenology	8
2 Aims of the study	10
3 Methodological approach	12
3.1 Study site	12
3.2 Data sets	13
3.2.1 In situ observations	13
3.2.2 Initial conditions and forcing for the physical-biological model	14
3.2.3 Sediment trap data	14
3.3 Methods applied	15
3.3.1 Environmental window	15
3.3.2 Model-based approach	17
3.3.3 Particle flux	17
3.3.4 Phenology metrics	18
4 Results and Discussion	20
4.1 Environmental window of cyanobacteria blooms	20
4.2 Cyanobacteria blooms and their response to environmental changes	22
4.3 Export production linked to cyanobacteria blooms	24
4.4 The future of cyanobacteria blooms in the eastern Baltic Sea	27

4.5	Global trends	31
4.6	Phytoplankton blooms: Insights and challenges in a changing climate	34
5	Summary and Outlook	36
	References	39
6	Contributions to manuscripts	52

List of Figures

1-1	Harmful algal bloom events since 1985 worldwide. The data was downloaded from the Harmful Algae Event Database (HAEDAT, http://haedat.iode.org) of the UNESCO Intergovernmental Oceanographic Commission.	2
1-2	Bacillariophyceae (diatoms) species frequently found in the Gotland Sea, Baltic Sea. The pictures were taken by R. Bahlo, S. Busch and R. Hansen, IOW-Image Gallery of Microalgae.	7
1-3	Cyanophyceae (cyanobacteria) species frequently found in the Gotland Sea, Baltic Sea. The pictures were taken by R. Bahlo, S. Busch and R. Hansen, IOW-Image Gallery of Microalgae.	7
3-1	Location of monitoring station TF271 in the Gotland Basin. Figure adapted from Publication III (Beltran-Perez et al., 2023).	13
3-2	Theoretical definition of an optimum environmental window based on the relationship between biomass and environmental conditions acting during each stage of the bloom. Figure adapted from Publication I (Beltran-Perez and Waniek, 2021).	16
3-3	Scheme of the coupled physical-biological model. Figure adapted from Publication II (Beltran-Perez and Waniek, 2022).	18
4-1	Influence of SST (A-B), wind (C-D) and net heat flux (E-F) on cyanobacteria biomass (between June and August) in the Gotland Basin. At the top of each plot is shown the year with the highest positive anomalies (left panel) and negative anomalies (right panel) for each variable. The blue line corresponds to the variable (left axes) and the red line to biomass (right axes) of diatoms (dashed line) and cyanobacteria (solid line). The diatom bloom is included only to illustrate its inter-annual cycle. Figure adapted from Publication II (Beltran-Perez and Waniek, 2022).	23
4-2	Annual cycle based on monthly means between 1999 and 2020 of A) total particle flux, B) particulate organic carbon, C) particulate organic nitrogen, D) biogenic silica, E) C:N ratio from sediment traps moored at 180 m depth in the Gotland Basin and F) Chlorophyll a derived from water column measurements. The central red line in each box represents the median over 22 years. The bottom and top edges in each box indicate the 25th and 75th percentiles, respectively. The whiskers extend to the most extreme data points. Figure adapted from Publication III (Beltran-Perez et al., 2023).	26

4-3	Phenology of cyanobacteria blooms in the eastern Baltic Sea using a) observations (1990-2017) Publication I (Beltran-Perez and Waniek, 2021), b) model results (1990-2019) Publication II (Beltran-Perez and Waniek, 2022) and c) the particulate organic carbon component of the total particle flux (1999-2020) Publication III (Beltran-Perez et al., 2023). In each box, the central red line indicates the median. The bottom and top edges in each box indicate the 25th and 75th percentiles, respectively. The whiskers extend to the most extreme data points; outlier observations are marked individually using the '+'.	28
4-4	Temporal change in the phenology of cyanobacteria blooms based on A) modeling results between 1990 and 2019 and B) sediment trap samples collected at 180 m depth in the Gotland Basin between 1999 and 2020. The circles connected with a black solid line represent the onset dates or the length of the bloom, see legend on the figure. The slope of the curves was estimated using the Mann-Kendall test with the non-parametric Sen method using 95% significance level.	30
4-5	Chlorophyll a concentration derived from satellite data. Monthly regional mean values are calculated by performing the average of 2D monthly mean (weighted by pixel area) over the Baltic Sea. The seasonal cycle is obtained by applying the X-11 seasonal adjustment methodology on the original time series, as described by Colella et al. (2016). The trend line was estimated using the Mann-Kendall test with the non-parametric Sen method. The data used were downloaded from the Baltic Sea Biogeochemistry Reanalysis data set provided by the Copernicus Marine Service.	31
4-6	Development of global coastal phytoplankton blooms between 2003 and 2020 using satellite observations from MODIS. The number of bloom counts within a year for each location was enumerated, and the long-term annual mean values were then estimated. Figure adapted from Dai et al. (2023).	32
4-7	Cyanobacteria bloom in August 2018 during the monitoring cruise EMB190 in the Gotland Basin, Baltic Sea. The pictures were taken by J. Waniek (IOW), personal communication.	33
4-8	Change in the number of algal blooms events between 1985 and 2018 in 9 global regions: East Coast America (ECA), Central America/Caribbean (CCA), South America (SAM), West Coast America (WCA), Australia/New Zealand (ANZ), South East Asia (SEA) and North East Asia (NAS), Mediterranean (MED) and Europe (EUR). The number of events is indicated by the blue line and the trend by the red line in each panel. Figure adapted from Hallegraeff et al. (2021b).	34

List of Tables

1-1	Harmful effects of microalgae in coastal and brackish waters. Table adapted from Zingone and Wyatt (2004).	3
4-1	Environmental conditions driving the development of cyanobacteria blooms in the eastern Baltic Sea. Table adapted from Publication I (Beltran-Perez and Waniek, 2021).	21
4-2	Seasonal means of total particle flux, POC, PON, P _{Si} , C:N, $\delta^{13}C$ and $\delta^{15}N$ from sediment traps moored at 180 m depth in the Gotland Basin between 1999 and 2020. The seasons were divided into spring (March-May), summer (June-August), autumn (September-November) and winter (December-February). Values in parentheses correspond to the percentage of the variable with respect to its total value over all seasons. Table adapted from Publication III (Beltran-Perez et al., 2023).	25

List of abbreviations

Abbreviation	Term
HAB	Harmful algal bloom
IPCC	Intergovernmental Panel on Climate Change
OEW	Optimum environmental window
IOW	Leibniz Institute for Baltic Sea Research Warnemünde
SMHI	Swedish Meteorological and Hydrological Institute
DWD	German Weather Service
<i>SST</i>	Sea surface temperature
T_a	Air temperature
Q_{sw}	Incoming solar radiation
Q_{lw}	Outgoing long-wave radiation
Q_{net}	Net heat flux
Q_h	Sensible heat flux
Q_l	Latent heat flux
<i>MLD</i>	Mixed layer depth
N^2	Brunt-Väisälä frequency
DIN	Dissolved inorganic nitrogen
PO_4	Phosphate
<i>WWP</i>	Weak wind period
R^2	Coefficient of determination
PLS	Partial least squares regression
VIP	Variable importance in projection
POC	Particulate organic carbon
PON	Particulate organic nitrogen
PSi	Particulate biogenic silica
<i>Chla</i>	Chlorophyll a
pCO_2	Partial pressure of carbon dioxide
MBI	Major Baltic Inflow
DOM	Dissolved organic matter
ECA	East Coast America

List of abbreviations

Abbreviation	Term
CCA	Central America/Caribbean
SAM	South America
WCA	West Coast America
ANZ	Australia/New Zealand
SEA	South East Asia
NAS	North East Asia
MED	Mediterranean
EUR	Europe

1 Introduction

1.1 Harmful algal blooms

The term "harmful algal bloom" (HAB) was originally conceived several decades ago to describe toxic events that could have an impact on humans, but has evolved over the years to include events that have an "adverse" ecological impact (Table 1-1). There are two broad categories of recognized harmful species (Zingone et al., 2022). The first includes species that produce toxins. These are chemical substances that can affect human health or marine animals by poisoning, either directly or through vector organisms that accumulate the toxins. In some cases, toxic events can lead to human illness and death (Tagmouti-Talha et al., 1996; García et al., 2004) along with mortality of fauna at higher trophic levels, such as seabirds or marine mammals (Gibble et al., 2021). The production of toxins varies within species because of intraspecific and physiological differences (Pizarro et al., 2009), which may also be affected by environmental conditions.

The second category of harmful species includes microalgae that do not produce any toxic substances. Although they are not toxic species, they can have a negative impact on marine animals, e.g., by mechanical damage to fish-gills (Bell, 1961) or anoxia (Pitcher and Probyn, 2011) or high ammonia concentrations (Okaichi and Nishio, 1976). Other adverse effects may include a change in the water color turning green-brown (Satta et al., 2010) or red-brown (Zohdi and Abbaspour, 2019), as well as the formation of mucilage, scums or foams (e.g., Peperzak et al., 2000) that negatively impact the use of coastal waters for fishing, recreation and tourism.

It can be difficult to differentiate between toxic and non-toxic events. Changes in water color can be due to toxin-producing species without involving the presence of toxins, whereas mass mortality can be related to toxins from microalgae, but also to mechanical damage or anoxia. This makes it difficult to distinguish between harmful and non-harmful events, as any species can have harmful effects when they reach high abundances. A clear example of this is provided by a large number of ecologically beneficial diatoms, which produce polyunsaturated fatty acids that can interfere with the reproduction and development of copepods during intense blooms (Ianora et al., 2004). Red tide is another well-known harmful bloom, usually

caused by dinoflagellates, that changes the color of the water to red or brown. Depending on the bloom-forming species, it can be toxic, with serious consequences for the aquatic ecosystem (Zohdi and Abbaspour, 2019).

Eutrophication, changes in environmental conditions and climate driven by global warming, human-introduced non-native species, and aquaculture development have all been identified as possible causes for the expansion and increase in the abundance of HABs (Hallegraeff, 2010; Hallegraeff et al., 2021a). However, evidence for such a global increase is weak (Hallegraeff et al., 2021b). Capacity and monitoring efforts to detect harmful species and events have also increased over the past four decades, resulting in more reports and data on harmful events in the global marine environment (Fig. 1-1).

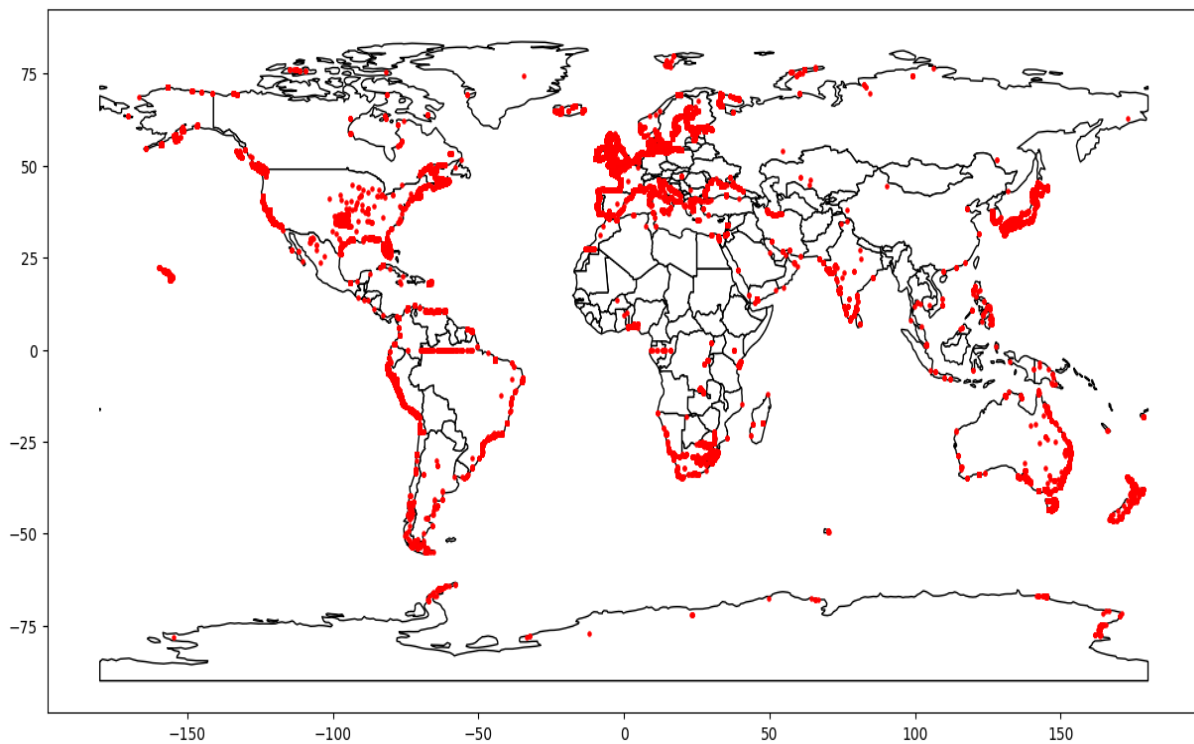


Fig. 1-1. Harmful algal bloom events since 1985 worldwide. The data was downloaded from the Harmful Algae Event Database (HAEDAT, <http://haedat.iode.org>) of the UNESCO Intergovernmental Oceanographic Commission.

1.2 Phytoplankton blooms

All forms of life begin at a small scale, even in the ocean. Microscopic organisms, phytoplankton, are the foundation of ocean ecosystems. They absorb carbon dioxide from the atmosphere like terrestrial plants, form the basis of the marine food web and influence fish abundance and global climate. The organic carbon produced in the ocean by phytoplankton

Table 1-1. Harmful effects of microalgae in coastal and brackish waters. Table adapted from Zingone and Wyatt (2004).

Adverse effects	Genus	Species
HUMAN HEALTH		
Paralytic shellfish poisoning (PSP)	Dinoflagellates	<i>Alexandrium</i> spp., <i>Pyrodinium bahamense</i> , <i>Gymnodinium catenatum</i>
	Cyanobacteria	<i>Anabaena circinalis</i> , <i>Aphanizomenon flos-aquae</i>
Neurotoxic shellfish poisoning (NSP)	Dinoflagellates	<i>Karenia brevis</i>
Ciguatera fish poisoning (CFP)	Dinoflagellates	<i>Gambierdiscus toxicus</i>
	Cyanobacteria	<i>Nodularia spumigena</i> , <i>Lyngbya majuscula</i>
Hepatotoxicity	Cyanobacteria	<i>Microcystis aeruginosa</i> , <i>Nodularia spumigena</i>
NATURAL AND CULTURED MARINE RESOURCES		
Haemolytic, hepatotoxic, osmoregulatory effects	Dinoflagellates	<i>Gymnodinium</i> spp., <i>Cochlodinium polykrikoides</i> , <i>Pfiesteria</i> spp., <i>Gonyaulax</i> spp., <i>Karenia</i> spp.
	Cyanobacteria	<i>Microcystis aeruginosa</i>
Mechanical damage	Diatoms	<i>Chaetoceros</i> spp.
Gill clogging and necrosis	Diatoms	<i>Thalassiosira</i> spp., <i>Cerataulina pelagica</i>
TOURISM AND RECREATIONAL ACTIVITIES		
Production of foams, mucilages, discoloration, repellent odours	Dinoflagellates	<i>Noctiluca scintillans</i> , <i>Prorocentrum</i> spp.
	Diatoms	<i>Cylindrotheca closterium</i> , <i>Coscinodiscus wailesii</i>
	Cyanobacteria	<i>Nodularia spumigena</i> , <i>Microcystis aeruginosa</i> <i>Lyngbya</i> spp., <i>Aphanizomenon flos-aquae</i>
MARINE ECOSYSTEM		
Hypoxia, anoxia	Dinoflagellates	<i>Noctiluca scintillans</i> , <i>Heterocapsa triquetra</i>
	Diatoms	<i>Skeletonema costatum</i> , <i>Cerataulina pelagica</i>
Negative effects on feeding behaviour, reduction of water clarity	Pelagophytes	<i>Aureococcus anophagefferens</i> , <i>Aureoumbra lagunensis</i>
Toxicity to wild marine fauna	Dinoflagellates	<i>Karenia brevis</i> , <i>Alexandrium</i> spp.
	Diatoms	<i>Pseudo-nitzschia australis</i>

is either passed through the food web or exported to the ocean floor as total particle flux by a process known as the biological carbon pump, a key natural process in the global carbon cycle that regulates atmospheric CO₂ levels (Basu and Mackey, 2018). This process transfers both organic and inorganic carbon fixed by primary producers, mostly phytoplankton, from

the surface to the sea floor locking away that carbon for centuries. The biological carbon pump is linked to other natural processes that also influence the climate. Ocean currents transport both energy (in the form of heat) and mass (dissolved solids and gases) thousands of meters below the surface. Cold and salty water favors the vertical exchange with lighter water in the upper layers ensuring ocean mixing and energy distribution through the water column. Therefore, even small changes in phytoplankton may significantly affect the ocean and climate.

There is evidence that global warming may substantially impact the patterns, distribution and intensity of phytoplankton blooms in marine, brackish and fresh water ecosystems, as the Intergovernmental Panel on Climate Change (IPCC) indicated in its Special Report on the Ocean and Cryosphere in a Changing Climate (SROCC) (IPCC, 2019). Phytoplankton species respond to alterations in the environment by physiological changes, shifts in distribution and phenology, or by genetic changes. Parmesan (2006) suggested that phytoplankton species are more likely to shift their seasonal cycles and distributions in response to climate change, rather than change their genetic material. Therefore, species that are better adapted to environmental conditions, such as cyanobacteria, may out compete other species changing the composition of the phytoplankton community and therefore the trophic chain. The increase in storms and cyclones will favor certain species of phytoplankton as suggested by Paerl et al. (2018), but large uncertainty remains about how these climate drivers might shape future blooms. Some common responses may be expected, as temperature increases affect species growth rates and water column stratification. However, the response of species to changes is not universal and depends on many other factors that influence the development of phytoplankton blooms at different temporal and spatial scales (Wells et al., 2020).

Phytoplankton species respond differently to changes in temperature as each species has different requirements and optimum temperatures for cell division, photosynthesis and growth (Wells et al., 2020). Thus, the effect of temperature alone is difficult to identify considering the influence of other factors (e.g. light, nutrients, mixing) on the development of the bloom (Behrenfeld et al., 2006; Paerl, 2014). The overwintering stages of phytoplankton cells may also be altered by seasonal changes in temperature. It is not possible to confirm whether there will be more frequent and intense blooms in the future due to global warming, but there are indications that phytoplankton blooms are favored by high temperatures (Paerl and Huisman, 2009; Neil et al., 2012; Paerl and Paul, 2012; Suikkanen et al., 2013). There is no doubt that temperature plays a major role in phytoplankton growth and water column structure.

Water column stratification and mixing influence substantially phytoplankton dynamics. A

stratified water column is not due purely to increases in temperature, precipitation and runoff also contribute to formation of strong stratification in the water column. Therefore, a greater variability in stratification can be expected as a consequence of increased storms, cyclones and sea level rise due to warming conditions (Wells et al., 2020). Phytoplankton response to changes in stratification depend on the spatial scale and physiology of the species. Some species become strong competitor under stratified conditions (e.g. dinoflagellates and cyanobacteria) as they can move through the water column in search of nutrients or adapt to stress conditions (Smayda and Reynolds, 2001; Wells et al., 2020). However, other species are more vulnerable to changes in the water column limiting their source of nutrients and therefore their occurrence.

Nutrient availability in the water column is affected in different forms by the changes in the environment. On the one hand, anthropogenic nutrient loading to the marine environment is increasing due to intensive land use and population density (Paerl et al., 2018; Burford et al., 2020). On the other hand, warming and increased stratification may inhibit the flux of nutrients from the sediment to the surface, which is driven by mixing, diffusion and upwelling (Sarmiento et al., 2004; Wells et al., 2020). The effect of wind, currents and mixing is more uncertain because they depend on local conditions. The continuous changes in the amount of nutrients in the water column may affect the magnitude, ratios and availability of macro- and micro-nutrients, thereby the growth of phytoplankton species (e.g. dinoflagellates and diatoms) that depend on them. It is still unknown how the nutrient uptake kinetics contribute to the competitive success and toxicity of phytoplankton species (Wells et al., 2020). pH reduction may also affect metabolic mechanisms, competitive balance among species and phytoplankton succession patterns as a result of the increase in the amount of dissolved carbon dioxide and carbon availability in marine environments (Beardall et al., 2009).

1.3 Phytoplankton blooms in the Baltic Sea

Regular blooms occur in all sub-basins of the Baltic Sea, frequently during spring and summer seasons (Groetsch et al., 2016; Kahru et al., 2016). The spring bloom is mainly dominated by diatoms. It develops from the south to the north of the Baltic Sea, with the first bloom appearing in mid-March in the Bay of Mecklenburg and the late bloom occurring in mid-April in the Gulf of Finland (Groetsch et al., 2016). Seasonality of spring blooms is mainly driven by light and nutrient availability (Sverdrup, 1953; Legendre, 1990). Overall, the spring bloom starts when water temperature and nutrients availability increase as direct response of incoming solar radiation and prior mixing in the water column. The end of the bloom is given by combined effects of nutrient depletion and grazing.

Diatoms exist globally, their small size and resistance to mixing enable them to be easily carried by currents throughout the ocean (Margalef, 1978). As part of their overwintering strategy, they accumulate in the sediment for long periods of time, providing refuge during adverse conditions (Spilling et al., 2018; Sundqvist et al., 2018). Diatoms have a diverse community (Fig. 1-2), their genetic variation makes them resistant to environmental changes (Godhe and Rynearson, 2017). Therefore, diatoms provide a stable base for the whole marine food web.

In contrast, the summer bloom is dominated by cyanobacteria, also called blue-green algae. Cyanobacteria may have been the first plankton to produce oxygen on earth, although they are prokaryotes and not eukaryotes like other plankton species (Lalonde and Konhauser, 2015). Cyanobacteria blooms start in June reaching maximum biomass during July and August in the Baltic Sea (Kahru et al., 2020). Cyanobacteria blooms give rise to environmental concern due to their ability to fix molecular nitrogen from the atmosphere accelerating eutrophication and oxygen depletion in deep waters (Larsson et al., 1985; Wasmund, 1997; Janssen et al., 2004). The most representative species of cyanobacteria encountered during blooms in the Baltic Sea are *N. spumigena*, *Aphanizomenon sp.* and *Dolichospermum spp.* (Fig. 1-3). These species may produce toxins including Microcystins, Nodularins, Cylindrospermopsins, Anatoxin-a and Lipopolysaccharides that are a major threat to organisms and humans, fishing and recreational use of coastal waters (Paerl and Huisman, 2009; Neil et al., 2012; Huisman et al., 2018).

Particularly for cyanobacteria, a common bloom-forming species in freshwater and marine environments, high temperatures and calm weather conditions often lead to intense blooms (Wasmund, 1997; Wasmund et al., 2011; Kahru and Elmgren, 2014; Kahru et al., 2016, 2020). Kanoshina et al. (2003) defined as driving factors of the bloom water temperature, stratification and wind. Wasmund (1997) also suggested water temperature as the main factor controlling the onset of the bloom. Kahru et al. (2020) indicated that the variability of cyanobacteria blooms is related to incoming solar radiation and sea surface temperature rather than biogeochemical variables. Therefore, increasing global temperature may lead to changes in intensity and distribution of cyanobacteria blooms when other environmental conditions (e.g. nutrients availability, calm wind conditions) are suitable for their growth. In the current climate scenarios, high carbon dioxide in the atmosphere have also been found to stimulate growth rates of cyanobacteria favoring bloom formation (Wells et al., 2020). Although the role of nutrient loading, temperature and other factors is recognized in bloom formation, a better understanding of the underlying causes of phytoplankton blooms and their phenology across the region is needed to evaluate how climate change might impact their dynamics, the marine food web and carbon cycle in a rapidly warming environment.

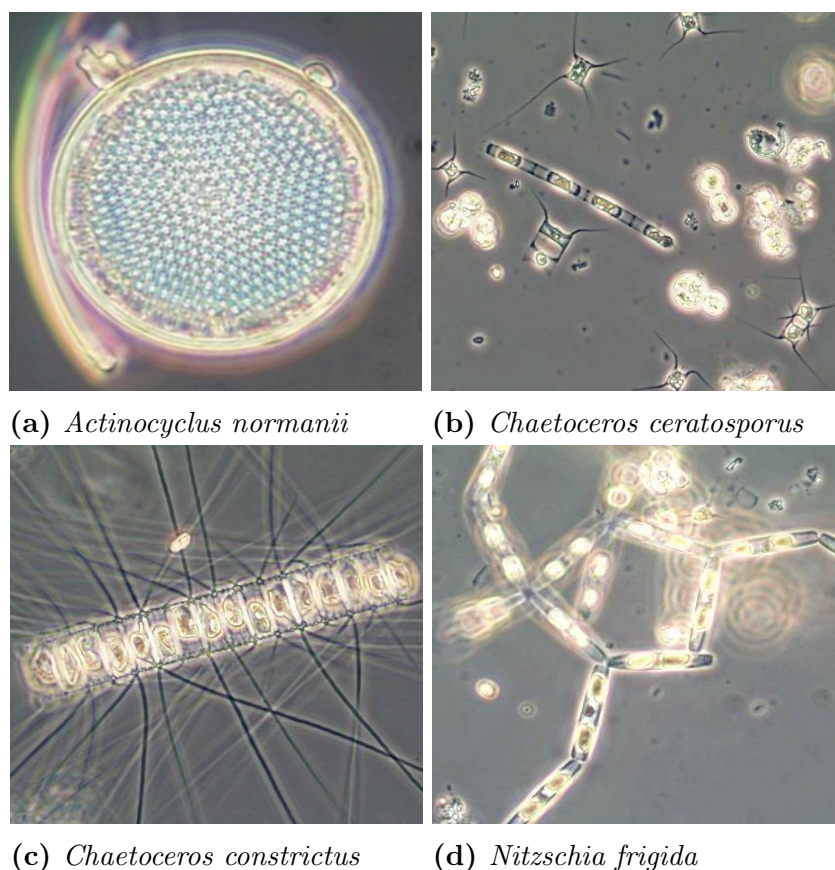


Fig. 1-2. Bacillariophyceae (diatoms) species frequently found in the Gotland Sea, Baltic Sea. The pictures were taken by R. Bahlo, S. Busch and R. Hansen, IOW-Image Gallery of Microalgae.

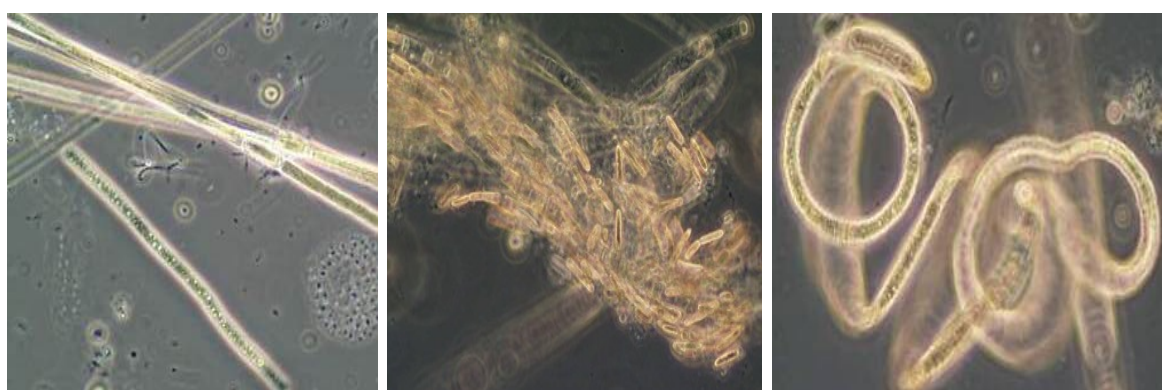


Fig. 1-3. Cyanophyceae (cyanobacteria) species frequently found in the Gotland Sea, Baltic Sea. The pictures were taken by R. Bahlo, S. Busch and R. Hansen, IOW-Image Gallery of Microalgae.

1.4 Phenology

Many species have developed strategies to exploit favorable periods of the year for growth and reproduction and to minimize exposure to stressful periods, i.e. an optimum environmental window (OEW) (Cury and Roy, 1989; Beltran-Perez and Waniek, 2021). However, there is usually a mismatch in timing, as the inter-annual variability of environmental conditions and individual species differs. Many phenological events are seasonal and therefore they can provide insight about the sensitivity of an ecosystem to environmental change in terms for example of population abundance, reproductive success, development status and timing of occurrence. Climate change is significantly altering the seasonal timing of a wide variety of organisms (Parmesan, 2006). In some places, like the North Atlantic, warmer water is causing a shift in the phytoplankton community moving warm water plankton species northward while colder water species are advected towards the pole (Gobler et al., 2017). North Atlantic diatom and dinoflagellate communities have shifted northwards and eastward by over 12.9 and 42.7 km per decade, respectively (Barton et al., 2016). The continuous changes in phytoplankton distribution have increased the attention to phenological variability of individual species and its ecosystem impacts over time.

The complexity of marine ecosystems is driven by nonlinear interaction of multiple forcing (Ji et al., 2010). Ji et al. (2007) showed that spatial pattern in the onset of the spring bloom are driven by water column stratification on the Northwest Atlantic shelf. In regions influenced by the California Current, the spring bloom was delayed by over a month in 2005 as a result of the late onset of upwelling-favorable winds (Kudela et al., 2006; Thomas and Brickley, 2006). Satellite imagery has shown significant changes in the distribution and inter-annual variability of phytoplankton blooms in different marine regions (Henson et al., 2009; Kahru et al., 2016). Broad ecosystem impacts are expected in the trophic chain as phenology changes may also involve changes in the succession and food quality of the bloom-forming species (Ji et al., 2010; SØreide et al., 2010).

Phytoplankton growing season plays an integral role in the marine food web and ecosystem functioning (Smith and Hollibaugh, 1993). Changes in phytoplankton phenology may affect the survival of higher trophic levels due to variations in the timing of food availability (match-mismatch hypothesis) (Smith and Hollibaugh, 1993; Winder and Schindler, 2004). It was observed for example a reduction of food availability for cod larvae and recruitment success in the North Sea as a consequence of changes in planktonic assemblage and copepod phenology (Beaugrand, 2009). The link between plankton phenology and higher trophic levels has been observed in other studies as well, including e.g. shrimps in the North Atlantic (Koeller et al., 2009) and zooplankton abundance and energy propagation up to fish and seabird predators

level in the Northeast Pacific (Mackas et al., 2007). Zooplankton species even depend on the match between their reproductive cycle and phytoplankton blooms for their survival (S reide et al., 2010).

There are several metrics to define the phenology of phytoplankton blooms i.e., the time at which the bloom starts, reaches maximum abundance and declines, its length and magnitude (Ji et al., 2010). The metric used depends on the phenological questions to be addressed, e.g. the timing of winter blooms instead of spring blooms to estimate zooplankton productivity and abundance (Durbin et al., 2003) or the occurrence of phytoplankton blooms in response to nutrient renewal by mixing (Sharples et al., 2006; Chen et al., 2021). Several metrics have been used to identify phytoplankton responses to environmental changes. A metric commonly used is based on the definition of thresholds at which the bloom exceeds a certain value (Ji et al., 2010). This metric has provided insight into environmental factors linked to bloom occurrence (Sharples et al., 2006; Henson et al., 2009). However, there is no criterion to define a threshold for a phytoplankton community or a single species, which limits the comparison of results between different studies.

2 Aims of the study

The ocean is a large sink for atmospheric CO₂ taking up nearly one third of anthropogenic CO₂ emissions from the atmosphere (Häder et al., 2014). Primary producers, mostly phytoplankton, are involved in carbon sequestration through a process known as the biological carbon pump. Phytoplankton is the base of the marine food web and account for 90% of oceanic productivity and half of all photosynthesis on Earth (Smith and Hollibaugh, 1993; Baumert and Petzoldt, 2008; Simon et al., 2009). Therefore, changes in phytoplankton may affect biogeochemical cycles in the ocean and the climate. Despite the major role that phytoplankton plays in the ecosystem, many questions remain open regarding its driving factors, temporal variability, contribution to the sinking material and response to future environmental changes.

The Intergovernmental Panel for Climate Change concluded that the occurrence of algal blooms, their toxicity and risk for natural and human systems are projected to increase with warming and rising CO₂ in the 21st century (IPCC, 2019). Marginal seas have warmed faster than the ocean (Belkin, 2009). The Baltic Sea is warming more than the average of all marginal seas and the global ocean, with areas increasing at a rate of 0.59°C per decade (HELCOM/Baltic Earth, 2021, and references therein). Water temperature is projected to increase by 1.1 to 3.2 °C along with rising precipitation and land runoff of organic matter and pollutants, a reduction in salinity is also expected (Andersson et al., 2015; HELCOM/Baltic Earth, 2021). These environmental changes are expected to have extensive effects on the ecosystem including shifts in composition, distribution, succession and timing of phytoplankton growth. As a result, phytoplankton may bloom too early or too late to feed the zooplankton and other species higher up the marine food chain that depend on them, altering the entire food web (the so called match-mismatch hypothesis) (Smith and Hollibaugh, 1993; Winder and Schindler, 2004). However, the response of phytoplankton to change is by no means universal (Hallegraeff et al., 2021b), as it depends on the species, the hydrographic and chemical properties of the water column, the interaction between the atmosphere and the upper ocean, as well as interactions between species and across the food web levels.

Environmental management programs have been in place in the Baltic Sea since 1974 to

monitor and control its environmental state (e.g. Helsinki Convention, EU Marine Strategy Framework Directive, Baltic Sea Action Plan), however massive blooms continue to occur in the Baltic Sea. The main bloom-forming species are diatoms in spring and cyanobacteria in summer. Although these blooms occur every year, the underlying conditions leading to their development, how they have changed over time and whether these changes are due purely to global warming or whether other factors are involved are unknown. A thorough understanding of the mechanisms driving diatom and cyanobacteria blooms must examine influences of a wide range of interacting biotic and abiotic factors in the context of a changing world (Downing et al., 2001; Paerl and Huisman, 2009; Paerl et al., 2011). Several approaches were used in this thesis with the aim of answering the following questions:

- 1) are there specific conditions that trigger the development of cyanobacteria blooms in the eastern Baltic Sea? An optimum environmental window for the occurrence of cyanobacteria blooms was defined based on in situ observations at different stages of the bloom and forcing associated with them (**Publication I**, Beltran-Perez and Waniek, 2021).
- 2) how do phytoplankton blooms vary over time and respond to changes in environmental conditions? A coupled physical-biological model was developed to investigate the temporal variability of spring and summer blooms and their interaction with the atmospheric forcing (**Publication II**, Beltran-Perez and Waniek, 2022).
- 3) how has the total particle flux changed over time in the Gotland Basin and how is it related to phytoplankton blooms? Sediment trap data were used to determine the long-term, inter-annual, seasonal and annual cycle of the total particle flux and its components, as well as the contribution of phytoplankton blooms to the sinking material (**Publication III**, Beltran-Perez et al., 2023).

3 Methodological approach

3.1 Study site

The Baltic Sea is a shallow, brackish sea in central Northern Europe with a narrow connection to the North Sea. The limited water exchange results in a long residence time and large seasonal and spatial variation in biological, physical and chemical properties of the water column (Schneider and Müller, 2018). In addition, the drainage basin of the Baltic Sea is shared by 14 countries (around 84 million people, Munkes et al., 2020), which exerts pressure on the entire ecosystem by increasing nutrient deposition, pollution and pressure on fish stocks. Climate change may exacerbate impacts on the ecosystem, but large uncertainty remains about how climate drivers might shape e.g. future phytoplankton blooms. Studies in the Baltic Sea have indicated that cyanobacteria blooms are as ancient as the present brackish water phase of the Baltic Sea (Bianchi et al., 2000). An increase in the intensity of the blooms has been observed since the 1980s (Kahru et al., 1994; Bianchi et al., 2000; Kaiser et al., 2020).

The Baltic Sea is divided into 17 basins, each basin with its own complexity and particular characteristics (HELCOM, 2013; Öberg, 2015; Kownacka et al., 2018). The Gotland Basin is the deepest basin in the Baltic Sea with a maximum depth of 249 m and characterized by mostly anoxic bottom conditions. A permanent halocline at 60–80 m depth functions as a barrier between anoxic bottom waters and the surface near layer (Schneider et al., 2000; Klais et al., 2011). Low oxygen levels lead to the production of hydrogen sulphide (H_2S) and release of phosphate and silicate from the sediments to the water column (HELCOM/Baltic Earth, 2021). The surplus of nutrients reaching the surface may contribute to the phytoplankton growth observed in this basin. Phytoplankton blooms occur regularly during spring, summer and autumn connecting the surface with the seafloor, as phytoplankton dominates primary production and comprises the major source of organic matter exported to the bottom (Leipe et al., 2008).

This thesis focuses on the Gotland Basin, specifically on the TF271 station located in the eastern part of the Baltic Sea at 57°19'12" N, 20°3'0" E (Fig. 3-1). This station has been monitored since 1979 in the frame of the HELCOM monitoring program (HELCOM, 2012).

However, a regular monitoring of phytoplankton blooms started just in 1990 (Wasmund, 1997).

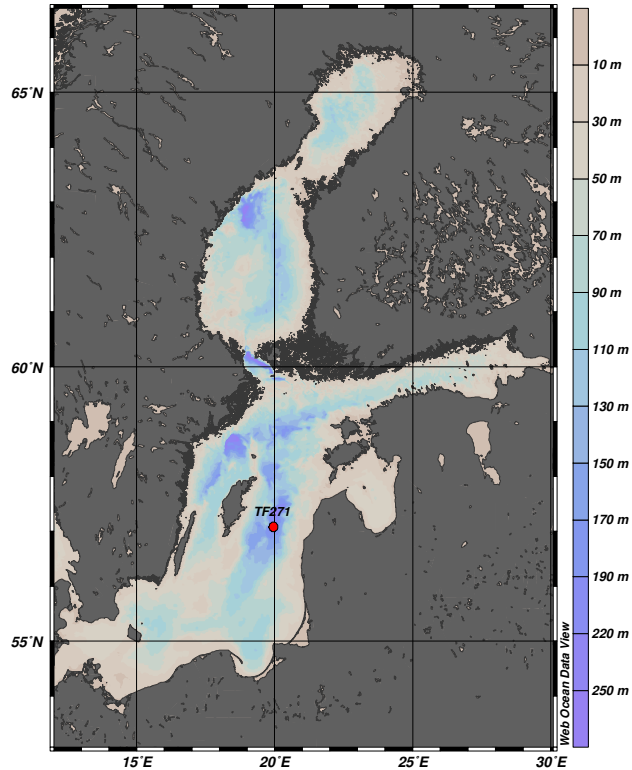


Fig. 3-1. Location of monitoring station TF271 in the Gotland Basin. Figure adapted from **Publication III** (Beltran-Perez et al., 2023).

3.2 Data sets

In this thesis, in situ observations, reanalysis data, model results and sediment trap data from different databases and sources were collected, the main data used are described below:

3.2.1 In situ observations

Cyanobacteria biomass and composition were determined by collecting and integrating water samples over 10 m depth at the sampling station TF271 (Fig. 3-1) and nearby stations between 1990 and 2017 as part of the monitoring program in the Baltic Sea. Preservation and counting of phytoplankton cells were carried out according to the method of Utermöhl (1958). Cyanobacteria biomass (wet weight) was calculated using conversion factors recommended by Olenina et al. (2006). The total cyanobacteria biomass was defined as the sum of biomass of the bloom-forming species *N. spumigena*, *Aphanizomenon sp.* and *Dolichospermum spp.*,

the most representative species of cyanobacteria encountered during summer blooms in the Baltic Sea. The biomass of the three cyanobacteria species was combined due to the sparse number of counts and irregular frequency of the observations. The analysis was focused on the time period between June and August as this is the period in which cyanobacteria blooms usually occur in the eastern Baltic Sea (Kahru et al., 2020). All data were accessed and downloaded from the Leibniz Institute for Baltic Sea Research Warnemünde (IOW) and the Swedish Meteorological and Hydrological Institute (SMHI). A complete description of the data used and the sources of information can be found in **Publication I** (Beltran-Perez and Waniek, 2021).

Forcing data were collected from stations located on the island of Gotland (Sweden) and Warnemünde (Germany). The forcing included incoming solar radiation, sea surface temperature, air temperature, wind speed, relative humidity, rainfall and cloud cover. Missing data in time series were filled by linear interpolation. The heat flux and its components (outgoing long-wave radiation, sensible and latent heat flux) were calculated following the empirical equations of Rahmstorf (1990). These data were downloaded from the SMHI and the German Weather Service (DWD). For more details about data sources, equations and calculations see **Publication I** (Beltran-Perez and Waniek, 2021).

3.2.2 Initial conditions and forcing for the physical-biological model

Vertical profiles of water column temperature, salinity and nutrients were taken from the monitoring station TF271 during December 2002 as initial conditions for the model approach. The initial concentration of diatom, cyanobacteria, zooplankton and detritus were defined according to observations made in the Baltic Sea and a previous literature review (see **Publication II** for more details, Beltran-Perez and Waniek, 2022). The model was forced with realistic daily atmospheric reanalysis data from the National Centers for Environmental Prediction (NCEP) for a period of 30 years (1990-2019) (Kalnay et al., 1996). The forcing used included cloud cover, relative humidity, wind speed, air temperature and incoming solar radiation.

3.2.3 Sediment trap data

The total particle flux and its components (particulate organic carbon (POC), particulate organic nitrogen (PON) and particulate biogenic silica (PSi)) were collected at 180 m depth using a funnel-shaped automated Kiel sediment trap (type S/MT 234, KUM, Germany) with 0.5 m² aperture and a revolver holding twenty-one collecting cups of 400 mm (Kremling et al., 1996). In addition, the C:N ratio and the isotopic composition of organic carbon and nitrogen were measured. A total of 740 sediment trap samples were collected at in-

tervals of 7 to 10 days between 15 May 1999 and 14 November 2020 at mooring station TF271 (57°18.3N, 20°0.46E) in the Gotland Basin. After recovery, the samples were sieved through a 400- μm gauze to remove large zooplankton organisms. The total particle flux was measured by filtering the sample onto a pre-weighed 0.45 μm pore size membrane filter, drying in an oven and weighing. POC, PON and stable carbon and nitrogen isotopes were determined using an elemental analyzer connected to an isotope ratio mass spectrometer (Thermo Fisher Scientific, US). The samples were previously filtered on precombusted glass fiber filters (GF/F, 500°C, 2 h) and dried at 60°C, according to the procedure described by Nieuwenhuize et al. (1994). Isotope values were given in δ -notation and parts per thousand (‰) relative to Vienna Pee Dee Belemnite (VPDB) and atmospheric nitrogen for carbon ($\delta^{13}\text{C}$) and nitrogen ($\delta^{15}\text{N}$), respectively. The precision of the method was $<0.2\text{‰}$ for both stable isotope ratios $\delta^{13}\text{C}$ and $\delta^{15}\text{N}$. P*Si* was analyzed using a photometric method, following the procedures described by Bodungen et al. (1991). Moreover, discrete measurements of surface chlorophyll a concentration (*Chla*) were downloaded from the SHARKweb database provided by the SMHI. Chlorophyll a data were used to relate the export production to the development of phytoplankton blooms. The partial pressure of carbon dioxide ($p\text{CO}_2$) was estimated from in situ observations and provided by the Copernicus Marine Service through the Global Ocean Surface Carbon product. Monthly $p\text{CO}_2$ were used between January 1999 and December 2020 with a spatial resolution of $1^\circ \times 1^\circ$. A more detailed description of the data used is given in **Publication III** (Beltran-Perez et al., 2023).

3.3 Methods applied

In this thesis, different methods were used to analyze the collected data given their characteristics and spatial and temporal constraints.

3.3.1 Environmental window

Phenology describes key stages in the life cycle of species, e.g., seeds germinating, birds migrating or phytoplankton growing. Environmental conditions greatly influence these stages. Therefore, many species have developed strategies to exploit favorable periods of the year to grow and reproduce in what is called an optimum environmental window (Cury and Roy, 1989). Some environmental conditions (e.g. low temperature, absence of light and strong mixing) restrict bloom formation while others (e.g. high temperature, calm weather conditions and light availability) favor it and support the accumulation of cells in the upper layers of the water column (t1), as it is illustrated in the Fig. **3-2**. Cells grow and reproduce as long as favorable conditions are maintained (from t1 to t2). The bloom reaches its maximum biomass when the limiting conditions are at their minimum (t2) and declines under unfav-

favorable environmental conditions such as strong mixing and nutrient depletion, returning to background levels (t_3). Based on these stages of the bloom, its phenology was determined. A partial least squares regression (PLS) was performed between the phenological dates and monthly averages of the environmental conditions in the water column and atmosphere to find out which conditions are related to each stage, i.e., the start of the bloom, its maximum abundance and its decline. The environmental conditions were interpolated at the corresponding phenological dates and normalized to make them comparable. This method provides explanatory variables and coefficients for the direction in which the dependent variable is affected. The variable importance in projection (VIP) scores was calculated as the weighted sum of the squared correlations between the PLS components and the dependent variable, where the variation explained by the PLS components was used as weight (Chong and Jun, 2005). The VIP was used to select explanatory variables ($VIP > 1$) avoiding multi-collinearity. The selected variables were averaged and compared to observations at the corresponding phenological dates. For more details see **Publication I** (Beltran-Perez and Waniek, 2021).

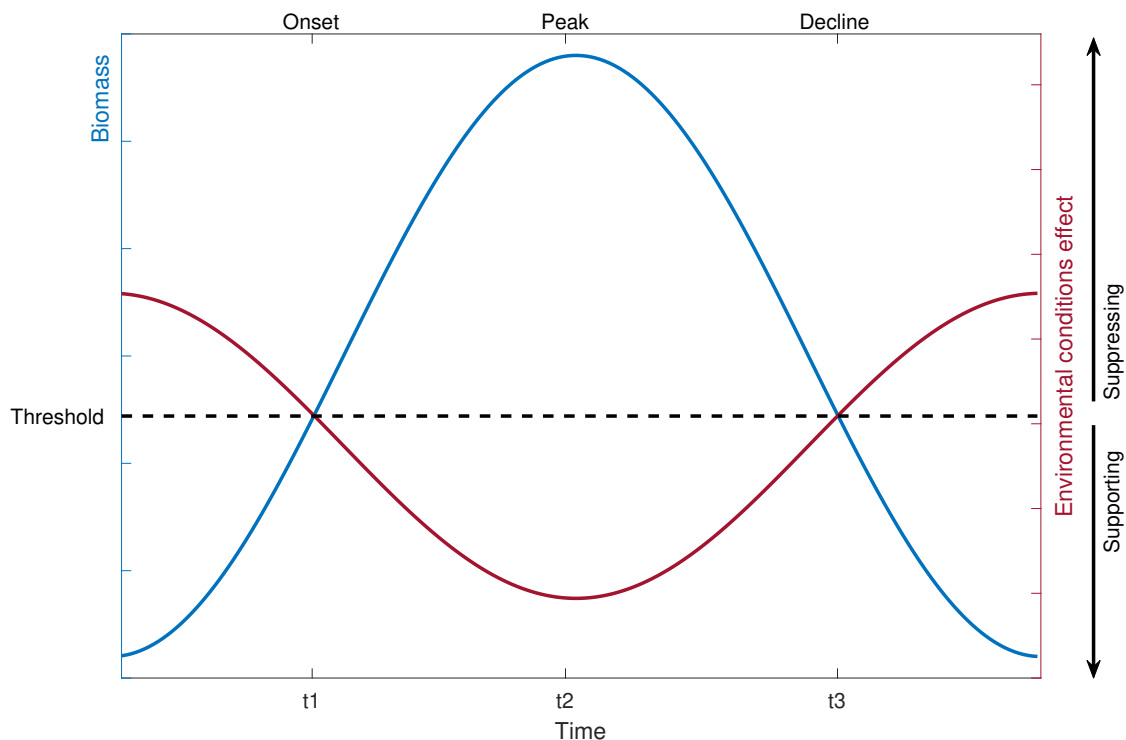


Fig. 3-2. Theoretical definition of an optimum environmental window based on the relationship between biomass and environmental conditions acting during each stage of the bloom. Figure adapted from **Publication I** (Beltran-Perez and Waniek, 2021).

3.3.2 Model-based approach

A physical-biological model was developed for cyanobacteria, the dominant bloom-forming species in the Baltic Sea during summer. The model is based on an initial model developed for diatom blooms in the northeast Atlantic by Waniek (2003). Modifications to the initial model included the addition of cyanobacteria species, the implementation of new initial conditions and forcing according to the Baltic Sea, simulation parameters (e.g., time step and vertical discretization), and physical parameters of the water column (e.g., maximum depth and attenuation coefficients). Specific biological parameters for diatoms and cyanobacteria were adjusted according to the values found in the literature for these species. The model was used to understand the interaction between physical and biological factors affecting phytoplankton blooms and their development over time, given the limitations of estimating the temporal variability of phytoplankton from observations alone. On the one hand, the physical model included a mixed-layer model for the surface layer and a advective-diffusion model for the thermocline (Waniek, 2003). Therefore, the physical component of the model is able to estimate the changes in temperature related to mixing, convection, upwelling and turbulent diffusion in the water column, redistributing the heat vertically in the water column. Moreover, the model uses realistic forcing and is coupled to the atmosphere through the heat flux terms. On the other hand, the biological model describes the dynamic of six state variables: nutrients expressed in terms of nitrogen concentration, two phytoplankton functional groups (diatoms and cyanobacteria), zooplankton fueled by grazing primarily on diatoms and detritus divided into two groups based on the sinking speed (Fig. 3-3). Thereby, the elements and processes included in this coupled physical-biological model provide a reliable approach to the conditions that influence the formation and development of blooms in the eastern Baltic Sea. A vertical discretization of 1 m to the bottom and a time step of 1 day were used in the final model configuration, which ran for a period of 30 years (1990-2019). A detailed description of the physical-biological model, equations and parameters can be found in Waniek (2003) and **Publication II** (Beltran-Perez and Waniek, 2022).

3.3.3 Particle flux

The long-term, inter-annual and seasonal variability of the total particle flux and its components (POC, PON and P_{Si}), C:N ratio, the isotopic composition of carbon and nitrogen were estimated as the arithmetic average of values in the same month, year and season, respectively, over the 22-year study period. The seasonal variability was determined by clustering the total particle flux and its components according to the pelagic seasons in the eastern Baltic Sea: spring (1 March to 31 May), summer (1 June to 31 August), autumn (1 September to 30 November) and winter (1 December to 28 February). In addition, the

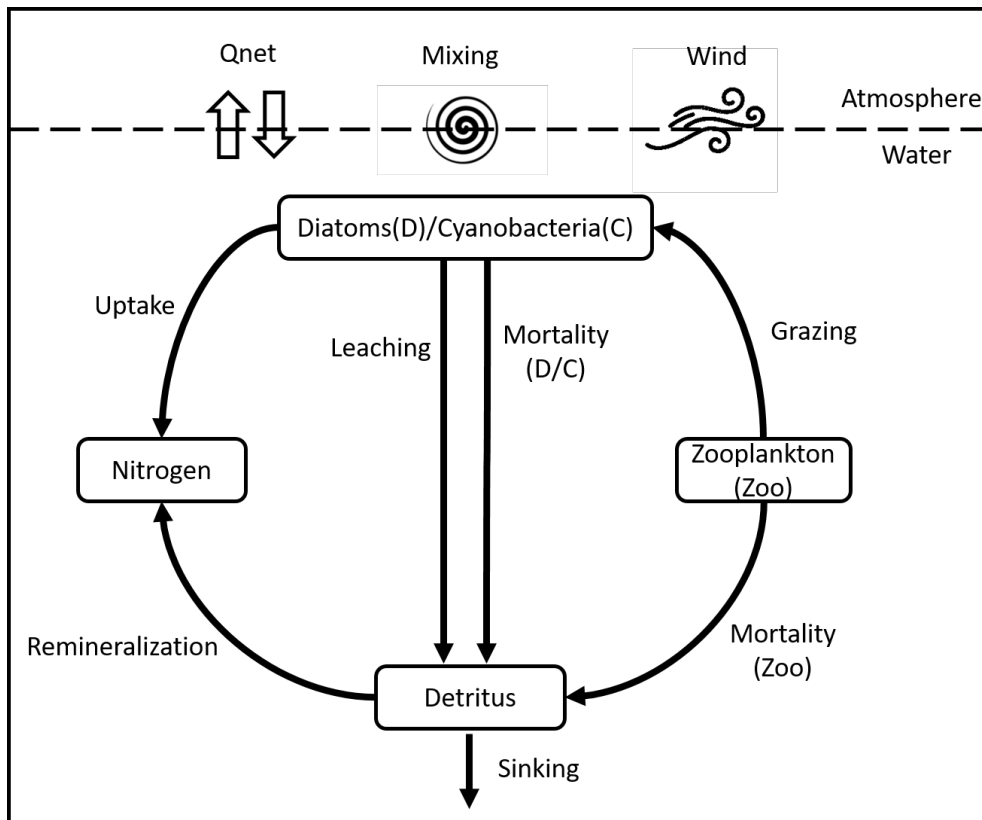


Fig. 3-3. Scheme of the coupled physical-biological model. Figure adapted from **Publication II** (Beltran-Perez and Waniek, 2022).

annual cycle of all variables was estimated by monthly means between 1999 and 2020. For a more detailed description of the sediment trap data and their processing see **Publication III** (Beltran-Perez et al., 2023).

3.3.4 Phenology metrics

There are several metrics to define phytoplankton phenology i.e., the time at which the bloom starts, reaches maximum abundance and declines as well as its length and magnitude (Ji et al., 2010). The number of in situ observations to estimate the bloom phenology was limited. Therefore, a Weibull function was used (**Publication I**, Beltran-Perez and Waniek, 2021). Based on in situ observations and sediment trap data, the onset and decline dates of the bloom were defined at the 10% quantile and 90% quantile of the time-integrated curve before and after the maximum abundance, respectively. However, the same criteria were not used for the model results because the phenology exceeded the period when diatom and cyanobacteria blooms occur in the Baltic Sea. Instead, the threshold method was used for the model results (see section 3.3.2). The threshold for cyanobacteria blooms was defined as an increase in biomass above $22 \mu\text{g L}^{-1}$, following the threshold proposed by Wasmund

(1997). This threshold was also used for diatom blooms, as it coincides with the biomass at which spring blooms are observed in the Baltic Sea. Thus, the onset of the bloom was defined as the time when the bloom biomass exceeded the threshold for the first time. The decline of the bloom was defined as the time when the bloom biomass dropped below the threshold after reaching its maximum abundance. The phenology of the bloom was calculated year by year by analyzing changes in phytoplankton biomass between February and May for the diatom bloom and between June and August for the cyanobacteria bloom. Overall, the length of the bloom was estimated as the difference between the onset and decline dates of the bloom.

Furthermore, the non-parametric Mann-Kendall test for monotonic downward or upward trends (Kendall, 1975) and the non-parametric Sen method for the slope estimate (Sen, 1968) were applied on the phenological dates identified for diatoms and cyanobacteria to define the changes over time in the occurrence of both blooms. Statistical tests were considered significant at p-value less than or equal to 0.05. All calculations and analyses were performed in MATLAB (version R2018b). For more details on the phenology metrics used and the analyses performed, see **Publication I** (Beltran-Perez and Waniek, 2021) and **Publication II** (Beltran-Perez and Waniek, 2022).

4 Results and Discussion

4.1 Environmental window of cyanobacteria blooms

The formation of cyanobacteria blooms in the Baltic Sea is influenced by various factors, such as water temperature, nutrient availability and incoming solar radiation. All of them directly or indirectly affect the bloom, but so far it remains unclear which of these factors affect the development of the bloom to a greater extent. Phytoplankton species have different needs as the bloom progresses, with an optimum environmental window in which favorable conditions promote growth and contribute to maintain the bloom until it eventually declines.

Beltran-Perez and Waniek (2021) (**Publication I**) observed that the conditions that favor cyanobacteria blooms change depending on the stage of the bloom (Table 4-1). It was found that the formation of the bloom is influenced by sea surface temperature (14 °C), air temperature (14 °C), outgoing long-wave radiation (-68 W m^{-2}), mixed layer depth (26 m), water column stability expressed as Brunt-Väisälä frequency (-0.02 s^{-2}), phosphate concentration (0.1 mmol m^{-3}) and wind speed (5 m s^{-1}). The maximum biomass of cyanobacteria is governed by sensible (-0.3 W m^{-2}) and latent (-0.04 W m^{-2}) heat fluxes, while the decline of the bloom is driven by incoming solar radiation (211 W m^{-2}), sensible heat flux (-1 W m^{-2}), latent heat flux (-0.1 W m^{-2}) and phosphate concentration (0.1 mmol m^{-3}). Thus, the early occurrence or extension of the cyanobacteria bloom depends on the combined effect of these explanatory variables from the water column and the atmosphere at each stage of the bloom. The interactions among these explanatory variables define the phenology of cyanobacteria blooms, accounting in part for their variability over time and space. The results indicated that the bloom cannot be attributed to one parameter alone, but instead results from the combined effect of several parameters forming the OEW and their interaction with each other (**Publication I**, Beltran-Perez and Waniek, 2021).

Numerous studies have shown that weather conditions play a role in bloom development (Suikkanen et al., 2010; Wasmund et al., 2011; Kahru et al., 2020). However, most of these studies only consider incoming solar radiation as forcing, since it provides energy for photosynthesis and growth of phytoplankton species. Recent findings demonstrated that the occurrence of phytoplankton blooms is not only influenced by incoming solar radiation, but

Table 4-1. Environmental conditions driving the development of cyanobacteria blooms in the eastern Baltic Sea. Table adapted from **Publication I** (Beltran-Perez and Waniek, 2021).

Variable	Stage	Mean \pm SD*
Sea surface temperature ($^{\circ}\text{C}$)	Onset	14 ± 1
Air temperature ($^{\circ}\text{C}$)	Onset	14 ± 1
Outgoing long-wave radiation (W m^{-2})	Onset	-68 ± 7
Mixed layer depth (m)	Onset	26 ± 15
Brunt-Väisälä frequency (s^{-2})	Onset	-0.02 ± 0.003
Phosphate (mmol m^{-3})	Onset	0.1 ± 0.05
Wind speed (m s^{-1})	Onset	5 ± 1
Sensible heat flux (W m^{-2})	Peak	41 ± 6
Latent heat flux (W m^{-2})	Peak	-3 ± 9
Incoming solar radiation (W m^{-2})	Decline	218 ± 11
Net heat flux (W m^{-2})	Decline	178 ± 22
Sensible heat flux (W m^{-2})	Decline	35 ± 7
Latent heat flux (W m^{-2})	Decline	-12 ± 10
Phosphate (mmol m^{-3})	Decline	0.1 ± 0.02

* Standard deviation.

also by the net heat flux or some of its components (Gittings et al., 2018; Beltran-Perez and Waniek, 2021), which can lead to early or late bloom development and to stratification of the water column. Furthermore, air temperature is often disregarded in studies of this type, attributing the formation of the bloom solely to changes in sea surface temperature, but air temperature also plays a role in bloom formation (**Publication I**, Beltran-Perez and Waniek, 2021). Therefore, to properly analyze cyanobacteria blooms, it is necessary to consider several factors, including the heat exchange between the water surface and the atmosphere and the properties of the water column, as well as the interplay between them.

The timing, duration and intensity of blooms are strongly influenced by the life cycle and environmental preferences of phytoplankton species, leading to significant variation in results between phenological studies among species and regions, as demonstrated by Groetsch et al. (2016) and Scharfe and Wiltshire (2019) analyzing spring blooms in the Baltic Sea and the North Sea. When different species are combined into a pooled variable, trends and shifts in the timing of the bloom may be masked, affecting the results. Despite international efforts over many years, the study of individual species is still challenging due to technical, financial, and practical constraints, which limit the number of samples that can be collected over time. Moreover, the time at which the bloom starts, reaches maximum abundance and declines is unpredictable, as there is no guarantee that the samples collected will contain sufficient

information to track the evolution of the bloom. Model-based approaches are being used more often to increase our understanding derived from observations alone, providing a more detailed view of the development of phytoplankton blooms over time and the mechanisms that influence their formation.

4.2 Cyanobacteria blooms and their response to environmental changes

Over the last decades, the spring and summer blooms in the eastern Baltic Sea have shown a strong temporal variability. Although their variability has been studied previously (Wasmund and Uhlig, 2003; Janssen et al., 2004; Wasmund et al., 2011), the phenology and response of these phytoplankton blooms to changing environmental conditions are still unclear, as pointed out by Kahru and Elmgren (2014); Groetsch et al. (2016); Kahru et al. (2016); Beltran-Perez and Waniek (2021). In particular, changes in sea surface temperature, wind, and net heat flux affect the occurrence of spring and summer blooms differently. Anomalies of SST, wind and net heat flux during each bloom period were calculated to better understand changes in the occurrence of summer blooms and their relationship to stratification and mixing in the water column (**Publication II**, Beltran-Perez and Waniek, 2022), as the mixing in the water column is associated with changes in density (through buoyancy forcing by the net heat flux) and therefore in the mixed layer depth. The years with the most positive and negative anomalies (see Fig. S3 in **Publication II**, Beltran-Perez and Waniek, 2022) during the development of the bloom were selected for the analysis and are shown in the Fig. 4-1.

Surface water temperature has risen steadily over the past 100 years. The temperature of the Baltic Sea is rising faster than that of other marginal seas and the global ocean, with areas increasing at a rate of 0.59°C per decade (HELCOM/Baltic Earth, 2021, and references therein). Therefore, an increase in water stratification is expected, resulting in favorable conditions for the summer bloom to occur (Kanoshina et al., 2003; Paerl and Huisman, 2009). Based on the results of the calibrated and validated model, Beltran-Perez and Waniek (2022) found significant differences in cyanobacteria biomass induced by positive and negative sea surface temperature (SST) anomalies. Cyanobacteria blooms developed higher biomass during warmer periods than during colder periods. However, it was observed that the length of the cyanobacteria bloom was associated with a positive net heat flux (i.e. with a higher heat gain) rather than higher temperature (Fig. 4-1). Strong heat gain during summertime, such as in 1997, 2002, and 2006, resulted in an extended bloom, whereas lower heat gain, such as in 1993, 1998, and 2000, resulted in a shorter bloom. A positive net heat

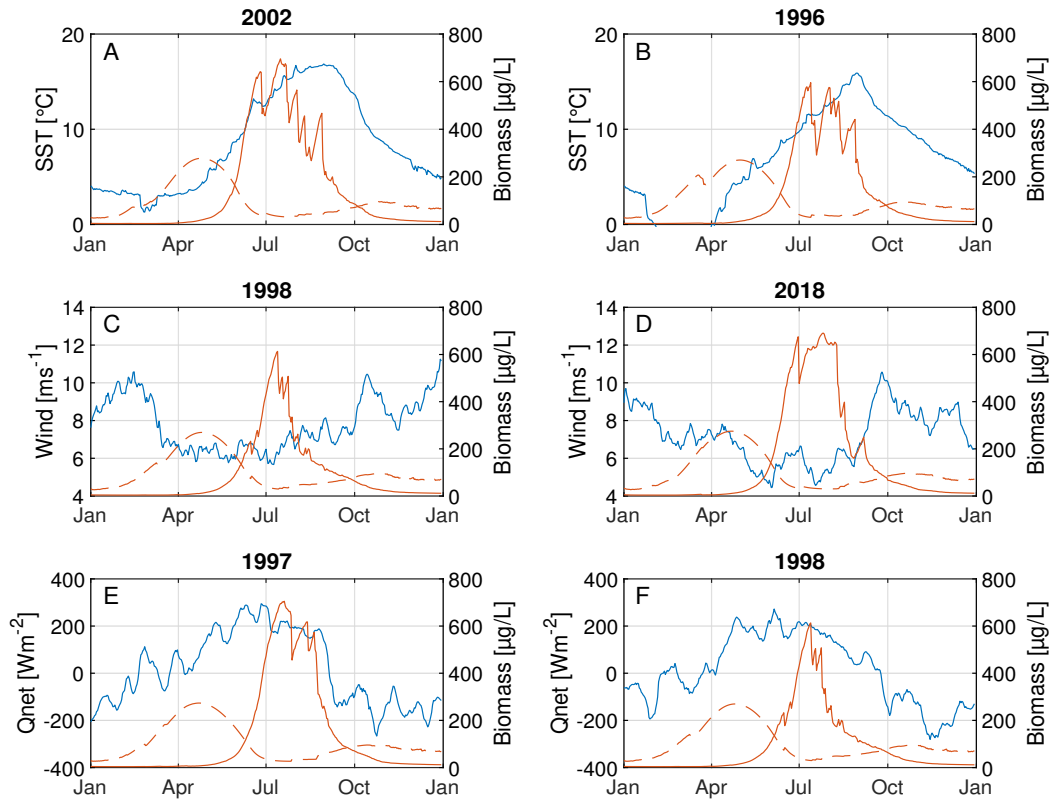


Fig. 4-1. Influence of SST (A-B), wind (C-D) and net heat flux (E-F) on cyanobacteria biomass (between June and August) in the Gotland Basin. At the top of each plot is shown the year with the highest positive anomalies (left panel) and negative anomalies (right panel) for each variable. The blue line corresponds to the variable (left axes) and the red line to biomass (right axes) of diatoms (dashed line) and cyanobacteria (solid line). The diatom bloom is included only to illustrate its inter-annual cycle. Figure adapted from **Publication II** (Beltran-Perez and Waniek, 2022).

flux also led to a bloom with higher abundance and maximum. The energy gain by the water column intensifies stratification and contributes significantly to the increase in bloom abundance, as a shallow mixed layer receives sufficient light for cell division and growth (critical depth hypothesis) (Sverdrup, 1953). Calm wind conditions are also favorable for the development of cyanobacteria blooms (Margalef, 1978), resulting in longer blooms. The highest cyanobacteria abundance coincides with calm wind conditions (Fig. 4-1), but there was no statistically significant difference found between the occurrence of the bloom and calm wind conditions (p -value > 0.05). These results are supported by Beltran-Perez and Waniek (2021), who showed that the phenology of cyanobacteria blooms is explained by the energy exchange between the atmosphere and the ocean. The role of energy exchange at

the ocean-atmosphere interface in the context of phenology studies has been highlighted in only few studies (Gittings et al., 2018; Beltran-Perez and Waniek, 2021). Thus, these results provide a first approach to the temporal variability and phenology of cyanobacteria blooms considering the interaction between the atmosphere and the water column in the eastern Baltic Sea, giving substantial information on the changes to which the bloom is exposed in a continuously changing environment.

4.3 Export production linked to cyanobacteria blooms

Based on sediment trap data from the Gotland Basin, the total particle flux and its components have shown large variability on the long-term and inter-annual time scales, with periods of exceptionally high particle flux in 2003, 2012 and 2015 (**Publication III**, Beltran-Perez et al., 2023). There are some indications that Major Baltic Inflows (MBIs) may have influenced the increase in total particle flux during these periods, but a detailed analysis of the effects of MBIs in the entire water column after their occurrence is beyond the scope of this thesis. The seasonal and annual cycle of particle flux in the Gotland Basin is strongly influenced by primary production in the surface layer, as reflected in studies by Leipe et al. (2008) and Schneider et al. (2017). The POC component of the flux has been found to consist mainly of recently produced biogenic material, according to Wasmund et al. (1998) and Cisternas-Novoa et al. (2019). As a result, the high POC component of the total particle flux observed in spring, summer, and autumn is related to near surface production, with diatoms dominating the export production in spring and autumn, and cyanobacteria in summer (Schneider et al., 2017; Beltran-Perez et al., 2023).

Monthly means over the period 1999 to 2020 were calculated and grouped by season to identify the seasonal variation in the total particle flux and its components (see Table 4-2). Seasons were divided into spring (March–May), summer (June–August), autumn (September–November) and winter (December–February), according to the pelagic seasons observed in the eastern Baltic Sea. The contribution of each parameter by season was determined as a percentage of its total signal over all seasons. Beltran-Perez et al. (2023) showed that the highest contribution to the total particle flux occurred in summer with about one third (31%) of the sinking material, followed by winter (27%), spring (24%), and autumn (19%) (Table 4-2). The total particle flux by season ranged from 118 to 193 mg m⁻² day⁻¹. The seasonal patterns of POC and PON mirrored each other, with higher values in summer and autumn than in winter and spring. The seasonal POC and PON components of the total particle flux were highest during summer. This indicates the contribution of cyanobacteria blooms to the sinking material. In contrast, the maximum and minimum seasonal P_{Si} component of the particle flux and C:N ratio occurred in winter (December, January, and February)

and summer (June, July, and August), respectively. The seasonal contributions of POC and PON to the total particle flux showed the opposite pattern to the seasonal PSi component of the flux and the C:N ratio, indicating the species succession from silica-rich species such as diatoms to species able to fix nitrogen from the atmosphere such as cyanobacteria in the Gotland Basin. The seasonal mean of $\delta^{13}C$ varied slightly between seasons (-26‰ to -25‰), whereas the seasonal mean of $\delta^{15}N$ reached higher values in spring (4.5‰) and lower in autumn (3.2‰).

Table 4-2. Seasonal means of total particle flux, POC, PON, PSi, C:N, $\delta^{13}C$ and $\delta^{15}N$ from sediment traps moored at 180 m depth in the Gotland Basin between 1999 and 2020. The seasons were divided into spring (March-May), summer (June-August), autumn (September-November) and winter (December-February). Values in parentheses correspond to the percentage of the variable with respect to its total value over all seasons. Table adapted from **Publication III** (Beltran-Perez et al., 2023).

Variable	Winter	Spring	Summer	Autumn	Total
Total particle flux [$\text{mg m}^{-2} \text{day}^{-1}$]	169.2 (26.8)	150.4 (23.8)	193.1 (30.6)	118.1 (18.7)	630.8
POC [$\text{mg m}^{-2} \text{day}^{-1}$]	15.9 (17.7)	19.8 (22.1)	29.6 (33.0)	24.4 (27.2)	89.7
PON [$\text{mg m}^{-2} \text{day}^{-1}$]	2.2 (19.5)	2.2 (19.5)	3.5 (31.0)	3.4 (30.1)	11.3
PSi [$\text{mg m}^{-2} \text{day}^{-1}$]	11.0 (33.7)	8.8 (27.0)	6.1 (18.7)	6.7 (20.6)	32.6
C:N	9.5 (27.1)	8.9 (25.4)	8.0 (22.9)	8.6 (24.6)	35.0
$\delta^{13}C$ [‰]	-26.1 (25.6)	-26.0 (25.5)	-25.1 (24.6)	-24.9 (24.4)	-102.1
$\delta^{15}N$ [‰]	4.2 (27.6)	4.5 (29.6)	3.3 (21.7)	3.2 (21.1)	15.2

The annual cycle of the total particle flux showed high values in April, July and November, reaching up to $97 \text{ mg m}^{-2} \text{day}^{-1}$ in the Gotland Basin (Fig. 4-2A). There was a low particle flux with high variability from December to March. The annual cycle of the POC component of the flux reached maximum values in November ($25 \text{ mg m}^{-2} \text{day}^{-1}$), followed by April and July with values of 16 and $9 \text{ mg m}^{-2} \text{day}^{-1}$, respectively (Fig. 4-2B). The minimum POC in the flux was mostly observed between January and March (around $3 \text{ mg m}^{-2} \text{day}^{-1}$). Maximum PON values occurred in April, July and November with large variability observed throughout the year (Fig. 4-2C). Thus, the POC and PON components of the flux reached maximum values during the same months than the total particle flux. The PSi in the flux had maximum values in April ($4 \text{ mg m}^{-2} \text{day}^{-1}$) and November ($6 \text{ mg m}^{-2} \text{day}^{-1}$) (Fig. 4-2D) with low values and variability in the remaining months, especially between June and September and minimum PSi values in July. The C:N ratio fluctuated between 7 and 9 with the highest C:N ratios between November and February and the lowest in July, August and September (Fig. 4-2E). The changes in the annual cycle of the total particle flux and POC indicated the contribution of phytoplankton blooms to the sinking material in the

Gotland Basin, while PON, P*Si* and C:N ratio reflected the species succession from diatoms to cyanobacteria and vice versa (as in autumn), with the corresponding effects on the nutrient pool (**Publication III**, Beltran-Perez et al., 2023).

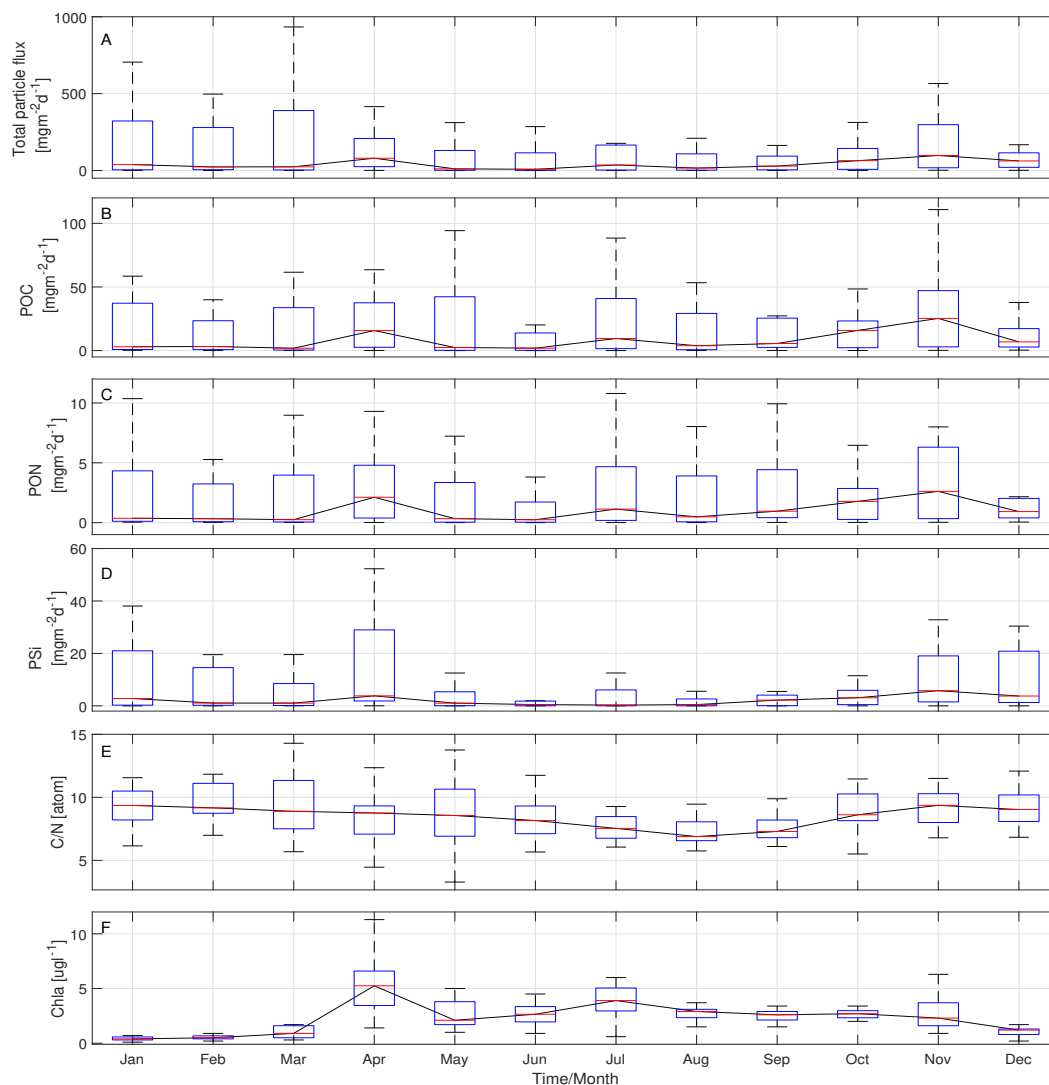


Fig. 4-2. Annual cycle based on monthly means between 1999 and 2020 of A) total particle flux, B) particulate organic carbon, C) particulate organic nitrogen, D) biogenic silica, E) C:N ratio from sediment traps moored at 180 m depth in the Gotland Basin and F) Chlorophyll a derived from water column measurements. The central red line in each box represents the median over 22 years. The bottom and top edges in each box indicate the 25th and 75th percentiles, respectively. The whiskers extend to the most extreme data points. Figure adapted from **Publication III** (Beltran-Perez et al., 2023).

The annual cycle of chlorophyll a, as a proxy for primary production, exhibited a consistent pattern with that of the particle flux and its components (Fig. 4-2F). Maximum chlorophyll a concentrations were observed in April ($6 \mu\text{g L}^{-1}$) and July ($4 \mu\text{g L}^{-1}$), which corresponded to the occurrence of spring and summer blooms and high particle flux in the Gotland Basin (Wasmund, 1997; Walve and Larsson, 2010; Kahru et al., 2016). The slow decrease in chlorophyll a concentration after the summer bloom may be linked to the autumn bloom (Wasmund and Uhlig, 2003), as indicated by the increase in total particle flux, POC, PON, and P*S*i in November. The chlorophyll a concentrations were low and had little variability between December and February, likely due to light limitations and deep mixing during these months. The total particle flux during the spring and autumn blooms was enriched in P*S*i, indicating the presence of diatoms in the sinking material (**Publication III**, Beltran-Perez et al., 2023). This observation was supported by moderate chlorophyll a concentrations and high POC and P*S*i in April and November (Fig. 4-2), as well as by microscopic analyses (Schneider et al., 2017).

4.4 The future of cyanobacteria blooms in the eastern Baltic Sea

The phenology of the cyanobacteria bloom is summarized in the Fig. 4-3. The phenology was derived from observations (**Publication I**, Beltran-Perez and Waniek, 2021), model results (**Publication II**, Beltran-Perez and Waniek, 2022) and the particulate organic carbon (POC) component of the total particle flux from sediment trap samples (**Publication III**, Beltran-Perez et al., 2023). Overall, the onset and maximum abundance of the cyanobacteria bloom occurred at similar times across all three data sets, with an average onset between days 157 and 172 and maximum concentrations between days 189 and 193. The decline of the bloom considering observations, model results and sediment trap data was on day 209, 236 and 226, respectively. The bloom length derived from the in situ observations and the sediment trap data was similar, resulting in a duration of 39 and 44 days, respectively, but it extended up to 80 days using model results. Notably, there were larger differences in the phenology determined with the three data sets, mostly at the end of the bloom, which affected its length as seen with the model results (Fig. 4-3).

The differences observed in the approaches for estimating phenology may be due to several reasons. For instance, in the case of observations, the grouping of three different species of cyanobacteria (*Nodularia spumigena*, *Aphanizomenon sp.* and *Dolichospermum spp.*) into a single one due to the lack of information to analyze each species separately may have caused discrepancies. Similarly, the implemented model account for the exchange of matter

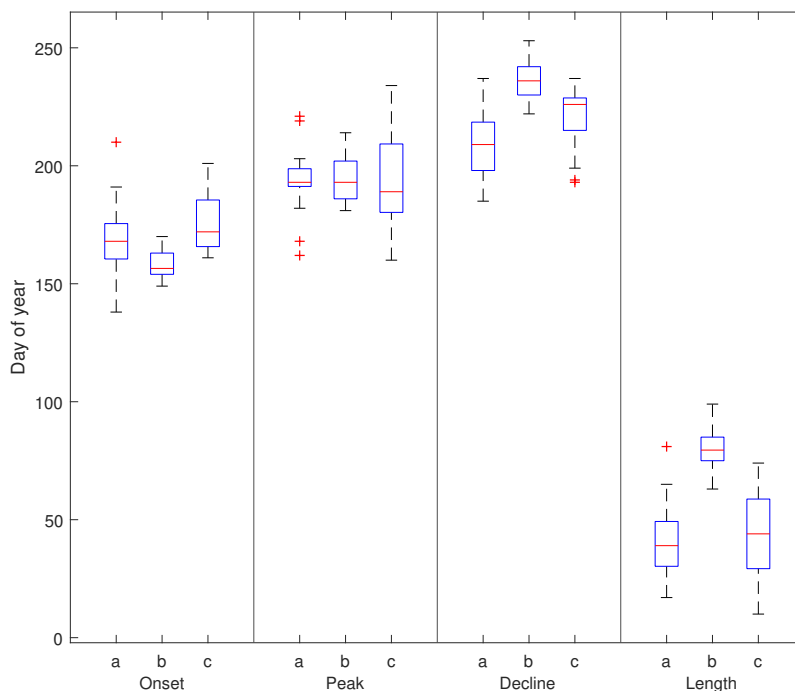


Fig. 4-3. Phenology of cyanobacteria blooms in the eastern Baltic Sea using a) observations (1990-2017) **Publication I** (Beltran-Perez and Waniek, 2021), b) model results (1990-2019) **Publication II** (Beltran-Perez and Waniek, 2022) and c) the particulate organic carbon component of the total particle flux (1999-2020) **Publication III** (Beltran-Perez et al., 2023). In each box, the central red line indicates the median. The bottom and top edges in each box indicate the 25th and 75th percentiles, respectively. The whiskers extend to the most extreme data points; outlier observations are marked individually using the '+'.

and energy through the water column, but not with the surroundings. In addition, the coupled model does not include other plankton species besides diatoms and cyanobacteria that may also appear throughout the year (e.g. dinoflagellates) in the Gotland Basin. These simplifications may have led to over- or underestimation of the simulated variables and contributed to the model error, which could also explain the differences to the observations and the sediment trap data. Overall, the temporal resolution and length of the data, as well as the definition of the threshold used to identify the onset and decline of the bloom strongly influence the results. There are different methods to define the bloom based on a threshold or the bloom distribution (Ji et al., 2010). However, no consensus on which method is more appropriate or a universal threshold applicable for each bloom-forming species exist, making comparisons between phenological studies challenging. A trend analysis may be an option for comparison with other studies, as the data are expected to reflect the same trend regardless of the threshold used, making it a more robust method.

The timing and duration of the cyanobacteria bloom exhibit significant temporal changes (p -value < 0.05) with both modeling results and sediment trap data (Fig. 4-4). According to the modeling results, summer blooms started 9 days earlier moving from day 161 in 1990 (10 June) to day 152 in 2019 (1 June) in the Gotland Basin. The length of the bloom also increased from 72 to 87 days, lasting 15 days longer in 2019 than in 1990. Similarly, the onset of cyanobacteria blooms was found to occur 30 days earlier, starting on day 166 in 2020 (14 June) instead of day 196 in 1999 (15 July) analyzing the particulate organic carbon component of the total particle flux over a 22-year period. The bloom length increased from 18 days in 1999 to 60 days in 2020. The modeling results indicate that summer blooms occur on average 0.3 days earlier and last 0.5 days longer per year. Sediment trap data shows a more pronounced trend, with blooms starting 1.4 days earlier and lasting 1.9 days longer per year. The days on which the cyanobacteria bloom reaches maximum abundance or declines did not show any significant temporal change based on modeling results and sediment trap data. In contrast to the temporal changes in the occurrence of the bloom previously indicated, in situ observations of the cyanobacteria bloom between 1990 and 2017 showed no significant changes. The limited frequency of observations in time and space may mask the presence of a trend or shifts in the timing of the bloom. In addition, in situ observations of phytoplankton biomass are usually integrated over the water column, which may lead to differences in the estimated biomass and phenology when compared to other studies even during similar periods of time and locations. These findings underscore the importance of using multiple data sources and robust analysis to accurately assess the inter-annual variability of cyanobacteria blooms and their phenology.

The results of this thesis are consistent with previous studies indicating that cyanobacteria blooms are starting earlier and lasting longer, regardless of how bloom phenology is defined. Kahru and Elmgren (2014) reported a progressive earlier accumulation of cyanobacteria in summer by about 0.6 days per year over a 35-year period in the Baltic Sea. Kahru et al. (2016) also found trends towards an earlier start of spring and summer blooms in the central Baltic Sea. However, Wasmund and Uhlig (2003) found no evidence that cyanobacteria blooms increased during the period 1979-1999, even a decreasing trend was observed in some basins of the Baltic Sea. Therefore, the future of cyanobacteria blooms remains uncertain in the Baltic Sea, as no consensus has been reached on whether they will increase or decrease (Wasmund and Uhlig, 2003; Kahru and Elmgren, 2014; Kahru et al., 2016; Meier et al., 2019). This uncertainty stems from the complex factors involved in the development of cyanobacteria blooms, the natural variability of the species itself, its interaction with grazers, and the physical, chemical and biological processes occurring at small scales and across scales.

Changes in the phenology of summer blooms and their relationship to global warming suggest

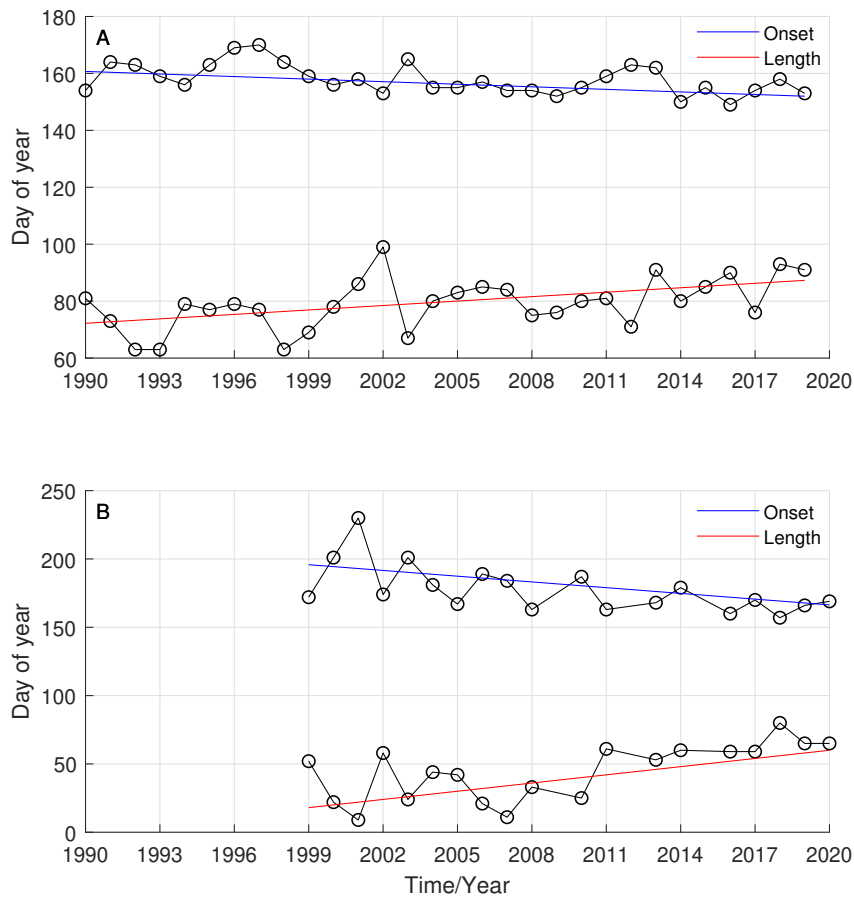


Fig. 4-4. Temporal change in the phenology of cyanobacteria blooms based on A) modeling results between 1990 and 2019 and B) sediment trap samples collected at 180 m depth in the Gotland Basin between 1999 and 2020. The circles connected with a black solid line represent the onset dates or the length of the bloom, see legend on the figure. The slope of the curves was estimated using the Mann-Kendall test with the non-parametric Sen method using 95% significance level.

that cyanobacteria blooms will continue to be a major concern for the Baltic Sea. Cyanobacteria blooms can accelerate eutrophication and oxygen depletion in the water (Larsson et al., 1985; Wasmund, 1997; Janssen et al., 2004). They can have significant impacts on fisheries and recreational use of coastal waters due to the production of toxins (Paerl and Huisman, 2009; Neil et al., 2012). Changes in the food web are also expected as the efficiency of energy transfer to higher trophic levels may be reduced due to the timing of food availability (match-mismatch hypothesis) (Smith and Hollibaugh, 1993; Winder and Schindler, 2004) and the poor quality of cyanobacteria as a food source for grazers (depending on the availability of other sources of food and the type of zooplankton and cyanobacteria species)

(Meyer-Harms et al., 1999; Ger et al., 2016; Munkes et al., 2020). A shift in the phytoplankton community may also affect the survival of zooplankton and fish, as larval spawning continues to match the original timing of the bloom prior to changes (Cole, 2014; Gittings et al., 2018). Therefore, changes in the phenology of phytoplankton blooms combined with current environmental changes may lead to potential negative impacts on the whole Baltic Sea ecosystem.

4.5 Global trends

Trends for phytoplankton blooms are difficult to resolve for the entire Baltic Sea or globally, owing to inconsistent sampling efforts and the diversity of the eco-environmental or socio-economic effects. Satellites have become an alternative to continuously monitor the ocean surface, enabling the detection of blooms in many regions (Dai et al., 2023). By analyzing chlorophyll a concentration from multiple satellites (MERIS, MODIS-AQUA, SeaWiFS, NPP-VIIRS and OLCI-A) merged at 1 km resolution, the chlorophyll a concentration in the Baltic Sea showed a positive trend with a slope of $0.67 \pm 0.46\%$ per year between 1997 and 2021 (Fig. 4-5).

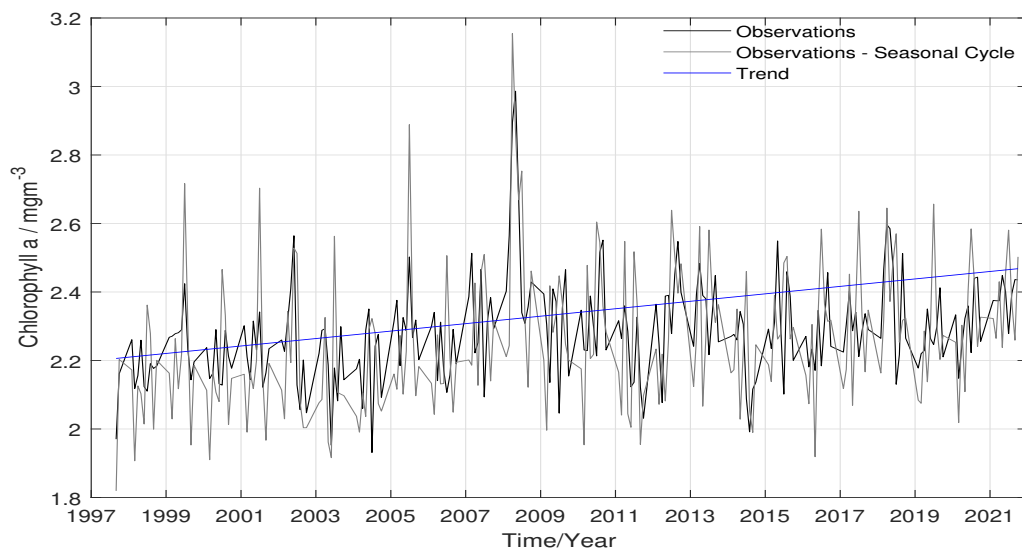


Fig. 4-5. Chlorophyll a concentration derived from satellite data. Monthly regional mean values are calculated by performing the average of 2D monthly mean (weighted by pixel area) over the Baltic Sea. The seasonal cycle is obtained by applying the X-11 seasonal adjustment methodology on the original time series, as described by Colella et al. (2016). The trend line was estimated using the Mann-Kendall test with the non-parametric Sen method. The data used were downloaded from the Baltic Sea Biogeochemistry Reanalysis data set provided by the Copernicus Marine Service.

Coastal waters are undergoing continuous changes through warming, acidification, and de-oxygenation that are likely to intensify in the future. Phytoplankton blooms have also shown changes in coastal waters. Dai et al. (2023) studied global marine coastal algal blooms between 2003 and 2020 using global satellite observations from the Moderate Resolution Imaging Spectroradiometer (MODIS) onboard NASA's Aqua satellite. The data set was derived using global, 1 km spatial resolution daily observations. Indeed, similar to the trend observed in the Baltic Sea, Dai et al. (2023) found a positive trend in coastal bloom events worldwide, increasing at a rate of 2.2% per year (Fig. 4-6).

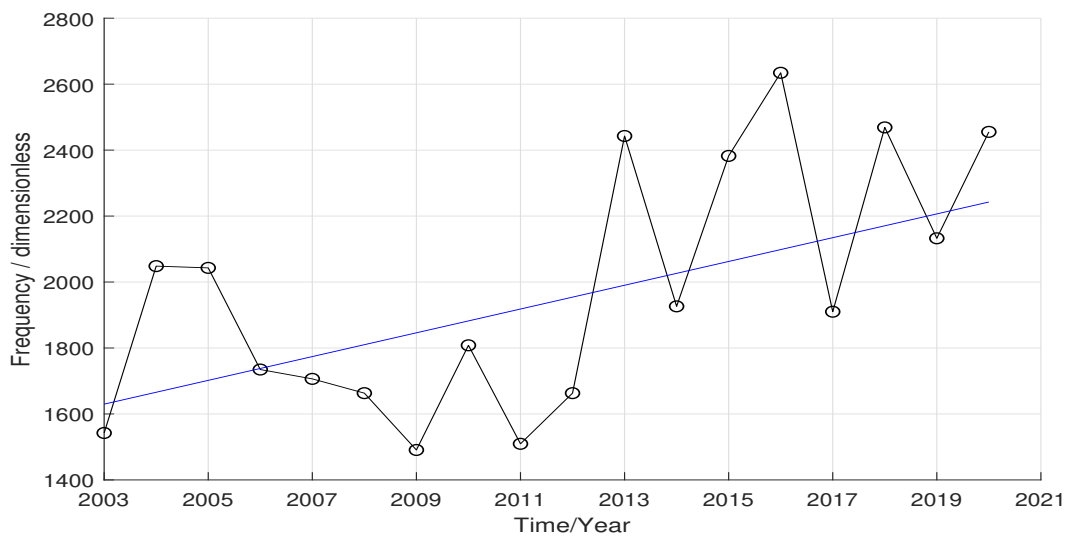


Fig. 4-6. Development of global coastal phytoplankton blooms between 2003 and 2020 using satellite observations from MODIS. The number of bloom counts within a year for each location was enumerated, and the long-term annual mean values were then estimated. Figure adapted from Dai et al. (2023).

Satellite data provide finer spatial and temporal resolution than in situ observations, but they are subject to other limitations. On one side, satellite data are affected by clouds, which interfere with the measurements as well as there are also restrictions when merging and processing data from different sensors/satellites. On the other side, satellites can only detect phytoplankton blooms when strong surface aggregations are formed. These usually occur at an advanced stage of the bloom and are directly related to cyanobacteria species such as *Nodularia spumigena*, the only bloom-forming species that forms dense surface accumulations in summer in the Baltic Sea (Kahru et al., 2020), Fig. 4-7. *Nodularia spumigena* is a co-dominant cyanobacteria species in the Baltic Sea, the other co-dominant species, *Aphanizomenon sp.* and *Dolichospermum spp.*, although both are present during the bloom, these species are typically found at the subsurface and are therefore not specifically detected by satellites (Kahru and Elmgren, 2014; Eigemann et al., 2018; Kahru et al., 2020).



Fig. 4-7. Cyanobacteria bloom in August 2018 during the monitoring cruise EMB190 in the Gotland Basin, Baltic Sea. The pictures were taken by J. Waniek (IOW), personal communication.

Harmful algal bloom (HAB) events have been recorded globally since 1985 in the Harmful Algae Event Database (HAEDAT, <http://haedat.iode.org>) of the UNESCO Intergovernmental Oceanographic Commission. The HAEDAT records for each HAB event the period (ranging from days to months) and geolocation. Hallegraeff et al. (2021b) through a meta-analysis showed increases in algal blooms events in different global regions (Fig. 4-8). Specifically, eight of the nine regions showed increasing trends (East Coast America (ECA), Central America/Caribbean (CCA), South America (SAM), West Coast America (WCA), Australia/New Zealand (ANZ), South East Asia (SEA), Mediterranean (MED) and Europe (EUR)), except for North East Asia (NAS) with a decreasing trend. Six of these trends showed statistically significant changes (ECA, CCA, WCA, SEA, MED, EUR). However, on a global scale no trend was found. The contrasting trends in individual regions were driven likely by differences in bloom species, type of HAB and impacts (seafood toxins, mass mortalities, high phytoplankton count, mucus). Effects of environmental changes will vary from species to species, as climate change alters different ocean regions at different rates and time scales. Therefore, differences in phytoplankton blooms among apparently similar sites remain in most cases unexplained, which calls for ecological studies addressed on a species-by-species and site-by-site basis (Hallegraeff et al., 2021b).

Overall, it appears that the combination of both in situ observations and satellite data provides a more comprehensive understanding of phytoplankton blooms. Thus, efforts to monitor phytoplankton blooms regardless of the technique should continue to increase our understanding of these events, their changes over time and potential impacts on marine ecosystems.

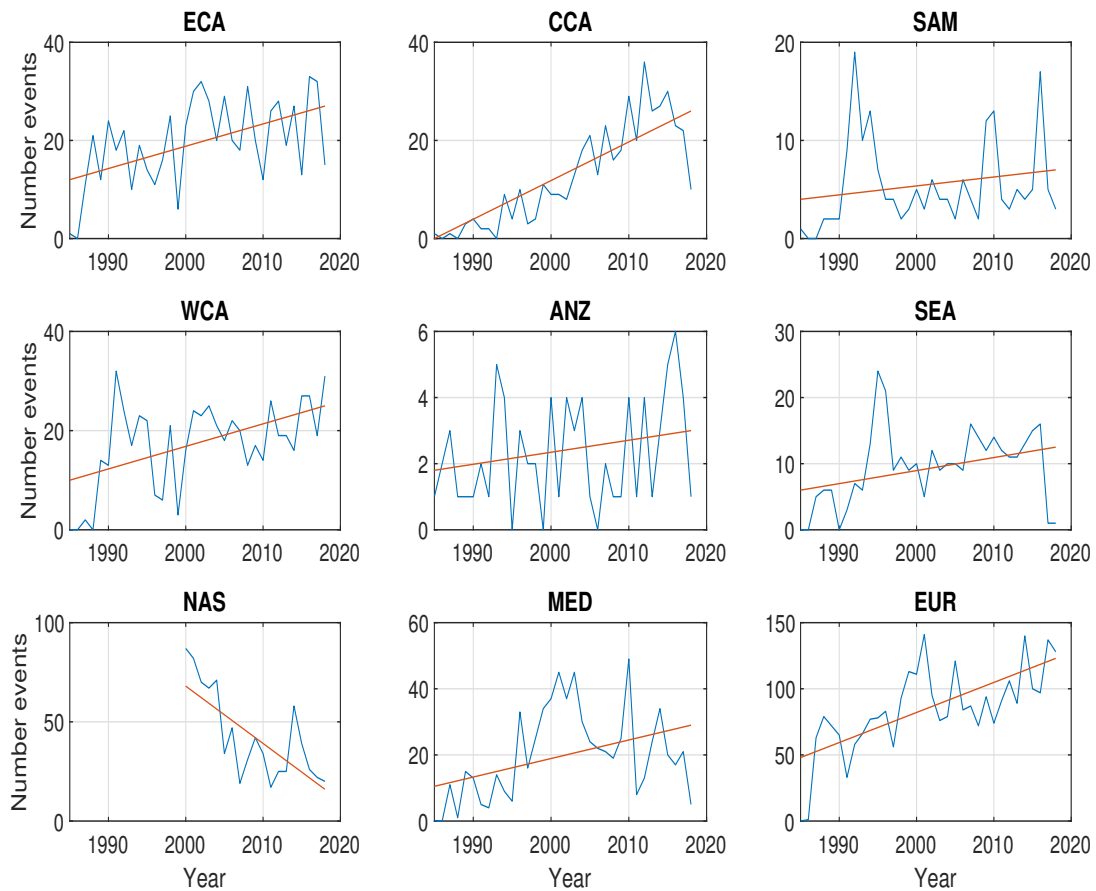


Fig. 4-8. Change in the number of algal blooms events between 1985 and 2018 in 9 global regions: East Coast America (ECA), Central America/Caribbean (CCA), South America (SAM), West Coast America (WCA), Australia/New Zealand (ANZ), South East Asia (SEA) and North East Asia (NAS), Mediterranean (MED) and Europe (EUR). The number of events is indicated by the blue line and the trend by the red line in each panel. Figure adapted from Hallegraeff et al. (2021b).

4.6 Phytoplankton blooms: Insights and challenges in a changing climate

Over the last decades, there has been growing concern about the impact of climate change on the entire ecosystem (Gruber, 2011). Temperatures are expected to rise to harmful levels causing physiological stress to marine organisms (Pörtner and Farrell, 2008). The dissolved oxygen in the ocean and coastal areas has decreased since the mid-twentieth century, as warmer waters contain less dissolved oxygen (Breitburg et al., 2018). Ocean acidification alters the pH and saturation state of calcium carbonate in the ocean, affecting the growth and

survival of both calcifying and non-calcifying organisms (Gobler and Baumann, 2016). In addition, external factors such as precipitation affect runoff intensity and the residence time of water, nutrient loading, salinity and the content of dissolved organic matter (DOM) and trace metals (Gledhiir and Buck, 2012; Creed et al., 2018). Internal loading of phosphorus along with decreasing N:P ratios may favor diazotrophic species such as cyanobacteria over other phytoplankton species e.g. in the Baltic Sea (Vahtera et al., 2007), shifting the phytoplankton community from eukaryotic (especially diatom) to cyanobacteria species (Paerl and Otten, 2013). Harmful species appear to benefit more than other species from increasing CO₂ levels, with growth rates steadily increasing as CO₂ increases (Brandenburg et al., 2019). Despite extensive research on these topics, it is still unclear to what extent climate change is exacerbating HABs.

There is a scientific consensus that harmful algal bloom impacts on public health, recreation, tourism, fishery and aquaculture have intensified in recent decades (Gobler, 2020). The observed trends in harmful algal blooms are driven partly by ocean warming, marine heatwaves, oxygen loss, eutrophication and pollution (IPCC, 2019). However, individual events are influenced by local, regional, and global forcing. The expansion of HABs induced by warming is the strongest signal to date of climate-related effects on phytoplankton blooms (IPCC, 2019). Several studies have shown that the maximum growth temperatures for many cyanobacteria species are higher than those for non-harmful eukaryotic species (Paerl and Huisman, 2009; Paerl and Otten, 2013). Warming has been linked to the intensification of HABs in several mid- and high-latitude regions, where a poleward migration of HABs has also been observed (Hallegraeff, 2010; Gobler et al., 2017; Griffith et al., 2019). The emergence of harmful species in new ecosystems may pose a risk to local species and nearby populations (Colin and Dam, 2002), as HABs may release toxins with negative effects in several sectors including food security, tourism, economy and human health (Gobler, 2020).

5 Summary and Outlook

This thesis contributes to the better understanding of phytoplankton blooms and their phenology in the Baltic Sea, highlighting the importance of considering different data sources and approaches when studying this complex events. While there are still many unresolved questions about phytoplankton blooms, the results provide insights that can guide future research. The first part of this thesis aimed to define the factors that trigger the development of cyanobacteria blooms in the eastern Baltic Sea (**Publication I**, Beltran-Perez and Waniek, 2021). Based on in situ observations, Beltran-Perez and Waniek (2021) defined the environmental window for the occurrence of cyanobacteria blooms. They respond to the combined effect of both oceanic and atmospheric variables at each development stage (onset, maximum abundance and decline), leading to a high degree of variability, both in time and space between the cyanobacteria blooms.

The frequency of in situ observations is not sufficient for a detailed analysis of the inter-annual variability of phytoplankton blooms, therefore in the second part of this thesis a model was developed and used to identify trends in the occurrence of spring and summer blooms in the eastern Baltic Sea (**Publication II**, Beltran-Perez and Waniek, 2022). Beltran-Perez and Waniek (2022) developed a one-dimensional, coupled physical-biological model based on equations governing the formation of the bloom and the interaction ocean-atmosphere driven by realistic forcing. The model reproduced the development and response of the bloom to changing environmental conditions with reliable results, providing a solid basis for testing phytoplankton bloom hypothesis. Overall, cyanobacteria are more sensitive to environmental changes than diatoms. Therefore, cyanobacteria blooms are expected to respond faster to changing environmental conditions in the Baltic Sea. It is not clear whether warming will lead to more frequent, intense and long cyanobacteria blooms in the future, but the results so far indicate that this is the most likely outcome.

Sinking particles provide the major connection between the surface and the deep water column. Therefore, the contribution of phytoplankton blooms to the total particle flux provides insight into the processes occurring in the water column (**Publication III**, Beltran-Perez et al., 2023). Despite the high temporal variability of the total particle flux and its components, three distinct periods over the year were identified and associated with surface

primary production in the Gotland Basin, eastern Baltic Sea. Diatoms blooms were the source of sinking material in spring and autumn. The large particle flux in summer was driven by the growth of nitrogen fixing cyanobacteria, mainly of the species *Aphanizomenon* and *Nodularia*. The winter season was characterized by low primary production due to light limitations and deep mixing.

The Baltic Sea is one of the most intensively monitored seas in the world. However, its observations are not sufficient to determine in detail phytoplankton phenology. Coupling of several sources of data on species-specific life cycles and succession to environment conditions (e.g. nutrient ratios, light, temperature), other organisms (e.g. prey, predators, competitors), and process-based models is necessary to explain the timing and intensity of phytoplankton blooms in the Baltic Sea, and most likely in other environments as well. It is worth considering not only how climate leads to local stresses that favor phytoplankton blooms, but also how to distinguish local human influences from those driven by the climate.

Significant progress has been made in understanding phytoplankton blooms, however, there are still several unanswered questions regarding their development and their impacts on human health, fisheries, and aquaculture that warrant exploration. While certain factors such as nutrient availability and light play a role in the formation of the bloom, the precise mechanisms in different regions and under varying environmental conditions are not fully understood. Understanding the competitive dynamics, interactions, and symbiotic relationships among various phytoplankton species within a bloom can provide insights into the overall bloom structure, species succession, and potential impacts on ecosystem functioning. Considerable attention has been given to the formation and maximum abundance stages of the bloom, but the ecological consequences and the fate of bloom-forming species after the decline of the bloom are still unclear. Therefore, exploring the impacts on nutrient cycling, carbon export, and microbial dynamics during the post-bloom phase can provide valuable insights into ecosystem responses and the entire carbon cycle.

Certain species within phytoplankton blooms can produce harmful toxins that accumulate in seafood and pose risks to human health. However, the specific factors influencing toxin production and the mechanisms by which they affect human health are still areas of active research. Furthermore, determining how phytoplankton blooms influence the abundance, distribution, and composition of fish populations and the potential impacts on aquaculture operations (e.g., fish health, feed availability), is crucial for sustainable fisheries management and aquaculture practices.

Future HABs will become more common in an anthropogenically-altered ocean and, therefore, their occurrence and impacts may differ from what we observe today. Although the

relationship between nutrients and phytoplankton is known, better quantification and linkage to their expansion are needed. In addition to nutrients, micronutrients (e.g. iron, zinc), trace metal, temperature, light regimes and heat exchange with the atmosphere have to be coupled to explain the dynamics of phytoplankton blooms. The spatio-temporal scales of interaction between forcing and phytoplankton blooms are also not well understood, most likely because of their natural variability. In the coming years, efforts may be directed towards more long-term monitoring programs including traditional sampling coupled to modern instruments (e.g. buoys, floats, gliders) and remote sensing, laboratory and field assays, molecular techniques (genomics, transcriptomics, proteomics, metabolomics) and modeling approaches to gain a better understanding of phytoplankton and HABs and their anthropogenic and natural forcing. Studies of the life cycle of bloom-forming species, predators (e.g. large zooplankton species, zebra mussels), viral and fungi interactions are needed as well. By gaining a more comprehensive understanding of phytoplankton blooms and their implications for human health, fisheries, aquaculture, and in general for the whole ecosystem, it may be possible the implementation of effective management strategies to mitigate risks and promote the sustainable use of the ocean.

References

- Andersson, A., Meier, H.E., Ripszam, M., Rowe, O., Wikner, J., Haglund, P., Eilola, K., Legrand, C., Figueroa, D., Paczkowska, J., Lindehoff, E., Tysklind, M., Elmgren, R., 2015. Projected future climate change and Baltic Sea ecosystem management. *Ambio* 44, 345–356. doi:10.1007/s13280-015-0654-8.
- Barton, A.D., Irwin, A.J., Finkel, Z.V., Stock, C.A., 2016. Anthropogenic climate change drives shift and shuffle in North Atlantic phytoplankton communities. *Proceedings of the National Academy of Sciences of the United States of America* 113, 2964–2969. doi:10.1073/pnas.1519080113.
- Basu, S., Mackey, K.R., 2018. Phytoplankton as key mediators of the biological carbon pump: Their responses to a changing climate. *Sustainability (Switzerland)* 10. doi:10.3390/su10030869.
- Baumert, H.Z., Petzoldt, T., 2008. The role of temperature, cellular quota and nutrient concentrations for photosynthesis, growth and light-dark acclimation in phytoplankton. *Limnologica* 38, 313–326. doi:10.1016/j.limno.2008.06.002.
- Beardall, J., Stojkovic, S., Larsen, S., 2009. Living in a high CO₂ world: Impacts of global climate change on marine phytoplankton. *Plant Ecology and Diversity* 2, 191–205. doi:10.1080/17550870903271363.
- Beaugrand, G., 2009. Decadal changes in climate and ecosystems in the North Atlantic Ocean and adjacent seas. *Deep-Sea Research Part II: Topical Studies in Oceanography* 56, 656–673. doi:10.1016/j.dsr2.2008.12.022.
- Behrenfeld, M.J., O'Malley, R.T., Siegel, D.A., McClain, C.R., Sarmiento, J.L., Feldman, G.C., Milligan, A.J., Falkowski, P.G., Letelier, R.M., Boss, E.S., 2006. Climate-driven trends in contemporary ocean productivity. *Nature* 444, 752–755. doi:10.1038/nature05317.
- Belkin, I.M., 2009. Rapid warming of Large Marine Ecosystems. *Progress in Oceanography* 81, 207–213. doi:10.1016/j.pocean.2009.04.011.
- Bell, G.R., 1961. Penetration of spines from a marine diatom into the gill tissue of lingcod (*Ophiodon elongatus*). *Nature* 192, 279. doi:10.1038/192279a0.

References

- Beltran-Perez, O.D., Voss, M., Pollehne, F., Liskow, I., Waniek, J.J., 2023. Temporal variability of particle flux and its components in the Gotland Basin, eastern Baltic Sea. *Frontiers in Earth Science* 11. doi:10.3389/feart.2023.1171917.
- Beltran-Perez, O.D., Waniek, J.J., 2021. Environmental window of cyanobacteria bloom occurrence. *Journal of Marine Systems* 224, 103618. doi:10.1016/j.jmarsys.2021.103618.
- Beltran-Perez, O.D., Waniek, J.J., 2022. Inter-annual variability of spring and summer blooms in the eastern Baltic Sea. *Frontiers in Marine Science* 9. doi:10.3389/fmars.2022.928633.
- Bianchi, T.S., Engelhaupt, E., Westman, P., Andr n, T., Rolff, C., Elmgren, R., 2000. Cyanobacterial blooms in the Baltic Sea: Natural or human-induced? *Limnology and Oceanography* 45, 716–726. doi:10.4319/lo.2000.45.3.0716.
- Bodungen, B.V., Wunsch, M., F rderer, H., 1991. Sampling and Analysis of Suspended and Sinking Particles in the Northern North Atlantic, in: Hurd, D.C., Spencer, D.W. (Eds.), *Marine Particles: Analysis and Characterization*. 63 ed.. Geophysical Monograph Series, American Geophysical Union (AGU), Washington, DC, pp. 47–56. doi:10.1029/GM063P0047.
- Brandenburg, K.M., Velthuis, M., Van de Waal, D.B., 2019. Meta-analysis reveals enhanced growth of marine harmful algae from temperate regions with warming and elevated CO2 levels. *Global Change Biology* 25, 2607–2618. doi:10.1111/gcb.14678.
- Breitburg, D., Levin, L.A., Oschlies, A., Gr goire, M., Chavez, F.P., Conley, D.J., Gar on, V., Gilbert, D., Guti rrez, D., Isensee, K., Jacinto, G.S., Limburg, K.E., Montes, I., Naqvi, S.W., Pitcher, G.C., Rabalais, N.N., Roman, M.R., Rose, K.A., Seibel, B.A., Telszewski, M., Yasuhara, M., Zhang, J., 2018. Declining oxygen in the global ocean and coastal waters. *Science* 359. doi:10.1126/science.aam7240.
- Burford, M.A., Carey, C.C., Hamilton, D.P., Huisman, J., Paerl, H.W., Wood, S.A., Wulff, A., 2020. Perspective: Advancing the research agenda for improving understanding of cyanobacteria in a future of global change. *Harmful Algae* 91, 101601. doi:10.1016/j.hal.2019.04.004.
- Chen, Z., Sun, J., Gu, T., Zhang, G., Wei, Y., 2021. Nutrient ratios driven by vertical stratification regulate phytoplankton community structure in the oligotrophic western Pacific Ocean. *Ocean Science* 17, 1775–1789. doi:10.5194/os-17-1775-2021.

- Chong, I.G., Jun, C.H., 2005. Performance of some variable selection methods when multicollinearity is present. *Chemometrics and Intelligent Laboratory Systems* 78, 103–112. doi:10.1016/j.chemolab.2004.12.011.
- Cisternas-Novoa, C., Le Moigne, F.A., Engel, A., 2019. Composition and vertical flux of particulate organic matter to the oxygen minimum zone of the central Baltic Sea: Impact of a sporadic North Sea inflow. *Biogeosciences* 16, 927–947. doi:10.5194/bg-16-927-2019.
- Cole, H.S., 2014. The natural variability and climate change response in phytoplankton. Doctoral dissertation. University of Southampton.
- Colella, S., Falcini, F., Rinaldi, E., Sammartino, M., Santoleri, R., 2016. Mediterranean ocean colour chlorophyll trends. *PLoS ONE* 11, 1–16. doi:10.1371/journal.pone.0155756.
- Colin, S.P., Dam, H.G., 2002. Latitudinal differentiation in the effects of the toxic dinoflagellate *Alexandrium* spp. on the feeding and reproduction of populations of the copepod *Acartia hudsonica*. *Harmful Algae* 1, 113–125. doi:10.1016/S1568-9883(02)00007-0.
- Creed, I.F., Bergström, A.K., Trick, C.G., Grimm, N.B., Hessen, D.O., Karlsson, J., Kidd, K.A., Kritzberg, E., McKnight, D.M., Freeman, E.C., Senar, O.E., Andersson, A., Ask, J., Berggren, M., Cherif, M., Giesler, R., Hotchkiss, E.R., Kortelainen, P., Palta, M.M., Vrede, T., Weyhenmeyer, G.A., 2018. Global change-driven effects on dissolved organic matter composition: Implications for food webs of northern lakes. *Global Change Biology* 24, 3692–3714. doi:10.1111/gcb.14129.
- Cury, P., Roy, C., 1989. Optimal Environmental Window and Pelagic Fish Recruitment Success in Upwelling Areas. *Canadian Journal of Fisheries and Aquatic Sciences* 46, 670–680. doi:10.1139/f89-086.
- Dai, Y., Yang, S., Zhao, D., Hu, C., Xu, W., Anderson, D.M., Li, Y., Song, X.P., Boyce, D.G., Gibson, L., Zheng, C., Feng, L., 2023. Coastal phytoplankton blooms expand and intensify in the 21st century. *Nature* 615. doi:10.1038/s41586-023-05760-y.
- Downing, J.A., Watson, S.B., Mccauley, E., 2001. Predicting Cyanobacteria dominance in lakes. *Canadian Journal of Fisheries and Aquatic Sciences* 58, 1905–1908. doi:10.1139/cjfas-58-10-1905.
- Durbin, E.G., Campbell, R.G., Casas, M.C., Ohman, M.D., Niehoff, B., Runge, J., Wagner, M., 2003. Interannual variation in phytoplankton blooms and zooplankton productivity

References

- and abundance in the Gulf of Maine during winter. *Marine Ecology Progress Series* 254, 81–100. doi:10.3354/meps254081.
- Eigemann, F., Schwartke, M., Schulz-Vogt, H., 2018. Niche separation of Baltic Sea cyanobacteria during bloom events by species interactions and autecological preferences. *Harmful Algae* 72, 65–73. doi:10.1016/j.hal.2018.01.001.
- García, C., Bravo, M.D.C., Lagos, M., Lagos, N., 2004. Paralytic shellfish poisoning: post-mortem analysis of tissue and body fluid samples from human victims in the Patagonia fjords. *Toxicon* 43, 149–158. doi:10.1016/J.TOXICON.2003.11.018.
- Ger, K.A., Urrutia-Cordero, P., Frost, P.C., Hansson, L.A., Sarnelle, O., Wilson, A.E., Lüring, M., 2016. The interaction between cyanobacteria and zooplankton in a more eutrophic world. *Harmful Algae* 54, 128–144. doi:10.1016/j.hal.2015.12.005.
- Gibble, C.M., Kudela, R.M., Knowles, S., Bodenstein, B., Lefebvre, K.A., 2021. Domoic acid and saxitoxin in seabirds in the United States between 2007 and 2018. *Harmful Algae* 103, 101981. doi:10.1016/j.hal.2021.101981.
- Gittings, J.A., Raitsos, D.E., Krokos, G., Hoteit, I., 2018. Impacts of warming on phytoplankton abundance and phenology in a typical tropical marine ecosystem. *Scientific Reports* 8, 1–12. doi:10.1038/s41598-018-20560-5.
- Gledhiir, M., Buck, K.N., 2012. The organic complexation of iron in the marine environment: A review. *Frontiers in Microbiology* 3, 1–17. doi:10.3389/fmicb.2012.00069.
- Gobler, C.J., 2020. Climate Change and Harmful Algal Blooms: Insights and perspective. *Harmful Algae* 91, 101731. doi:10.1016/j.hal.2019.101731.
- Gobler, C.J., Baumann, H., 2016. Hypoxia and acidification in ocean ecosystems: Coupled dynamics and effects on marine life. *Biology Letters* 12. doi:10.1098/rsbl.2015.0976.
- Gobler, C.J., Doherty, O.M., Hattenrath-Lehmann, T.K., Griffith, A.W., Kang, Y., Litaker, R.W., 2017. Ocean warming since 1982 has expanded the niche of toxic algal blooms in the North Atlantic and North Pacific oceans. *Proceedings of the National Academy of Sciences of the United States of America* 114, 4975–4980. doi:10.1073/pnas.1619575114.
- Godhe, A., Rynearson, T., 2017. The role of intraspecific variation in the ecological and evolutionary success of diatoms in changing environments. *Philosophical Transactions of the Royal Society B: Biological Sciences* 372. doi:10.1098/rstb.2016.0399.

- Griffith, A.W., Doherty, O.M., Gobler, C.J., 2019. Ocean warming along temperate western boundaries of the Northern Hemisphere promotes an expansion of *Cochlodinium polykrikoides* blooms. *Proceedings of the Royal Society B: Biological Sciences* 286. doi:10.1098/rspb.2019.0340.
- Groetsch, P.M., Simis, S.G., Eleveld, M.A., Peters, S.W., 2016. Spring blooms in the Baltic Sea have weakened but lengthened from 2000 to 2014. *Biogeosciences* 13, 4959–4973. doi:10.5194/bg-13-4959-2016.
- Gruber, N., 2011. Warming up, turning sour, losing breath: ocean biogeochemistry under global change. *Philos. Trans. R. Soc. A* doi:10.1098/rsta.2011.0003.
- Häder, D.P., Villafañe, V.E., Helbling, E.W., 2014. Productivity of aquatic primary producers under global climate change. *Photochemical and Photobiological Sciences* 13, 1370–1392. doi:10.1039/c3pp50418b.
- Hallegraeff, G., Enevoldsen, H., Zingone, A., 2021a. Global harmful algal bloom status reporting. *Harmful Algae* 102. doi:10.1016/j.hal.2021.101992.
- Hallegraeff, G.M., 2010. Ocean climate change, phytoplankton community responses, and harmful algal blooms: A formidable predictive challenge. *Journal of Phycology* 46, 220–235. doi:10.1111/j.1529-8817.2010.00815.x.
- Hallegraeff, G.M., Anderson, D.M., Belin, C., Bottein, M.Y.D., Bresnan, E., Chinain, M., Enevoldsen, H., Iwataki, M., Karlson, B., McKenzie, C.H., Sunesen, I., Pitcher, G.C., Provoost, P., Richardson, A., Schweibold, L., Tester, P.A., Trainer, V.L., Yñiguez, A.T., Zingone, A., 2021b. Perceived global increase in algal blooms is attributable to intensified monitoring and emerging bloom impacts. *Communications Earth & Environment* 2. doi:10.1038/s43247-021-00178-8.
- HELCOM, 2012. Manual for Marine Monitoring in the COMBINE Programme of HELCOM. Technical Report. Helsinki Commission - Baltic Marine Environment Protection Commission.
- HELCOM, 2013. Climate change in the Baltic Sea Area HELCOM thematic assessment in 2013. Technical Report. Helsinki Commission - Baltic Marine Environment Protection Commission.
- HELCOM/Baltic Earth, 2021. Climate Change in the Baltic Sea. 2021 Fact Sheet. Technical Report. Helsinki Commission – HELCOM.

References

- Henson, S.A., Dunne, J.P., Sarmiento, J.L., 2009. Decadal variability in North Atlantic phytoplankton blooms. *Journal of Geophysical Research: Oceans* 114, 1–11. doi:10.1029/2008JC005139.
- Huisman, J., Codd, G.A., Paerl, H.W., Ibelings, B.W., Verspagen, J.M., Visser, P.M., 2018. Cyanobacterial blooms. *Nature Reviews Microbiology* 16, 471–483. doi:10.1038/s41579-018-0040-1.
- Ianora, A., Miralto, A., Poulet, S.A., Carotenuto, Y., Buttino, I., Romano, G., Casotti, R., Pohnert, G., Wichard, T., Colucci-D'Amato, L., Terrazzano, G., Smetacek, V., 2004. Aldehyde suppression of copepod recruitment in blooms of a ubiquitous planktonic diatom. *Nature* 429, 403–407. doi:10.1038/nature02526.
- IPCC, 2019. IPCC Special Report on the Ocean and Cryosphere in a Changing Climate. of the Intergovernmental Panel on Climate Change. Technical Report.
- Janssen, F., Neumann, T., Schmidt, M., 2004. Inter-annual variability in cyanobacteria blooms in the Baltic Sea controlled by wintertime hydrographic conditions. *Marine Ecology Progress Series* 275, 59–68. doi:10.3354/meps275059.
- Ji, R., Davis, C.S., Chen, C., Townsend, D.W., Mountain, D.G., Beardsley, R.C., 2007. Influence of ocean freshening on shelf phytoplankton dynamics. *Geophysical Research Letters* 34, 1–5. doi:10.1029/2007GL032010.
- Ji, R., Edwards, M., MacKas, D.L., Runge, J.A., Thomas, A.C., 2010. Marine plankton phenology and life history in a changing climate: current research and future directions. *Journal of Plankton Research* 32, 1355–1368. doi:10.1093/plankt/fbq062.
- Kahru, M., Elmgren, R., 2014. Multidecadal time series of satellite-detected accumulations of cyanobacteria in the Baltic Sea. *Biogeosciences* 11, 3619–3633. doi:10.5194/bg-11-3619-2014.
- Kahru, M., Elmgren, R., Kaiser, J., Wasmund, N., Savchuk, O., 2020. Cyanobacterial blooms in the Baltic Sea: Correlations with environmental factors. *Harmful Algae* 92, 101739. doi:10.1016/j.hal.2019.101739.
- Kahru, M., Elmgren, R., Savchuk, O.P., 2016. Changing seasonality of the Baltic Sea. *Biogeosciences* 13, 1009–1018. doi:10.5194/bg-13-1009-2016.
- Kahru, M., Horstmann, U., Rud, O., 1994. Satellite detection of increased cyanobacterial blooms in the Baltic Sea: natural fluctuation or ecosystem change? *Ambio* 23, 469–472.

- Kaiser, J., Wasmund, N., Kahru, M., Wittenborn, A.K., Hansen, R., Häusler, K., Moros, M., Schulz-Bull, D., Arz, H.W., 2020. Reconstructing N₂-fixing cyanobacterial blooms in the Baltic Sea beyond observations using 6- and 7-methylheptadecane in sediments as specific biomarkers. *Biogeosciences* doi:10.5194/bg-17-2579-2020.
- Kalnay, E., Kanamitsu, M., Kistler, R., Collins, W., Deaven, D., Gandin, L., Iredell, M., Saha, S., White, G., Woollen, J., Zhu, Y., Chelliah, M., Ebisuzaki, W., Higgins, W., Janowiak, J., Mo, K.C., Ropelewski, C., Wang, J., Leetmaa, A., Reynolds, R., Jenne, R., Joseph, D., 1996. The NCEP/NCAR 40-Year Reanalysis Project. *Bulletin of the American Meteorological Society* 77, 437–472. doi:10.1175/1520-0477(1996)077<0437:TNYRP>2.0.CO;2.
- Kanoshina, I., Lips, U., Leppänen, J.M., 2003. The influence of weather conditions (temperature and wind) on cyanobacterial bloom development in the Gulf of Finland (Baltic Sea). *Harmful Algae* 2, 29–41. doi:10.1016/S1568-9883(02)00085-9.
- Kendall, M., 1975. *Multivariate analysis*. Charles Griffin & Co, London.
- Klais, R., Tamminen, T., Kremp, A., Spilling, K., Olli, K., 2011. Decadal-scale changes of Dinoflagellates and Diatoms in the Anomalous Baltic Sea spring bloom. *PLoS ONE* 6, 10. doi:10.1371/journal.pone.0021567.
- Koeller, P., Fuentes-Yaco, C., Platt, T., Sathyendranath, S., Richards, A., Ouellet, P., Orr, D., Skúladóttir, U., Wieland, K., Savard, L., Aschan, M., 2009. Basin-scale coherence in phenology of shrimps and phytoplankton in the North Atlantic Ocean. *Science* 324, 791–793. doi:10.1126/science.1170987.
- Kownacka, J., Busch, S., Göbel, J., Gromisz, S., Hällfors, H., Högländer, H., Huseby, S., Jaanus, A., Jakobsen, H., Johansen, M., Johansson, M., Jurgensone, I., Kraśniewski, W., Lehtinen, S., Olenina, I., V.Weber, M., Wasmund, N., 2018. Cyanobacteria biomass 1990-2018. HELCOM Baltic Sea Environment Fact Sheets 2018.
- Kremling, K., Lentz, U., Zeitzschel, B., Schulz-Bull, D.E., Duinker, J.C., 1996. New type of time-series sediment trap for the reliable collection of inorganic and organic trace chemical substances. *Review of Scientific Instruments* 67, 4360–4363. doi:10.1063/1.1147582.
- Kudela, R.M., Cochlan, W.P., Peterson, T.D., Trick, C.G., 2006. Impacts on phytoplankton biomass and productivity in the Pacific Northwest during the warm ocean conditions of 2005. *Geophysical Research Letters* 33, 1–6. doi:10.1029/2006GL026772.

References

- Lalonde, S.V., Konhauser, K.O., 2015. Benthic perspective on Earth's oldest evidence for oxygenic photosynthesis. *Proceedings of the National Academy of Sciences of the United States of America* 112, 995–1000. doi:10.1073/pnas.1415718112.
- Larsson, U., Elmgren, R., Wulff, F., 1985. Eutrophication and the Baltic Sea: causes and consequences. *AMBIO* 14.
- Legendre, L., 1990. The significance of microalgal blooms for fisheries and for the export of particulate organic carbon in oceans. *Journal of Plankton Research* 12, 681–699. doi:10.1093/plankt/12.4.681.
- Leipe, T., Harff, J., Meyer, M., Hille, S., Pollehne, F., Schneider, R., Kowalski, N., Brüggmann, L., 2008. Sedimentary Records of Environmental Changes and Anthropogenic Impacts during the Past Decades, in: *State and Evolution of the Baltic Sea, 1952-2005: A Detailed 50-Year Survey of Meteorology and Climate, Physics, Chemistry, Biology, and Marine Environment*. John Wiley & Sons, Ltd. chapter 14, pp. 395–439. doi:10.1002/9780470283134.CH14.
- Mackas, D.L., Batten, S., Trudel, M., 2007. Effects on zooplankton of a warmer ocean: Recent evidence from the Northeast Pacific. *Progress in Oceanography* 75, 223–252. doi:10.1016/j.pocean.2007.08.010.
- Margalef, R., 1978. Life-forms of phytoplankton as survival alternatives in an unstable environment. *Oceanologica Acta* 1, 493–509. doi:10.1007/BF00202661.
- Meier, H.E., Dieterich, C., Eilola, K., Gröger, M., Höglund, A., Radtke, H., Saraiva, S., Wählström, I., 2019. Future projections of record-breaking sea surface temperature and cyanobacteria bloom events in the Baltic Sea. *Ambio* 48, 1362–1376. doi:10.1007/s13280-019-01235-5.
- Meyer-Harms, B., Reckermann, M., Voss, M., Siegmund, H., Von Bodungen, B., 1999. Food selection by calanoid copepods in the euphotic layer of the Gotland Sea (Baltic Proper) during mass occurrence of N₂-fixing cyanobacteria. *Marine Ecology Progress Series* 191, 243–250. doi:10.3354/meps191243.
- Munkes, B., Löptien, U., Dietze, H., 2020. Cyanobacteria Blooms in the Baltic Sea: A Review of Models and Facts. *Biogeosciences Discussions* doi:10.5194/bg-2020-151.
- Neil, J.M.O., Davis, T.W., Burford, M.A., Gobler, C.J., 2012. The rise of harmful cyanobacteria blooms: The potential roles of eutrophication and climate change. *Harmful Algae* 14, 313–334. doi:10.1016/j.hal.2011.10.027.

- Nieuwenhuize, J., Maas, Y., Middelburg, J., 1994. Rapid analysis of organic carbon and nitrogen in particulate materials. *Marine Chemistry* 45, 217–224.
- Öberg, J., 2015. Cyanobacteria blooms in the Baltic Sea. Technical Report I.
- Okaichi, T., Nishio, S., 1976. Identification of ammonia as the toxic principle of red tide of *Noctiluca miliaris*. *Bulletin of Plankton Society of Japan* 23, 25–30.
- Olenina, I., Hajdu, S., Edler, L., Andersson, A., Wasmund, N., Busch, S., Göbel, J., Gromisz, S., Huseby, S., Huttunen, M., Jaanus, A., Kokkonen, P., Ledaine, I., Niemkiewicz, E., 2006. Biovolumes and Size-Classes of Phytoplankton in the Baltic Sea. *HELCOM Balt.Sea Environ. Proc.* , 144.
- Paerl, H.W., 2014. Mitigating harmful cyanobacterial blooms in a human- and climatically-impacted world. *Life* 4, 988–1012. doi:10.3390/life4040988.
- Paerl, H.W., Hall, N.S., Calandrino, E.S., 2011. Controlling harmful cyanobacterial blooms in a world experiencing anthropogenic and climatic-induced change. *The Science of the total environment* 409, 1739–45. doi:10.1016/j.scitotenv.2011.02.001.
- Paerl, H.W., Huisman, J., 2009. Climate change: A catalyst for global expansion of harmful cyanobacterial blooms. *Environmental Microbiology Reports* 1, 27–37. doi:10.1111/j.1758-2229.2008.00004.x.
- Paerl, H.W., Otten, T.G., 2013. Harmful Cyanobacterial Blooms: Causes, Consequences, and Controls. *Microbial Ecology* 65, 995–1010. doi:10.1007/s00248-012-0159-y.
- Paerl, H.W., Otten, T.G., Kudela, R., 2018. Mitigating the Expansion of Harmful Algal Blooms Across the Freshwater-to-Marine Continuum. *Environmental Science and Technology* 52, 5519–5529. doi:10.1021/acs.est.7b05950.
- Paerl, H.W., Paul, V.J., 2012. Climate change: Links to global expansion of harmful cyanobacteria. *Water Research* 46, 1349–1363. doi:10.1016/j.watres.2011.08.002.
- Parmesan, C., 2006. Ecological and evolutionary responses to recent climate change. *Annual Review of Ecology, Evolution, and Systematics* 37, 637–669. doi:10.1146/annurev.ecolsys.37.091305.110100.
- Peperzak, L., Duin, R.N., Colijn, F., Gieskes, W.W., 2000. Growth and mortality of flagellates and non-flagellate cells of *Phaeocystis globosa* (Prymnesiophyceae). *Journal of Plankton Research* 22, 107–119. doi:10.1093/plankt/22.1.107.

References

- Pitcher, G.C., Probyn, T.A., 2011. Anoxia in southern Benguela during the autumn of 2009 and its linkage to a bloom of the dinoflagellate *Ceratium balechii*. *Harmful Algae* 11, 23–32. doi:10.1016/j.hal.2011.07.001.
- Pizarro, G., Paz, B., González-Gil, S., Franco, J.M., Reguera, B., 2009. Seasonal variability of lipophilic toxins during a *Dinophysis acuta* bloom in Western Iberia: Differences between picked cells and plankton concentrates. *Harmful Algae* 8, 926–937. doi:10.1016/j.hal.2009.05.004.
- Pörtner, H.O., Farrell, A.P., 2008. Physiology and Climate Change. *Science* , 690–692doi:10.1126/science.1163156.
- Rahmstorf, S., 1990. An oceanic mixing model : application to global climate and to the New Zealand West Coast. Ph.D. thesis. Victoria University.
- Sarmiento, J.L., Slater, R., Barber, R., Bopp, L., Doney, S.C., Hirst, A.C., Kleypas, J., Matear, R., Mikolajewicz, U., Monfray, P., Soldatov, V., Spall, S.A., Stouffer, R., 2004. Response of ocean ecosystems to climate warming. *Global Biogeochemical Cycles* 18. doi:10.1029/2003GB002134.
- Satta, C.T., Pulina, S., Padedda, B.M., Penna, A., Sechi, N., Lugliè, A., 2010. Water discoloration events caused by the harmful dinoflagellate *Alexandrium taylorii* Balech in a new beach of the Western Mediterranean Sea (Platamona beach, North Sardinia). *Italian Association of Oceanography and Limnology* 1, 259–269. doi:10.1080/19475721.2010.528947.
- Scharfe, M., Wiltshire, K.H., 2019. Modeling of intra-annual abundance distributions: Constancy and variation in the phenology of marine phytoplankton species over five decades at Helgoland Roads (North Sea). *Ecological Modelling* 404, 46–60. doi:10.1016/j.ecolmodel.2019.01.001.
- Schneider, B., Dellwig, O., Kuliński, K., Omstedt, A., Pollehne, F., Rehder, G., Savchuk, O., 2017. Biogeochemical cycles, in: Snoeijs-Leijonmalm, P., Schubert, H., Radziejewska, T. (Eds.), *Biological Oceanography of the Baltic Sea*. Springer, Dordrecht. chapter 3, pp. 87–122. doi:10.1007/978-94-007-0668-2_3/COVER.
- Schneider, B., Müller, J.D., 2018. The Main Hydrographic Characteristics of the Baltic Sea, in: *Springer Oceanography* (Ed.), *Biogeochemical Transformations in the Baltic Sea*. Springer, Cham, pp. 35–41. doi:10.1007/978-3-319-61699-5_3.

- Schneider, B., Nagel, K., Struck, U., 2000. Carbon fluxes across the halocline in the eastern Gotland Sea. *Journal of Marine Systems* 25, 261–268. doi:10.1016/S0924-7963(00)00020-8.
- Sen, P.K., 1968. Estimates of the Regression Coefficient Based on Kendall's Tau. *Journal of the American Statistical Association* 63, 1379–1389. doi:10.1080/01621459.1968.10480934.
- Sharples, J., Ross, O.N., Scott, B.E., Greenstreet, S.P., Fraser, H., 2006. Inter-annual variability in the timing of stratification and the spring bloom in the North-western North Sea. *Continental Shelf Research* 26, 733–751. doi:10.1016/j.csr.2006.01.011.
- Simon, N., Cras, A.L., Foulon, E., Lemée, R., 2009. Diversity and evolution of marine phytoplankton. *Comptes Rendus - Biologies* 332, 159–170. doi:10.1016/j.crv.2008.09.009.
- Smayda, T.J., Reynolds, C.S., 2001. Community assembly in marine phytoplankton: Application of recent models to harmful dinoflagellate blooms. *Journal of Plankton Research* 23, 447–461. doi:10.1093/plankt/23.5.447.
- Smith, S.V., Hollibaugh, J.T., 1993. Coastal metabolism and the oceanic organic carbon balance. *Reviews of Geophysics* 31, 75–89. doi:10.1029/92RG02584.
- SØreide, J.E., Leu, E.V., Berge, J., Graeve, M., Falk-Petersen, S., 2010. Timing of blooms, algal food quality and *Calanus glacialis* reproduction and growth in a changing Arctic. *Global Change Biology* 16, 3154–3163. doi:10.1111/j.1365-2486.2010.02175.x.
- Spilling, K., Olli, K., Lehtoranta, J., Kremp, A., Tedesco, L., Tamelander, T., Klais, R., Peltonen, H., Tamminen, T., 2018. Shifting diatom-dinoflagellate dominance during spring bloom in the Baltic Sea and its potential effects on biogeochemical cycling. *Frontiers in Marine Science* 5, 1–17. doi:10.3389/fmars.2018.00327.
- Suikkanen, S., Kaartokallio, H., Hällfors, S., Huttunen, M., Laamanen, M., 2010. Life cycle strategies of bloom-forming, filamentous cyanobacteria in the Baltic Sea. *Deep-Sea Research Part II: Topical Studies in Oceanography* doi:10.1016/j.dsr2.2009.09.014.
- Suikkanen, S., Pulina, S., Engström-Öst, J., Lehtiniemi, M., Lehtinen, S., Brutemark, A., 2013. Climate Change and Eutrophication Induced Shifts in Northern Summer Plankton Communities. *PLoS ONE* 8. doi:10.1371/journal.pone.0066475.

References

- Sundqvist, L., Godhe, A., Jonsson, P.R., Sefbom, J., 2018. The anchoring effect—long-term dormancy and genetic population structure. *ISME Journal* 12, 2929–2941. doi:10.1038/s41396-018-0216-8.
- Sverdrup, H.U., 1953. On conditions for the vernal blooming of phytoplankton. *ICES Journal of Marine Science* 18, 287–295. doi:10.1093/icesjms/18.3.287.
- Tagmouti-Talha, F., Chafak, H., Fellat-Zarrouk, K., Talbi, M., Blaghen, M., Mikou, A., Guittet, E., 1996. Detection of toxins in bivalves on the Moroccan coasts, in: Yasumoto, T., Oshima, T., Fukuyo, Y. (Eds.), *Harmful and Toxic Algal Blooms. Proceedings of the 7th International Conference on Toxic Phytoplankton.. Intergovernmental Oceanographic Commission of UNESCO, Sendai, Japan*, pp. 85–87.
- Thomas, A.C., Brickley, P., 2006. Satellite measurements of chlorophyll distribution during spring 2005 in the California current. *Geophysical Research Letters* 33, 1–5. doi:10.1029/2006GL026588.
- Utermöhl, H., 1958. Zur Vervollkommnung der quantitativen Phytoplankton-Methodik. *Internationale Vereinigung für Theoretische und Angewandte Limnologie* 9, 1–38. doi:10.1080/05384680.1958.11904091.
- Vahtera, E., Conley, D.J., Gustafsson, B.G., Kuosa, H., Pitkänen, H., Savchuk, O.P., Tamminen, T., Viitasalo, M., Voss, M., Wasmund, N., Wulff, F., 2007. Internal Ecosystem Feedbacks Enhance Nitrogen-fixing Cyanobacteria Blooms and Complicate Management in the Baltic Sea. *Ambio* 36, 186–194. doi:10.1579/0044-7447(2007)36[186:IEFENC]2.0.CO;2.
- Walve, J., Larsson, U., 2010. Seasonal changes in Baltic Sea seston stoichiometry: The influence of diazotrophic cyanobacteria. *Marine Ecology Progress Series* 407, 13–25. doi:10.3354/meps08551.
- Waniek, J.J., 2003. The role of physical forcing in initiation of spring blooms in the northeast Atlantic. *Journal of Marine Systems* 39, 57–82. doi:10.1016/S0924-7963(02)00248-8.
- Wasmund, N., 1997. Occurrence of cyanobacterial blooms in the Baltic Sea in relation to environmental conditions. *Internationale Revue der gesamten Hydrobiologie und Hydrographie* 82, 169–184. doi:10.1002/iroh.19970820205.
- Wasmund, N., Alheit, J., Pollehne, F., Siegel, H., Zettler, M.L., 1998. Ergebnisse des Biologischen Monitorings der Ostsee im Jahre 1997 im Vergleich mit bisherigen Untersuchungen. Technical Report 32. Institut für Ostseeforschung Warnemünde.

-
- Wasmund, N., Tuimala, J., Suikkanen, S., Vandepitte, L., Kraberg, A., 2011. Long-term trends in phytoplankton composition in the western and central Baltic Sea. *Journal of Marine Systems* 87, 145–159. doi:10.1016/j.jmarsys.2011.03.010.
- Wasmund, N., Uhlig, S., 2003. Phytoplankton trends in the Baltic Sea. *ICES Journal of Marine Science* 60, 177–186. doi:10.1016/S1054-3139(02)00280-1.
- Wells, M.L., Karlson, B., Wulff, A., Kudela, R., Trick, C., Asnaghi, V., Berdalet, E., Cochlan, W., Davidson, K., De Rijcke, M., Dutkiewicz, S., Hallegraeff, G., Flynn, K.J., Legrand, C., Paerl, H., Silke, J., Suikkanen, S., Thompson, P., Trainer, V.L., 2020. Future HAB science: Directions and challenges in a changing climate. *Harmful Algae* 91. doi:10.1016/j.hal.2019.101632.
- Winder, M., Schindler, D.E., 2004. Climate change uncouples trophic interactions in an aquatic ecosystem. *Ecology* 85, 2100–2106. doi:10.1890/04-0151.
- Zingone, A., Escalera, L., Bresnan, E., Enevoldsen, H., Provoost, P., Anthony J. Richardson, G.H., 2022. Databases for the study of harmful algae, their global distribution and their trends, in: *Guidelines for the study of climate change effects on HAB*. chapter 5, pp. 79–103.
- Zingone, A., Wyatt, T., 2004. Harmful algal blooms: keys to the understanding of the phytoplankton ecology. volume 13.
- Zohdi, E., Abbaspour, M., 2019. Harmful algal blooms (red tide): a review of causes, impacts and approaches to monitoring and prediction. *International Journal of Environmental Science and Technology* 16, 1789–1806. doi:10.1007/s13762-018-2108-x.

6 Contributions to manuscripts

Publication I

Beltran-Perez, O.D., Waniek, J.J., 2021. Environmental window of cyanobacteria bloom occurrence. *Journal of Marine Systems*. 224, 103618. doi:10.1016/j.jmarsys.2021.103618.

O. Beltran-Perez and J.J. Waniek contributed to the conception of the study. J.J. Waniek supervised the study and O. Beltran-Perez compiled data, carried out the data analysis, produced the figures and wrote the manuscript. O. Beltran-Perez and J.J. Waniek contributed to the interpretation and discussion of the results and edition of the manuscript. Both authors have read and approved the manuscript for publication. Contribution to this study by O. Beltran-Perez of approximately 80%.

Publication II

Beltran-Perez, O.D., Waniek, J.J., 2022. Inter-annual variability of spring and summer blooms in the eastern Baltic Sea. *Frontiers in Marine Science*. doi:10.3389/fmars.2022.928633.

O. Beltran-Perez and J.J. Waniek contributed to the conception of the study. J.J. Waniek provided the initial version of the model and supervised the study. O. Beltran-Perez extended the model to other phytoplankton species, calibrated and validated the model results, analyzed the data, produced the figures and wrote the manuscript. O. Beltran-Perez and J.J. Waniek contributed to the interpretation of results, the discussion and subsequent edits of the manuscript. Both authors have read and approved the manuscript for publication. Contribution to this study by O. Beltran-Perez of approximately 75%.

Publication III

Beltran-Perez, O.D., Voss, M., Pollehne, F., Liskow, I., Waniek, J.J., 2023. Temporal variability of particle flux in the Gotland Basin, eastern Baltic Sea. *Frontiers in Earth Science*. Special issue on "The Oceanic Particle Flux and its Cycling Within the Deep Water Column-Volume II". doi.org/10.3389/feart.2023.1171917.

F. Pollehne provided the bulk parameters of the sediment trap data set. M. Voss and I. Liskow provided the isotope data, M. Voss also contributed to their interpretation and discussion. J.J. Waniek supervised all data analyses and interpretation of results. O. Beltran-Perez explored, harmonized and analyzed the data, prepared the figures and wrote the manuscript. All authors have read and approved the manuscript for publication. Contribution to this study by O. Beltran-Perez of approximately 75%.



Contents lists available at ScienceDirect

Journal of Marine Systems

journal homepage: www.elsevier.com/locate/jmarsys

Environmental window of cyanobacteria bloom occurrence

Oscar Dario Beltran-Perez^{*}, Joanna J. Waniek

Leibniz Institute for Baltic Sea Research Warnemünde, Seestraße 15, 18119 Rostock, Germany

ARTICLE INFO

Keywords:

Cyanobacteria
Bloom
Phenology
Driving conditions
Stage
Baltic Sea

ABSTRACT

Summer cyanobacteria blooms regularly occur in the Baltic Sea. The phenology of the bloom, however, is mostly unknown. Data of total biomass of the bloom-forming species *Nodularia spumigena*, *Aphanizomenon sp.* and *Dolichospermum spp.*, water column variables, nutrients and weather conditions were used to study and define the phenology and optimum environmental window for the occurrence of cyanobacteria blooms in the Gotland Basin during the period 1990–2017. The intra-annual variability of cyanobacteria biomass was modeled using a Weibull function and a partial least squares regression was used to define the variables that explain the timing of the onset, peak and decline stages of the bloom. On average blooms lasted 41 ± 16 days, starting in mid-June, reaching the maximum of observed biomass by mid-July and ending by the end of July with a total biomass in the three stages of 79, 353 and $161 \mu\text{g L}^{-1}$, respectively. The timing of the onset of the bloom was driven by sea surface temperature ($14 \text{ }^\circ\text{C}$), air temperature ($14 \text{ }^\circ\text{C}$), outgoing long-wave radiation (-68 W m^{-2}), mixed layer depth (26 m), water column stability expressed as Brunt–Väisälä frequency (-0.02 s^{-2}), phosphate concentration (0.1 mmol m^{-3}) and wind speed (5 m s^{-1}). The time of maximum cyanobacteria biomass occurrence was controlled by sensible (41 W m^{-2}) and latent (-3 W m^{-2}) heat flux. The timing of the decline of the bloom was driven by incoming solar radiation (218 W m^{-2}), net heat flux (178 W m^{-2}), sensible heat flux (35 W m^{-2}), latent heat flux (-12 W m^{-2}) and phosphate concentration (0.1 mmol m^{-3}). If the bloom occurs early or lasts longer depends on the overall effect that these explanatory variables have on each stage of the bloom. The results show that the phenology of the bloom depends in part on the heat exchange that takes place between the water surface and the overlying atmosphere, however, heat flux components are rarely included in bloom-related studies. The results also show that the Weibull function and the optimum environmental window can be used as an approach to define the phenology of a bloom and the environmental conditions that favor it.

1. Introduction

Cyanobacteria are naturally present and not inherently problematic in aquatic systems (Bianchi et al., 2000; Whitton and Potts, 2000). They provide ecosystem services, particularly as biogeochemical mediators of nitrogen and phosphorus (Codd et al., 2005). In general, the rapid increase of phytoplankton biomass and accumulation in the water column is known as a bloom. Cyanobacteria are special in that they form dense, visible blooms at the surface (Wasmund, 1997). Studies of pigments in Baltic Sea sediments indicate that blooms of filamentous cyanobacteria are as ancient as the present brackish water phase of the Baltic Sea (Bianchi et al., 2000). These studies have also shown an increase in intensity of cyanobacteria blooms in the Baltic Sea since the 1960s (Poutanen and Nikkilä, 2001), coinciding with increasing eutrophication (Finni et al., 2001) and warmer climate conditions (Kahru et al., 1994; Kanoshina et al., 2003; Stal et al., 2003; Lips and Lips, 2008). The most abundant cyanobacteria species are the

heterocystous species *Nodularia spumigena*, *Aphanizomenon sp.* and the species *Dolichospermum spp.* formerly known as *Anabaena* (Wasmund, 1997; Lips and Lips, 2008).

Cyanobacteria blooms give rise to environmental concern due to their ability to fix molecular nitrogen from the atmosphere accelerating eutrophication and oxygen depletion in deep waters (Larsson et al., 1985; Wasmund, 1997; Janssen et al., 2004). Dense cyanobacteria blooms also increase the turbidity of water suppressing the establishment and growth of aquatic macrophytes and seagrass beds (Hall et al., 1999) and thereby disrupting food web and ecosystem dynamics for many invertebrates and fish species (Havens, 2008; Moore et al., 2008). As many cyanobacteria species may produce toxins (including hepatotoxins, neurotoxins, cytotoxins and dermatotoxins), cyanobacteria blooms are a major threat to fishing and recreational use of coastal waters (Paerl and Huisman, 2009; Neil et al., 2012).

^{*} Corresponding author.

E-mail address: oscar.beltran@io-warnemuende.de (O.D. Beltran-Perez).

<https://doi.org/10.1016/j.jmarsys.2021.103618>

Received 25 August 2020; Received in revised form 20 July 2021; Accepted 2 August 2021

Available online 16 August 2021

0924-7963/© 2021 Elsevier B.V. All rights reserved.

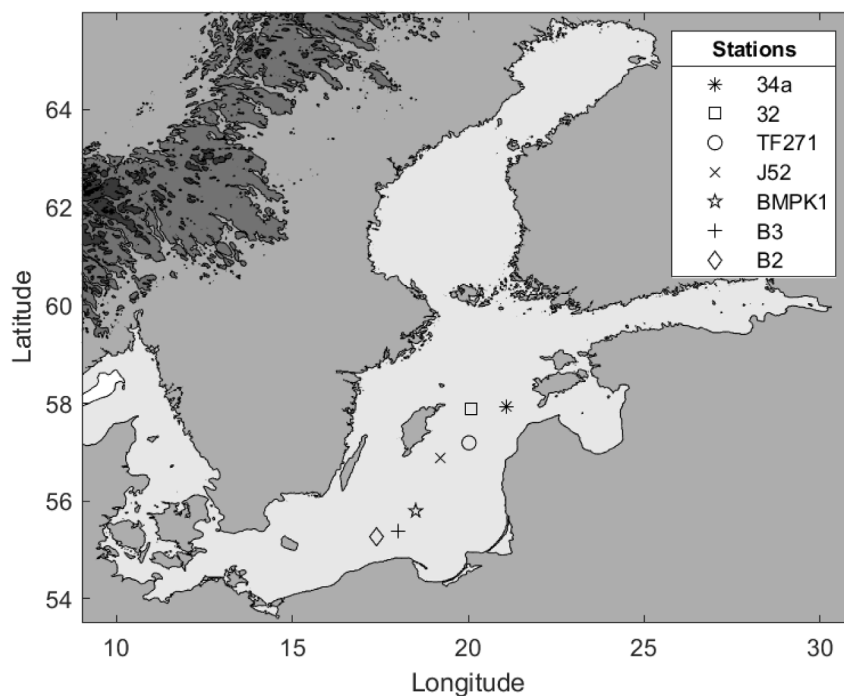


Fig. 1. Location of the phytoplankton monitoring stations in the study region.

An increase in the extent and intensity of cyanobacteria blooms during the last few decades was generally linked to eutrophication (Paerl, 1988; Chorus and Bartram, 1999; Janssen et al., 2004; Rönnerberg and Bonsdorff, 2004; Hudnell and Dortch, 2008). However, nowadays blooms of filamentous cyanobacteria are expected to be influenced by climate change, reaching higher intensities and lengths as a result of increased sea surface temperature (BACC, 2008; HELCOM, 2013). Projections for the Baltic Sea future show an accelerated warming, rising precipitation and land runoff of organic matter and pollutants as well as a reduction in salinity (Andersson et al., 2015). Another study projects the extension of periods with temperature above 18 °C by 10 to 30 days as well as the disappearance of record breaking cyanobacteria blooms because of the lower nutrient loads to the Baltic Sea (Meier et al., 2019). Under this scenario it is likely that cyanobacteria blooms will disappear in the future, however, how and when this will actually happen depends on the sensitivity of cyanobacteria blooms to changes in the environmental conditions.

Changes in the phenology of cyanobacteria blooms as a consequence of changing climate in the Baltic Sea have been already reported (Neumann et al., 2012; Kahru and Elmgren, 2014; Kahru et al., 2016). Kanoshina et al. (2003) defined water temperature as the main factor controlling the initiation of the bloom in the Baltic Sea, while vertical stratification seemed to influence the intensity of the bloom at species level and wind their spatial distribution. Kanoshina et al. (2003) also indicated that blooms at the surface are dispersed by wind speeds over 6 ms^{-1} . Wasmund (1997) suggested water temperature as the main trigger for the onset of a cyanobacteria bloom, whereas incoming solar radiation and wind speed determined the end of the bloom in the Baltic Sea. In addition, Kahru et al. (2020) found that inter-annual variations in the frequency of cyanobacteria surface accumulations are related to incoming solar radiation and sea surface temperature rather than biogeochemical variables using satellite data from the central Baltic Sea Proper.

While it is clear that summer cyanobacteria blooms regularly occur in the Baltic Sea and environmental conditions such as high water temperature, intense solar radiation and periods of weak wind speed may favor such blooms, the underlying causes and phenology of cyanobacteria blooms are still not well understood. Moreover, climate change is

expected to increase water temperature by 2 to 4 °C (HELCOM, 2013; Andersson et al., 2015) in the Baltic Sea favoring cyanobacteria dominance due to their competitive traits relative to other phytoplankton species (Carey et al., 2012). Therefore, a thorough understanding of the mechanisms driving cyanobacteria blooms must examine influences of a wide range of interacting biotic and abiotic factors in the context of a changing world (Downing et al., 2001; Paerl and Huisman, 2009; Paerl et al., 2011). In this sense, this study examines the role of environmental variables from both the water and the atmosphere on the occurrence of cyanobacteria blooms in the Gotland Basin. The variables studied are sea surface temperature (SST), air temperature (T_a), mixed layer depth (MLD), Brunt–Väisälä frequency (N^2), wind speed, weak wind period (WWP), incoming solar radiation (Q_{sw}), outgoing long-wave radiation (Q_{lw}), sensible heat flux (Q_h), latent heat flux (Q_l), net heat flux (Q_{net}), dissolved inorganic nitrogen (DIN) and phosphate (PO_4). Data collected on regular monitoring cruises in the Gotland Basin were used for this study. We hypothesize that sea surface temperature, net heat flux and wind speed define the phenology of the bloom and there is an optimum environmental window where a specific range of these variables trigger the development of cyanobacteria blooms in the Gotland Basin.

2. Methods

2.1. Study site

The Baltic Sea is a brackish, shallow (mean depth of 55 m), semi-enclosed sea with narrow connections to the North Sea, which results in a large seasonal temperature variation and salinity gradient in both north-south and east-west direction (Schneider and Müller, 2018). Spatial differences are also observed in seasonal cycles of biological and chemical variables of the water column, the weather and even in the distribution of phytoplankton blooms. This spatial heterogeneity leads to the need of studying the Baltic Sea basin by basin, each with its own complexity and particular characteristics (HELCOM, 2013; Öberg, 2015; Kownacka et al., 2018). Cyanobacteria blooms are frequent in the Baltic Sea, especially in the Gotland Basin, a sub-basin with a maximum depth of 249 m in the eastern Baltic Sea. We restrict our analyses to this basin, specifically to the station TF271 (Fig. 1) located

Table 1
Mean cyanobacteria biomass in June, July and August.
The number of samples is given in parentheses.

Year	Monthly mean [$\mu\text{g L}^{-1}$]		
	June	July	August
1990	–	252(2)	5(1)
1991	36(1)	627(4)	186(4)
1992	8(1)	781(3)	4(2)
1993	22(2)	–	186(9)
1994	–	–	626(8)
1995	127(4)	–	320(7)
1996	–	–	234(6)
1997	76(2)	–	636(11)
1998	57(2)	395(1)	84(8)
1999	199(2)	598(5)	281(6)
2000	34(2)	364(5)	143(5)
2001	64(2)	354(4)	58(7)
2002	51(3)	647(4)	169(5)
2003	27(2)	192(6)	53(5)
2004	37(3)	195(6)	558(5)
2005	60(3)	531(10)	247(4)
2006	213(6)	213(7)	181(14)
2007	33(1)	114(4)	91(10)
2008	318(3)	342(4)	54(9)
2009	66(3)	264(7)	74(10)
2010	12(2)	131(5)	69(6)
2011	8(2)	567(2)	88(12)
2012	38(2)	220(4)	66(4)
2013	23(3)	692(2)	38(8)
2014	105(5)	323(4)	89(7)
2015	56(4)	191(4)	118(1)
2016	351(3)	54(1)	141(5)
2017	123(3)	285(3)	72(2)

east of the Gotland Island at 57°19'12" N, 20°3'0" E. This station has been monitored since 1979 in the frame of the HELCOM phytoplankton monitoring program by the Leibniz Institute for Baltic Sea Research, Warnemünde (Germany), the Department of Marine Research of the Environmental Protection Agency (Lithuania), the Department of Ecology, Environment and Plant Sciences, Stockholm University (Sweden), the Institute of Meteorology and Water Management, Maritime Branch (Poland), the National Marine Fisheries Research Institute (Poland), the Finnish Environment Institute, Marine Research Centre (Finland) and the Swedish Meteorological and Hydrological Institute (Sweden).

2.2. Data sets

Cyanobacteria biomass and composition were determined by collecting and integrating water samples over 10 m depth at sampling station TF271 and complemented by nearby stations (Fig. 1), station-specific information is given in the HELCOM program documentation (HELCOM, 2012). Each water sample (250 mL) was preserved using 1 mL of acetic Lugol solution. The sedimentation of subsamples (25 mL) and the counting under an inverted microscope were carried out according to the method of Utermöhl (1958). Cyanobacteria biomass (wet weight) was calculated using conversion factors recommended by Olenina et al. (2006). A detailed description of the instruments, sampling procedures, methods and biomass conversion can be found in the guidelines of the HELCOM monitoring program (HELCOM, 2012).

While research efforts have been undertaken since the seventies of the last century, a regular monitoring of blooms started in 1990 (Wasmund, 1997). Thus, the period analyzed in this study covers the years from 1990 to 2017. The total cyanobacteria biomass was defined as the sum of biomass of the cyanobacteria species *N. spumigena*, *Aphanizomenon sp.* and *Dolichospermum spp.* (Table 1). The biomass of the three cyanobacteria species was combined due to the sparse number of counts for the individual species. It shall be noted that this approach leads to a simplification of the results.

The water temperature (T_w) was measured using a CTD (conductivity–temperature–depth) probe coupled with a rosette water sampler

(Table 2). Water temperature and salinity were used to calculate density and water column stability expressed as Brunt–Väisälä frequency (N^2), defined as $N^2 = \frac{-g}{\rho} * \frac{d\rho}{dz}$ where ρ , z and g correspond to density, depth and gravitational acceleration, respectively. The mixed layer depth (MLD) was calculated as the depth at which the density difference between the surface and the water column below $\Delta\rho(z) = \rho(z) - \rho(z_0)$ exceeds the threshold of 0.125 kg m^{-3} ; here $\rho(z_0)$ is the surface density used as reference calculated as the mean density between 0 and 10 m depth. Samples for ammonium, nitrate, nitrite and phosphate were taken every 5 m and analyzed by colorimetric methods according to the guidelines of the HELCOM monitoring program (HELCOM, 2012). Dissolved inorganic nitrogen (DIN) contains nitrate, nitrite and ammonium concentrations in the water. Average values in the water column were determined as the arithmetical average over the upper 10 m depth. Monthly averages were calculated over the period 1990–2017 only for variables that contain at least 2 observations per month (see Table S1 in the supplementary material). The analysis was focused on the time period between June and August as this is the time frame in which cyanobacteria blooms usually occur in the Gotland Basin.

Air temperature, wind speed and relative humidity were obtained from Östergarnsholm A station. Sea surface temperature, rainfall and cloud cover were collected respectively from Hoburg, Fårösund Ar A and Visby Flygplats stations. All stations are located on Gotland Island and were chosen based on the availability of continuous data over the period 1990–2017 (Table 2). Meteorological data were also complemented by incoming solar radiation data from the Warnemünde station of the German Weather Service (DWD), closest station with available and continuous solar radiation data since 1998. Missing data in daily time series were filled by linear interpolation. Monthly averages of all atmospheric variables were calculated over the study period. The outgoing long-wave radiation, sensible, latent and net heat flux were calculated and averaged by month from 1998 onwards following empirical equations (Table S2). In this study we use the notation where heat gain by the ocean is expressed using positive values and heat loss by the ocean is given by negative values of net heat flux and its components (incoming solar radiation, outgoing long-wave radiation, sensible and latent heat flux). The number of days with wind speed below 6 m s^{-1} was defined as the weak wind period (WWP), based on Kanoshina et al. (2003) who indicated that blooms at the surface are dispersed by wind speeds over $6\text{--}8 \text{ m s}^{-1}$.

Independent data sources were used to validate the ranges of explanatory variables at the stages of the bloom. These data sources include ERA-Interim daily reanalysis data (VAL1) and NCEP reanalysis data (VAL2), both for locations nearby the study area (Table 2). Furthermore, satellite images describing bloom developments in the Baltic Sea were used in order to validate the phenology of the bloom estimated with the Weibull function (Table 2). The images classify blooms according to a color scale: strong (red), weak (yellow) and uncertain (gray). Although it is not possible to compare the magnitude of the bloom between observations and satellite images due to incompatibility of scales, it is possible to follow the development of the bloom and verify the dates on which blooms occur.

2.3. Phenology model-based approach

The scarce biomass data describing cyanobacteria blooms in the Gotland Basin and their irregular sampling frequency (Fig. S1) make it necessary to use a model-based approach to describe changes in the phenology of the blooms. We applied a Weibull function following the method proposed by Rolinski et al. (2007), also implemented in other phenological studies of phytoplankton (Groetsch et al., 2016; Scharfe and Wiltshire, 2019). Weibull functions adapt to different distributions providing information on shape parameters while preserving the characteristics of the bloom (Scharfe and Wiltshire, 2019). If a Weibull function is fitted to a biomass curve, it allows the determination of the onset, peak and decline stages of the bloom. We applied the Weibull

Table 2

Data used in this study. Data were acquired from the Leibniz Institute for Baltic Sea Research Warnemünde (IOW), the Swedish Meteorological and Hydrological Institute (SMHI), the German Weather Service (DWD), the NOAA Physical Sciences Laboratory (PSL) and the European Centre for Medium-Range Weather Forecasts (ECMWF). *n* refers to the number of observations and VAL1 and VAL2 refer to the data sources used to validate the results.

Variable	<i>n</i>	Years	Resolution	Station/Area	Data source
Biomass	344	1990–2017	Discrete samples ^a	Gotland Basin	N. Wasmund, IOW, pers. communication https://sharkweb.smhi.se/hamta-data/ https://odin2.io-warnemuende.de/ https://sharkweb.smhi.se/hamta-data/
Water temp. (T_w)	583 ^b	1990–2017	Discrete samples	TF271	
NO_3	308 ^b	1990–2017			
NO_2	308 ^b	1990–2017			
NH_4	252 ^b	1990–2017			
PO_4	307 ^b	1990–2017			
SST	326	1990–2017	Monthly	Hoburg	https://www.smhi.se/data/oceanografi/ladda-ner-oceanografiska-observationer/#param=seatemperature,stations=all
Air temp. (T_a)	244	1995–2017		Östergarnsholm	
Wind speed	244	1995–2017		Östergarnsholm	
Relative humidity	244	1995–2017		Östergarnsholm	
Rainfall	268	1995–2017		Färösund Ar A	
Cloud cover	172	1990–2017		Visby Flygplats	
Q_{sw}	7062	1998–2017		Warnemünde	https://opendata.dwd.de/climate_environment/CDC/observations_germany/climate/daily/solar/algsituationen/1.121633 https://apps.ecmwf.int/datasets/data/interim-full-daily/levtype=sfc/ https://psl.noaa.gov/data/gridded/data.ncep.reanalysis.surfaceflux.html
Satellite images	1353	2002–2017	Daily ^a	Baltic Sea	
VAL1: SST, T_a , wind speed, Q_{sw} , Q_{lw} , Q_h , Q_l	10227	1990–2017	Daily	Model	https://apps.ecmwf.int/datasets/data/interim-full-daily/levtype=sfc/
VAL2: T_a , wind speed, Q_{sw} , Q_{lw} , Q_h , Q_l	10227	1990–2017	Daily	Model	https://psl.noaa.gov/data/gridded/data.ncep.reanalysis.surfaceflux.html

^aOnly between June and August.

^bObservations details in Table S1 in supplementary material.

function on cyanobacteria biomass observations between June and August (Table 1). The Weibull function with six parameters takes the form

$$w(t) = (p_4 + \exp(-(\frac{t}{p_5})^{p_6})) * (1 - p_1 * \exp(-(\frac{t}{p_2})^{p_3}))$$

Where t is time and p_1 to p_6 are fitting parameters describing increasing and decreasing branches of the curve and thresholds before and after a peak. First, the biomass data are scaled to the interval [0, 1] based on the maximum peak (y_{max}) and then the function parameters are determined by fitting a nonlinear regression of the function w to the scaled values. The goodness of the fit was estimated by the coefficient of determination (R^2) between the observation and the fitted curve. The phenological dates were then determined based on the fitted curve. All calculations were performed using the CDW (cardinal dates using Weibull curves) algorithm implemented in the R-package cardidates (Rolinski et al., 2018).

We determined the total biomass of a bloom based on its peak size, considering the onset and decline dates as thresholds because the increasing and decreasing branches of the fitted curve are asymmetric (Fig. 2). The onset and decline dates of a bloom were defined at the 10% quantile and 90% quantile of the integral of the fitted curve, before and after the peak, respectively. These quantiles were chosen because they include the period of the year in which the beginning and decline of the bloom are usually reported in the Baltic Sea, i.e. June and August. The length of the bloom was defined as the difference between the decline and onset dates of the bloom. We applied the Weibull function separately for each year and visually inspected the curve to ensure correct fitting and interpretation. Only years with at least 8 samples between June and August (Table 1) and fitted curves with a R^2 equal to or greater than 0.7 were included in the analysis.

2.4. Environmental window

An environmental window refers to a specific range of environmental conditions under which an optimum response of the system is reached while the effect of the constraint factors is minimized (Cury and Roy, 1989). The optimum environmental window was initially

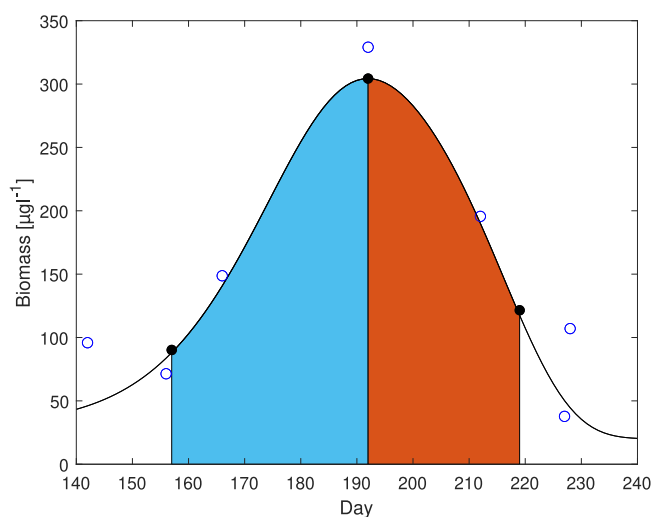


Fig. 2. Scheme of the modeling approach for the cyanobacteria bloom in 2017. Observations (open circles), onset (157), peak (192) and decline (219) days from left to right (black circles) and fitted Weibull function (line). The length of the bloom is indicated in blue from onset to peak and in orange from peak to decline.

developed for the analysis of fish recruitment (Cury and Roy, 1989; Roy, 1993), but nowadays it has also been applied for the occurrence of blooms (Díaz et al., 2016; Tobin et al., 2019).

Conditions in the water column such as low temperature, strong mixing, limited light availability and weak water column stability restrict the development of blooms keeping cells dispersed without bloom formation, as it is suggested in Fig. 3 before the onset of the bloom (t1). Under favoring conditions like calm weather, reduced mixing and increasing temperature, cells start to accumulate defining the onset of the bloom. In contrast, strong mixing conditions may delay or even suppress the bloom. Cells are growing and reproducing as long as favoring conditions are maintained. The bloom reaches maximum biomass when constraint conditions have the minimum effect (t2). After this point, the environmental conditions turn unfavorable for the bloom dissipating it and therefore reducing its biomass until background levels are reached (t3).

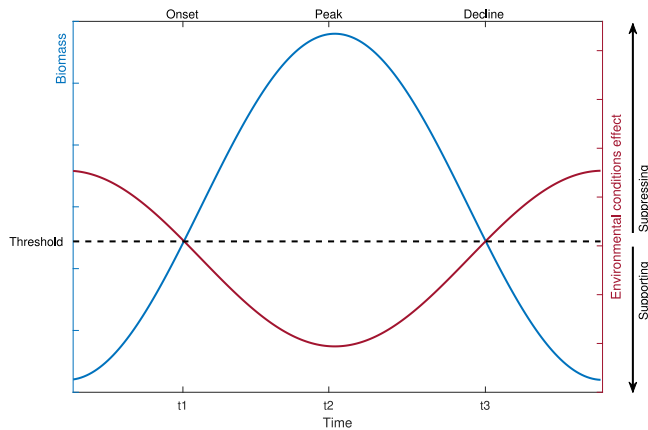


Fig. 3. Theoretical definition of an optimum environmental window based on the relationship between biomass and environmental conditions acting during each stage of the bloom.

2.5. Statistical analysis

A partial least squares regression (PLS) was performed between the phenological dates identified with the Weibull function and atmospheric variables (Q_{sw} , Q_{lw} , Q_{net} , Q_h , Q_l , T_a , wind speed, WWP), water column variables (SST , MLD , N^2) and nutrients (DIN , PO_4). PLS analysis describes variation in predictor and response variables by orthogonal scores and weighted factors, it is particularly useful when multi-collinearity exists among variables (Rosipal and Krämer, 2006). This method provides explanatory variables for the variation in the dependent variable as well as coefficients for the direction in which that influence is exerted. The variables for the analysis were normalized in order to make them comparable, i.e. each variable was centered to have a mean equal to zero and scaled to have standard deviation equal to 1. The analysis was run separately for the onset, peak and decline stages of the bloom using interpolated values of the environmental variables at the corresponding phenological dates.

The variable importance in projection (VIP) scores were used to select predictor variables from the PLS regression avoiding multi-collinearity. The VIP score of a variable is calculated as a weighted sum of the squared correlations between the PLS components and the original variable (Chong and Jun, 2005). The weights correspond to the percentage variation explained by the PLS components. Variables with a VIP score greater than 1 are considered explanatory variables for the timing of the bloom. The resulting variables were averaged and compared to observations in the corresponding phenological dates. All calculations and statistical analyses were performed in Matlab 2018b.

3. Results

3.1. Phenology of cyanobacteria blooms

The Weibull function was applied to each year of the 28-year biomass data set, however, it was only possible in 19 years to identify the phenology of the bloom. The mean R^2 of all fitted curves was 0.92 with a standard deviation of 0.08 (Table S3). The bloom in 2017 was chosen to illustrate the method (Fig. 2). Day 157 (June 6) represents the 10% quantile for the cyanobacteria bloom in 2017. After reaching the maximum biomass on day 192 (July 11), a rapid decline was observed resulting in the end of the bloom on day 219 (August 7) (90% quantile). This method identifies the onset and decline of the bloom based on the position of the peak and differences in biomass even with an irregular number of samples as in this study, which is an advantage of this method (Rolinski et al., 2007). The coefficients of the Weibull function

as well as the total biomass of the bloom for each fitted curve are presented in Table S3 in the supplementary material.

Based on the Weibull function results, on average the bloom started on day 168 (June 17) ± 16 days (± 16 refers to standard deviation) (Fig. 4A), reached the maximum observed biomass on day 193 (July 12) ± 14 (Fig. 4B) and declined after day 209 (July 28) ± 13 (Fig. 4C) with an average biomass in the three stages of 79, 353 and 161 $\mu\text{g L}^{-1}$, respectively. Thereby, bloom-forming species took around 25 ± 15 days to reach the maximum observed biomass (Fig. 5A) and then 16 ± 10 days to end the bloom (Fig. 5B). The mean length of the bloom has been estimated to be 41 ± 16 days (Fig. 5C). The longest blooms occurred in the summers of 1995, 2015 and 2017 with lengths of 81, 65 and 61 days, respectively, followed by summers in 2003 and 2008 both with lengths of around 50 days (Fig. 5C). The bloom in 1995 was the longest and strongest in biomass considering the time between the onset and peak of the bloom (Fig. 5A). However, short blooms can also have high biomass as for example in 2002 (Fig. 5B) and in 2002 and 2008 (Fig. 5C). Therefore, longest blooms are not necessarily the blooms with highest biomass.

Phenological dates were compared with daily satellite images taken over the Baltic Sea. The phenological dates were confirmed if the images report a strong or weak bloom event during the same date. For example, in 2013 the bloom started on June 22 according to the Weibull fit, reached the peak on July 14 and declined on July 27. Satellite images reported both weak and strong bloom accumulations in the eastern Baltic Sea at those dates. We consider it as a confirmation of the occurrence of the bloom and therefore of our results. In general, the onset, peak and decline dates identified with the Weibull function coincided with cyanobacteria blooms reported by satellite images in the Baltic Sea 43, 100 and 83% of the time, respectively. The images are available since 2002 and they allowed to confirm the onset, peak and decline dates of the bloom in 7, 12 and 12 years, respectively. Cloudy days reduced the satellite view of the water surface and therefore the availability of images.

3.2. Changes in environmental variables

Sea surface temperature increased from 14 °C in June to 17 °C in July reaching a maximum temperature of 18 °C by mid-August (Fig. 6A). The increase of water temperature coincided with the development of bloom-forming cyanobacteria. The bloom began when the water temperature was above 14 °C and reached its maximum biomass at 17 °C. The bloom declined when the water temperature was still close to 17 °C. Air temperature showed similar patterns as sea surface temperature (Fig. 6B). The maximum air temperature was reached at 17 °C by mid-August. The bloom started when the air temperature rose up to 14 °C and reached its maximum biomass at 17 °C. The bloom declined when air temperature was still at its maximum value, similarly to SST.

Incoming solar radiation increased from beginning of the year to mid-June, rising from a monthly mean of 176 W m^{-2} in April up to a maximum of 242 W m^{-2} in June (Fig. 6C). In the following period the incoming solar radiation slowly decreased until it reached roughly 129 W m^{-2} in September. The onset of the bloom fell together with the period of maximum incoming solar radiation, but the bloom continued growing as the incoming solar radiation reduced. The onset, peak and decline dates of the bloom were reached at 241, 227 and 210 W m^{-2} , respectively. Outgoing long-wave radiation decreased from -75 W m^{-2} in April to -64 W m^{-2} in July and increased again to -69 W m^{-2} in September (Fig. 6D). The peak of the bloom coincided with the weakest outgoing long-wave radiation in the consideration period, i.e. -64 W m^{-2} .

The net heat flux increased from 109 W m^{-2} in April to a maximum of 228 W m^{-2} by mid-June (Fig. 6E). It decreased during the rest of the summer period reaching -11 W m^{-2} by the middle of September. The bloom started near the maximum net heat flux and continued to

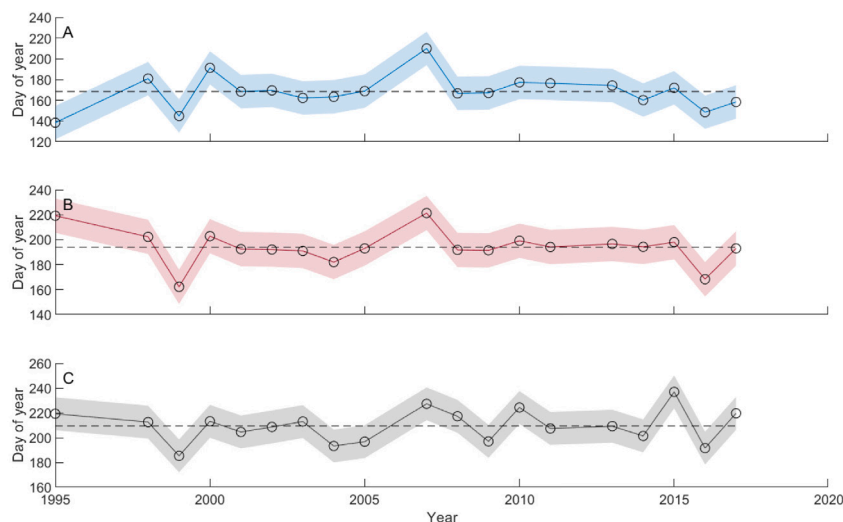


Fig. 4. Timing of cyanobacteria bloom onset (A), peak (B) and decline (C). The dashed line corresponds to the mean timing day and the shaded area to standard deviation. For biomass details see Tables 1 and 2.

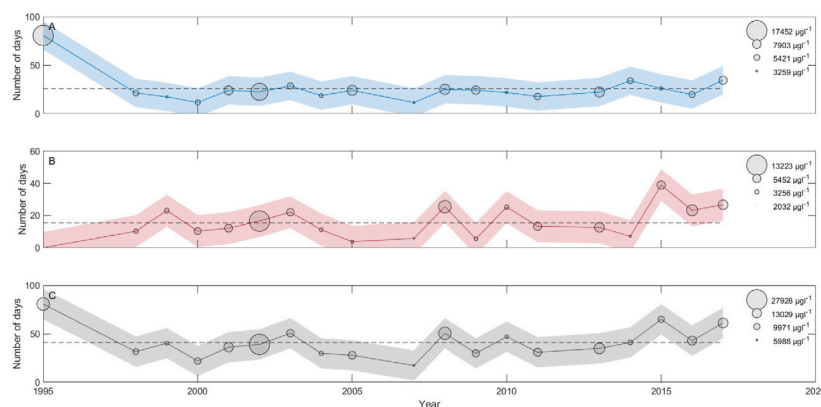


Fig. 5. Length of cyanobacteria bloom stages: (A) from onset to peak, (B) from peak to decline and (C) from onset to decline. The dashed line corresponds to the mean length and the shaded area to standard deviation. Circles represent total biomass of the blooms based on the size of their peaks (see Table S3). For biomass details see Tables 1 and 2.

grow, reaching its maximum biomass at 211 W m^{-2} . From this time on, both bloom and net heat flux gradually decreased. The sensible and latent heat flux showed small temporal changes throughout the development of the bloom (Fig. S2 in supplementary material). Wind speed remained below 6 m s^{-1} throughout the bloom period (Fig. 6F). Weak wind conditions continued during summer reaching 5.5 m s^{-1} by the middle of August and then 6.5 m s^{-1} by the middle of September when the bloom already finished.

The mixed layer depth became shallower from April, before the onset of the cyanobacteria bloom (Fig. 6G). The mixed layer depth changed from 30 m at the beginning of June to 14 m in July during the peak of the bloom. It reached 20 m at the beginning of September when the bloom has already finished. The bloom development (onset, peak and decline) coincided with a shallower mixed layer indicating a stratified water column. The bloom developed as the Brunt-Väisälä frequency increased, i.e. as the stratification of the water column became stronger, supporting the results obtained for the mixed layer depth (Fig. 6H). The bloom started at a Brunt-Väisälä frequency of -0.02 s^{-2} at the end of June and then it reached its peak at -0.03 s^{-2} in July. The bloom ended at a Brunt-Väisälä frequency of -0.03 s^{-2} by the middle of August.

The highest DIN concentration was found to be 0.6 mmol m^{-3} in early April, it decreased drastically to a concentration of 0.1 mmol m^{-3} in May just before the onset of the cyanobacteria bloom (Fig. 6I). DIN concentration remained at 0.1 mmol m^{-3} during the entire bloom. The

highest phosphate concentration was reached in April (0.4 mmol m^{-3}). The concentration decreased to 0.1 mmol m^{-3} before the onset of the bloom and it remained at this level over the entire bloom (Fig. 6J). The low concentrations of phosphate and DIN (both around 0.1 mmol m^{-3}) during the bloom suggest that such low nutrient concentrations in the water column do not prevent the bloom to occur and to evolve.

3.3. Effect of environmental variables on the phenology of the bloom

The PLS analysis indicated sea surface temperature, air temperature, outgoing long-wave radiation, mixed layer depth, Brunt-Väisälä frequency, wind speed and phosphate concentration as explanatory variables for the timing of the onset of the cyanobacteria bloom (Fig. 7A). Variables with a VIP score below 1 were considered collinear of the explanatory variables. The coefficients of the PLS regression determined in which sense each explanatory variable affects the phenological dates, i.e. if the changes in the explanatory variables lead to blooms appearing early or being delayed. SST, N^2 and wind speed had positive coefficients for the onset of the bloom (Fig. 7B), indicating that increases in these variables have a delaying effect on the onset of the bloom. The coefficients for T_a , Q_{lw} , MLD and PO_4 were negative, indicating that increases in these variables lead to an early occurrence of the bloom.

Sensible and latent heat flux had the highest VIP scores explaining the timing of the peak of the bloom (Fig. 7C). The coefficient for sensible heat flux was positive while the coefficient for latent heat flux

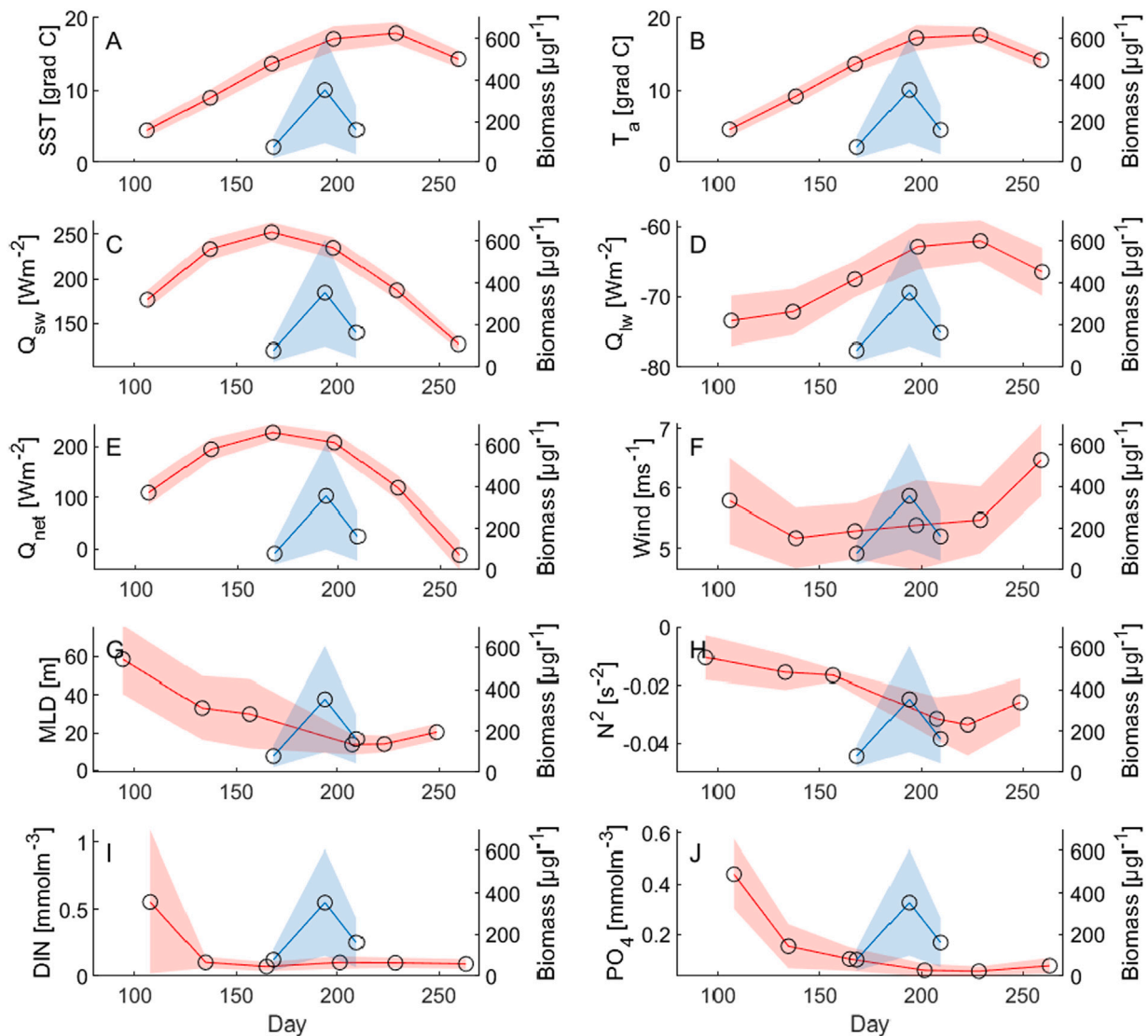


Fig. 6. Monthly averages of (A) sea surface temperature, (B) air temperature, (C) incoming solar radiation, (D) outgoing long-wave radiation, (E) net heat flux, (F) wind speed, (G) mixed layer depth, (H) Brunt-Väisälä frequency, (I) dissolved inorganic nitrogen and (J) phosphate. The red line corresponds to the variable (left axis) and the blue line to average total biomass (right axis). The shaded area corresponds to the standard deviation of each variable. Please note that monthly averages for incoming solar radiation and heat flux components were carried out from 1998 onwards, data sets details can be found in Table 2 and Table S1 in supplementary material.

was negative (Fig. 7D), i.e. increases in the latent heat flux lead to an early appearance of the peak while increases in sensible heat flux delay its appearance. Therefore, the heat exchange affects the timing at which the bloom reaches its maximum biomass.

Net heat flux components (Q_{sw} , Q_h , Q_l), net heat flux and phosphate concentration had the highest VIP scores explaining the timing of the decline of the bloom (Fig. 7E). With the exception of Q_{net} and Q_l , all other explanatory variables had negative coefficients in the regression model (Fig. 7F). This implies that increases in Q_{net} and Q_l extend the length of the bloom while increases in Q_{sw} , Q_h and PO_4 reduce it.

All explanatory variables were evaluated on the phenological dates using daily data sets compiled in VAL1 and VAL2 (Table 2) and the results were compared with the ranges given by the environmental window. The probability of finding the explanatory variables in the range of values indicated by the environmental window was calculated (Table 3). In general, the calculated probabilities were below 60% and differed between VAL1 and VAL2 with the exception of air temperature at the beginning of the bloom and latent heat flux at the peak of the bloom which showed some consistency with both data sets.

4. Discussion

4.1. Bloom timing

In the context of ongoing environmental changes, phenological studies provide a framework to identify changes in the development of blooms. This study provides insights of the phenology of cyanobacteria blooms in the Gotland Basin. We showed how a Weibull function can be used to model cyanobacteria biomass based on sparse and irregular data sets. Although detailed long-time series are expected for phenological studies, in most cases technical, financial and practical reasons restrict the number of samples to a few samples over a period of weeks or even months. In addition, the exact time at which the bloom begins is not known in advance. Therefore, there is no guarantee that the samples collected contain the information necessary to follow the evolution of the bloom. Here is where the model approach used comes into play. Our results provide a first approach to the phenology of cyanobacteria blooms using in-situ observations in combination with meteorological data from the eastern Baltic Sea. An approach that has not been carried out before and that provides substantial information

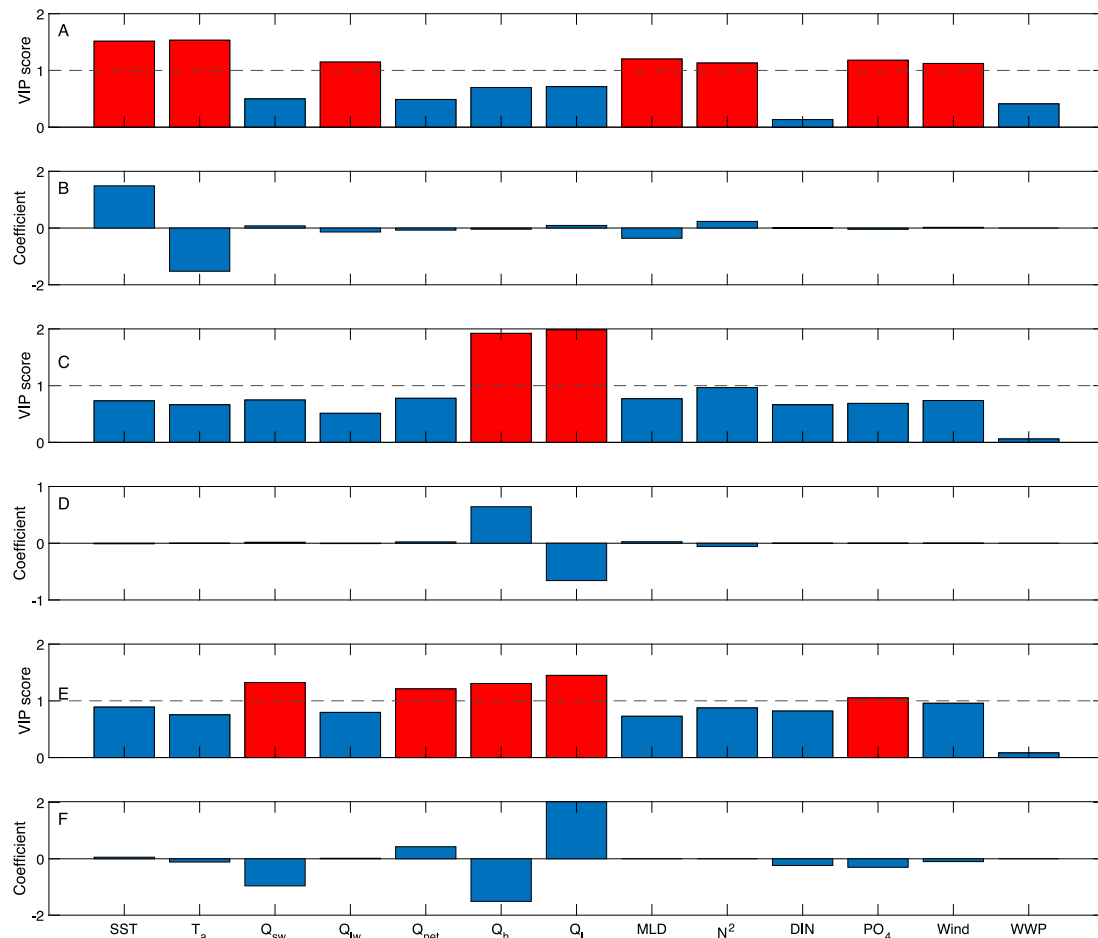


Fig. 7. Variable importance in projection (VIP) scores and regression coefficients for PLS regression model (A-B) onset, (C-D) peak and (E-F) decline. Variables with a VIP score greater than 1 are considered explanatory variables for the timing of the bloom (red bars). From left to right: sea surface temperature (*SST*), air temperature (*T_a*), incoming solar radiation (*Q_{sw}*), outgoing long-wave radiation (*Q_{lw}*), net heat flux (*Q_{net}*), sensible heat flux (*Q_h*), latent heat flux (*Q_l*), mixed layer depth (MLD), Brunt–Väisälä frequency (*N²*), dissolved inorganic nitrogen (DIN), phosphate (*PO₄*), wind speed and weak wind period (WWP).

Table 3

Validation of environmental conditions during phenological dates. *P* refers to the probability of finding the explanatory variables (from the PLS analysis) in the range of values obtained from the environmental window; *n* refers to the number of years used to calculate the probability and the dash represents explanatory variables for which no daily information is available to validate the defined ranges. VAL1 and VAL2 data sets details are reported in Table 2 and years analyzed in Table S3.

Variable	Stage	Mean ±SD	VAL1		VAL2	
			<i>P</i> (%)	<i>n</i>	<i>P</i> (%)	<i>n</i>
Sea surface temperature	Onset	14±1	53	19	–	19
Air temperature	Onset	14±1	58	19	53	19
Outgoing long-wave radiation	Onset	–68±7	0	19	37	19
Mixed layer depth	Onset	26±15	–	19	–	19
Brunt–Väisälä frequency	Onset	–0.02±0.003	–	19	–	19
Phosphate	Onset	0.1±0.05	–	19	–	19
Wind speed	Onset	5±1	53	19	32	19
Sensible heat flux	Peak	41±6	53	19	26	19
Latent heat flux	Peak	–3±9	11	19	11	19
Incoming solar radiation	Decline	218±11	0	19	63	19
Net heat flux	Decline	178±22	5	19	21	19
Sensible heat flux	Decline	35±7	74	19	47	19
Latent heat flux	Decline	–12±10	16	19	42	19
Phosphate	Decline	0.1±0.02	–	19	–	19

on the changes to which the bloom is subjected in a continuously changing environment.

The presence of cyanobacteria species of *N. spumigena*, *Aphanizomenon sp.* and *Dolichospermum spp.* has been regularly reported during

June, July and August in the eastern Baltic Sea. Although there is a wide variation in the biomass of surface accumulations of these cyanobacteria species in the water, they usually form blooms between mid-June and late July as it is observed in Fig. 4 and suggested by Kahru et al. (2020) in the central Baltic Sea Proper through satellite-derived time series. Öberg (2015) reported cyanobacteria blooms as seen in satellite images starting in the first week of July through August 25, 2015 in the eastern Gotland Basin, which means that the bloom has a length of about 55 days. This length is less than the 65 days estimated with the Weibull function for 2015. The average length of blooms in our study corresponded to 41 ± 16 days, a shorter length compared with other phytoplankton studies (Kahru et al., 2016; Wasmund et al., 2019).

The phenological dates of bloom occurrence were confirmed by daily satellite images taken over the Baltic Sea (Table 2). However, it has to be taken into account that blooms occurrence is subject to a strong variability in terms of magnitude and timing as observed in Figs. 4 and 5. A delay in blooms identified through satellite images may be expected as a result of the time it takes cells to accumulate and form visible blooms identifiable from satellite imagery. Comparison of observed onset dates with reported dates from satellite images coincided 43% of the time, in part possibly due to the delay in the formation of visible surface accumulations. The difference between phenological dates from observations and satellite images was reduced as blooms accumulate more cells in the water as shown by the percentages reported for the peak (100%) and decline of the bloom (83%). Satellite images are limited to surface accumulations, which in principle differs

from in-situ observations taken from different depths of the water column. This difference generates a discrepancy both in magnitude and timing when comparing results from both data sources. Additionally, the difference between our results and those from satellite images comes from the limitations of satellites measurements because of the cloud cover, mathematical algorithm and type of sensors used as on one side. On other side it results from the in-situ data coverage in space and time.

There are several phenological studies of cyanobacteria in lakes, seas and even in the Baltic Sea (Kahru et al., 2016; Zhang et al., 2018) using satellite techniques, but results vary greatly as there is no consensus on the metric for defining the bloom in addition to the difference between techniques. Kahru et al. (2016) defined phenological indicators based on a threshold value. Indeed, Kahru et al. (2016) studied frequency of cyanobacteria accumulations using satellite images and found that the period with chlorophyll a concentration higher than 3 mg m^{-3} was approximately 220 days in 2013, which is twice as high as the 110-day period estimated in 1998. In general, the differences between this study and our results are not surprising due to the periods, study sites and methods used. However, the study of Kahru et al. (2016) is the only one reporting the length of cyanobacteria blooms in the Baltic Sea.

Another reason for the difference between our results and other studies is linked to the cyanobacteria species studied. Kahru et al. (2016) studied only one species of cyanobacteria represented by *N. spumigena* while our study included three different species as a pooled variable. Considering an individual species or a group of species make a substantial difference in the phenology of the bloom. The bloom-forming cyanobacteria species have different life cycles and environmental preferences, which influence the timing, length and magnitude of the bloom from year to year. This makes the results of phenological studies vary greatly among species and even between regions as shown by Groetsch et al. (2016) and Scharfe and Wiltshire (2019) studying spring blooms in the Baltic Sea and the North Sea. In this sense, the combination of biomass of three different species as a pooled variable may be masking trends and shifts in the timing of the bloom in our results. Unfortunately, despite international efforts over many years a study of each species alone is still not possible.

4.2. Environmental forcing

The phenology of the bloom depends on different environmental conditions. It was found that the bloom begins when sea surface temperature is between 13 and 15 °C which is lower than the temperature reported by Wasmund (1997) of 16 °C for cyanobacteria blooms in the Baltic Sea. The reason for the onset of the bloom at a lower temperature is not clear, but may be linked to a change in the physiology of the bloom-forming species or the presence of early favorable conditions given by air temperature, outgoing long-wave radiation, mixed layer depth and phosphate concentration. Nevertheless, *Dolichospermum spp.*, *N. spumigena* and *Aphanizomenon sp.* are able to grow at temperatures above 10 °C (Nordin and Stein, 1980; Paerl and Otten, 2013; Cirés and Ballot, 2016). *N. spumigena* and *Dolichospermum spp.* have high temperature preference in comparison to *Aphanizomenon sp.* in the Baltic Sea (Lehtimäki et al., 1997; Suikkanen et al., 2010), with optimum growth rates for cyanobacteria species above 25 °C (Eigemann et al., 2018).

While several studies have highlighted the role of weather conditions in the development of blooms (Suikkanen et al., 2010; Wasmund et al., 2011; Kahru et al., 2020), often only incoming solar radiation is considered because it provides energy for the photosynthesis and growth of the bloom-forming species. Our results show that not only incoming solar radiation but also other heat flux components affect the occurrence of the bloom, favoring early or late blooms occurrence. The same applies to air temperature, which is usually left out in studies of this type, attributing blooms development only to changes in sea

surface temperature. Therefore, the heat exchange between the water surface and the overlying atmosphere and other variables such as air temperature and wind speed have to be taken into account when analyzing the phenology of cyanobacteria blooms. In fact, in our results incoming solar radiation is not an explanatory variable for the timing of the onset of the bloom, which is contrary to other studies where it is considered as one of the bloom triggers (Wasmund, 1997; Kahru et al., 2020).

Brunt-Väisälä frequency, mixed layer depth and wind speed are explanatory variables for the timing of the onset of the bloom (Table 3). These variables are directly associated with the stability of the water column. A stronger stratification creates a shallow mixed layer where cells accumulate and receive sufficient light for cell division and growth (critical depth hypothesis Sverdrup, 1953), as it was observed in the results (Fig. 6G-H) and previously reported in other studies (Reynolds, 1997; Kanoshina et al., 2003; Paerl and Huismann, 2009; Hjerne et al., 2019). In general, during blooms the wind speed did not exceed 6 m s^{-1} favoring the timing for the onset of the bloom as it was indicated by Kanoshina et al. (2003). It is particularly interesting that wind speed and not WWP affect the occurrence of the bloom since it is expected that prolonged calm conditions increase the water column stability and hence favor the bloom.

The maximum DIN (0.6 mmol m^{-3}) and phosphate (0.4 mmol m^{-3}) concentrations were observed in April before the onset of the bloom (Fig. 6I-J). Wasmund (1997) reported the occurrence of large cyanobacteria blooms of *N. spumigena* and *Aphanizomenon sp.* mostly at phosphate concentrations below 0.2 mmol m^{-3} and DIN concentrations around 0.3 mmol m^{-3} between 1979–1993 in the Baltic Sea Proper. Phosphate and DIN concentrations before cyanobacteria blooms may be linked to the release of soluble nitrogen and phosphorus by decomposed phytoplankton cells from the spring bloom, mainly composed of diatoms and dinoflagellates (Fallon and Brock, 1979; Wasmund et al., 2011). DIN and phosphate concentrations decreased to minimum values around 0.1 mmol m^{-3} before the bloom took place, which is consistent with other studies reporting cyanobacteria bloom development under nutrient depleted conditions (Wasmund, 1997; Lignell et al., 2003). However, nutrient depleted conditions do not mean that the bloom develops without nutrients, but that bloom-forming species have already taken them up, stored and consumed as Wasmund et al. (2011) found for long-term trends of phytoplankton composition in the western and central Baltic Sea. The relationship between nutrients and bloom biomass becomes even more complex if multiple nutrient sources in the ocean (e.g. remineralization, mixing, upwelling, lateral advection) are considered.

Both *Aphanizomenon sp.* and *N. spumigena* species possess high affinity for uptake and intracellular storage of nitrogen and phosphorus (Flores and Herrero, 2005), enabling them to maintain growth and survive for days under limited nutrient conditions (Kanoshina et al., 2003). The ability of diazotrophic cyanobacteria to fix biologically available nitrogen from the atmosphere (Fogg, 1969; Jöhnk et al., 2008; Paerl et al., 2011) makes phosphorus the limiting nutrient for their growth (Lignell et al., 2003). According to the results, phosphate concentration appears to be an explanatory variable for the timing of the onset of the bloom while DIN seems to have no effect on the bloom development. Phosphate also appears to be an explanatory variable for the timing of decline of the bloom. However, at this stage it is not possible to define if the effect of phosphate on the bloom is indeed associated with the decline of the bloom because of the time the bloom needs to respond to changes in nutrients concentrations. Vahtera et al. (2005) reported a two to three-week time lag in the response of cyanobacteria biomass to phosphate-rich upwelled water.

Climate change may lead to early and more frequent cyanobacteria blooms (Neumann et al., 2012; Andersson et al., 2015) as already indicated by Kahru and Elmgren (2014). This is contradicting projections for the Baltic Sea that predict a higher number of days (about

10–30 days) with water temperatures above 18 °C but less cyanobacteria blooms (Meier et al., 2019). This shows the uncertainty that persists regarding the phenology of blooms and its changes in relation to the environmental conditions. The probabilities calculated for the explanatory variables also reflect part of this uncertainty with both independent data sets. In addition to the uncertainty of the data and processes studied, part of the uncertainty may be attributed to the phenological dates estimated with the Weibull function, the defined environmental window and the compiling of biomass of three species into a single variable.

Based on our results, it is likely that the accelerated changes in the marine environment caused by global warming (including increasing temperatures and more severe storms) may have an effect on the timing at which blooms develop. Whether a bloom occurs early or is delayed depends on the overall effect that the explanatory variables have on each stage of the bloom. An increase in the explanatory variables T_a , Q_{lw} , MLD, PO_4 at the onset of the bloom, Q_h at the peak of the bloom, and Q_{net} and Q_l at the decline of the bloom may result in longer blooms as a consequence of an early onset of the bloom, a delay in the occurrence of the peak and a late decline of the bloom. An increase in the explanatory variables SST, N^2 and wind speed at the onset of the bloom, Q_l at the peak of the bloom, Q_{sw} , Q_h and PO_4 at the decline of the bloom may result in shorter blooms as a result of a delay in the onset of the bloom, an early appearance of the peak as well as an early decline of the bloom. In summary, changes in the explanatory variables and their interplay lead to the observed variability in bloom phenology.

5. Conclusions

The compilation of biomass data for species that co-occur in time and space may be an alternative to overcome difficulties when studying individual species, for which just sparse data exist. Although the behavior of each species in the bloom may be masked, our approach provides a way to track and understand which factors are favoring a representative part of the whole community. Our results show the reliability of the Weibull function and the optimum environmental window as an approach to study the phenology of cyanobacteria blooms in the Gotland Basin.

In summary, the timing of the onset of the bloom is driven by sea surface temperature, air temperature, outgoing long-wave radiation, mixed layer depth, Brunt-Väisälä frequency, phosphate concentration and wind speed. The timing of maximum cyanobacteria biomass is controlled by sensible and latent heat flux, showing the importance of the exchange that occurs between the water surface and the overlying atmosphere. The timing of the decline of the bloom is driven by incoming solar radiation, net heat flux, sensible heat flux, latent heat flux and phosphate concentration. These variables and the way they interact with each other define the phenology of cyanobacteria blooms and partly explain its variability, since a bloom does not depend on only one variable but on the combined effect of these oceanic and atmospheric variables at each stage of the bloom. The role of phosphate in the timing of the onset and decline of the bloom has to be carefully analyzed because of the time lag of the response of cyanobacteria biomass to changes in phosphate concentration.

Until now cyanobacteria studies solely focused on changes in water temperature and incoming radiation. Our results show the need for consideration of other variables in the water column and overlying atmosphere to avoid misleading conclusions. The possible increase in intensity, frequency and duration of cyanobacteria blooms in response to both direct and indirect effects of changing climate conditions requires additional research efforts. Moreover, further related observational studies and modeling approaches are required in order to broaden the understanding of cyanobacteria blooms, their phenology and role in the ecosystem.

Declaration of competing interest

The authors declare that they have no known competing financial interests or personal relationships that could have appeared to influence the work reported in this paper.

Acknowledgments

The authors would like to thank the DAAD for the funding granted by the program: Research Grants - Doctoral Programmes in Germany 2018/19 and the Leibniz Institute for Baltic Sea Research (IOW) for the facilities, data access and support provided during the writing of the manuscript. We want to acknowledge Susanne Feistel for her support with the ODIN platform to obtain data collected by the IOW within its monitoring program, Norbert Wasmund (IOW) for the biomass data set and his comments on the first draft of this manuscript, Ralf Prien and the anonymous reviewers for their constructive and helpful comments and the HELCOM monitoring program of the Baltic Sea, the German Weather Service (DWD), the Swedish Meteorological and Hydrological Institute (SMHI), the European Centre for Medium-Range Weather Forecasts (ECMWF) and the National Oceanic and Atmospheric Administration (NOAA) for the data provided.

Appendix A. Supplementary data

Supplementary material related to this article can be found online at <https://doi.org/10.1016/j.jmarsys.2021.103618>.

References

- Andersson, A., Meier, H.E., Ripszám, M., Rowe, O., Wikner, J., Haglund, P., Eilola, K., Legrand, C., Figueroa, D., Paczkowska, J., Lindehoff, E., Tysklind, M., Elmgren, R., 2015. Projected future climate change and Baltic Sea ecosystem management. *Ambio* 44 (3), 345–356. <http://dx.doi.org/10.1007/s13280-015-0654-8>.
- BACC, 2008. Assessment of Climate Change for the Baltic Sea Basin. Springer Berlin Heidelberg, Berlin, Heidelberg, <http://dx.doi.org/10.1007/978-3-540-72786-6>.
- Bianchi, T.S., Engelhaupt, E., Westman, P., Andrén, T., Rolff, C., Elmgren, R., 2000. Cyanobacterial blooms in the Baltic Sea: Natural or human-induced? *Limnol. Oceanogr.* 45 (3), 716–726. <http://dx.doi.org/10.4319/lo.2000.45.3.0716>.
- Carey, C.C., Ibelings, B.W., Hoffmann, E.P., Hamilton, D.P., Brookes, J.D., 2012. Eco-physiological adaptations that favour freshwater cyanobacteria in a changing climate. *Water Res.* 46 (5), 1394–1407. <http://dx.doi.org/10.1016/J.WATRES.2011.12.016>.
- Chong, I.G., Jun, C.H., 2005. Performance of some variable selection methods when multicollinearity is present. *Chemometr. Intell. Lab. Syst.* 78 (1), 103–112. <http://dx.doi.org/10.1016/j.chemolab.2004.12.011>.
- Chorus, I., Bartram, J., 1999. *Toxic Cyanobacteria in Water: A Guide to Their Public Health Consequences, Monitoring and Management*. Technical Report, World Health Organization.
- Cirés, S., Ballot, A., 2016. A review of the phylogeny, ecology and toxin production of bloom-forming Aphanizomenon spp. and related species within the Nostocales (cyanobacteria). *Harmful Algae* 54, 21–43. <http://dx.doi.org/10.1016/j.hal.2015.09.007>.
- Codd, G.A., Morrison, L.F., Metcalf, J.S., 2005. Cyanobacterial toxins: risk management for health protection. *Toxicol. Appl. Pharmacol.* 203 (3), 264–272. <http://dx.doi.org/10.1016/J.TAAP.2004.02.016>.
- Cury, P., Roy, C., 1989. Optimal environmental window and pelagic fish recruitment success in upwelling areas. *Can. J. Fish. Aquat. Sci.* 46 (4), 670–680. <http://dx.doi.org/10.1139/f89-086>.
- Díaz, P.A., Ruiz-Villarreal, M., Pazos, Y., Moita, T., Reguera, B., 2016. Climate variability and dinophysia acuta blooms in an upwelling system. *Harmful Algae* 53, 145–159. <http://dx.doi.org/10.1016/j.hal.2015.11.007>.
- Downing, J.A., Watson, S.B., Mccauley, E., 2001. Predicting cyanobacteria dominance in lakes. *Can. J. Fish. Aquat. Sci.* 58, 1905–1908. <http://dx.doi.org/10.1139/cjfas-58-10-1905>.
- Eigemann, F., Schwartke, M., Schulz-Vogt, H., 2018. Niche separation of Baltic Sea cyanobacteria during bloom events by species interactions and autecological preferences. *Harmful Algae* 72, 65–73. <http://dx.doi.org/10.1016/j.hal.2018.01.001>.
- Fallon, R.D., Brock, T.D., 1979. Decomposition of blue-green algal (cyanobacterial) blooms in lake mendota, wisconsin. *Appl. Environ. Microbiol.* 37 (5), 820–830.

- Finni, T., Kononen, K., Olsonen, R., Wallström, K., 2001. The history of cyanobacterial blooms in the Baltic Sea. *Ambio* 30 (4), 172–178. <http://dx.doi.org/10.1579/0044-7447-30.4.172>.
- Flores, E., Herrero, A., 2005. Nitrogen assimilation and nitrogen control in cyanobacteria. *Biochem. Soc. Trans.* 33 (1), 164–167. <http://dx.doi.org/10.1042/BST0330164>.
- Fogg, G.E., 1969. The physiology of an algal nuisance. *Proc. R. Soc. B* 173 (1031), 175–189. <http://dx.doi.org/10.1098/rspb.1969.0045>.
- Groetsch, P.M., Simis, S.G., Eleveld, M.A., Peters, S.W., 2016. Spring blooms in the Baltic Sea have weakened but lengthened from 2000 to 2014. *Biogeosciences* 13 (17), 4959–4973. <http://dx.doi.org/10.5194/bg-13-4959-2016>.
- Hall, M.O., Durako, M.J., Fourqurean, J.W., Zieman, J.C., 1999. Decadal changes in seagrass distribution and abundance in Florida Bay. *Estuaries* 22 (2), 445–459. <http://dx.doi.org/10.2307/1353210>.
- Havens, K.E., 2008. Cyanobacteria blooms: effects on aquatic ecosystems. In: Hudnell, H.K. (Ed.), *Cyanobacterial Harmful Algal Blooms: State of the Science and Research Needs*, Vol. 619. Springer New York, pp. 733–747. http://dx.doi.org/10.1007/978-0-387-75865-7_33.
- HELCOM, 2012. *Manual for Marine Monitoring in the COMBINE Programme of HELCOM*. Technical Report, Helsinki Commission - Baltic Marine Environment Protection Commission.
- HELCOM, 2013. *Climate Change in the Baltic Sea Area HELCOM Thematic Assessment In 2013*. Technical Report, Helsinki Commission - Baltic Marine Environment Protection Commission.
- Hjerne, O., Hajdu, S., Larsson, U., Downing, A., Winder, M., 2019. Climate driven changes in timing, composition and size of the Baltic Sea phytoplankton spring bloom. *Front. Mar. Sci.* 6 (JUL), 1–15. <http://dx.doi.org/10.3389/fmars.2019.00482>.
- Hudnell, H.K., Dortch, Q., 2008. A synopsis of research needs identified at the interagency, international symposium on cyanobacterial harmful algal blooms (ISOC-HAB). In: Hudnell, H.K. (Ed.), *Cyanobacterial Harmful Algal Blooms: State of the Science and Research Needs*, Vol. 619. Springer New York, pp. 17–43. http://dx.doi.org/10.1007/978-0-387-75865-7_2.
- Janssen, F., Neumann, T., Schmidt, M., 2004. Inter-annual variability in cyanobacteria blooms in the Baltic Sea controlled by wintertime hydrographic conditions. *Mar. Ecol. Prog. Ser.* 275, 59–68. <http://dx.doi.org/10.3354/meps275059>.
- Jöhnk, K.D., Huisman, J., Sharples, J., Sommeijer, B., Visser, P.M., Stroom, J.M., 2008. Summer heatwaves promote blooms of harmful cyanobacteria. *Global Change Biol.* 14 (3), 495–512. <http://dx.doi.org/10.1111/j.1365-2486.2007.01510.x>.
- Kahru, M., Elmgren, R., 2014. Multidecadal time series of satellite-detected accumulations of cyanobacteria in the Baltic Sea. *Biogeosciences* 11 (13), 3619–3633. <http://dx.doi.org/10.5194/bg-11-3619-2014>.
- Kahru, M., Elmgren, R., Kaiser, J., Wasmund, N., Savchuk, O., 2020. Cyanobacterial blooms in the Baltic Sea: Correlations with environmental factors. *Harmful Algae* 92 (August 2019), 101739. <http://dx.doi.org/10.1016/j.hal.2019.101739>.
- Kahru, M., Elmgren, R., Savchuk, O.P., 2016. Changing seasonality of the Baltic Sea. *Biogeosciences* 13, 1009–1018. <http://dx.doi.org/10.5194/bg-13-1009-2016>.
- Kahru, M., Horstmann, U., Rud, O., 1994. Satellite detection of increased cyanobacterial blooms in the Baltic Sea: natural fluctuation or ecosystem change? *Ambio* 23 (8), 469–472.
- Kanoshina, I., Lips, U., Leppänen, J.M., 2003. The influence of weather conditions (temperature and wind) on cyanobacterial bloom development in the Gulf of Finland (Baltic Sea). *Harmful Algae* 2 (1), 29–41. [http://dx.doi.org/10.1016/S1568-9883\(02\)00085-9](http://dx.doi.org/10.1016/S1568-9883(02)00085-9).
- Kownacka, J., Busch, S., Göbel, J., Gromisz, S., Hällfors, H., Högländer, H., Huseby, S., Jaanus, A., Jakobsen, H., Johansen, M., Johansson, M., Jurgensone, I., Kraśniewski, W., Lehtinen, S., Olenina, I., Weber, M.V., Wasmund, N., 2018. Cyanobacteria biomass 1990–2018. HELCOM baltic sea environment fact sheets 2018. URL: <https://helcom.fi/baltic-sea-trends/environment-fact-sheets/eutrophication/cyanobacteria-biomass/>.
- Larsson, U., Elmgren, R., Wulff, F., 1985. Eutrophication and the Baltic Sea: causes and consequences. *AMBIO* 14.
- Lehtimäki, J., Moisander, P., Sivonen, K., Kononen, K., 1997. Growth, nitrogen fixation, and nodularin production by two Baltic Sea cyanobacteria. *Appl. Environ. Microbiol.* <http://dx.doi.org/10.1128/aem.63.5.1647-1656.1997>.
- Lignell, R., Seppälä, J., Kuoppo, P., Tamminen, T., Andersen, T., Gismervik, I., 2003. Beyond bulk properties: Responses of coastal summer plankton communities to nutrient enrichment in the northern Baltic Sea. *Limnol. Oceanogr.* 48 (1), 189–209. <http://dx.doi.org/10.4319/lo.2003.48.1.0189>.
- Lips, I., Lips, U., 2008. Abiotic factors influencing cyanobacterial bloom development in the Gulf of Finland (baltic sea). *Hydrobiologia* 614 (1), 133–140. <http://dx.doi.org/10.1007/s10750-008-9449-2>.
- Meier, H.E., Dieterich, C., Eilola, K., Gröger, M., Höglund, A., Radtke, H., Saraiva, S., Wählström, I., 2019. Future projections of record-breaking sea surface temperature and cyanobacteria bloom events in the Baltic Sea. *Ambio* 48 (11), 1362–1376. <http://dx.doi.org/10.1007/s13280-019-01235-5>.
- Moore, S.K., Trainer, V.L., Mantua, N.J., Parker, M.S., Laws, E.A., Backer, L.C., Fleming, L.E., 2008. Impacts of climate variability and future climate change on harmful algal blooms and human health. *Environ. Health* 7 (Suppl. 2), S4. <http://dx.doi.org/10.1186/1476-069X-7-S2-S4>.
- Neil, J.M.O., Davis, T.W., Burford, M.A., Gobler, C.J., 2012. The rise of harmful cyanobacteria blooms: The potential roles of eutrophication and climate change. *Harmful Algae* 14, 313–334. <http://dx.doi.org/10.1016/j.hal.2011.10.027>.
- Neumann, T., Eilola, K., Gustafsson, B., Müller-Karulis, B., Kuznetsov, I., Meier, H.E.M., Savchuk, O.P., 2012. Extremes of temperature, oxygen and blooms in the Baltic Sea in a changing climate. *AMBIO* 41 (6), 574–585. <http://dx.doi.org/10.1007/s13280-012-0321-2>.
- Nordin, R.N., Stein, J.R., 1980. Taxonomic revision of *Nodularia* (Cyanophyceae/Cyanobacteria). *Can. J. Bot.* 58 (11).
- Öberg, J., 2015. Cyanobacteria Blooms in the Baltic Sea. Technical Report I, URL: <http://helcom.fi/baltic-sea-trends/environment-fact-sheets/eutrophication/cyanobacterial-blooms-in-the-baltic-sea/>.
- Olenina, I., Hajdu, S., Edler, L., Andersson, A., Wasmund, N., Busch, S., Göbel, J., Gromisz, S., Huseby, S., Huttunen, M., Jaanus, A., Kokkonen, P., Ledaine, I., Niemkiewicz, E., 2006. Biovolumes and size-classes of phytoplankton in the baltic sea. In: HELCOM Balt. Sea Environ. Proc., No. 106. p. 144.
- Paerl, H.W., 1988. Nuisance phytoplankton blooms in coastal, estuarine, and inland waters. *Limnol. Oceanogr.* 33 (4, part 2), 823–847. <http://dx.doi.org/10.4319/lo.1988.33.4part2.0823>.
- Paerl, H.W., Hall, N.S., Calandrino, E.S., 2011. Controlling harmful cyanobacterial blooms in a world experiencing anthropogenic and climatic-induced change. *Sci. Total Environ.* 409 (10), 1739–1745. <http://dx.doi.org/10.1016/j.scitotenv.2011.02.001>.
- Paerl, H.W., Huisman, J., 2009. Climate change: A catalyst for global expansion of harmful cyanobacterial blooms. *Environ. Microbiol. Rep.* 1 (1), 27–37. <http://dx.doi.org/10.1111/j.1758-2229.2008.00004.x>.
- Paerl, H.W., Otten, T.G., 2013. Harmful cyanobacterial blooms: Causes, consequences, and controls. *Microb. Ecol.* 65 (4), 995–1010. <http://dx.doi.org/10.1007/s00248-012-0159-y>.
- Poutanen, E.L., Nikkilä, K., 2001. Carotenoid pigments as tracers of cyanobacterial blooms in recent and postglacial sediments of the Baltic Sea. *Ambio* 30 (4–5), 179–183.
- Reynolds, C.S., 1997. Vegetation processes in the pelagic: A model for ecosystem theory. In: *Excellence in Ecology*. <http://dx.doi.org/10.2216/i0031-8884-37-1-70.1>.
- Rolinski, S., Horn, H., Petzoldt, T., Paul, L., 2007. Identifying cardinal dates in phytoplankton time series to enable the analysis of long-term trends. *Oecologia* 153 (4), 997–1008. <http://dx.doi.org/10.1007/s00442-007-0783-2>.
- Rolinski, S., Sachse, R., Petzoldt, T., 2018. Identification of cardinal dates in ecological time series. <http://dx.doi.org/10.1007/s0044200707832>, R Package “Carditates”, Version 0. URL: <http://carditates.r-forge.r-project.org>.
- Rönnerberg, C., Bonsdorff, E., 2004. Baltic Sea eutrophication: area-specific ecological consequences. *Hydrobiologia* 514 (1–3), 227–241. <http://dx.doi.org/10.1023/B:HYDR.0000019238.84989.7f>.
- Rosipal, R., Krämer, N., 2006. Overview and recent advances in partial least squares. In: *Transactions on Petri Nets and Other Models of Concurrency XV*. pp. 34–51. http://dx.doi.org/10.1007/11752790_2.
- Roy, C., 1993. The optimal environmental window hypothesis: a non linear environmental process affecting recruitment success. In: *ICES Statutory Meeting 1993*. 1993. pp. 1–13.
- Scharfe, M., Wiltshire, K.H., 2019. Modeling of intra-annual abundance distributions: Constancy and variation in the phenology of marine phytoplankton species over five decades at Helgoland Roads (North Sea). *Ecol. Model.* 404 (January), 46–60. <http://dx.doi.org/10.1016/j.ecolmodel.2019.01.001>.
- Schneider, B., Müller, J.D., 2018. The main hydrographic characteristics of the baltic sea. In: *Springer Oceanography* (Ed.), *Biogeochemical Transformations in the Baltic Sea*. Springer, Cham, pp. 35–41. http://dx.doi.org/10.1007/978-3-319-61699-5_3.
- Stal, L.J., Albertano, P., Bergman, B., Von Bröckel, K., Gallon, J.R., Hayes, P.K., Sivonen, K., Walsby, A.E., 2003. BASIC: Baltic Sea cyanobacteria. An investigation of the structure and dynamics of water blooms of cyanobacteria in the Baltic Sea - Responses to a changing environment. *Cont. Shelf Res.* 23 (17–19), 1695–1714. <http://dx.doi.org/10.1016/j.csr.2003.06.001>.
- Suikkanen, S., Kaartokallio, H., Hällfors, S., Huttunen, M., Laamanen, M., 2010. Life cycle strategies of bloom-forming, filamentous cyanobacteria in the Baltic Sea. *Deep-Sea Res. II* <http://dx.doi.org/10.1016/j.dsr2.2009.09.014>.
- Sverdrup, H.U., 1953. On conditions for the vernal blooming of phytoplankton. *ICES J. Mar. Sci.* 18 (3), 287–295. <http://dx.doi.org/10.1093/icesjms/18.3.287>.
- Tobin, E.D., Wallace, C.L., Crumpton, C., Johnson, G., Eckert, G.L., 2019. Environmental drivers of paralytic shellfish toxin producing *Alexandrium catenella* blooms in a fjord system of northern Southeast Alaska. *Harmful Algae* 88 (February), 101659. <http://dx.doi.org/10.1016/j.hal.2019.101659>.
- Utermöhl, H., 1958. Zur Vervollkommnung der quantitativen Phytoplankton-Methodik. *Int. Ver. Theor. Angew. Limnol.* 9 (1), 1–38. <http://dx.doi.org/10.1080/05384680.1958.11904091>.

- Vahtera, E., Laanemets, J., Pavelson, J., Huttunen, M., Kononen, K., 2005. Effect of upwelling on the pelagic environment and bloom-forming cyanobacteria in the western Gulf of Finland, Baltic Sea. *J. Mar. Syst.* 58 (1–2), 67–82. <http://dx.doi.org/10.1016/j.jmarsys.2005.07.001>.
- Wasmund, N., 1997. Occurrence of cyanobacterial blooms in the Baltic Sea in relation to environmental conditions. *Int. Rev. Gesamten Hydrobiol. Hydrogr.* 82 (2), 169–184. <http://dx.doi.org/10.1002/iroh.19970820205>.
- Wasmund, N., Nausch, G., Gerth, M., Busch, S., Burmeister, C., Hansen, R., Sadkowiak, B., 2019. Extension of the growing season of phytoplankton in the western Baltic Sea in response to climate change. *Mar. Ecol. Prog. Ser.* 622, 1–16. <http://dx.doi.org/10.3354/meps12994>.
- Wasmund, N., Tuimala, J., Suikkanen, S., Vandepitte, L., Kraberg, A., 2011. Long-term trends in phytoplankton composition in the western and central Baltic Sea. *J. Mar. Syst.* 87 (2), 145–159. <http://dx.doi.org/10.1016/j.jmarsys.2011.03.010>.
- Whitton, B.A., Potts, M., 2000. Introduction to the cyanobacteria. In: *The Ecology of Cyanobacteria: Their Diversity in Time and Space*. Springer Netherlands, pp. 1–11. <http://dx.doi.org/10.1007/0-306-46855-7>.
- Zhang, D., Lavender, S., Muller, J.P., Walton, D., Zou, X., Shi, F., 2018. MERIS Observations of phytoplankton phenology in the Baltic Sea. *Sci. Total Environ.* 642, 447–462. <http://dx.doi.org/10.1016/j.scitotenv.2018.06.019>.

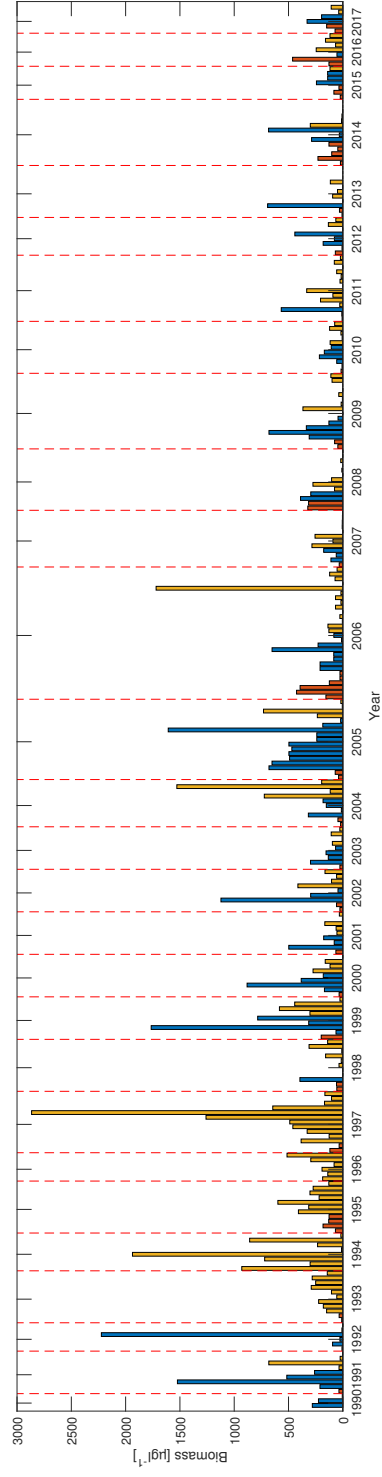


Fig. S1. Biomass observations in June (orange), July (blue) and August (yellow). The reported biomass corresponds to the sum of the three cyanobacteria species biomass (*N. spumigena*, *Aphanizomenon sp.* and *Dolichospermum spp.*). The red dashed lines divide the observations by year. Data set was provided by Norbert Wasmund, pers. communication.

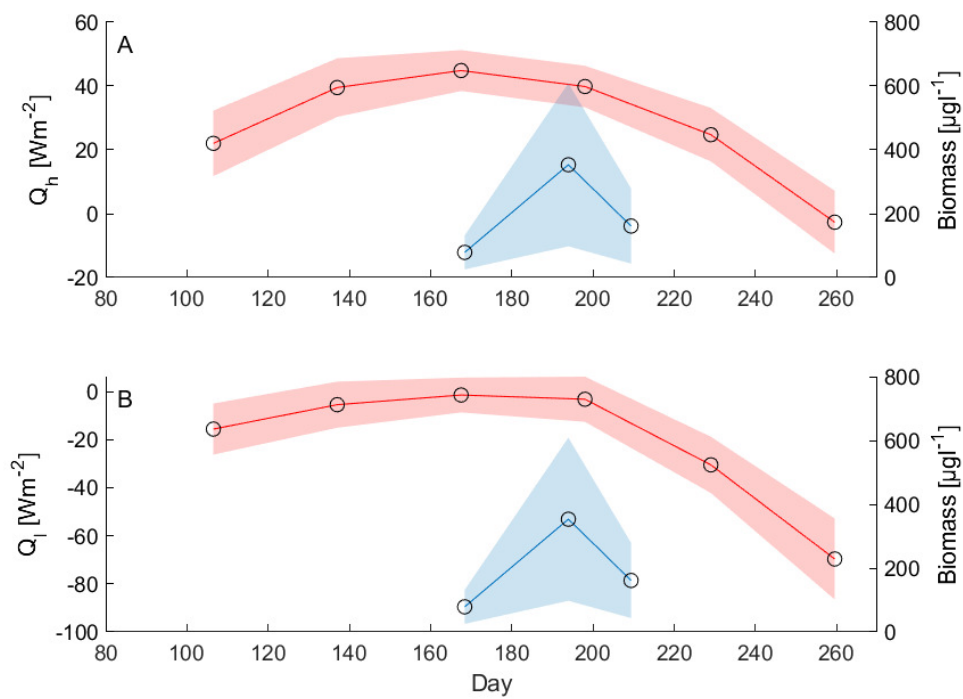


Fig. S2. Monthly averages of (A) sensible heat flux and (B) latent heat flux. The red line corresponds to the variable (left axis) and the blue line to average total biomass (right axis). The shaded area corresponds to the standard deviation of each variable.

Table S1

Mean value of water temperature, ammonium, nitrate, nitrite and phosphate concentrations. Number of samples per month in parentheses.

Year	Month	T_w	NH_4	NO_3	NO_2	PO_4
1990	May	8 (1)	0.395 (2)	0.088 (2)	0.028 (2)	0.116 (2)
	July	15 (1)	0.267 (1)	0.08 (1)	0.027 (1)	0.007 (1)
	August	17 (1)	0.07 (1)	0.1 (1)	0.037 (1)	0.067 (1)
1991	April	3 (1)	0.53 (1)	5.39 (1)	0 (1)	0.58 (1)
	May	6 (2)	0.355 (2)	0.265 (2)	0.015 (2)	0.211 (2)
	June	7 (4)	- (-)	0.054 (2)	0.033 (2)	0.165 (2)
	July	18 (3)	0.2 (1)	0.11 (1)	0.013 (1)	0 (1)
	September	- (-)	0.337 (1)	0.1 (1)	0.023 (1)	0.033 (1)
1992	May	6 (2)	0.324 (2)	0.108 (2)	0.018 (2)	0.12 (2)
	July	17 (2)	- (-)	- (-)	- (-)	- (-)
	August	17 (5)	0.247 (1)	0.136 (3)	0.015 (3)	0.069 (3)
1993	April	3 (2)	0.3 (2)	3.155 (2)	0.098 (2)	0.502 (2)
	May	10 (6)	0.34 (3)	0.053 (3)	0.005 (3)	0.052 (3)
	June	- (-)	0.193 (1)	- (-)	0.047 (1)	0.083 (1)
	July	- (-)	0.22 (1)	- (-)	0.02 (1)	0.05 (1)
	August	17 (3)	0.213 (3)	0.18 (3)	0.058 (3)	0.043 (3)
1994	April	2 (1)	0.357 (1)	3.477 (1)	0.12 (1)	0.455 (1)
	May	5 (6)	0.371 (4)	0.081 (4)	0.024 (4)	0.05 (4)
	July	18 (1)	0.51 (1)	- (-)	0.027 (1)	0.068 (1)
	August	21 (2)	0.268 (2)	0.08 (2)	0.033 (2)	0.03 (2)
	September	12 (1)	0.09 (1)	- (-)	0.043 (1)	0.075 (1)
1995	April	4 (1)	0.147 (1)	2.51 (1)	0.083 (1)	0.43 (1)
	May	7 (2)	0.175 (2)	0.035 (2)	0.017 (2)	0.146 (2)
	June	12 (1)	0.05 (1)	- (-)	0.033 (1)	0.125 (1)
	July	14 (1)	0.05 (1)	- (-)	0.02 (1)	0.05 (1)
	August	18 (5)	0.074 (3)	0.085 (3)	0.012 (3)	0.044 (3)
	September	14 (3)	0.147 (1)	- (-)	0.02 (1)	0.075 (1)
1996	April	2 (1)	0.135 (1)	0.1 (1)	0.025 (1)	0.25 (1)
	May	5 (8)	0.306 (2)	0.055 (2)	0.015 (2)	0.076 (2)
	June	10 (14)	0.08 (1)	- (-)	0.043 (1)	0.08 (1)
	July	15 (1)	0.11 (1)	- (-)	0.03 (1)	0.085 (1)
	August	18 (7)	0.13 (2)	0.02 (2)	0.052 (2)	0.036 (2)
	September	11 (1)	0.103 (1)	- (-)	0.02 (1)	0.09 (1)
1997	April	- (-)	0.24 (1)	2.677 (1)	0.153 (1)	0.44 (1)
	May	4 (3)	0.19 (1)	0.06 (1)	0.015 (1)	0.13 (1)
	June	9 (1)	- (-)	- (-)	0.023 (1)	0.13 (1)
	July	19 (1)	0.137 (1)	- (-)	0.063 (1)	0.088 (1)
	August	21 (6)	0.187 (2)	0.06 (3)	0.048 (3)	0.058 (3)
	September	13 (1)	0.123 (1)	- (-)	0.03 (1)	0.103 (1)

(continued on next page)

Table S1 (continued)

Year	Month	T_w	NH_4	NO_3	NO_2	PO_4
1998	April	3 (1)	0.16 (1)	2.26 (1)	0.133 (1)	0.443 (1)
	May	7 (10)	0.206 (5)	0.03 (5)	0.007 (5)	0.119 (5)
	June	9 (2)	0.06 (2)	- (-)	0.042 (2)	0.148 (2)
	July	15 (1)	0.103 (1)	- (-)	0.08 (1)	0.123 (1)
	August	16 (3)	0.113 (3)	0.07 (3)	0.01 (3)	0.068 (3)
	September	15 (1)	0.05 (1)	0.1 (1)	0.067 (1)	0.093 (1)
1999	April	3 (1)	0.12 (1)	0.13 (1)	0.033 (1)	0.19 (1)
	May	5 (4)	0.205 (3)	0.17 (3)	0.021 (3)	0.138 (3)
	June	11 (1)	0.08 (1)	- (-)	0.03 (1)	0.093 (1)
	July	17 (1)	0.143 (1)	- (-)	0.117 (1)	0.103 (1)
	August	20 (3)	0.231 (3)	0.02 (3)	0.043 (3)	0.068 (3)
	September	16 (1)	0.05 (1)	- (-)	0.02 (1)	0.03 (1)
2000	April	4 (2)	0.15 (2)	4.23 (2)	0.065 (2)	0.415 (2)
	May	7 (4)	0.313 (2)	0 (2)	0.015 (2)	0.087 (2)
	June	10 (1)	0.253 (1)	- (-)	0.027 (1)	0.11 (1)
	July	15 (1)	0.143 (1)	- (-)	0.03 (1)	0.053 (1)
	August	17 (6)	0.19 (3)	0.163 (4)	0.023 (4)	0.055 (4)
	September	- (-)	- (-)	- (-)	- (-)	- (-)
2001	April	4 (1)	0.33 (1)	- (-)	0.02 (1)	0.143 (1)
	May	6 (13)	0.266 (4)	0.081 (4)	0.015 (4)	0.088 (4)
	June	12 (1)	0.107 (1)	0.1 (1)	0.093 (1)	0.047 (1)
	July	18 (35)	0.22 (2)	0 (2)	0.025 (2)	0.038 (2)
	August	19 (18)	0.264 (5)	0.013 (6)	0.028 (6)	0.047 (6)
	September	18 (28)	- (-)	- (-)	- (-)	- (-)
2002	April	4 (5)	0.111 (2)	2.393 (4)	0.067 (4)	0.445 (4)
	May	7 (5)	0.28 (2)	0.023 (4)	0.017 (4)	0.121 (4)
	June	16 (1)	0.103 (1)	- (-)	0.033 (1)	0.063 (1)
	July	18 (3)	0.453 (2)	0.03 (2)	0.032 (2)	0.06 (2)
	August	20 (2)	0.205 (2)	- (-)	0.03 (2)	0.052 (2)
	September	16 (1)	0.26 (1)	- (-)	0.04 (1)	0.07 (1)
2003	April	1 (1)	0.247 (1)	2.743 (1)	0.147 (1)	0.67 (1)
	May	3 (5)	0.177 (2)	0.078 (4)	0.025 (4)	0.435 (4)
	June	12 (1)	0.137 (1)	- (-)	0.023 (1)	0.113 (1)
	July	19 (5)	0.227 (4)	0.03 (5)	0.027 (5)	0.032 (5)
	August	17 (1)	0.09 (1)	- (-)	0.027 (1)	0.06 (1)
	September	15 (1)	0.14 (1)	- (-)	0.03 (1)	0.057 (1)
2004	April	4 (1)	0.147 (1)	- (-)	0.02 (1)	0.347 (1)
	May	7 (3)	0.2 (2)	0.02 (3)	0.015 (3)	0.147 (3)
	June	10 (1)	0.05 (1)	0.14 (1)	0.027 (1)	0.12 (1)
	July	15 (5)	0.161 (4)	0 (5)	0.023 (5)	0.038 (5)
	August	18 (1)	0.333 (1)	- (-)	0.03 (1)	0.083 (1)

(continued on next page)

Table S1 (continued)

Year	Month	T_w	NH_4	NO_3	NO_2	PO_4
2005	September	14 (1)	0.217 (1)	- (-)	0.02 (1)	0.17 (1)
	April	3 (6)	0.118 (4)	1.06 (5)	0.065 (5)	0.545 (5)
	May	6 (4)	0.112 (2)	0 (3)	0.012 (3)	0.183 (3)
	June	12 (1)	0.05 (1)	- (-)	0.023 (1)	0.083 (1)
	July	18 (4)	0.113 (2)	0.05 (4)	0.04 (4)	0.053 (4)
	August	18 (1)	0.137 (1)	0.1 (1)	0.05 (1)	0.057 (1)
2006	September	16 (2)	0.087 (2)	- (-)	0.025 (2)	0.09 (2)
	April	4 (1)	0.107 (1)	- (-)	0.02 (1)	0.31 (1)
	May	7 (4)	0.122 (3)	0 (4)	0.019 (4)	0.163 (4)
	June	11 (1)	0.05 (1)	- (-)	0.02 (1)	0.093 (1)
	July	19 (4)	0.142 (2)	0.05 (4)	0.025 (4)	0.05 (4)
	August	20 (2)	0.082 (2)	- (-)	0.032 (2)	0.063 (2)
2007	September	16 (1)	0.217 (1)	- (-)	0.033 (1)	0.053 (1)
	April	5 (1)	0.05 (1)	- (-)	0.02 (1)	0.337 (1)
	May	8 (6)	0.197 (2)	0.065 (3)	0.013 (3)	0.205 (3)
	June	15 (1)	0.05 (1)	- (-)	0.033 (1)	0.067 (1)
	July	15 (6)	0.077 (1)	0.07 (4)	0.05 (4)	0.046 (4)
	August	17 (2)	0.145 (2)	- (-)	0.04 (2)	0.072 (2)
2008	September	14 (1)	0.14 (1)	- (-)	0.06 (1)	0.077 (1)
	April	4 (1)	0.137 (1)	0.1 (1)	0.053 (1)	0.487 (1)
	May	8 (8)	0.213 (3)	0.03 (4)	0.017 (4)	0.095 (4)
	June	13 (1)	0.05 (1)	- (-)	0.023 (1)	0.123 (1)
	July	18 (2)	0.05 (2)	- (-)	0.043 (2)	0.083 (2)
	August	19 (3)	0.168 (3)	0.01 (3)	0.023 (3)	0.06 (3)
2009	September	15 (1)	0.083 (1)	- (-)	0.033 (1)	0.123 (1)
	April	5 (1)	0.073 (1)	- (-)	0.023 (1)	0.373 (1)
	May	7 (3)	0.128 (3)	0 (3)	0.01 (3)	0.15 (3)
	June	10 (1)	0.073 (1)	- (-)	0.033 (1)	0.07 (1)
	July	16 (10)	0.052 (2)	- (-)	0.037 (2)	0.077 (2)
	August	18 (1)	0.117 (1)	- (-)	0.037 (1)	0.053 (1)
2010	September	17 (1)	0.05 (1)	- (-)	0.023 (1)	0.073 (1)
	April	3 (1)	0.117 (1)	- (-)	0.02 (1)	0.31 (1)
	May	5 (31)	0.18 (2)	0.05 (4)	0.01 (4)	0.167 (4)
	June	8 (1)	0.057 (1)	- (-)	0.02 (1)	0.09 (1)
	July	20 (7)	0.198 (3)	0.05 (6)	0.017 (6)	0.047 (5)
	August	21 (1)	0.05 (1)	- (-)	0.037 (1)	0.067 (1)
2011	September	15 (1)	0.05 (1)	- (-)	0.02 (1)	0.057 (1)
	April	1 (1)	0.2 (1)	2.963 (1)	0.163 (1)	0.64 (1)
	May	7 (7)	0.12 (2)	0.01 (4)	0.04 (4)	0.02 (4)
	June	13 (1)	0.2 (1)	- (-)	0.037 (1)	0.07 (1)
	July	18 (1)	0.2 (1)	- (-)	0.033 (1)	0.05 (1)

(continued on next page)

Table S1 (continued)

Year	Month	T_w	NH_4	NO_3	NO_2	PO_4
2012	August	19 (13)	0.222 (5)	0.01 (5)	0.012 (5)	0.035 (5)
	September	13 (1)	0.26 (1)	- (-)	0.033 (1)	0.117 (1)
	April	3 (1)	0.21 (1)	2.217 (1)	0.163 (1)	0.677 (1)
	May	6 (12)	0.393 (2)	0.04 (4)	0.02 (4)	0.253 (4)
	July	16 (15)	0.17 (3)	0.18 (4)	0.028 (4)	0.058 (4)
2013	August	17 (1)	0.23 (1)	- (-)	0.023 (1)	0.07 (1)
	April	2 (1)	0.2 (1)	2.45 (1)	0.153 (1)	0.543 (1)
	May	7 (10)	0.2 (3)	- (-)	0.02 (5)	0.14 (5)
	June	13 (1)	0.2 (1)	- (-)	0.027 (1)	0.05 (1)
	July	18 (1)	0.2 (1)	- (-)	0.033 (1)	0.047 (1)
2014	August	18 (7)	0.11 (3)	0.11 (5)	0.03 (5)	0.043 (5)
	September	17 (1)	0.2 (1)	- (-)	0.02 (1)	0.06 (1)
	April	5 (1)	0.2 (1)	- (-)	0.023 (1)	0.38 (1)
	May	5 (7)	0.13 (2)	0.04 (4)	0.02 (4)	0.28 (4)
	June	11 (1)	0.2 (1)	- (-)	0.037 (1)	0.107 (1)
2015	July	18 (17)	0.115 (3)	0.09 (6)	0.028 (6)	0.06 (6)
	August	20 (1)	0.2 (1)	- (-)	0.083 (1)	0.09 (1)
	September	16 (1)	0.2 (1)	- (-)	0.043 (1)	0.077 (1)
	April	5 (1)	0.2 (1)	0.1 (1)	0.03 (1)	0.567 (1)
	May	7 (7)	0.25 (2)	0.15 (4)	0.02 (4)	0.32 (4)
2016	June	11 (1)	0.2 (1)	0.1 (1)	0.02 (1)	0.273 (1)
	July	16 (14)	0.265 (4)	0.095 (5)	0.018 (5)	0.073 (5)
	August	19 (4)	- (-)	- (-)	- (-)	- (-)
	September	18 (1)	0.2 (1)	0.1 (1)	0.023 (1)	0.047 (1)
	April	5 (1)	0.2 (1)	0.1 (1)	0.023 (1)	0.47 (1)
2017	May	8 (9)	0.14 (2)	0.05 (4)	0.01 (4)	0.115 (4)
	June	- (-)	- (-)	0.1 (1)	0.02 (1)	0.093 (1)
	July	18 (1)	0.2 (1)	0.1 (1)	0.02 (1)	0.073 (1)
	August	18 (10)	0.19 (3)	0.1 (5)	0.02 (5)	0.038 (5)
	September	17 (1)	0.2 (1)	0.1 (1)	0.02 (1)	0.063 (1)
2017	April	4 (1)	0.2 (1)	0.1 (1)	0.02 (1)	0.4 (1)
	May	7 (15)	0.15 (3)	0.05 (3)	0.01 (3)	0.2 (3)
	June	11 (1)	0.2 (1)	0.1 (1)	0.02 (1)	0.093 (1)
	July	15 (1)	0.2 (1)	0.1 (1)	0.045 (1)	0.07 (1)
	August	18 (6)	0.21 (2)	0.3 (2)	0.06 (2)	0 (2)
September	16 (1)	0.2 (1)	0.1 (1)	0.02 (1)	0.063 (1)	

Table S2

Parameters and empirical equations used for estimation of heat flux components.

Parameter	Equation	Reference
Net long-wave radiation [W m^{-2}]	$Q_{lw} = qlw_{in} - qlw_{out}$	
Long-wave radiation in [W m^{-2}]	$qlw_{in} = (1 - r_{water}) * K_{emp} * K_{SB} * T_a^6 * (1 + (0.17 * clouds^2))$	Fischer et al. (1979)
Water surface reflectivity	$r_{water} = 0.03$	Henderson-Sellers (1986)
Empirical coefficient [K^{-2}]	$K_{emp} = 9.3700e - 06$	
Stefan-Boltzmann constant [$\text{W m}^{-2} \text{K}^4$]	$K_{SB} = 5.73e - 08$	
Air temperature [$^{\circ}\text{C}$]	T_a	
Cloud cover	clouds	
Long-wave radiation out [W m^{-2}]	$qlw_{out} = e_{water} * K_{SB} * SST^4$	Fischer et al. (1979)
Water emissivity	$e_{water} = 0.97$	
Sea surface temperature [$^{\circ}\text{C}$]	SST	
Sensible heat flux [W m^{-2}]	$Q_h = 1.56 + 1.84 * (T_a - SST) * Wind$	Rahmstorf (1990)
Wind speed [m s^{-1}]	Wind	
Latent heat flux [W m^{-2}]	$Q_l = (\rho_{air} * K_{DN} * Wind * 0.622 * p^{-1} * (ea - es)) * L_w$	Fischer et al. (1979)
Air density [kg m^{-3}]	$\rho_{air} = 1.2$	
Dalton number	$K_{DN} = 1.5e - 3$	
Atmospheric pressure [Pa]	p	
Vapour pressure for air [mbar]	$ea = h * 6.11 * 10^{(7.5 * T_a / (T_a + 237.3))}$	Rahmstorf (1990)
Humidity [%]	h	
Vapour pressure for water [mbar]	$es = h * 6.11 * 10^{(7.5 * SST / (SST + 237.3))}$	Rahmstorf (1990)
Water latent heat flux [J kg^{-1}]	$L_w = 2.56e6$	
Incoming solar radiation [W m^{-2}]	Q_{sw}	
Net heat flux [W m^{-2}]	$Q_{net} = Q_{sw} + Q_{lw} + Q_h + Q_l$	

Table S3

Coefficient of determination (R^2), coefficients of the Weibull function and total biomass of the bloom for each fitted curve.

Year	R^2	y_{max}	Weibull function coefficients						Total biomass [$\mu\text{g L}^{-1}$]		
			p_1	p_2	p_3	p_4	p_5	p_6	Onset- Peak	Peak- Decline	Onset- Decline
1995	0.667	598	1.073	218.2	4.5	0.255	222.2	49.6	17452	9	17461
1998	0.972	395	0.890	193.0	24.3	0.045	211.2	52.4	5083	2998	8081
1999	0.986	199	0.969	153.6	25.3	0.227	177.5	12.9	2151	3256	5407
2000	0.794	881	0.980	198.9	48.8	0.046	209.7	32.0	4459	4551	9010
2001	0.943	581	0.975	182.8	19.9	0.114	202.3	36.1	7903	5126	13029
2002	0.958	1124	0.996	181.4	22.2	0.069	206.2	27.8	14706	13223	27928
2003	0.936	322	0.953	178.5	16.6	0.125	208.3	18.6	5466	4952	10418
2004	0.981	320	0.973	174.6	25.6	0.072	192.3	38.8	3415	2573	5988
2005	0.980	666	0.994	182.8	19.8	0.025	196.0	183.5	8793	2032	10826
2007	0.860	256	0.715	216.8	51.5	0.010	226.0	93.6	1814	1021	2834
2008	0.872	389	0.219	181.8	19.5	0.021	218.5	27.8	8889	8126	17014
2009	0.921	680	0.989	185.7	18.3	0.103	195.6	86.3	7424	2547	9971
2010	0.900	216	0.981	189.2	24.3	0.010	217.5	15.4	2321	2906	5226
2011	0.978	567	0.997	185.6	29.4	0.072	205.2	33.9	5762	5337	11099
2013	0.978	692	1.000	186.3	22.7	0.046	207.6	39.3	8716	6291	15007
2014	0.869	288	0.998	183.2	13.0	0.131	200.3	77.7	5215	1622	6838
2015	0.856	243	0.938	185.0	19.9	0.022	233.6	7.3	3259	5452	8710
2016	0.967	462	0.978	159.7	22.8	0.141	186.4	14.6	5421	7262	12683
2017	0.981	329	0.914	176.6	13.6	0.061	216.7	18.8	7161	6315	13476

References

- Fischer, H., List, E., Koh, R., Imberger, J., Brooks, N., 1979. *Mixing in inland and coastal waters*. New York.
- Henderson-Sellers, B., 1986. Calculating the surface energy balance for lake and reservoir modeling: A review. *Reviews of Geophysics* 24, 625.
doi:10.1029/RG024i003p00625.
- Rahmstorf, S., 1990. *An oceanic mixing model: application to global climate and to the New Zealand West Coast*. Ph.D. thesis. Victoria University.



Inter-Annual Variability Of Spring And Summer Blooms In The Eastern Baltic Sea

Oscar Dario Beltran-Perez* and Joanna J. Waniek

Department of Marine Chemistry, Leibniz Institute for Baltic Sea Research Warnemünde, Rostock, Germany

Changes in environmental conditions may have an effect on the occurrence and intensity of phytoplankton blooms. However, few studies have been carried out on this subject, mainly due to the lack of long-term in situ observations. We study the inter-annual variability and phenology of spring and summer blooms in the eastern Baltic Sea using a physical-biological model. The one-dimensional NPZD model simulates the development of both blooms in the water column with realistic atmospheric forcing and initial conditions representative of the eastern Baltic Sea between 1990 and 2019. On average, the spring bloom started on day 85 ± 7 , reached its maximum biomass on day 115 ± 6 and declined after day 144 ± 5 . The summer bloom started on day 158 ± 5 , had its maximum biomass on day 194 ± 9 and ended after day 237 ± 8 . The results showed that the summer bloom occurs 9 days earlier and last 15 days longer over the 30-year simulation period, but changes in the phenology of the spring bloom were not statistically significant. There is strong evidence that warmer periods favor both blooms, but in different ways. Warmer periods caused spring blooms to peak earlier, while summer blooms reached higher abundance. Additionally, a higher energy gain by the ocean led to longer summer blooms of greater abundance and higher biomass maxima. Overall, summer blooms are more sensitive to changes in the environment than spring blooms, being therefore more vulnerable to changes generated by climate change in the Baltic Sea.

Keywords: cyanobacteria, diatoms, bloom, phenology, Baltic Sea, modeling approach

OPEN ACCESS

Edited by:

Jesper H. Andersen,
NIVA Denmark Water
Research, Denmark

Reviewed by:

Urmas Lips,
Tallinn University of
Technology, Estonia
Kalle Olli,
Estonian University of Life
Sciences, Estonia

*Correspondence:

Oscar Dario Beltran-Perez
Oscar.beltran@io-warnemuende.de

Specialty section:

This article was submitted to
Marine Ecosystem Ecology,
a section of the journal
Frontiers in Marine Science

Received: 26 April 2022

Accepted: 22 June 2022

Published: 02 August 2022

Citation:

Beltran-Perez OD and Waniek JJ
(2022) Inter-Annual Variability
Of Spring And Summer Blooms
In The Eastern Baltic Sea.
Front. Mar. Sci. 9:928633.
doi: 10.3389/fmars.2022.928633

INTRODUCTION

The phytoplankton growing season plays an integral role in the marine food web and ecosystem functioning, as phytoplankton comprises the base of the marine food web and represents 90% of ocean productivity (Smith and Hollibaugh, 1993). Phenology studies describe the key stages of the life cycle of species, e.g. seed sprouting, bird migration or phytoplankton growth. Many phenological events are seasonal and therefore they provide insight about the sensitivity of an ecosystem to environmental change. Alteration in phytoplankton phenology may influence the survival of higher trophic levels due to variations in the timing of food availability (match-mismatch hypothesis) (Smith and Hollibaugh, 1993; Winder and Schindler, 2004). Regular phytoplankton blooms occur in all sub-basins of the Baltic Sea, frequently during spring and summer seasons. However, there is still uncertainty about the phenology and factors governing the development of those blooms.

Overall, diatoms dominate the spring bloom but in the Baltic Sea diatoms and dinoflagellates occur at the same time and build up the spring bloom biomass (Klais et al., 2011). The last decades

have shown a highly variable proportion of diatoms and dinoflagellates in the spring bloom of the Baltic Sea in both time and space (Klais et al., 2011). Therefore, no common pattern can be defined for all sub-basins, indicating a strong influence of local mechanisms driving the bloom. The conditions, factors and mechanisms promoting the success of cold-water dinoflagellates in dominating the spring phytoplankton community remain poorly understood, as well as their conspicuous dominance in the ice-free central part of the Baltic Sea (Klais et al., 2011). Diatom and dinoflagellate blooms are difficult to track independently with low frequency data due to the co-occurrence of both species, diatom blooms grow faster, but dinoflagellate blooms may last longer (Lips et al., 2014).

The decrease in availability of dissolved silica (DSi) and the reduction of DSi:N ratios associated with eutrophication (Rahm et al., 1996; Papush and Danielsson, 2006) have been suggested to limit diatom growth in the Baltic Sea, indirectly supporting the expansion of dinoflagellate blooms. However, it was shown that spring bloom species in the Baltic Sea are well adapted to low DSi availability and are not directly affected by reduced surface concentrations of DSi (Spilling et al., 2010). Diatoms are effectively seeded even from minor inocula of resting propagules (McQuoid and Godhe, 2004), as in the Gotland Basin where the permanent halocline (at 60–80 m depth) is a strong barrier for local cyst re-suspension from the sediment to the euphotic layer. Additionally, the anoxic sediments and bottom waters are not favorable for cyst germination (Rengefors and Anderson, 1998; Kremp and Anderson, 2000). Small fast-growing diatoms thrive in unstable, turbulent conditions giving them a competitive advantage through building a superior head-start biomass over slow-growing, large and motile dinoflagellates that require a specific habitat setting for bloom formation (Klais et al., 2011).

Spring blooms develop from the south to the north of the Baltic Sea, with the first blooms peaking in mid-March in the Bay of Mecklenburg and the last blooms occurring in mid-April in the Gulf of Finland (Groetsch et al., 2016) and in May/June in the Bothnian Bay with biomass much lower than in most other parts of the Baltic Sea (Spilling et al., 2018). Despite the phenological changes by sub-basin, the bloom length is similar between basins (43 ± 2 day), except for the Bay of Mecklenburg (36 ± 11 day) (Groetsch et al., 2016). Summer blooms are dominated by the cyanobacteria species *Nodularia spumigena*, *Aphanizomenon* sp. and *Dolichospermum* spp. Studies in the Baltic Sea have observed an increase in the intensity and duration of cyanobacteria blooms since the 1960s (Bianchi et al., 2000; Poutanen and Nikkilä, 2001; Kahru and Elmgren, 2014; Kahru et al., 2016; HELCOM/Baltic Earth, 2021). Cyanobacteria blooms give rise to environmental concern due to their ability to fix molecular nitrogen from the atmosphere and the production of toxins by some species that may lead to the death of mammals, fish and filtering organisms in the water (Paerl, 2014). Cyanobacteria blooms usually begin in June and reach their maximum biomass during July and August (Kahru et al., 2020; Beltran-Perez and Waniek, 2021).

Although environmental management programs (e.g. Helsinki Convention, EU Marine Strategy Framework Directive,

Baltic Sea Action Plan) have been in place in the Baltic Sea to monitor and control its environmental state for decades, massive blooms continue to occur especially those that produce toxins (Paerl, 2014; Munkes et al., 2020). Eutrophication by nutrients entering the Baltic Sea through rivers, nitrogen fixation from the atmosphere by cyanobacteria species, the organic material subsequently sinking to depth and the turnover of phosphorus from sediments (Vahtera et al., 2007; Paerl and Scott, 2010) are still the major concerns of the environmental authorities in the Baltic Sea (HELCOM/Baltic Earth, 2021). Subsequent remineralization at depth by bacteria depletes oxygen concentration and creates low-oxygen conditions that are lethal to fish (Gustafsson, 2012; Breitburg et al., 2018). Another concern are increasing temperatures, which have been linked to changes in phytoplankton dynamics in terms of abundance, composition and phenology (Carey et al., 2012; HELCOM/Baltic Earth, 2021).

Despite the regular occurrence of spring and summer blooms in the Baltic Sea and their role in the ecosystem, species-specific life cycles, succession and bloom alterations under changing environmental conditions are still not well understood, partly due to the lack of long-term *in situ* data sets. In recent decades, coupled biological-physical models have been used to define how the phenology of blooms is affected by environmental forcing in different coastal (Sharples et al., 2006; Ji et al., 2008) and marine environments (Hashioka et al., 2009; Henson et al., 2009; Gittings et al., 2018), including the Baltic Sea (Neumann et al., 2012; Dzierzbicka-Głowacka et al., 2013; Daewel and Schrum, 2017). Models include processes on different spatial and temporal scales, their complexity increases depending on the number of processes included and parametrization used. One-dimensional models may provide insight into the mechanisms driving phytoplankton phenology when the dynamics are dominated by local forcing (Sharples et al., 2006) such as in the Baltic Sea, where there are significant changes in the environmental conditions (e.g. in terms of temperature, stratification, mixing) from one basin to another (Schneider and Müller, 2018; Hjerne et al., 2019; HELCOM/Baltic Earth, 2021) regulating the bloom.

Usually phenological studies and models include temperature, solar radiation and wind among other factors as the main bloom drivers, but not heat flux. It has recently been observed that heat flux plays an important role in bloom phenology (Gittings et al., 2018; Beltran-Perez and Waniek, 2021). Our model seeks to define the influence of atmospheric forcing on bloom phenology. Therefore, realistic atmospheric forcing (wind, air temperature, solar radiation, relative humidity, cloud cover) was used in the simulation of the heat budget and energy transfer from the atmosphere to the water column and vice versa. In this study, we hypothesize that (1) the inter-annual variability of spring and summer blooms can be reproduced by a one-dimensional (water column) model including the main forcing affecting bloom formation and biological interactions between phytoplankton, zooplankton, detritus and nutrients, and (2) the phenology of spring and summer blooms has changed, leading to longer and more intense bloom as a consequence of changes in heat flux in the Gotland Basin.

METHODS

Study Site

The Baltic Sea is a shallow, semi-enclosed brackish sea in northern Europe (Figure 1). Its drainage basin is shared by 14 countries (around 84 million people), which exerts pressure on all the Baltic Sea ecosystem by increasing eutrophication, pollution and pressure on fish stocks (HELCOM, 2018). The limited water exchange with the North Sea results in a long residence time and a large seasonal and spatial variation in the biological, physical and chemical properties of the water column and the distribution of phytoplankton species (Schneider and Müller, 2018). The high buffer capacity of the system has led to a slow response to nutrient load reductions implemented for decades by the Baltic Sea countries (Savchuk, 2018; Murray et al., 2019). Furthermore, climate change affects the entire ecosystem causing increasing temperatures, declining ice cover and increasing annual precipitation in the Baltic Sea (HELCOM/Baltic Earth, 2021). Therefore, human-induced environmental pressures coupled with climate change may exacerbate changes in the phytoplankton community, especially in the Baltic Sea where the sea surface temperature is increasing faster than the average for the global ocean (HELCOM/Baltic Earth, 2021).

The Baltic Sea is divided into 17 basins, each basin with its own complexity and particular characteristics (Hjerne et al., 2019; HELCOM/Baltic Earth, 2021). The Gotland Basin is the deepest basin in the Baltic Sea with a maximum depth of 249 m, characterized by a permanent halocline at 60–80 m depth which functions as a barrier between anoxic sediments and bottom waters and the euphotic layer (Klais et al., 2011). Low oxygen levels lead to the production of hydrogen sulphide and release of phosphate from the sediments to the water column which further amplifies primary production and consequently oxygen demand (Vahtera et al., 2007; Murray et al., 2019). This study focuses on the Gotland Basin, specifically the station TF271 (Figure 1) located in the eastern part of the Baltic Sea at 57°19'12" N, 20°3'0" E. This station has been monitored since 1979 in the frame of the HELCOM monitoring program (HELCOM, 2012). However, regular monitoring of blooms began only in 1990 (Wasmund, 1997).

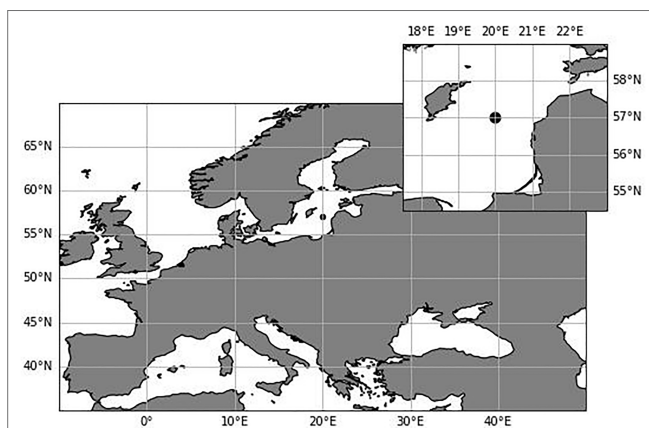


FIGURE 1 | Location of the monitoring station TF271 (black dot) in the Gotland Basin, Baltic Sea.

Model-Based Approach

We used a coupled physical-biological model to understand the interactions between the physical and biological conditions of the water column that affect the development of spring and summer blooms in the Gotland Basin. This model is an adaptation of an early version developed by Waniek (2003) to study the physical factors controlling phytoplankton growth in the northeast Atlantic and the Irminger Sea (Waniek, 2003; Waniek and Holliday, 2006). The physical model basically consists of an integrated mixed-layer model for the surface layer embedded into an advective-diffusion model for the thermocline. The model is therefore able to estimate the changes in temperature with depth from kinetic energy and thermal budgets solving wind mixing, convection, upwelling and turbulent diffusion processes in the water column, giving a reliable approach to the physical processes that influence bloom formation. In addition to the changes in the water column, the model incorporates the feedback between the water surface and the atmosphere through the net heat flux terms (incoming solar radiation, long-wave radiation, sensible and latent heat flux) calculated from standard bulk formulae for each time step. A detailed description of the physical model can be found in Waniek (2003).

The biological model is a simplified representation of the phytoplankton cycle conceived primarily to describe the dynamics of six state variables (Figure 2): nitrogen concentration as limiting nutrient, two functional groups of phytoplankton composed of diatoms (*Diatoms*) and cyanobacteria (*Cyano*), zooplankton (*Zoo*) fueled by grazing on mainly diatoms, and detritus, which sinks at two different velocities and is remineralized or lost to the sediment (see Figure 2). In this study the spring bloom was modeled on the basis of diatoms because they usually begin the spring bloom and are considered superior to dinoflagellates as competitors because of their relatively high growth rates and nutrient uptake capacities (Suikkanen et al., 2011). Furthermore, reliable, high frequency data to identify and validate the beginning and end of each bloom individually are still scarce in the Gotland Basin (Klais et al., 2011; Lips et al., 2014). Therefore, the results may combine the behavior of diatoms and dinoflagellates, as both species have basically comparable nutrient requirements (excluding the need for silica) and appear to provide similar ecosystem services with respect to the annual new production and nutrient uptake (Kremp et al., 2008; Klais et al., 2011). All concentrations in the biological model are expressed in terms of nitrogen, i.e. mmol N m^{-3} , as nitrogen is usually the limiting nutrient in the ocean and the common unit in coupled models (Janssen et al., 2004; Beckmann and Hense, 2007; Sonntag and Hense, 2011; Hense et al., 2013). Carbon and phosphate concentrations were transformed into nitrogen using the Redfield ratio between carbon, nitrogen and phosphorus (C:N:P) of 106:16:1 (Redfield, 1958).

The growth rate of phytoplankton is determined by a “Michaelis-Menten” equation, which depends on the availability of nutrients and light (Tables 1, 2). The light term depends on the maximum growth rate of phytoplankton (μ_{growth}), on the slope of the growth-light curve (α) and the light intensity in the water column. The light in the water column is given by the fraction

of photosynthetically active radiation (PAR), the incoming solar radiation (Q_{sw}) and the attenuation of light through the water column due to water (k_w) and chlorophyll a (k_{chl}). The sink terms for phytoplankton are grazing by zooplankton, leaching and mortality including viral lysis and extracellular release (μ_m).

Zooplankton is included in the model for the sole purpose of closing the trophic food chain and to provide the grazing pressure on diatoms, given the limited reliable data regarding zooplankton and their interaction with phytoplankton e.g. in terms of growth, grazing and assimilation rates. Therefore, zooplankton equation does not reflect its life cycle nor the complete interactions of zooplankton with other organisms in the water column. The grazing pressure on diatoms is determined by the maximum grazing rate (μ_{gz}) and the catching rate of zooplankton (μ_c). Thus, the grazing rate is given by the grazing pressure, the assimilation efficiency (γ_1), the excretion rate (γ_2) and the mortality rate of zooplankton μ_{mZoo} .

The remineralization of organic material comprising dead diatoms, cyanobacteria and zooplankton is described by the detritus pool. The detritus pool was split into two groups (fast and slow) based on the sinking speed. Part of the dead organic material may form aggregates that sink rapidly (100 m d^{-1}) while fine organic particles may stay longer in the water column and sink at a slower rate (1 m d^{-1}). The fraction of fast and slow detritus pool within the model is determined by the interaction of detritus with the other model compartments (**Figure 2**), i.e. it depends on the amount of dead phytoplankton and zooplankton, remineralization rate (μ_r) and sinking speed (fast (w_f) and slow (w_s)) in each time step.

The change in nutrient concentration at each time step depends on the remineralization rate of both detritus pools, the excretion rate of zooplankton and phytoplankton uptake during growth. The equations and parameters for the biological state variables are given in **Tables 1, 2**, respectively. DSi concentrations was assumed to be sufficient during the early phase of the spring

bloom when the head-start population had been established (Kremp et al., 2008). At this point, nutrient levels, nutrient ratios or light intensity had only a limited effect on the biomass distribution (Kremp et al., 2008), therefore an aligned Redfield ratio was also assumed.

The ability to fix molecular nitrogen from the atmosphere allows cyanobacteria to circumvent the general summer nitrogen limitation, making phosphorus the primary limiting nutrient for N-fixing cyanobacteria (Walve and Larsson, 2007; Karlsson et al., 2015). Furthermore, cyanobacteria studies have highlighted the role of physical forcing and phosphorus over other nutrients during bloom development. Lips and Lips (2008) have shown that blooms for example of *Aphanizomenon* sp. are initiated by upwelling of phosphorus-rich deeper waters, whereas growth of *Nodularia spumigena* is mostly related to increases in incoming solar radiation and temperature as well as the ability of this species to make use of regenerated phosphorus pools during the low nutrient concentration periods. Nitrogen fixation by cyanobacteria as well as additional processes involved in bloom formation such as atmospheric nutrient deposition and water column-sediment interaction were not included in the model because they are beyond the scope of this study. Quantification of these processes and parameters such as carbon to chlorophyll a ratio, growth, mortality and remineralization rates is still an active field of research where many questions remain unresolved and valid parametrization for a numerical approach does not exist yet.

One of the limitations of our model is to consider the water column as a rigid parcel of water, where mass and energy exchange takes place through the water column but not with its surroundings. This assumption has implications for all simulated physical, chemical and biological variables, leading to over- or underestimation of these variables and contributing to the model error. In addition, the model was elaborated based on diatoms and cyanobacteria without considering plankton succession or other species such as dinoflagellates that co-occur during the spring bloom because of the limited data to reliably validate each bloom individually and species by species. This simplification may likely affect our results and therefore contribute to the difference observed with other studies and partly observations.

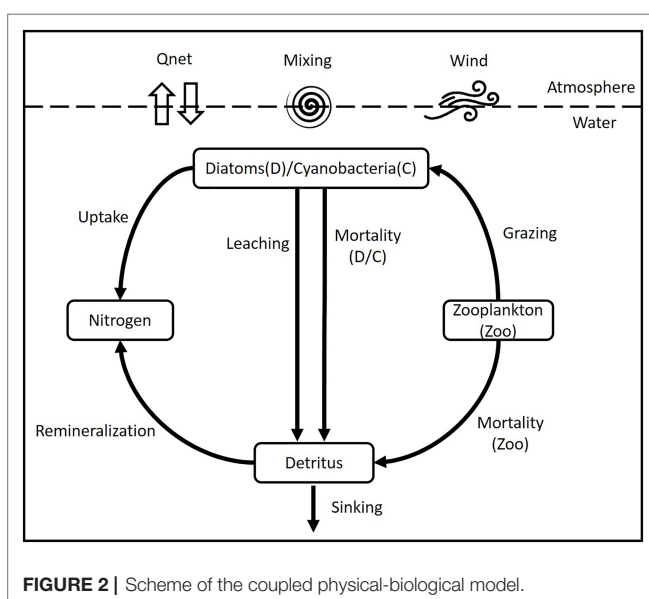


FIGURE 2 | Scheme of the coupled physical-biological model.

Model Setup and Validation

Vertical profiles of water column temperature and phosphate were taken from the monitoring station TF271 during December 2002 as initial conditions for the model (**Table 3**). The initial concentration of cyanobacteria and diatoms has a decreasing exponential distribution over depth with a surface value of 0.05 and $0.3 \text{ mmol N m}^{-3}$, respectively. The chlorophyll a concentration was expressed in terms of nitrogen using a chlorophyll a :carbon (Chl a :C) ratio of 1:50 and a Redfield ratio between carbon and nitrate (C:N) of 6.6 (Redfield, 1958). The initial concentration of zooplankton was set at $0.1 \text{ mmol N m}^{-3}$ on the surface with a decreasing exponential distribution within a vertical scale of 100 m . An initial concentration of $10^{-4} \text{ mmol N m}^{-3}$ was used for both detritus pools.

TABLE 1 | Equations of the biological model.

Variable	Equation
Attenuation light	$\beta = PAR * Q_{sw} * exp\left(-k_w * z - \int_z^0 k_{chl} * Phy * dz\right)$ (1)
Light	$\lambda = \frac{\mu_{gPhy} * \alpha_{Phy} * \beta}{\sqrt{\mu_{gPhy}^2 + \alpha_{Phy}^2 * \beta^2}}$ (2)
Grazing pressure	$\eta = Zoo * \frac{\mu_{gzPhy} * \mu_{cPhy} * Phy^2}{\mu_{gzPhy} + \mu_{cPhy} * Phy^2}$ (3)
Growth	$\Delta Phy = Phy + \left(\left(\frac{P}{P + k_{upPhy}}\right) * \lambda * Phy\right) - (\mu_{mPhy} * Phy^2) - \eta$ (4)
Grazing	$\Delta Zoo = (\gamma_1 * \eta) - (\gamma_2 * Zoo) - (\mu_{mZoo} * Zoo^2)$ (5)
Detritus fast	$\Delta Df = (\mu_{mPhy} * Phy^2) - (Df * \mu_r) - w_f \frac{dDf}{dz}$ (6)
Detritus slow	$\Delta Ds = ((1 - \gamma_1) * \eta) + (\mu_{mZoo} * Zoo^2) - (Ds * \mu_r) - w_s \frac{dDs}{dz}$ (7)
Nutrient	$\Delta P = (Df * \mu_r) + (Ds * \mu_r) + (\gamma_2 * Zoo) - \left(\left(\frac{P}{P + k_{upPhy}}\right) * \lambda * Phy\right)$ (8)

Phy refers to diatoms or cyanobacteria.

TABLE 2 | List of biological parameters used in the model.

Parameter	Symbol	Value	Range	Reference
Attenuation coefficient water (m ⁻¹)	<i>k_w</i>	0.04	–	Kirk (1994)
Attenuation coefficient chlorophyll a (m ⁻¹)	<i>k_{chl}</i>	0.03	–	Kirk (1994)
Fraction of photosynthetically active radiation	<i>PAR</i>	0.43	–	–
Maximum growth rate diatoms (d ⁻¹)	<i>μ_{gDiatoms}</i>	0.04	1-1.3*	Munkes et al. (2020)
Maximum growth rate cyanobacteria (d ⁻¹)	<i>μ_{gCyano}</i>	0.12	0.33-1*	Munkes et al. (2020)
Slope of P-I curve diatoms	<i>α_{Diatoms}</i>	1	0.025-0.72	Waniek (2003)
Slope of P-I curve cyanobacteria	<i>α_{Cyano}</i>	0.0034	0.035	Jöhnk et al. (2008)
Mortality rate diatoms (d ⁻¹)	<i>μ_{mDiatoms}</i>	0.02	0.02-0.6*	Munkes et al. (2020)
Mortality rate cyanobacteria (d ⁻¹)	<i>μ_{mCyano}</i>	0.03	0.02-0.4*	Munkes et al. (2020)
Half-saturation constant for nitrogen uptake diatoms (mmol m ⁻³)	<i>k_{upDiatoms}</i>	2	0.05-1.5*	Munkes et al. (2020)
Half-saturation constant for phosphate uptake cyanobacteria (mmol m ⁻³)	<i>k_{upCyano}</i>	2.5e-5	0.05-1.5*	Munkes et al. (2020)
Assimilation efficiency	<i>γ₁</i>	0.1	0.46, 0.76	Fasham and Evans (1995)
Excretion rate (d ⁻¹)	<i>γ₂</i>	0.03	0.03-0.11	Waniek (2003)
Maximum grazing rate diatoms (d ⁻¹)	<i>μ_{gzDiatoms}</i>	1	0.09-1.95*	Munkes et al. (2020)
Maximum grazing rate cyanobacteria (d ⁻¹)	<i>μ_{gzCyano}</i>	0.1	0.03-0.9*	Munkes et al. (2020)
Capture rate diatoms	<i>μ_{cDiatoms}</i>	3.0	1.0	Oschlies and Garçon (1999)
Capture rate cyanobacteria	<i>μ_{cCyano}</i>	1.0	1.0	Oschlies and Garçon (1999)
Grazing pressure cyanobacteria	<i>η_{Cyano}</i>	0	–	Meyer-Harms et al. (1999)
Mortality rate Zoo	<i>μ_{mZoo}</i>	0.1	0.1-0.28	Waniek (2003)
Remineralization rate (d ⁻¹)	<i>μ_r</i>	0.05	0.05	Oschlies and Garçon (1999)
Sinking velocity fast detritus (m d ⁻¹)	<i>w_f</i>	100	10	Evans and Garçon (1997)
Sinking velocity slow detritus (m d ⁻¹)	<i>w_s</i>	1.0	1.0	Evans and Garçon (1997)

*From models CEMBS, ECOSMO, ERGOM, SCOB1 and BALTSEM.

TABLE 3 | Data sets used for model setup and validation.

Variable	Type	Period	Reference/Data source
Cyanobacteria	Observations	1970-2005	Hense and Burchard (2010)
	Satellite data	1997-2013	Kahru et al. (2016)
	Observations	1990-2017	Beltran-Perez and Waniek (2021)
Diatoms	Observations	2000-2014	Groetsch et al. (2016)
Phosphate	Observations	1990-2017	https://odin2.io-warnemuende.de/
Temperature	Observations	1990-2017	https://sharkweb.smhi.se/hamta-data/ https://www.smhi.se/data/oceanografi/ladda-ner-oceanografiska-observationer/ https://sharkweb.smhi.se/hamta-data/
Net heat flux	NCEP Reanalysis	1990-2019	https://psl.noaa.gov/data/gridded/data.ncep.reanalysis.surfaceflux.html

The model was forced with daily atmospheric reanalysis data from the National Centers for Environmental Prediction (NCEP) (Kalnay et al., 1996). Forcing include air temperature, incoming solar radiation, wind speed, relative humidity and cloud cover (**Figure S1**). These data provide the basis for calculating the net heat flux and its components (long-wave radiation, sensible and latent heat flux) based on standard bulk formulation (Rahmstorf, 1990) and the estimated temperature at each time step to account for the interaction between the surface and the atmosphere. The model was implemented with a finite differential scheme of 1 m vertical resolution down to the bottom at 240 m and a daily time step. The simulations were done for each year using the same initial conditions and the respective forcing for the year, beginning in 1990 and covering a 30-year period. Thus, the observed variability in spring and summer blooms is driven by the net effect of forcing on the phenology of the bloom. A spin-up time was not included in the simulations.

The results of the model and analyses are restricted to the surface and variables directly related to the development of spring and summer blooms (**Figure 3**). These variables include nutrients in the form of nitrogen and phosphate (the latter expressed in nitrogen units using the Redfield ratio 1:16 between nitrogen and phosphorus), sea surface temperature, mixed layer depth (MLD), wind speed and net heat flux. The inter-annual variability of diatom and cyanobacteria blooms is compared with observations and satellite data from the study region. Phosphate concentration, sea surface temperature (SST) and net heat flux (Qnet) were also compared with reference data sets in order to evaluate the performance of the model (**Table 3**).

Phenology Metrics

The threshold criterion was used to identify the phenological dates for spring and summer blooms (Ji et al., 2010). It was defined as an increase in the biomass concentration above a certain level. Wasmund (1997) defined a concentration of $22\mu\text{g L}^{-1}$ as a threshold for cyanobacteria blooms in the Baltic Sea. We have taken this value as threshold for spring and summer blooms as it coincides with the biomass at which the onset and decline dates are usually reported for both blooms in the Baltic Sea. However, this threshold strongly influences the results as well as restricts in part the possibility of comparing results with other studies. For this reason we included a trend analysis to

make it more robust and comparable with other studies. Overall, the spring bloom begins on day 84 ± 6 (± 6 refers to standard deviation) and ends on day 128 ± 9 (Groetsch et al., 2016), while the summer bloom begins on day 168 ± 16 and declines after day 209 ± 13 (Beltran-Perez and Waniek, 2021). The onset of the bloom was defined as the time when the biomass is above the threshold for the first time. The decline of the bloom was set as the time after the biomass maximum reduces to values below the threshold. The duration of the bloom was estimated as the difference between the onset and decline dates of the bloom. The phenology of the bloom was calculated year by year by analyzing the biomass changes between February and May for the spring bloom and between June and August for the summer bloom.

Trend Analyses

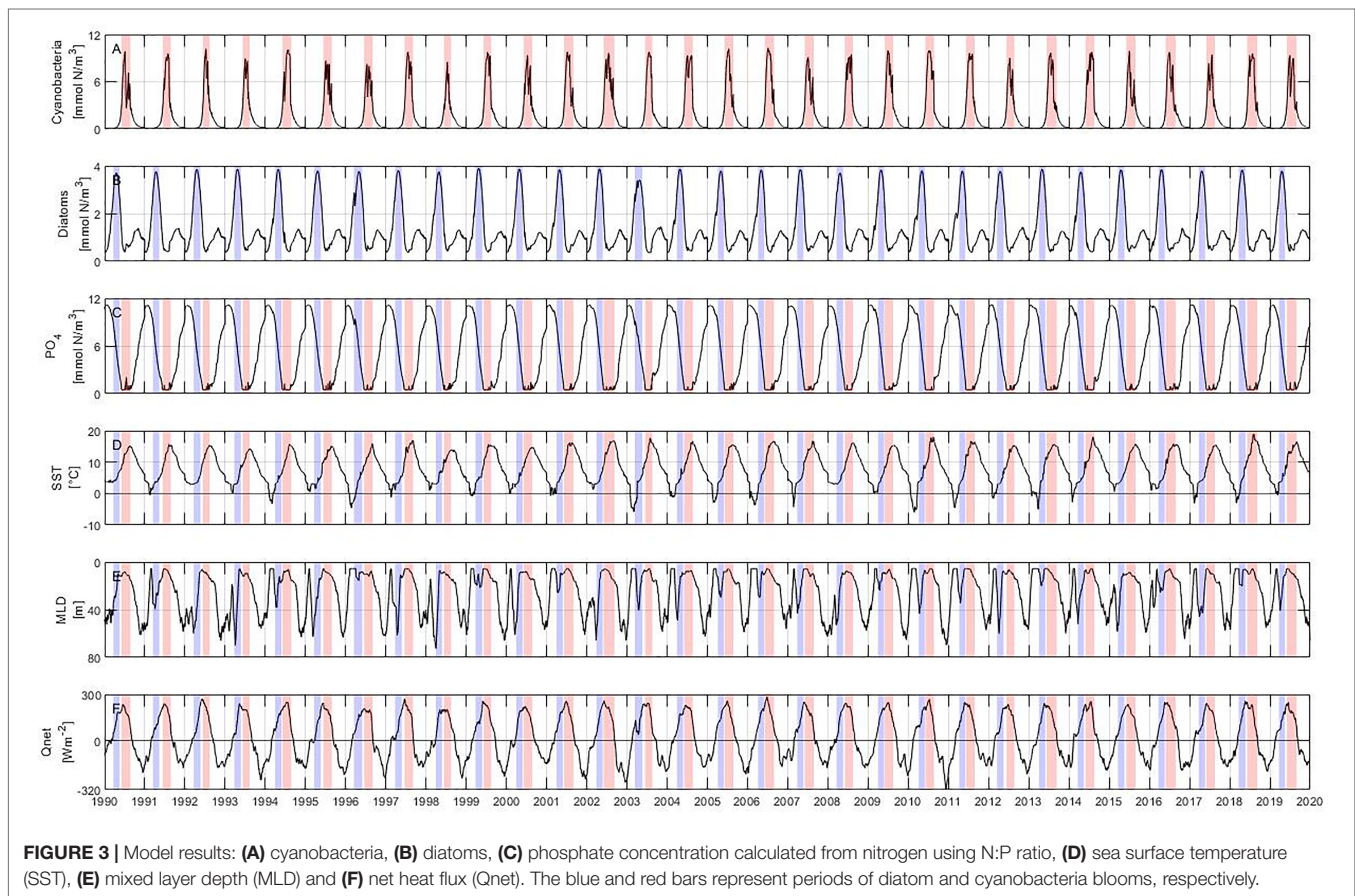
The non-parametric Mann-Kendall test (Kendall, 1975) was applied for monotonic downward or upward trends together with the non-parametric Sen method (Sen, 1968) for the slope estimate. This test tolerates outliers and it is independent of the data distribution. This method was applied on the phenological dates identified over the 30-year period for the spring and summer blooms to investigate changes in their occurrence. All calculations and trend analyses were performed in Matlab R2018b. Statistical tests were considered significant with a p-value less than or equal to 0.05.

RESULTS

Inter-Annual Variability

Summer blooms start at the beginning of June and last until the end of August, reaching their maximum concentration in mid-July (**Figure 3A**). In general, summer blooms have a length of about 3 months and reach a maximum concentration of 10 mmol N m^{-3} . Spring blooms begin on average at the end of March and last until the end of May (**Figure 3B**) with an average length of roughly 2 months. Their maximum concentrations are observed at the end of April with values around 4 mmol N m^{-3} . Diatoms usually develop a second bloom of lower abundance in autumn that is also captured by the model, but it is outside the scope of this study.

The phosphate concentration shows a cycle where the maximum concentration (around 11 mmol N m^{-3}) is reached



during January before the onset of the spring bloom (Figure 3C). The phosphate concentration decreases as the spring bloom is formed, reaching concentrations below $0.5 \text{ mmol N m}^{-3}$ at the beginning of the summer bloom. Phosphate concentration remains low throughout the summer bloom and increases only at the end of the year. The SST shows a pronounced annual cycle with a minimum in mid-February and a maximum in early August (Figure 3D).

The mixed layer depth is directly linked to changes in temperature and mixing intensity, becoming shallower as the solar radiation intensifies and temperature rises (Figure 3E). The shallowest mixed layer depth is reached at around 10 m during the summer bloom, i.e. between June and August. The highest energy gain by the ocean coincides with the end of the spring bloom and the beginning and maximum abundance of the summer bloom (Figure 3F).

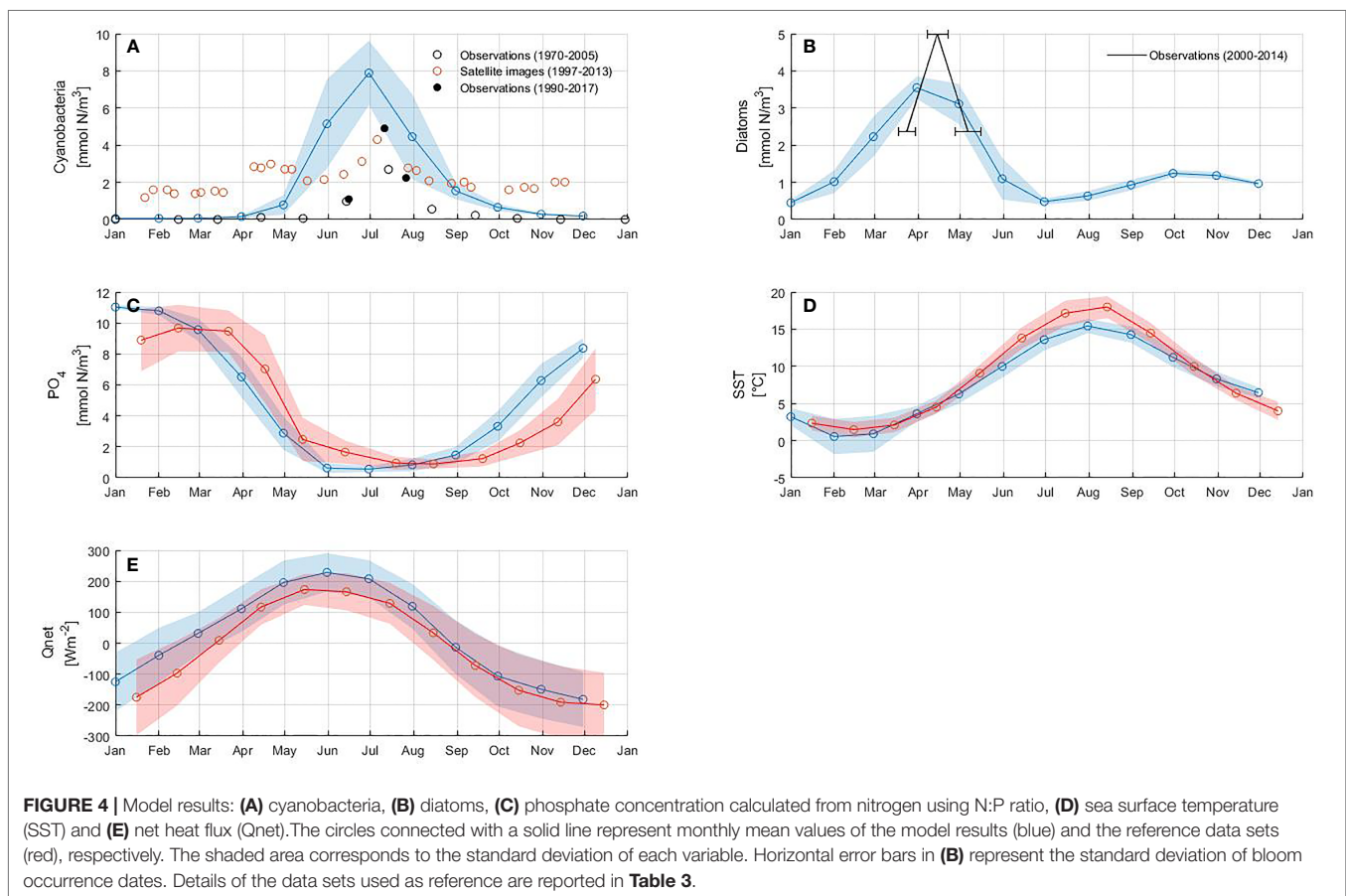
The model reproduces the typical annual cycle for spring and summer blooms (Figure 4). The inter-annual variability of both blooms is in good agreement with that derived from observations and satellite data (Figures 4A, B). However, the model underestimates the maximum concentration of the spring bloom and overestimates it for the summer bloom. The pattern of phosphate concentration, SST and net heat flux in Figures 4C–E bears a strong resemblance to the summer bloom pattern, suggesting that the highest cyanobacteria abundance coincides

with the minimum in phosphate concentration, high SST and positive net heat flux. The onset of the spring bloom coincides with the maximum phosphate concentration as well as with the increase in SST and net heat flux.

Changes in Phenology of Diatom and Cyanobacteria Blooms

The phenology of the spring and summer blooms is summarized in Tables S1, S2, respectively. The phenology of both blooms is compared with phenological dates derived from observations and satellite data in Figures 5, 6. The onset of the spring bloom coincides with the average onset reported by Groetsch et al. (2016) on day 85 ± 7 . The peak and decline dates occur on day 115 ± 6 and 144 ± 5 , respectively. Therefore, the length of the bloom is on average 59 ± 4 days. Our phenological dates differ to the observed peak and decline dates by 9 and 17 days, respectively, with the largest differences occurring at the end of the bloom.

Based on the results of the model, the summer bloom starts on day 158 ± 5 , reaches its maximum biomass on day 194 ± 9 and declines on day 237 ± 8 . On average the bloom lasts 79 ± 9 days. Similar to the results for the spring bloom, there is a discrepancy between our results, observations and satellite data. The bloom begins 9 and 38 days earlier than in observations and satellite data, respectively. The occurrence of the maximum coincides with *in situ* observations, but not with satellite data.



The maximum occurs on day 194 in the model and observations, but 15 days later in satellite data. The largest difference is at the end of the bloom. According to our results the bloom ends on day 237, but using observations and satellite data it ends 27 and 22 days earlier, respectively.

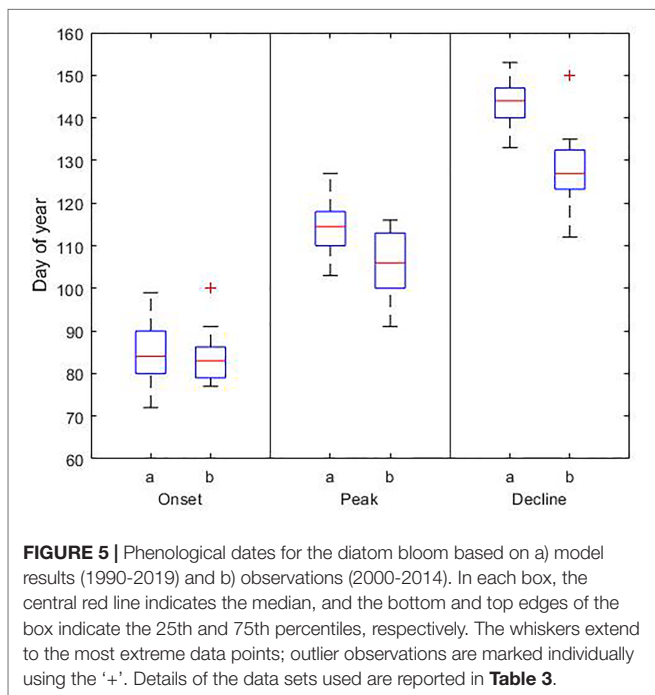
The inter-annual variability of the summer bloom showed significant temporal changes (p -value < 0.05) in the onset and length of the bloom (**Figure 7**). Summer blooms occur 9 days earlier, starting on day 152 in 2019 instead of day 161 in 1990 in the Gotland Basin. They last 15 days longer, increasing their length from 72 days in 1990 to 87 days in 2019. However, a longer bloom did not necessarily lead to a higher abundance of cyanobacteria. No temporal changes were found for the peak or decline dates of the summer bloom. The spring bloom showed no statistically significant changes in phenology and abundance over the 30-year period.

Effect of Environmental Variables on Bloom Phenology

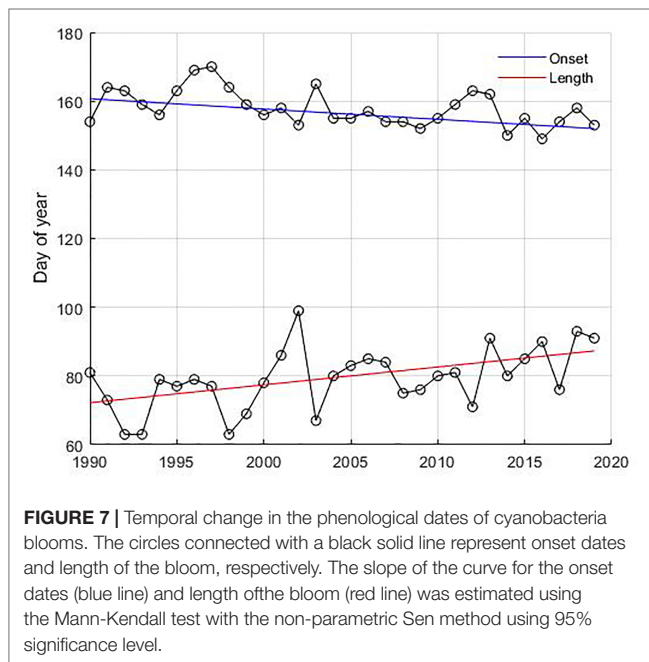
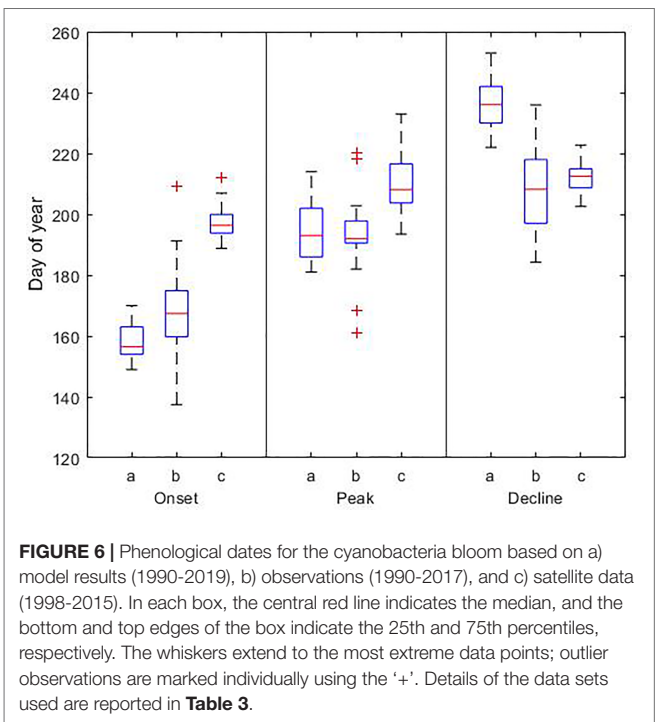
To emphasize the changes in spring and summer blooms occurrence and their relationship with SST, wind and net heat flux we have calculated the anomalies for SST, wind and net heat flux with respect to each bloom period (**Figures S2, S3**). We selected years with the higher positive and negative anomalies for

each variable during the development of each bloom, i.e. during February and May for the spring bloom and June and August for the summer bloom (**Tables 4, 5** and **Figures 8, 9**). During the spring bloom, the SST was around 1.5°C higher than average in 1990, 2008 and 2015 and lower roughly 2 °C in 1996, 2003 and 2010 (**Figure S2A**). Summer blooms were observed at SST roughly 0.5°C higher than average in 1990, 2002 and 2018 and 0.5°C lower in 1996, 2015 and 2017 (**Figure S3A**). SST anomalies indicate that the spring and summer seasons were warmer than average during 1990, while colder during 1996. In 2015 a warm spring followed by a cold summer was observed, both seasons were characterized by particularly strong winds (**Figures S2B, S3B**). Winds 1 ms⁻¹ higher than average were found during spring blooms in 1997, 2015 and 2019. The stronger winds during summer blooms are roughly 0.5 ms⁻¹ higher than average and occurred in 1998, 2004 and 2015. The response of the spring bloom changes over time but a strong relationship with the heat exchange between atmosphere and surface ocean was not observed (**Figure S2C**). On the contrary, summer blooms are generally observed to coincide with positive net heat flux anomalies (high energy gain) and negative wind anomalies (calm wind conditions), which are linked to higher water column stability (**Figure S3C**).

There is a statistically significant change in the occurrence of the spring bloom with respect to SST (**Table 4**). During warmer



periods the peak of the bloom occurs on average on day 109, while in cooler periods it occurs on day 121. As a result, spring blooms reach maximum biomass 12 days earlier in warmer periods. No further significant changes in phenology or abundance were found for the spring bloom.



A significant difference in cyanobacteria biomass is found when comparing positive and negative SST anomalies (**Table 5**). Cyanobacteria blooms develop higher biomass during warmer periods than during colder periods. There is also a significant difference in the biomass, decline dates, length and maximum peak of the summer bloom when comparing positive and negative net heat flux anomalies. Thus, a higher energy gain (positive net heat flux) by the ocean leads to a bloom with higher abundance and maximum peak as well as the extension of the bloom by delaying its end by around 19 days.

The highest cyanobacteria abundance coincides with calm wind conditions (**Figure 9**), however no statistically significant difference was found between the occurrence of the bloom and calm wind (p -value > 0.05, **Table 5**). Similarly, the spring bloom did not show a statistically significant difference with respect to the wind strength (**Table 4**).

DISCUSSION

Inter-annual and temporal variability of spring and summer blooms in the Gotland Basin has been described by Wasmund and Uhlig (2003); Janssen et al. (2004); Wasmund et al. (2011), but the phenology and response of these blooms to changing environmental conditions have been studied less extensively and remain unclear (Kahru and Elmgren, 2014; Groetsch et al., 2016; Kahru et al., 2016). Our results show that the occurrence of spring and summer blooms is affected differently by changes in SST, wind and net heat flux. The mixing in the water column is largely related to density changes (through buoyancy forcing by net heat flux) that drive the variability of the mixed layer (**Figures 3D-F**).

The onset of the spring bloom is consistent with the findings of Groetsch et al. (2016), who estimated the phenology of

TABLE 4 | Diatoms biomass integrated over the bloom period (February-May) calculated for the periods with the highest (+) and smallest (-) anomalies in SST, wind and net heat flux (Qnet).

Anomaly	Year	Day of year			Length (days)	Max peak ($\mu\text{g L}^{-1}$)	Biomass ($\mu\text{g L}^{-1}$)
		Onset	Peak	Decline			
SST (+) (warmer periods)	1990	80	107	135	55	267	13438
	2008	79	111	139	60	266	14459
	2015	80	108	138	58	276	14526
SST (-) (colder periods)	1996	75	122	151	76	271	17634
	2003	72	117	140	68	245	15345
	2010	96	123	150	54	274	13455
Wind (+) (stronger wind)	1997	84	113	144	60	274	14933
	2015	80	108	138	58	276	14526
	2019	82	109	138	56	272	13887
Wind (-) (weaker wind)	2009	90	118	146	56	275	13990
	2010	96	123	150	54	274	13455
	2016	83	111	140	57	277	14316
Qnet (+) (higher gain)	2003	72	117	140	68	245	15345
	2010	96	123	150	54	274	13455
	2014	80	107	136	56	270	13790
Qnet (-) (less gain)	1991	75	103	133	58	270	14273
	1997	84	113	144	60	274	14933
	2005	95	123	149	54	272	13376

The values in bold correspond to values with a significant difference by comparing the positive and negative anomaly (p -value < 0.05).

the spring bloom from a 15-year time series (2000–2014) of ship-of-opportunity chlorophyll a fluorescence observations for different regions in the Baltic Sea. However, in our results the average peak and decline dates occur later than in the aforementioned study. The use of a fixed threshold in our study ($22 \mu\text{g L}^{-1}$) instead of the 10th and 90th percentiles before and after the bloom peak used by Groetsch et al. (2016) resulted in a later occurrence of the peak and decline dates, as more time is allowed for spring and summer blooms to exceed the specified threshold value. The discrepancy between both studies may be explained by

the method used to quantify the biomass, and the threshold criteria used for the computation of the phenological dates. The definition of the threshold at which bloom begins or ends differs between studies, a trend analysis is more robust and therefore it was used to compare with other studies.

Earlier spring blooms have previously been reported for the Baltic Sea (Fleming and Kaitala, 2006; Klais et al., 2013). Our study showed that higher temperatures cause the spring bloom to peak earlier, but this was not observed over the 30-year period, i.e. changes in the timing of the peak occurrence over the 30-year

TABLE 5 | Cyanobacteria biomass integrated over the bloom period (June-August) calculated for the periods with the highest (+) and smallest (-) anomalies in SST, wind and net heat flux (Qnet).

Anomaly	Year	Day of year			Length (days)	Max peak ($\mu\text{g L}^{-1}$)	Biomass ($\mu\text{g L}^{-1}$)
		Onset	Peak	Decline			
SST (+) (warmer periods)	1990	154	187	235	81	710	33481
	2002	153	198	252	99	696	44621
	2018	158	208	251	93	691	43678
SST (-) (colder periods)	1996	169	195	248	79	596	32618
	2015	155	185	240	85	713	33305
	2017	154	204	230	76	682	32044
Wind (+) (stronger wind)	1998	164	195	227	63	613	21902
	2004	155	185	235	80	673	42030
	2015	155	185	240	85	713	33305
Wind (-) (weaker wind)	1999	159	193	228	69	702	37174
	2006	157	188	242	85	740	44206
	2018	158	208	251	93	691	43678
Qnet (+) (higher gain)	1997	170	202	247	77	705	38374
	2002	153	198	252	99	696	44621
	2006	157	188	242	85	740	44206
Qnet (-) (less gain)	1993	159	183	222	63	645	27667
	1998	164	195	227	63	613	21902
	2000	156	192	234	78	675	32895

The values in bold correspond to values with a significant difference by comparing the positive and negative anomaly (p -value < 0.05).

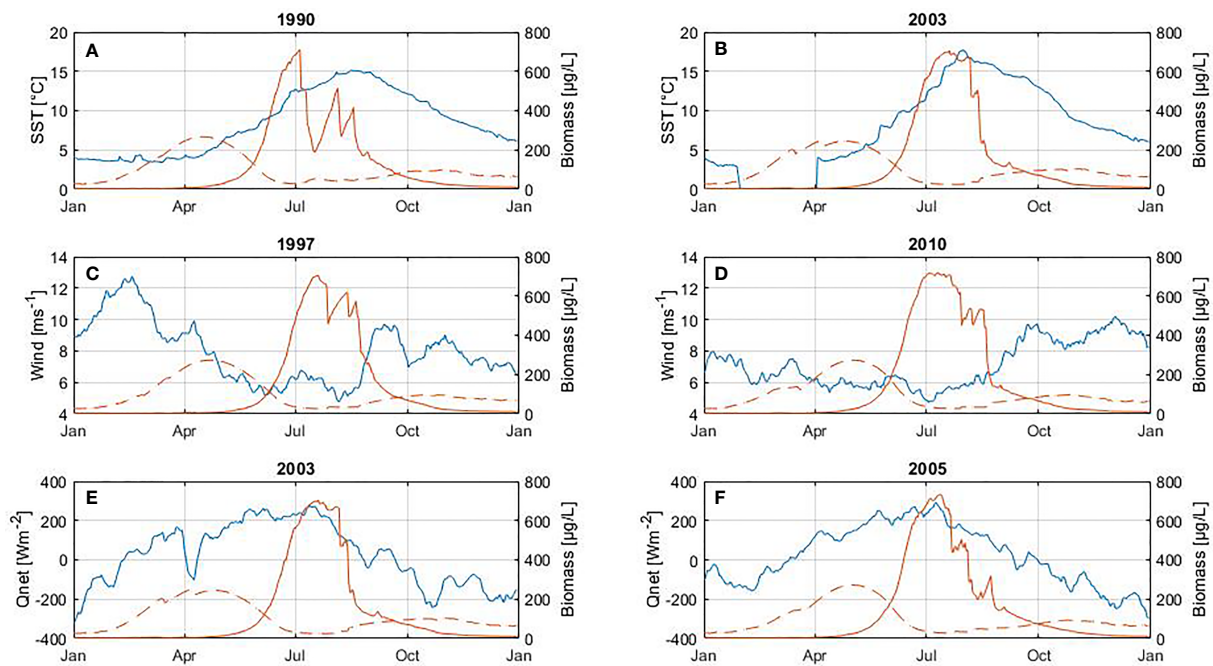


FIGURE 8 | Influence of SST (A, B), wind (C, D) and net heat flux (E, F) on diatom biomass (between February and May). At the top of each plot is shown the year with the highest positive anomalies (left panel) and negative anomalies (right panel) for each variable. The blue line corresponds to the variable (left axes) and the red line to biomass (right axes) of diatoms (dashed line) and cyanobacteria (solid line). The cyanobacteria bloom is included only to illustrate its inter-annual cycle.

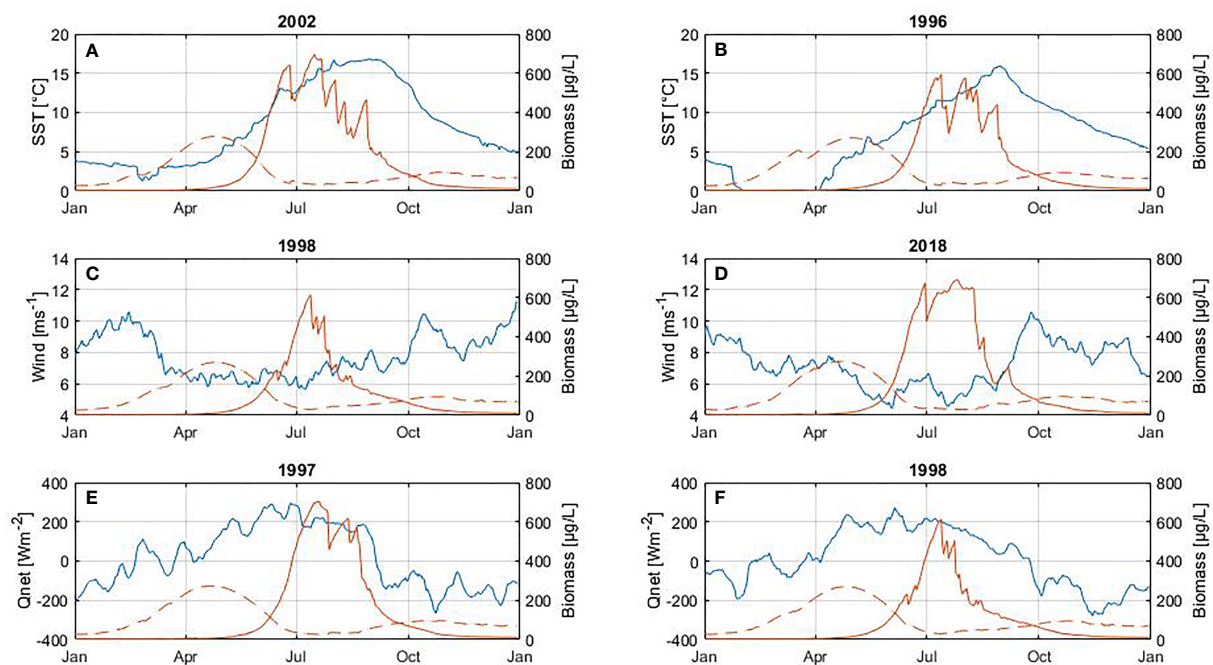


FIGURE 9 | Influence of SST (A, B), wind (C, D) and net heat flux (E, F) on cyanobacteria biomass (between June and August). At the top of each plot is shown the year with the highest positive anomalies (left panel) and negative anomalies (right panel) for each variable. The blue line corresponds to the variable (left axes) and the red line to biomass (right axes) of diatoms (dashed line) and cyanobacteria (solid line). The diatom bloom is included only to illustrate its inter-annual cycle.

period were not statistically significant (p -value > 0.05). Wasmund et al. (2011) also reported that there is no trend for the spring bloom in the eastern Baltic Sea during the period 1979 to 2005. However, other studies have found that spring blooms tend to develop earlier and less intense. Kahru et al. (2016) showed an advance of the growth season at a mean rate of 1.6 days per year for the spring bloom in the entire Baltic Sea. Groetsch et al. (2016) found a positive trend in the bloom length of 1 ± 0.20 day per year and a negative trend in chlorophyll a maximum of 0.31 ± 0.10 mg m⁻³ per year for the spring bloom over the period 2000 to 2014, attributing it to the gradual reduction of nutrients load in the Baltic Sea. Long-term data sets from 1979 to 2011 also showed a decrease in diatom abundance during the spring bloom in the Baltic Proper (Wasmund and Uhlig, 2003; Wasmund et al., 2013).

The phenology of the spring bloom seems to be affected only by SST (**Figure 8** and **Table 4**), which result in the spring bloom reaching its maximum abundance earlier. Higher temperatures favor the spring bloom by intensifying stratification, which increases light in a shallow mixed layer following the critical depth hypothesis (Sverdrup, 1953), as Sommer et al. (2012) confirmed using several temperatures and light levels in a series of mesocosm experiments. Light is necessary for phytoplankton photosynthesis and growth, while temperature influences growth rates and stratification. Wind has a dual effect on the bloom. On the one hand, strong winds induce mixing that favors redistribution of the resting stages of diatoms and nutrients in the water column (Hjerne et al., 2019). On the other hand, calm wind conditions are associated with lower energy losses or energy gain on the surface, increasing temperature and stratification of the water column (Wasmund et al., 1998; Wasmund and Uhlig, 2003; Wasmund et al., 2013). Therefore, according to our results and those from other studies (Groetsch et al., Reynolds et al., 1984; Spilling and Markager, 2008; Sommer et al., 2012; Wasmund et al., 2013), the spring bloom is favored by the ability of diatoms to proliferate despite strong wind (**Figure 3B** and **Figure S1C**) following Margalef's mandala (Margalef, 1978), the availability of nutrients during the first months of the year (**Figures 3B, C**) and the increasing amount of light as well (**Figure 3B** and **Figure S1B**) following Sverdrup's hypothesis (Sverdrup, 1953).

We found evidence that the occurrence of earlier maximum abundance in the spring bloom was related to warm weather conditions (**Figure 8** and **Table 4**). Changes in the spring bloom phenology may influence the survival of higher trophic levels due to variations in timing of food availability (match-mismatch hypothesis) (Smith and Hollibaugh, 1993; Winder and Schindler, 2004), i.e. the energy and carbon transfer from primary production to pelagic fish production (Sommer et al., 2012). A shift in the spring bloom may inhibit the survival of zooplankton and fish, affecting the recruitment of larvae as larval spawning continues to match the original timing of the bloom prior to changes (Cole, 2014; Gittings et al., 2018). As a result, potential negative impacts can be expected on the Baltic Sea ecosystem if changes in the phenology of phytoplankton blooms continue in conjunction with current changes in the environment.

The occurrence of the maximum cyanobacteria abundance in the model coincides with *in situ* observations but not with that estimated based on satellite data. There are, however, differences in

the onset and decline of the bloom probably due to the definition of the threshold at which species abundance exceeds normal values in the water. The lack of consensus on the definition of thresholds in phenological studies makes it difficult to compare the results between them. In fact, using thresholds defined on a percentile basis like in other studies, our results deviate from the time at which cyanobacteria blooms usually occur in the Baltic Sea (i.e. between June and August). Additionally, to the uncertainty surrounding the defined threshold at which the bloom develops, it is not surprising that our results vary from the phenological dates identified based on satellite imagery. Remote sensing is able to detect blooms only when strong surface aggregations are formed, which usually occurs at an advanced bloom stage and directly related with the cyanobacteria species *Nodularia spumigena*, the only species of the summer bloom in the Baltic Sea that forms dense surface accumulations. *Nodularia spumigena* is a co-dominant cyanobacteria species in the Baltic Sea, the other co-dominant species, *Aphanizomenon* sp. and *Dolichospermum* spp., although both are present during the bloom, these species are typically found at the subsurface and therefore not specifically detected through satellites (Kahru and Elmgren, 2014; Eigemann et al., 2018; Kahru et al., 2020).

Until now, there has been no consensus on whether cyanobacteria blooms will increase or decrease in the future (Wasmund and Uhlig, 2003; Kahru and Elmgren, 2014; Kahru et al., 2016; Meier et al., 2019). Our results support the findings of other studies which point to summer blooms starting earlier and lasting longer. We found that the summer bloom is occurring 0.3 days earlier each year and extending its length by 0.5 days per year. Kahru and Elmgren (2014) found progressively earlier accumulations of cyanobacteria in summer by approximately 0.6 days per year over a 35-year period. Kahru et al. (2016) also found trends towards an earlier start of the spring and summer blooms. Contrary to these results, Wasmund and Uhlig (2003) found no indication that cyanobacteria blooms have increased during the period 1979–1999, even if there is a tendency to decrease in some basins of the Baltic Sea. On the one hand, observations from satellites in the Baltic Sea are based on chlorophyll a and focused on specific species of cyanobacteria such as *Nodularia spumigena*, which forms dense surface accumulations (Kahru and Elmgren, 2014; Kahru et al., 2020). On the other hand, *in situ* observations of phytoplankton biomass are usually integrated over the water column and the frequency of observations is limited in time and space, which in case of blooms may lead to differences in the estimated biomass and phenology of the bloom when compared to other studies even during similar periods of time and locations. Although the results from observations and satellites may vary, they are the closest approximations available to identify and validate bloom phenology as long-term *in situ* data sets and studies defining bloom phenology are still scarce. Therefore, they have been used in this study and compared despite their significant differences, being aware of the limitations of both approaches (Kahru and Elmgren, 2014; Gittings et al., 2019).

Overall, cyanobacteria species are able to uptake a large amount of nutrients and store them to maintain growth and survive for days (Kanoshina et al., 2003; Flores and Herrero, 2005). Therefore, cyanobacteria blooms are able to develop under

depleted phosphorus (limiting nutrient) conditions (**Figures 3C, 4C**) (Wasmund, 1997; Lignell et al., 2003). Cyanobacteria abundance is coupled with SST at seasonal and inter-annual time scales (**Figures 3, 4**), signifying that warmer periods favor cyanobacteria growth (**Table 5**) as other studies have also indicated (Hense et al., 2013). Warm years characterised by higher cyanobacteria biomass (e.g. 1990, 2002 and 2018) coincide with a shallower MLD and stratified water column (**Figures 3A, D-F**).

The change in the length of the summer bloom was not observed in connection with temperature, but rather with net heat flux (**Figure 9** and **Table 5**). For years with a strong heat gain during summertime such as 1997, 2002, 2006 the bloom extends on average 19 days compared to years with lower heat gain such as 1993, 1998, 2000, which is in agreement with the trend observed for the summer bloom to extend its length over the entire 30-year period. The energy gain by the water column contributes significantly to the increase in bloom abundance by intensifying stratification. Cyanobacteria blooms do not tolerate turbulence so calm wind conditions and a strongly stratified water column favor their development resulting in longer blooms (**Table 5**). These results are supported by Beltran-Perez and Waniek (2021) who demonstrated that the phenology of cyanobacteria blooms is explained by the energy exchange between the atmosphere and the ocean. Only a few studies have highlighted the role of energy exchange at the ocean-atmosphere interface that regulates mixing in the water column in the context of phenology studies so far (Gittings et al., 2018; Beltran-Perez and Waniek, 2021).

Our results showed that changes in wind strength do not lead to changes in bloom phenology as Kahru et al. (2020) also indicated for cyanobacteria accumulations and wind on a decadal and inter-annual time scale. Calm wind may have an influence on the development of the bloom as reported by other studies (Wasmund, 1997; Kanoshina et al., 2003), but in this study, if there is such an influence, it was not statistically significant.

Water temperature has been increasing during the past 100 years and it is projected to further increase between 1.1°C to 3.2 °C by the end of this century in the Baltic Sea (HELCOM/ Baltic Earth, 2021). Higher temperatures intensify stratification and therefore favor the occurrence of summer blooms. Our results support the occurrence of earlier and longer blooms, but there is much uncertainty about whether cyanobacteria blooms may increase in the future. The observed changes in the phenology of summer blooms and their relationship with global warming suggest that cyanobacteria blooms will remain a major concern for the Baltic Sea. They may accelerate eutrophication and oxygen depletion in the water column (Larsson et al., 1985; Wasmund, 1997; Janssen et al., 2004) and have stronger impacts on fishing and recreational use of coastal waters (Paerl and Huisman, 2009; Neil et al., 2012), as many species of cyanobacteria produce toxins. Alterations in the food web are also expected as the efficiency of energy transfer to higher trophic levels may reduce due to the poor food quality of cyanobacteria for grazers, depending on the availability of other sources of food and the type of zooplankton and cyanobacteria species (Meyer-Harms et al., 1999; Ger et al., 2016; Munkes et al., 2020).

The Baltic Sea is one of the most intensively monitored seas in the world; however, its observations are not sufficient to determine

in detail phytoplankton phenology. Coupling of data on species-specific life cycles and succession to environment conditions (e.g. nutrient ratios, light, temperature), other organisms (e.g. prey, predators, competitors), as well as to process-based models appears necessary to explain the timing and intensity of spring and summer blooms in the study area and neighboring habitats. A simple, one-dimensional, coupled physical-biological model based on the basic equations governing bloom formation was able to reproduce the development of the bloom with reliable results and showed the effect of forcing on phenology of both blooms. Therefore, the use of models provides a solid basis for testing phytoplankton bloom hypothesis as observations are limited and may not necessarily cover the bloom development because samples are usually taken during specific very limited time periods and locations.

CONCLUSIONS

Overall, the model reproduces the inter-annual and temporal variability of spring and summer blooms considering the constraints and limitations of the model. On average the spring bloom started on day 85, reached its maximum on day 115 and declined on day 144. Warmer periods cause the spring bloom to peak earlier, but no statistically significant trend was found for the spring bloom over the period 1990 to 2019. The summer bloom started on day 158, had its maximum on day 194 and declined after day 237. Summer blooms were found to occur 9 days earlier and last 15 days longer over a 30 year period. Our results differ from results of other phenological studies mainly at the end of both blooms. More phenological studies are needed to define with certainty the changes in the occurrence of spring and summer blooms over time.

The influence of environmental variables such as sea surface temperature, wind and net heat flux on the occurrence of spring and summer blooms was confirmed. It was observed that warmer periods affect the spring and summer blooms differently. The spring bloom reaches its maximum earlier whereas the summer bloom increases its abundance. The heat exchange between the water and the atmosphere also had a significant influence on the summer bloom. A stronger heat gain delays the end of the summer bloom, increases its length, abundance and leads to higher biomass maxima due to greater water column stability. Overall, summer blooms are more sensitive to changes in the environment than spring blooms, therefore summer blooms are expected to react more quickly to the changes generated by climate change in the Baltic Sea. However, minor changes in the spring bloom may significantly affect the quantity and quality of food reaching the seafloor, leading to alterations in the entire ecosystem. Further research is needed to follow in detail the development of phytoplankton blooms and succession changes that may occur in response to changes in the environment.

Process-based models provide process- and feedback-understanding, since observations alone are usually limited in time and space. However, parameterization remains one of the main sources of uncertainty in all models. Our one-dimensional

model provides reliable insight into the inter-annual variability of spring and summer blooms and the effect of forcing on phenology of both blooms considering model limitations and assumptions. The threshold method showed the best results with respect to the metrics used to identify bloom phenology. However, phytoplankton response to changes and threshold values is far from universal and depends on species-by-species and site-by-site basis (Hallegraeff et al., 2021). There is an urgent need defining a threshold, which should full fill the following criteria: 1) be valid for different blooms, 2) be applicable to blooms around the globe and 3) be set up based on observations. Right now the only threshold that meets partly these characteristics corresponds to $22 \mu\text{g L}^{-1}$ ($2.7 \text{ mmol N m}^{-3}$). It was previously reported by Wasmund (1997) in the identification of cyanobacteria bloom in the Baltic Sea, but its general applicability to define bloom phenology was not yet tested, as far as we are aware of.

More complex models or techniques such as statistical models, genetic algorithm and machine learning need to be explored in more detail in order to improve the modeling of phytoplankton blooms and thus their phenology. Overall, more frequent observations of e.g. growth and mortality rates, isotope markers or other physiological indicators (e.g. genomics, transcriptomics, proteomics, metabolomics) provide a broader understanding of bloom phenology and longer data sets for model initialization and validation, data sets needed to improve the performance of our and other models.

DATA AVAILABILITY STATEMENT

Publicly available data sets were used in this study. The data can be found here: <https://odin2.io-warnemuende.de/>, <https://sharkweb.smhi.se/hamta-data/>, <https://www.smhi.se/data/oceanografi/ladda-ner-oceanografiska-observationer/> and <https://psl.noaa.gov/data/gridded/data.ncep.reanalysis.surfaceflux.html>.

REFERENCES

- Beckmann, A. and Hense, I. (2007). Beneath the surface: Characteristics of Oceanic Ecosystems Under Weak Mixing Conditions - A Theoretical Investigation. *Prog. Oceanogr.* 75, 771–796. doi: 10.1016/j.pocean.2007.09.002
- Beltran-Perez, O. D. and Waniek, J. J. (2021). Environmental window of cyanobacteria bloom occurrence. *J. Mar. Syst.* 224, 103618. doi: 10.1016/j.jmarsys.2021.103618
- Bianchi, T. S., Engelhaupt, E., Westman, P., Andr n, T., Rolff, C. and Elmgren, R. (2000). Cyanobacterial Blooms in the Baltic Sea: Natural or Human-Induced? *Limnol. Oceanogr.* 45, 716–726. doi: 10.4319/lo.2000.45.3.0716
- Breitburg, D., Levin, L. A., Oschlies, A., Gr goire, M., Chavez, F. P., Conley, D. J., et al. (2018). Declining Oxygen In the Global Ocean and Coastal Waters. *Science* 359. doi: 10.1126/science.aam7240. (80), 1–11.
- Carey, C. C., Ibelings, B. W., Hoffmann, E. P., Hamilton, D. P. and Brookes, J. D. (2012). Eco-Physiological Adaptations That Favour Freshwater Cyanobacteria in a Changing Climate. *Water Res.* 46, 1394–1407. doi: 10.1016/J.WATRES.2011.12.016
- Cole, H. S. (2014). *The Natural Variability and Climate Change Response in Phytoplankton* (UK: University of Southampton). Doctoral Dissertation.
- Resource Identification Initiative: MATLAB, RRID: SCR_001622, NCBI Taxon: 2836, NCBI Taxin: 2864, NCBI Taxon: 1117.

AUTHOR CONTRIBUTIONS

JW provided the initial version of the model and supervised the study. OB-P extended the model to other phytoplankton species, calibrated and validated the model outputs, analyzed the data, produced the figures and wrote the manuscript. JW and OB-P contributed to the interpretation of results, the discussion and subsequent edits of the manuscript. Both authors have read and agreed to the published version of the manuscript.

FUNDING

Funding granted by the DAAD program: Research Grants - Doctoral Programmes in Germany 2018/19.

ACKNOWLEDGMENTS

The authors thank the DAAD for the funding granted and the Leibniz Institute for Baltic Sea Research (IOW) for the facilities, data access, and support provided during the writing of the manuscript. We want to acknowledge the anonymous reviewers for their constructive comments that helped us to improve the quality of the manuscript.

SUPPLEMENTARY MATERIAL

The Supplementary Material for this article can be found online at: <https://www.frontiersin.org/articles/10.3389/fmars.2022.928633/full#supplementary-material>

- Daewel, U. and Schrum, C. (2017). Low-Frequency Variability in North Sea and Baltic Sea Identified Through Simulations with the 3-D Coupled Physical-Biochemical Model ECOSMO. *Earth Syst. Dyn.* 8, 801–815. doi: 10.5194/esd-8-801-2017
- Dzierzbicka-Głowacka, L., Janecki, M., Nowicki, A. and Jakacki, J. (2013). Activation of the Operational Ecohydrodynamic Model (3D CEMBS) - The Ecosystem Module. *Oceanologia* 55, 543–572. doi: 10.5697/oc.55-3.543
- Eigemann, E., Schwartke, M. and Schulz-Vogt, H. (2018). Niche Separation of Baltic Sea Cyanobacteria During Bloom Events by Species Interactions and Autecological Preferences. *Harmful Algae* 72, 65–73. doi: 10.1016/j.hal.2018.01.001
- Evans, G. and Garçon, V. C. (1997). "One-Dimensional Models of Water Column Biogeochemistry," in *JGOFS Rep. 23/97* (Bergen, Norway: Scientific Committee on Oceanic Research), 4–7.
- Fasham, M. J. and Evans, G. T. (1995). The Use of Optimization Techniques to Model Marine Ecosystem Dynamics at the JGOFS Station at 47° N 20° W. *Philos. Trans. R. Soc. London. Ser. B Biol. Sci.* 348, 203–209. doi: 10.1098/RSTB.1995.0062
- Fleming, V. and Kaitala, S. (2006). Phytoplankton Spring Bloom Intensity Index for the Baltic Sea Estimated for the Years 1992 to 2004. *Hydrobiologia* 554, 57–65. doi: 10.1007/s10750-005-1006-7

- Flores, E. and Herrero, A. (2005). Nitrogen Assimilation and Nitrogen Control in Cyanobacteria. *Biochem. Soc. Trans.* 33, 164–167. doi: 10.1042/BST0330164
- Ger, K. A., Urrutia-Cordero, P., Frost, P. C., Hansson, L. A., Sarnelle, O., Wilson, A. E., et al. (2016). The Interaction Between Cyanobacteria and Zooplankton in a More Eutrophic World. *Harmful Algae* 54, 128–144. doi: 10.1016/j.hal.2015.12.005
- Gittings, J. A., Raitos, D. E., Kheireddine, M., Racault, M. F., Claustre, H. and Hoteit, I. (2019). Evaluating Tropical Phytoplankton Phenology Metrics Using Contemporary Tools. *Sci. Rep.* 9, 1–9. doi: 10.1038/s41598-018-37370-4
- Gittings, J. A., Raitos, D. E., Krokos, G. and Hoteit, I. (2018). Impacts of Warming on Phytoplankton Abundance and Phenology in a Typical Tropical Marine Ecosystem. *Sci. Rep.* 8, 1–12. doi: 10.1038/s41598-018-20560-5
- Groetsch, P. M., Simis, S. G., Eleveld, M. A. and Peters, S. W. (2016). Spring Blooms in the Baltic Sea have Weakened but Lengthened from 2000 to 2014. *Biogeosciences* 13, 4959–4973. doi: 10.5194/bg-13-4959-2016
- Gustafsson, E. (2012). Modelled Long-Term Development of Hypoxic Area and Nutrient Pools in the Baltic Proper. *J. Mar. Syst.* 94, 120–134. doi: 10.1016/j.jmarsys.2011.11.012
- Hallegraeff, G. M., Anderson, D. M., Belin, C., Bottein, M.-Y. D., Bresnan, E., Chinain, M., et al. (2021). *Perceived Global Increase in Algal Blooms is Attributable to Intensified Monitoring and Emerging Bloom Impacts* (Commun). doi: 10.1038/s43247-021-00178-8
- Hashioka, T., Sakamoto, T. T. and Yamanaka, Y. (2009). Potential Impact of Global warming on North Pacific spring blooms projected by an eddy-permitting 3-D Ocean Ecosystem Model. *Geophys. Res. Lett.* 36, 1–5. doi: 10.1029/2009GL038912
- HELCOM/Baltic Earth (2021). “Climate Change in the Baltic Sea,” in *2021 Fact Sheet. Tech. rep.* (Helsinki, Finland: Helsinki Commission - HELCOM)
- HELCOM (2012). *Manual for Marine Monitoring in the COMBINE Programme of HELCOM* (Helsinki, Finland: Helsinki Commission - Baltic Marine Environment Protection Commission).
- HELCOM (2018). “Diatom / Dinoflagellate index,” in *HELCOM pre-core Indic. Rep.*, vol. 2, 1–15.
- Hense, I. and Burchard, H. (2010). Modelling Cyanobacteria in Shallow Coastal Seas. *Ecol. Modell.* 221, 238–244. doi: 10.1016/j.ecolmodel.2009.09.006
- Hense, I., Meier, H. E. and Sonntag, S. (2013). Projected Climate Change Impact on Baltic Sea Cyanobacteria: Climate Change Impact on Cyanobacteria. *Clim. Change* 119, 391–406. doi: 10.1007/s10584-013-0702-y
- Henson, S. A., Dunne, J. P. and Sarmiento, J. L. (2009). Decadal Variability in North Atlantic Phytoplankton Blooms. *J. Geophys. Res. Ocean.* 114, 1–11. doi: 10.1029/2008JC005139
- Hjerne, O., Hajdu, S., Larsson, U., Downing, A. and Winder, M. (2019). Climate Driven Changes in Timing, Composition and Size of the Baltic Sea Phytoplankton Spring Bloom. *Front. Mar. Sci.* 6. doi: 10.3389/fmars.2019.00482
- Janssen, F., Neumann, T. and Schmidt, M. (2004). Inter-annual Variability in Cyanobacteria Blooms in the Baltic Sea Controlled by Wintertime Hydrographic Conditions. *Mar. Ecol. Prog. Ser.* 275, 59–68. doi: 10.3354/meps275059
- Ji, R., Davis, C. S., Chen, C., Townsend, D. W., Mountain, D. G. and Beardsley, R. C. (2008). Modeling the Influence of Low-Salinity Water Inflow on Winter-Spring Phytoplankton Dynamics in the Nova Scotian Shelf-Gulf of Maine Region. *J. Plankton Res.* 30, 1399–1416. doi: 10.1029/2007GL032010
- Ji, R., Edwards, M., MacKas, D. L., Runge, J. A. and Thomas, A. C. (2010). Marine Plankton Phenology and Life History in a Changing Climate: Current Research and Future Directions. *J. Plankton Res.* 32, 1355–1368. doi: 10.1093/plankt/fbq062
- Jöhnk, K. D., Huisman, J., Sharples, J., Sommeijer, B., Visser, P. M. and Stroom, J. M. (2008). Summer Heatwaves Promote Blooms of Harmful Cyanobacteria. *Glob. Change Biol.* 14, 495–512. doi: 10.1111/j.1365-2486.2007.01510.x
- Kahru, M. and Elmgren, R. (2014). Multidecadal Time Series of Satellite-Detected Accumulations of Cyanobacteria in the Baltic Sea. *Biogeosciences* 11, 3619–3633. doi: 10.5194/bg-11-3619-2014
- Kahru, M., Elmgren, R., Kaiser, J., Wasmund, N. and Savchuk, O. (2020). Cyanobacterial Blooms in the Baltic Sea: Correlations with Environmental Factors. *Harmful Algae* 92, 101739. doi: 10.1016/j.hal.2019.101739
- Kahru, M., Elmgren, R. and Savchuk, O. P. (2016). Changing Seasonality of the Baltic Sea. *Biogeosciences* 13, 1009–1018. doi: 10.5194/bg-13-1009-2016
- Kalnay, E., Kanamitsu, M., Kistler, R., Collins, W., Deaven, D., Gandin, L., et al. (1996). The NCEP/NCAR 40-Year Reanalysis Project. *Bull. Am. Meteorol. Soc.* 77, 437–472. doi: 10.1175/1520-0477(1996)077<0437:TNYRP>2.0.CO;2
- Kanoshina, I., Lips, U. and Leppänen, J. M. (2003). The Influence of Weather Conditions (Temperature and Wind) on Cyanobacterial Bloom Development in the Gulf of Finland (Baltic Sea). *Harmful Algae* 2, 29–41. doi: 10.1016/S1568-9883(02)00085-9
- Karlson, A. M., Duberg, J., Motwani, N. H., Hogfors, H., Klawonn, I., Ploug, H., et al. (2015). Nitrogen Fixation by Cyanobacteria Stimulates Production in Baltic Food Webs. *Ambio* 44, 413–426. doi: 10.1007/s13280-015-0660-x
- Kendall, M. (1975). *Rank Correlation Methods* (London: Charles Griffin).
- Kirk, J. T. O. (1994). Light and Photosynthesis in Aquatic Ecosystems. *Chemtracts* 16, 48–52. doi: 10.1017/CBO9780511623370
- Klais, R., Tamminen, T., Kremp, A., Spilling, K., An, B. W., Hajdu, S., et al. (2013). Spring Phytoplankton Communities Shaped by Interannual Weather Variability and Dispersal Limitation: Mechanisms of Climate Change Effects on Key Coastal Primary Producers. *Limnol. Oceanogr.* 58, 753–762. doi: 10.4319/lo.2013.58.2.0753
- Klais, R., Tamminen, T., Kremp, A., Spilling, K. and Olli, K. (2011). Decadal-scale Changes of Dinoflagellates and Diatoms in the Anomalous Baltic Sea Spring Bloom. *PLoS One* 6, 1–10. doi: 10.1371/journal.pone.0021567
- Kremp, A. and Anderson, D. M. (2000). Factors Regulating Germination of Resting Cysts of the Spring Bloom Dinoflagellate *Scrippsiella Hangoei* from the Northern Baltic Sea. *J. Plankton Res.* 22, 1311–1327. doi: 10.1093/plankt/22.7.1311
- Kremp, A., Tamminen, T. and Spilling, K. (2008). Dinoflagellate Bloom Formation in Natural Assemblages with Diatoms: Nutrient Competition and Growth Strategies in Baltic Spring Phytoplankton. *Aquat. Microb. Ecol.* 50, 181–196. doi: 10.3354/ame01163
- Larsson, U., Elmgren, R. and Wulff, F. (1985). Eutrophication and the Baltic Sea: Causes and Consequences. *Ambio* 14, 1–6.
- Lignell, R., Seppälä, J., Kuoppo, P., Tamminen, T., Andersen, T. and Gismervik, I. (2003). Beyond Bulk Properties: Responses of Coastal Summer Plankton Communities to Nutrient Enrichment in the Northern Baltic Sea. *Limnol. Oceanogr.* 48, 189–209. doi: 10.4319/lo.2003.48.1.0189
- Lips, I. and Lips, U. (2008). Abiotic Factors Influencing Cyanobacterial Bloom Development in the Gulf of Finland (Baltic Sea). *Hydrobiologia* 614, 133–140. doi: 10.1007/s10750-008-9449-2
- Lips, I., Rünk, N., Kikas, V., Meerits, A. and Lips, U. (2014). High-Resolution Dynamics of the Spring Bloom in the Gulf of Finland of the Baltic Sea. *J. Mar. Syst.* 129, 135–149. doi: 10.1016/j.jmarsys.2013.06.002
- Margalef, R. (1978). Life-Forms of Phytoplankton as Survival Alternatives in an Unstable Environment. *Oceanol. Acta* 1, 493–509. doi: 10.1007/BF00202661
- McQuoid, M. R. and Godhe, A. (2004). Recruitment of Coastal Planktonic Diatoms from Benthic Versus Pelagic Cells: Variations in Bloom Development and Species Composition. *Limnol. Oceanogr.* 49, 1123–1133. doi: 10.4319/lo.2004.49.4.1123
- Meier, H. E., Dieterich, C., Eilola, K., Gröger, M., Höglund, A., Radtke, H., et al. (2019). Future Projections of Record-Breaking Sea Surface Temperature and Cyanobacteria Bloom Events in the Baltic Sea. *Ambio* 48, 1362–1376. doi: 10.1007/s13280-019-01235-5
- Meyer-Harms, B., Reckermann, M., Voß, M., Siegmund, H. and Von Bodungen, B. (1999). Food Selection by Calanoid Copepods in the Euphotic Layer of the Gotland Sea (Baltic Proper) During Mass Occurrence of N₂-Fixing Cyanobacteria. *Mar. Ecol. Prog. Ser.* 191, 243–250. doi: 10.3354/meps191243
- Munkes, B., Löptien, U. and Dietze, H. (2020). Cyanobacteria Blooms in the Baltic Sea: A Review of Models and Facts. *Biogeosciences Discuss.* 1–54. doi: 10.5194/bg-2020-151
- Murray, C. J., Müller-Karulis, B., Carstensen, J., Conley, D. J., Gustafsson, B. G. and Andersen, J. H. (2019). Past, Present and Future Eutrophication Status of the Baltic Sea. *Front. Mar. Sci.* 6. doi: 10.3389/fmars.2019.00002
- Neil, J. M. O., Davis, T. W., Burford, M. A. and Gobler, C. J. (2012). The rise of harmful cyanobacteria blooms: The Potential Roles of Eutrophication and Climate Change. *Harmful Algae* 14, 313–334. doi: 10.1016/j.hal.2011.10.027
- Neumann, T., Eilola, K., Gustafsson, B., Müller-Karulis, B., Kuznetsov, I., Meier, H. E. M., et al. (2012). Extremes of Temperature, Oxygen and Blooms in the Baltic Sea in a Changing Climate. *Ambio* 41, 574–585. doi: 10.1007/s13280-012-0321-2
- Oschlies, A. and Garçon, V. (1999). An Eddy-Permitting Coupled Physical-Biological Model of the North Atlantic. 1. Sensitivity to Advection Numerics and Mixed Layer Physics. *Global Biogeochem. Cycles* 14, 499–523. doi: 10.1029/98GB02811

- Paerl, H. W. (2014). Mitigating Harmful Cyanobacterial Blooms in a Human- and Climatically-Impacted World. *Life* 4, 988–1012. doi: 10.3390/life4040988
- Paerl, H. W. and Huisman, J. (2009). Climate Change: A Catalyst for Global Expansion of Harmful Cyanobacterial Blooms. *Environ. Microbiol. Rep.* 1, 27–37. doi: 10.1111/j.1758-2229.2008.00004.x
- Paerl, H. W. and Scott, J. T. (2010). Throwing Fuel on the Fire: Synergistic Effects of Excessive Nitrogen Inputs and Global Warming on Harmful Algal Blooms. *Environ. Sci. Technol.* 44, 7756–7758. doi: 10.1021/es102665e
- Papush, L. and Danielsson, Å. (2006). Silicon in the Marine Environment: Dissolved Silica Trends in the Baltic Sea. *Estuar. Coast. Shelf Sci.* 67, 53–66. doi: 10.1016/j.ECSSS.2005.09.017
- Poutanen, E. L. and Nikkilä, K. (2001). Carotenoid Pigments as Tracers of Cyanobacterial Booms in Recent and Postglacial Sediments of the Baltic Sea. *Ambio* 30, 179–183. doi: 10.1579/0044-7447-30.4.179
- Rahm, L., Conley, D., Sandén, P., Wulff, F. and Stålnacke, P. (1996). Time Series Analysis of Nutrient Inputs to the Baltic Sea and Changing DSi:DIN Ratios. *Mar. Ecol. Prog. Ser.* 130, 221–228. doi: 10.3354/meps130221
- Rahmstorf, S. (1990). *An Oceanic Mixing Model: Application to Global Climate and to the New Zealand West Coast* (New Zealand: Victoria University).
- Redfield, A. C. (1958). The Biological Control of Chemical Factors in the Environment. *Am. Sci.* 46, 205–221.
- Rengefors, K. and Anderson, D. M. (1998). Environmental and Endogenous Regulation of Cyst Germination in Two Freshwater Dinoflagellates. *J. Phycol.* 577, 568–577. doi: 10.1046/j.1529-8817.1998.340568.x
- Reynolds, C. S., Wiseman, S. W. and Clarke, M. J. O. (1984). Growth- and Loss-Rate Responses of Phytoplankton to Intermittent Artificial Mixing and their Potential Application to the Control of Planktonic Algal Biomass. *J. Appl. Ecol.* 21, 11. doi: 10.2307/2403035
- Savchuk, O. P. (2018). Large-Scale Nutrient Dynamics in the Baltic Sea 1970–2016. *Front. Mar. Sci.* 5, doi: 10.3389/fmars.2018.00095
- Schneider, B. and Müller, J. D. (2018). The Main Hydrographic Characteristics of the Baltic Sea. *Biogeochem. Transform. Balt. Sea*, 35–41. doi: 10.1007/978-3-319-61699-5_3
- Sen, P. K. (1968). Estimates of the Regression Coefficient Based on Kendall's Tau. *J. Am. Stat. Assoc.* 63, 1379–1389. doi: 10.1080/01621459.1968.10480934
- Sharples, J., Ross, O. N., Scott, B. E., Greenstreet, S. P. and Fraser, H. (2006). Inter-Annual Variability in the Timing of Stratification and the Spring Bloom in the North-Western North Sea. *Cont. Shelf Res.* 26, 733–751. doi: 10.1016/j.csr.2006.01.011
- Smith, S. V. and Hollibaugh, J. T. (1993). Coastal Metabolism and the Oceanic Organic Carbon Balance. *Rev. Geophys.* 31, 75–89. doi: 10.1029/92RG02584
- Sommer, U., Aberle, N., Lengfellner, K. and Lewandowska, A. (2012). The Baltic Sea Spring Phytoplankton Bloom in a Changing Climate: An Experimental Approach. *Mar. Biol.* 159, 2479–2490. doi: 10.1007/s00227-012-1897-6
- Sonntag, S. and Hense, I. (2011). Phytoplankton Behavior Affects Ocean Mixed Layer Dynamics Through Biological-Physical Feedback Mechanisms. *Geophys. Res. Lett.* 38, 1–6. doi: 10.1029/2011GL048205
- Spilling, K. and Markager, S. (2008). Ecophysiological Growth Characteristics and Modeling of the Onset of the Spring Bloom in the Baltic Sea. *J. Mar. Syst.* 73, 323–337. doi: 10.1016/j.jmarsys.2006.10.012
- Spilling, K., Olli, K., Lehtoranta, J., Kremp, A., Tedesco, L., Tamelander, T., et al. (2018). Shifting Diatom–Dinoflagellate Dominance During Spring Bloom in the Baltic Sea and its Potential Effects on Biogeochemical Cycling. *Front. Mar. Sci.* 5, doi: 10.3389/fmars.2018.00327
- Spilling, K., Tamminen, T., Andersen, T. and Kremp, A. (2010). Nutrient Kinetics Modeled from Time Series of Substrate Depletion and Growth: Dissolved Silicate Uptake of Baltic Sea Spring Diatoms. *Mar. Biol.* 157, 427–436. doi: 10.1007/s00227-009-1329-4
- Suikkanen, S., Hakanen, P., Spilling, K. and Kremp, A. (2011). Allelopathic Effects of Baltic Sea Spring Bloom Dinoflagellates on Co-Occurring Phytoplankton. *Mar. Ecol. Prog. Ser.* 439, 45–55. doi: 10.3354/meps09356
- Sverdrup, H. U. (1953). On Conditions for the Vernal Blooming of Phytoplankton. *ICES J. Mar. Sci.* 18, 287–295. doi: 10.1093/icesjms/18.3.287
- Vahtera, E., Conley, D. J., Gustafsson, B. G., Kuosa, H., Pitkänen, H., Savchuk, O. P., et al. (2007). Internal Ecosystem Feedbacks Enhance Nitrogen-fixing Cyanobacteria Blooms and Complicate Management in the Baltic Sea. *Ambio* 36, 186–194. doi: 10.1579/0044-7447(2007)36[186:IEFENC]2.0.CO;2
- Walve, J. and Larsson, U. (2007). Blooms of Baltic Sea Aphanizomenon sp. (Cyanobacteria) Collapse After Internal Phosphorus Depletion. *Aquat. Microb. Ecol.* 49, 57–69. doi: 10.3354/ame01130
- Waniek, J. J. (2003). The Role of Physical Forcing in Initiation of Spring Blooms in the Northeast Atlantic. *J. Mar. Syst.* 39, 57–82. doi: 10.1016/S0924-7963(02)00248-8
- Waniek, J. J. and Holliday, N. P. (2006). Large-Scale Physical Controls on Phytoplankton Growth in the Irminger Sea, Part II: Model Study of the Physical and Meteorological Preconditioning. *J. Mar. Syst.* 59, 219–237. doi: 10.1016/j.jmarsys.2005.10.005
- Wasmund, N. (1997). Occurrence of Cyanobacterial Blooms in the Baltic Sea in Relation to Environmental Conditions. *Int. Rev. der gesamten Hydrobiol. und Hydrogr.* 82, 169–184. doi: 10.1002/iroh.19970820205
- Wasmund, N., Nausch, G. and Feistel, R. (2013). Silicate Consumption: An Indicator for Long-Term Trends in Spring Diatom Development in the Baltic Sea. *J. Plankton Res.* 35, 393–406. doi: 10.1093/plankt/fbs101
- Wasmund, N., Nausch, G. and Matthäus, W. (1998). Phytoplankton Spring Blooms in the Southern Baltic sea - Spatio-Temporal Development and Long-Term Trends. *J. Plankton Res.* 20, 1099–1117. doi: 10.1093/plankt/20.6.1099
- Wasmund, N., Tuimala, J., Suikkanen, S., Vandepitte, L. and Kraberg, A. (2011). Long-Term Trends in Phytoplankton Composition in the Western and Central Baltic Sea. *J. Mar. Syst.* 87, 145–159. doi: 10.1016/j.jmarsys.2011.03.010
- Wasmund, N. and Uhlig, S. (2003). Phytoplankton Trends in the Baltic Sea. *ICES J. Mar. Sci.* 60, 177–186. doi: 10.1016/S1054-3139(02)00280-1
- Winder, M. and Schindler, D. E. (2004). Climate Change Uncouples Trophic Interactions in an Aquatic Ecosystem. *Ecology* 85, 2100–2106. doi: 10.1890/04-0151

Conflict of Interest: The authors declare that the research was conducted in the absence of any commercial or financial relationship that could be construed as a potential conflict of interest.

Publisher's Note: All claims expressed in this article are solely those of the authors and do not necessarily represent those of their affiliated organizations, or those of the publisher, the editors and the reviewers. Any product that may be evaluated in this article, or claim that may be made by its manufacturer, is not guaranteed or endorsed by the publisher.

Copyright © 2022 Beltran-Perez and Waniek. This is an open-access article distributed under the terms of the Creative Commons Attribution License (CC BY). The use, distribution or reproduction in other forums is permitted, provided the original author(s) and the copyright owner(s) are credited and that the original publication in this journal is cited, in accordance with accepted academic practice. No use, distribution or reproduction is permitted which does not comply with these terms.

Supplementary Material

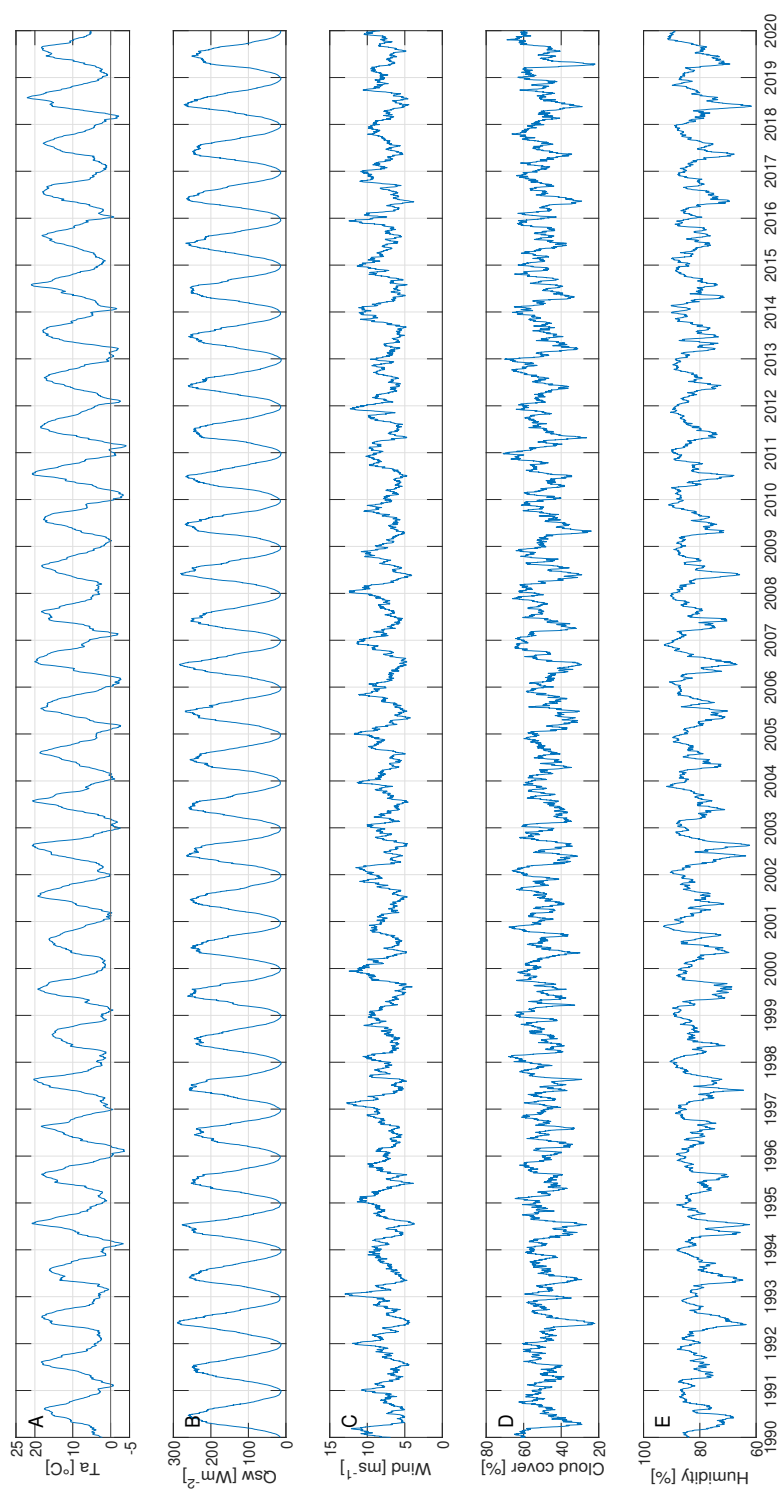


Figure S1. Atmospheric reanalysis data from NCEP used to calculate the forcing for the model (1990-2019): (A) air temperature, (B) incoming solar radiation, (C) wind speed, (D) cloud cover and (E) relative humidity.

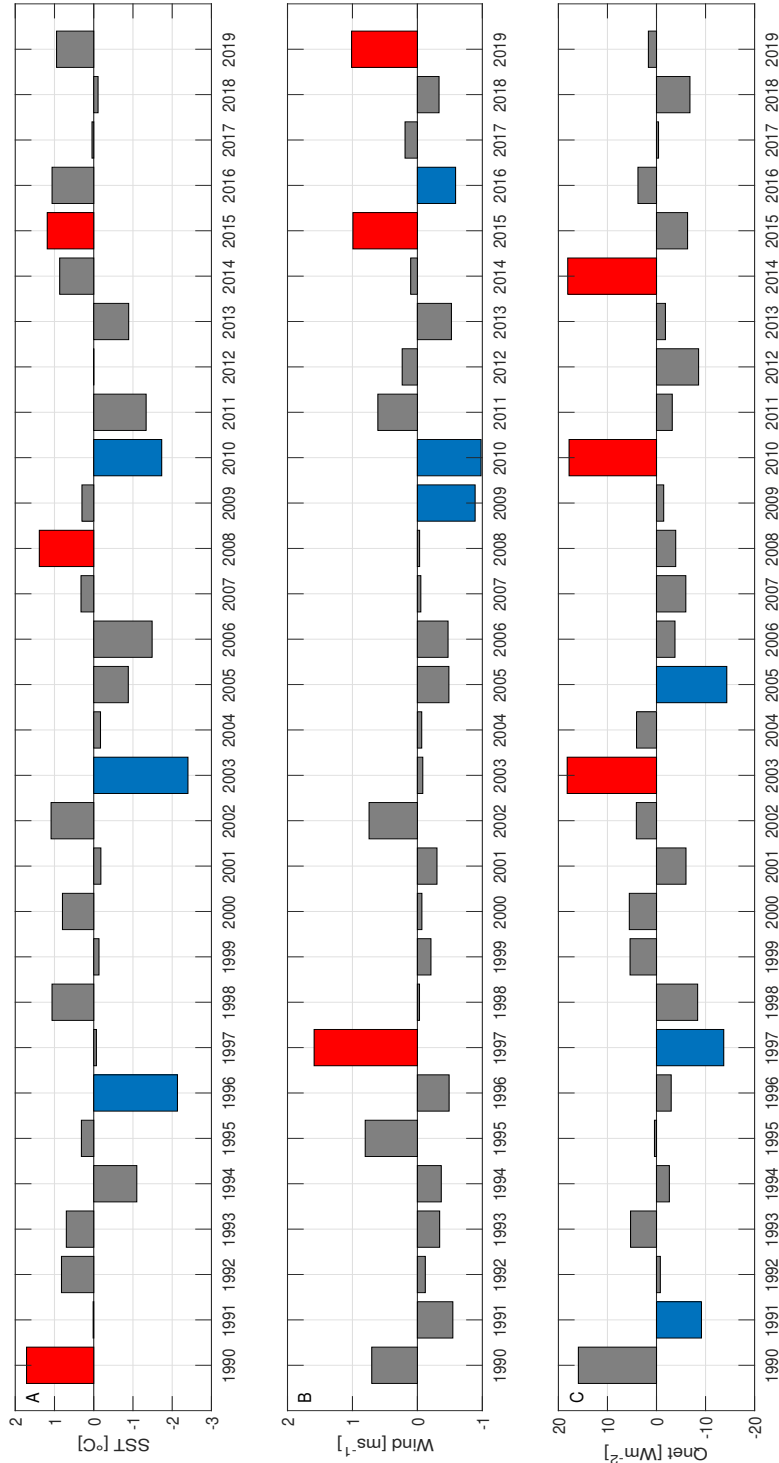


Figure S2. Anomaly (observed value minus overall mean) of (A) SST, (B) wind and (C) net heat flux calculated for the diatom bloom period (February-May). The bars in red represent for each subplot warmer periods, stronger wind and higher energy gain, respectively. The bars in blue represent for each subplot colder periods, weaker wind and less energy gain, respectively.

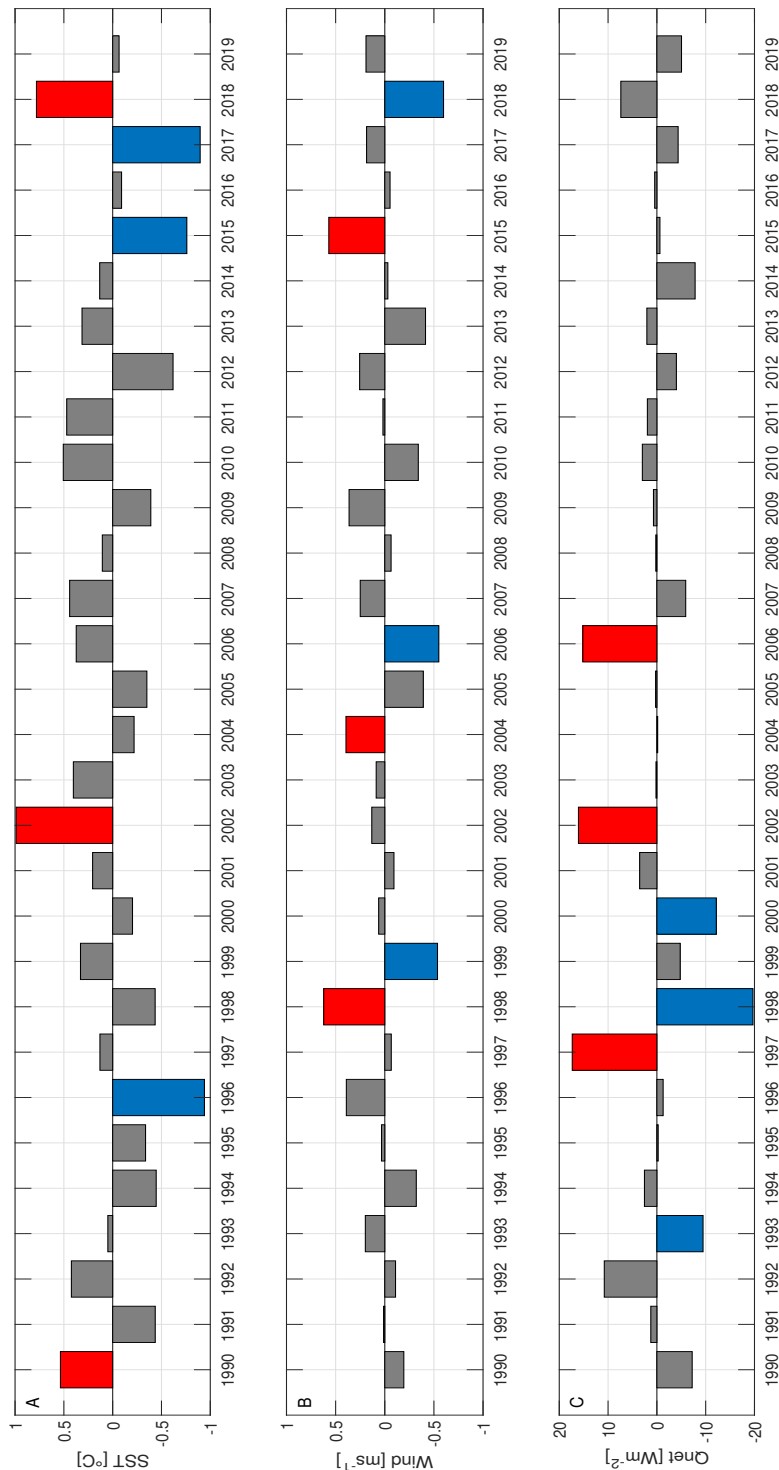


Figure S3. Anomaly (observed value minus overall mean) of (A) SST, (B) wind and (C) net heat flux calculated for the cyanobacteria bloom period (June-August). The bars in red represent for each subplot warmer periods, stronger wind and higher energy gain, respectively. The bars in blue represent for each subplot colder periods, weaker wind and less energy gain, respectively.

Table S1. Diatom phenology and biomass integrated over the bloom period (February-May).

Year	Day of year			Length (days)	Max peak ($\mu\text{g L}^{-1}$)	Biomass ($\mu\text{g L}^{-1}$)
	Onset	Peak	Decline			
1990	80	107	135	55	267	13438
1991	75	103	133	58	270	14273
1992	80	109	141	61	277	15307
1993	84	113	144	60	278	15036
1994	90	119	147	57	278	14364
1995	78	110	140	62	272	15294
1996	75	122	151	76	271	17634
1997	84	113	144	60	274	14933
1998	89	117	145	56	270	13787
1999	85	114	145	60	281	15201
2000	90	118	147	57	279	14390
2001	89	117	147	58	276	14494
2002	88	116	145	57	278	14368
2003	72	117	140	68	245	15345
2004	89	117	146	57	278	14366
2005	95	123	149	54	272	13376
2006	97	124	152	55	275	13771
2007	87	115	144	57	277	14293
2008	79	111	139	60	266	14459
2009	90	118	146	56	275	13990
2010	96	123	150	54	274	13455
2011	99	127	153	54	272	13382
2012	77	106	137	60	272	14793
2013	92	121	150	58	277	14571
2014	80	107	136	56	270	13790
2015	80	108	138	58	276	14526
2016	83	111	140	57	277	14316
2017	84	112	141	57	273	14147
2018	81	113	143	62	275	15379
2019	82	109	138	56	272	13887

Table S2. Cyanobacteria phenology and biomass integrated over the bloom period (June-August).

Year	Day of year			Length (days)	Max peak ($\mu\text{g L}^{-1}$)	Biomass ($\mu\text{g L}^{-1}$)
	Onset	Peak	Decline			
1990	154	187	235	81	710	33481
1991	164	212	237	73	692	34792
1992	163	192	226	63	733	29966
1993	159	183	222	63	645	27667
1994	156	209	235	79	725	40913
1995	163	185	240	77	625	32661
1996	169	195	248	79	596	32618
1997	170	202	247	77	705	38374
1998	164	195	227	63	613	21902
1999	159	193	228	69	702	37174
2000	156	192	234	78	675	32895
2001	158	189	244	86	706	39957
2002	153	198	252	99	696	44621
2003	165	202	232	67	705	35743
2004	155	185	235	80	673	42030
2005	155	194	238	83	733	39127
2006	157	188	242	85	740	44206
2007	154	186	238	84	656	35704
2008	154	214	229	75	682	37813
2009	152	181	228	76	720	37427
2010	155	193	235	80	719	43873
2011	159	191	240	81	693	40014
2012	163	193	234	71	650	30190
2013	162	199	253	91	696	39865
2014	150	207	230	80	704	42390
2015	155	185	240	85	713	33305
2016	149	183	239	90	704	39902
2017	154	204	230	76	682	32044
2018	158	208	251	93	691	43678
2019	153	182	244	91	676	38757



OPEN ACCESS

EDITED BY

Gerhard Josef Herndl,
University of Vienna, Austria

REVIEWED BY

Carolina Cisternas-Novoa,
Memorial University of Newfoundland,
Canada

Susanne Neuer,
Arizona State University, United States

*CORRESPONDENCE

Oscar Dario Beltran-Perez,
✉ oscar.beltran@io-warnemuende.de

RECEIVED 22 February 2023

ACCEPTED 07 June 2023

PUBLISHED 22 June 2023

CITATION

Beltran-Perez OD, Voss M, Pollehne F,
Liskow I and Waniek JJ (2023), Temporal
variability of particle flux and its
components in the Gotland Basin,
eastern Baltic Sea.

Front. Earth Sci. 11:1171917.

doi: 10.3389/feart.2023.1171917

COPYRIGHT

© 2023 Beltran-Perez, Voss, Pollehne,
Liskow and Waniek. This is an
open-access article distributed under
the terms of the [Creative Commons
Attribution License \(CC BY\)](https://creativecommons.org/licenses/by/4.0/). The use,
distribution or reproduction in other
forums is permitted, provided the
original author(s) and the copyright
owner(s) are credited and that the
original publication in this journal is
cited, in accordance with accepted
academic practice. No use, distribution
or reproduction is permitted which does
not comply with these terms.

Temporal variability of particle flux and its components in the Gotland Basin, eastern Baltic Sea

Oscar Dario Beltran-Perez*, Maren Voss, Falk Pollehne,
Iris Liskow and Joanna Jadwiga Waniek

Leibniz Institute for Baltic Sea Research Warnemünde, Rostock, Germany

Sinking particles were studied by analyzing samples collected in a sediment trap at 180 m depth in the Gotland Basin, eastern Baltic Sea between 1999 and 2020. The aim of this study was to determine the temporal variability of the particle flux and its components and how their changes are linked to phytoplankton blooms. The variables studied included total particle flux, particulate organic carbon and nitrogen, biogenic silica, C:N ratio and the isotopic composition of organic carbon and nitrogen. The total particle flux and its components reached maximum values in 2003, 2012 and 2015. Long-term means over the 22-year period of the total particle flux and its components particulate organic carbon and nitrogen, biogenic silica were estimated at around 152, 22, 3 and 8 mg m⁻² d⁻¹, respectively. The C:N ratio and the isotopic composition of organic carbon and nitrogen showed high variability around their long-term means of 9, -25‰ and 4‰, respectively. The annual variability of the components of the flux particulate organic carbon (3–65 mg m⁻² d⁻¹), particulate organic nitrogen (0.4–9 mg m⁻² d⁻¹) and biogenic silica (1–24 mg m⁻² d⁻¹) exhibited the same general pattern as the total particle flux (11–450 mg m⁻² d⁻¹) over the study period. On the seasonal scale, sinking material in summer contributed roughly one-third (31%) to the total particle flux, followed by winter (27%), spring (24%) and autumn (19%). The highest particle flux occurred mostly in April, July and November, during and after the appearance of phytoplankton blooms in the Gotland Basin. The phytoplankton community changed from silicon-rich species to nitrogen-fixing cyanobacteria, indicating a shift in nitrogen sources from nitrate-based to N₂-based over the year. The spring bloom, dominated by diatoms, was characterized by a lighter carbon and heavier nitrogen isotopic composition, while the summer bloom, mainly of diazotrophic cyanobacteria, was characterized in contrary by heavier carbon and lighter nitrogen isotopes. Although no trend was found in the data, the variability observed in the sinking material was related to the changes over time in the phytoplankton community in the Gotland Basin. The findings of this study provide new and valuable information for our understanding of the temporal variability of sinking material linked to the development of phytoplankton blooms and nutrient sources in the Gotland Basin, and underscore the importance of continued monitoring to understand the potential impacts of environmental changes on this fragile ecosystem.

KEYWORDS

sediment trap, temporal variability, particle flux, phytoplankton, bloom, Baltic Sea

1 Introduction

Particle flux measurements provide important insights into the pelagic system and the productivity of surface waters. This is especially true for systems like the Baltic Sea, a brackish, shallow, semi-enclosed sea in northern Europe (Figure 1), which is affected by eutrophication (Fleming-Lehtinen et al., 2008), rapid warming (Belkin, 2009; HELCOM/Baltic Earth, 2021) and acidification (Havenhand, 2012). The Baltic Sea is strongly stratified relative to other continental shelf seas with a strong seasonal pycnocline at around 10–20 m depth (Gustafsson et al., 2004). The long residence time influenced by the limited water exchange with the North Sea and the long-term excessive nutrient loading (Schneider and Müller, 2018) have contributed to the reduced phosphorus binding capacity of the sediment under anoxic conditions (Lehtoranta et al., 2008). Eutrophication and excess deposition of particles in environments with slow water renewal, as in the Baltic Sea, may have adverse effects on ecosystem structure and functioning (e.g., hypoxia of near-bottom water and sediment) (Vahtera et al., 2007; Diaz and Rosenberg, 2008; Carstensen et al., 2014; Tamelander et al., 2017).

Stagnation periods frequently occur in the deep basins of the Baltic Sea as a result of both the limited water exchange with the North Sea and the permanent stratification (Carstensen et al., 2014). Changes in stagnation periods strongly affect nutrient conditions (Mohrholz et al., 2015). Phosphate remains fixed in the sediment under oxic conditions, otherwise phosphate and iron ions are released, changing the chemistry of the water column (e.g.,

increasing phosphate concentration in the water and decreasing the N:P ratio). Moreover, inorganic nitrogen compounds are present mainly as nitrate under oxic conditions. However, under anoxic conditions, nitrate is denitrified to molecular nitrogen gas (N_2). Ammonium from the sediments or produced during mineralization cannot be oxidized under these conditions and is enriched. Enriched nutrients can be transported upwards by vertical mixing (Reissmann et al., 2009), reaching the euphotic surface layer and therefore determining to a large extent the intensity of phytoplankton blooms (Vahtera et al., 2007; Murray et al., 2019).

Deep water ventilation in the central Baltic basins can only take place by extreme inflow events - called Major Baltic Inflows (MBIs) - which transport large amounts of salt and oxygen into the deep basins of the Baltic Sea (Mohrholz, 2018). MBIs were recorded frequently in the last century, however since the mid-1970s their frequency and intensity have decreased (Mohrholz et al., 2015). A strong inflow event in January 1993 along with smaller inflows in winter 1993/1994 terminated the longest stagnation period ever recorded in the Baltic Sea (from the beginning of 1983 until the end of 1992). Subsequent MBIs occurred in 2003, 2011 and 2014. The strong inflow at the end of 2014 was even able to renew the bottom water in the eastern Gotland Basin (Mohrholz et al., 2015).

The Gotland Basin is the major basin of the Baltic Proper, with a maximum depth of 249 m. It is characterized by a permanent halocline at 60–80 m depth, which functions as a barrier between anoxic bottom waters and the surface near layer (Schneider et al., 2000; Klais et al., 2011). Diatom-dominated blooms occur in spring and autumn, while cyanobacteria blooms are more common in summer. These blooms connect the surface with the seafloor, as phytoplankton dominate primary production and are the major source of organic matter exported to the bottom. The estimated annual export of particulate organic carbon varies between 18 and 60 $gCm^{-2}year^{-1}$ over the entire Baltic Sea (Tamelander et al., 2017), considering only the central Baltic Sea, the annual export is around 50 $gCm^{-2}year^{-1}$ according to a study between 1998 and 2000 (Gustafsson et al., 2013). The sinking material increases during and after the phytoplankton bloom, i.e., when primary production is at its highest (Leipe et al., 2008; Schneider et al., 2017). However, the sinking material varies more strongly in summer than in spring (Tamelander et al., 2017), probably due to the greater sensitivity of cyanobacteria to environmental changes than diatom-dominated spring blooms (Beltran-Perez and Waniek, 2022).

Climate projections indicate that phytoplankton biomass in the Baltic Sea is likely to increase in the future due to higher nutrient loading (Meier et al., 2011) and an increase in wind stress, as well as continued loss of seasonal sea ice (Christensen et al., 2015), which may increase resuspension in coastal areas. In fact, resuspended particles represent about 50% of the material deposited on the seafloor in a coastal area of the Baltic Sea, as measured by sediment traps (Blomqvist and Larsson, 1994). Model simulations have also confirmed that resuspension events are likely to become more frequent and severe in the future (Eilola et al., 2013). As a result, sinking material may settle again locally or be transported offshore contributing to deposition in deeper areas as well (Almroth-Rosell et al., 2011). The freshwater runoff is projected to increase by 15%–22% due to higher precipitation in the Baltic Sea (Meier et al., 2012), however, in the open Baltic Sea waters the influence of terrestrial sources is minimal (Tamelander et al., 2017).

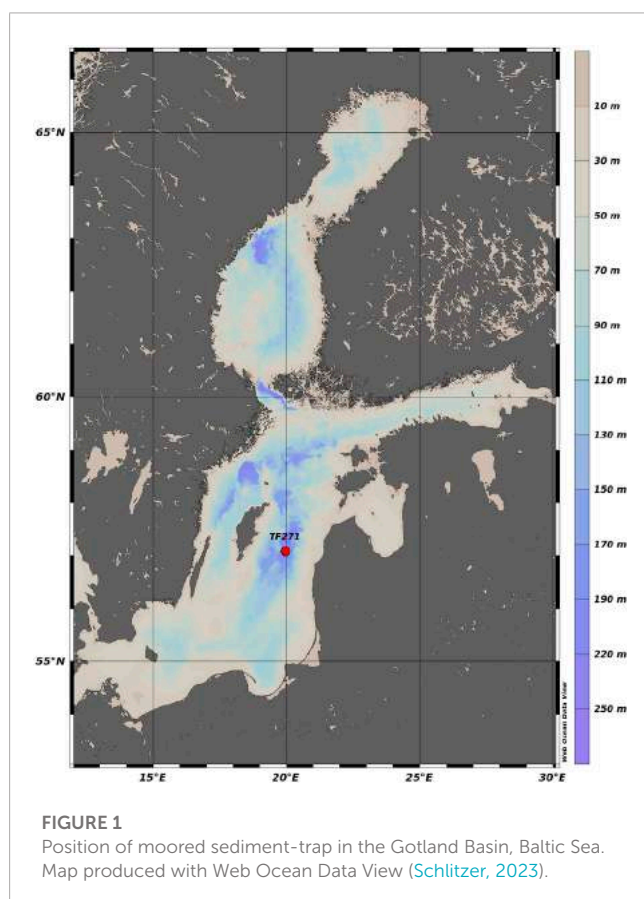


FIGURE 1
Position of moored sediment-trap in the Gotland Basin, Baltic Sea. Map produced with Web Ocean Data View (Schlitzer, 2023).

Previous studies of organic matter export in the Baltic Sea have indicated its spatial and temporal variability in relation to primary production (Elmgren, 1984), phytoplankton dynamics (Heiskanen and Kononen, 1994; Tamelander and Heiskanen, 2004), pelagic food web structure (Smetacek et al., 1984) and hydrodynamic forcing (Blomqvist and Heiskanen, 2001; Tamelander and Heiskanen, 2004). However, the temporal changes of the particle flux have not been comprehensively addressed so far in the Gotland Basin. Understanding the changes to which the particle flux is exposed in a permanently stratified basin with regular phytoplankton blooms, low water renewal and anoxic conditions at the bottom provide insights into the factors that dominate the particle flux, its components and impacts on ecosystems increasingly affected by climate change. Therefore, the aim of this study is to determine the temporal variability of the particle flux and its components as well as its relationship with phytoplankton blooms and environmental changes using sediment trap data collected at ca. 180 m depth between 1999 and 2020 in the Gotland Basin, eastern Baltic Sea (Figure 1).

2 Material and methods

2.1 Sediment trap and sample analyses

The particle flux was measured in sediment trap samples from ca. 180 m depth at mooring station TF271 (57°18.3N, 20°0.46E) in the Gotland Basin between 1999 and 2020. The instrument used was a funnel-shaped automated Kiel sediment trap (type S/MT 234, KUM, Germany) with aperture of 0.5 m² and a revolver holding twenty-one collecting cups of 400 mm (Kremling et al., 1996). The sampling intervals were 7–10 days. Collecting cups were filled with formalin (4%) as fixative to retard microbial activity. After recovery, the samples were sieved through a 400- μ m gauze to remove large organisms and stored separately in formalin (4%). The samples were split into subsets using a 4-fold sample-splitter for bulk analyses. To determine the total particle flux, a representative volume of the sample was filtered onto a pre-weighed membrane filter (0.45 μ m pore size), dried in an oven at 60°C and weighed to calculate the particle flux.

Samples were filtered on precombusted glass fiber filters (GF/F, 500°C, 2 h) for analysis of particulate organic carbon (POC) and nitrogen (PON) according to the procedure described by Nieuwenhuize et al. (1994). The POC was determined after the filters were treated with concentrated HCl for 24 h to remove inorganic carbon. A second filter was prepared for PON analysis. After drying at 60°C, POC, PON and stable carbon and nitrogen isotopes were measured using an elemental analyzer (Thermo Scientific) connected to a Delta isotope ratio mass spectrometer (Thermo Scientific) via a Conflow interface (Thermo Fisher Scientific, US). Acetanilide (manufactured by Merck) was used as the calibration material for C and N analysis. The analytical precision of the measurement was <0.2‰ for both stable isotope ratios $\delta^{13}\text{C}$ and $\delta^{15}\text{N}$ (Nieuwenhuize et al., 1994). Isotope values were expressed in parts per thousand (‰) relative to Vienna Pee Dee Belemnite (VPDB) and atmospheric nitrogen for carbon ($\delta^{13}\text{C}$) and nitrogen ($\delta^{15}\text{N}$), respectively, using the conventional δ -notation (Mariotti, 1983). Finally, particulate biogenic silica (PSi) was analyzed using

photometric detection after filtration on cellulose acetate filters and digestion using a wet alkaline extraction, following the procedures described by Bodungen et al. (1991).

2.2 Additional data

Chlorophyll a concentration (*Chla*) was downloaded from the SHARKweb database provided by the Swedish Meteorological and Hydrological Institute (SMHI). Discrete measurements of *Chla* at the surface of the Gotland Basin were used to calculate monthly mean values between January 1999 and December 2020. The partial pressure of carbon dioxide ($p\text{CO}_2$) was estimated from *in-situ* observations and provided by the Copernicus Marine Service through the Global Ocean Surface Carbon product. Monthly $p\text{CO}_2$ data were used from 15 January 1999 to 15 December 2020 with a spatial resolution of 1° × 1°. The $p\text{CO}_2$ data were interpolated to the deployment area of the sediment trap for the analysis.

2.3 Data analysis

A total of 740 sediment trap samples were collected at intervals of 7–10 days according to total exposition time and season between 15 May 1999 and 14 November 2020. Sampling periods of more than 10 days with no measurements were identified and excluded from the analysis (Table 1). These gaps were caused by malfunctioning of the trap, its loss or available ship time for mooring turnover. A moving median over a 10 days window was used to fill gaps of less than 10 days. Monthly, seasonal and annual means of total particle flux, particulate organic carbon and nitrogen, biogenic silica, molar C:N ratio, isotopic composition of organic carbon and nitrogen were calculated based on the sediment trap data at each interval. Monthly, seasonal and annual means of chlorophyll a and partial pressure of carbon dioxide were estimated from water column measurements in the Gotland Basin. The long-term, inter-annual and seasonal variability were estimated as the arithmetic average of values in the same month, year and season between 1999 and 2020, respectively. For the seasonal variability, sinking particles were grouped into spring (1 March to 31 May), summer (1 June to 31 August), autumn (1 September to 30 November) and winter (1 December to 28 February) using the pelagic seasons in the eastern Baltic Sea. The annual cycle was estimated as monthly means between 1999 and 2020. Mean $\delta^{15}\text{N}$ and $\delta^{13}\text{C}$ values were estimated based on a weighted mean over the sampling interval (i) (Equation 1; Voss et al., 2005). Single values outside the standard deviation of the mean were considered as outliers and were not used in further calculations and interpretations. The relationship and interplay of sinking material with primary production were explored by calculating linear correlations between the total particle flux and its components (POC, PON, PSi), isotopic composition, chlorophyll a and partial pressure of carbon dioxide. Correlations were considered significant at a p -value of less than or equal to 0.05. All calculations and analyses were performed in MATLAB (version R2018b).

$$\delta^{15}\text{N}_i = \frac{\sum_i \delta^{15}\text{N}_i * \text{PON}_i}{\sum_i \text{PON}_i} \quad (1)$$

TABLE 1 Sediment trap sampling periods of more than 10 days with no measurements due to trap malfunction, loss or available ship time for mooring turnover.

Date start	Date end	Length (days)
22-Nov-1999	06-Dec-1999	14
16-Apr-2002	10-May-2002	24
08-Aug-2005	03-Nov-2005	87
31-Dec-2008	05-Sep-2009	248
21-Jan-2011	04-Apr-2011	73
20-Jan-2012	16-Feb-2012	27
03-Jun-2012	14-Nov-2012	164
24-Nov-2013	15-Feb-2014	83
11-Dec-2014	14-Feb-2015	65
29-Jun-2015	16-Nov-2015	140
30-Nov-2018	10-Feb-2019	72
29-Apr-2020	18-May-2020	19

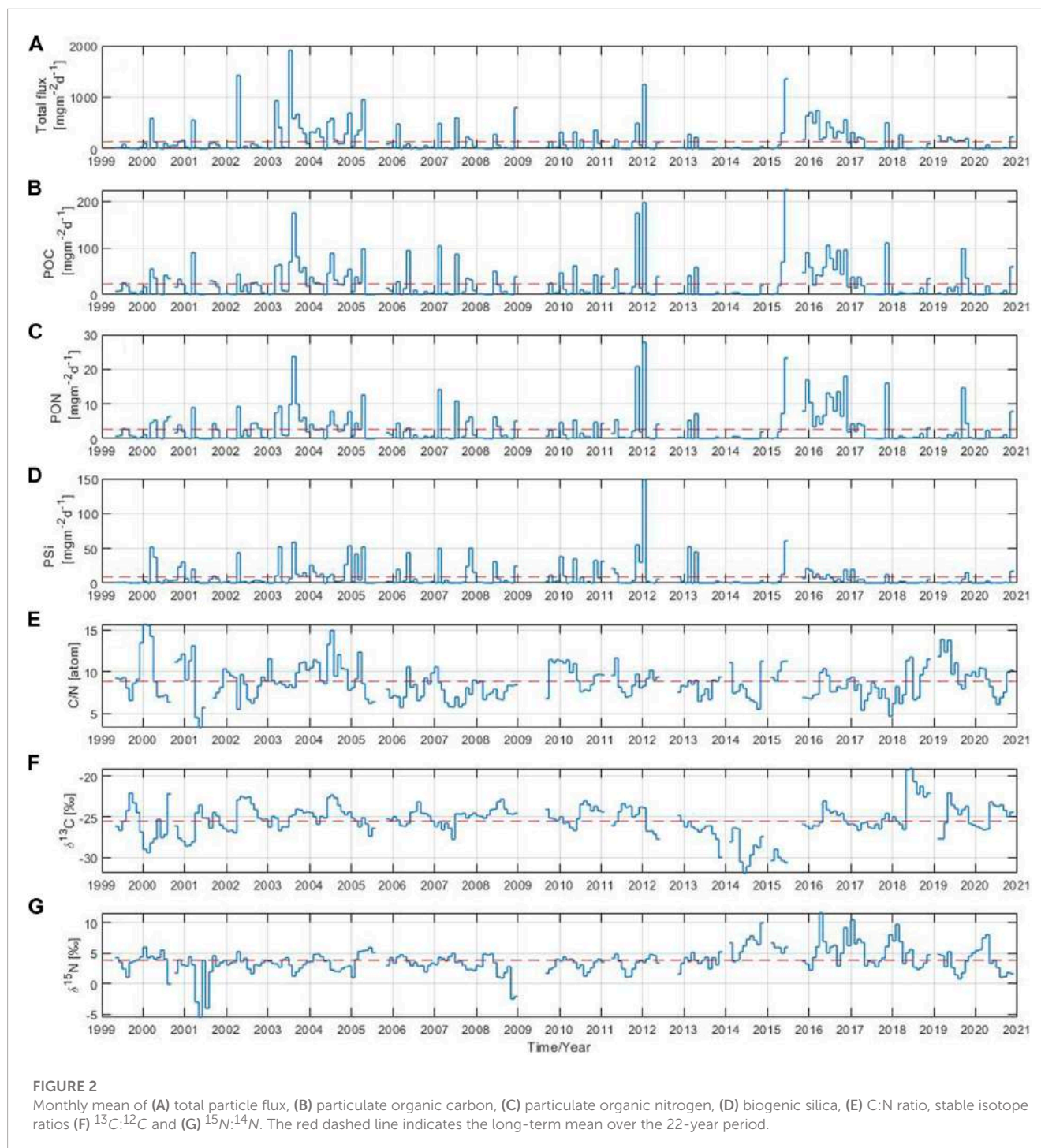
3 Results

3.1 Long-term variability

The total particle flux and its components were measured for a total of 22 years, from 1999 to 2020, in the Gotland Basin. Monthly means of the total particle flux showed differences in the magnitude and timing of sinking particles (Figure 2A). The absolute maximum of the total particle flux during the entire observation period occurred in July 2003 reaching up to $1907 \text{ mg m}^{-2} \text{ d}^{-1}$, whereas the long-term mean was $152 \text{ mg m}^{-2} \text{ d}^{-1}$. Elevated particle flux was also occasionally observed in other years. The monthly particle flux was mainly above the long-term mean in 2000–2008, 2012 and between 2015 and 2017, with maxima once or twice a year usually observed in March (2000, 2001, 2003, 2004, 2007), April (2002, 2005), July (2003, 2004, 2007) and December (2004, 2008). In 2008, a peak occurred only at the end of the year. However, it was not possible to follow this maximum because measurements were missing between the end of 2008 and the first half of 2009. Furthermore, in February 2006, January 2012, June 2015 and November 2017, a high particle flux was observed with values of 481, 1,245, 1,354 and $503 \text{ mg m}^{-2} \text{ d}^{-1}$, respectively. The total particle flux in 2016 was above the average over the entire year with maximum values in January, March, June and November of 705, 744, 517 and $566 \text{ mg m}^{-2} \text{ d}^{-1}$, respectively. Elevated values of the total particle flux were also observed in 1999, 2009–2011, 2013–2014 and 2018–2020, but the total particle flux in 1999 was only measured from May onwards. The lowest monthly values were observed in May 2001, May 2005, May 2007, August 2013 and June 2014. Overall, the long-term variability of the total particle flux followed the periods of high primary production in the eastern Baltic Sea, usually driven by diatom blooms in spring and autumn and cyanobacteria blooms in summer, as shown in Supplementary Figure S1 and also reported by Wasmund et al. (2000); Kudryavtseva et al. (2011). The total particle flux decreased after October, as the primary production at the end of the year was generally lower than during the previous months.

A high monthly POC component of the flux was observed in August 2003, November 2011, January 2012 and June 2015 with values above 100 up to a maximum of $225 \text{ mg m}^{-2} \text{ d}^{-1}$ reached in 2015 (Figure 2B). The long-term mean of POC over the study period was $22 \text{ mg m}^{-2} \text{ d}^{-1}$. Monthly POC values above the long-term mean were observed in February 2007, March 2001, April (2003, 2005, 2013), May (2006, 2010, 2011), July (2004, 2007), September 2019, November (2017, 2020) and December 2015. In addition, the POC component of the flux remained above the long-term mean throughout 2016 with elevated values in June, September and November. The POC contributed about 31% to the total particle flux (Supplementary Figure S2A). The monthly PON component of the flux had high values in August 2003, November 2011, January 2012 and June 2015 of 24, 21, 28, $23 \text{ mg m}^{-2} \text{ d}^{-1}$, respectively (Figure 2C). The long-term mean of PON was around $3 \text{ mg m}^{-2} \text{ d}^{-1}$. Monthly PON values exceeded the long-term mean in February 2007, March 2001, April (2002, 2003, 2005, 2013), July (2004, 2007), September 2019, November (2017, 2020) and December (2004, 2015). The PON remained above the long-term mean in 2016 with maximum values of 13, 14 and $18 \text{ mg m}^{-2} \text{ d}^{-1}$ in June, September and November, respectively. The PON contributed around 5% to the total particle flux (Supplementary Figure S2B). The long-term mean of P_{Si} over the observation period was $8 \text{ mg m}^{-2} \text{ d}^{-1}$ contributing around 8% to the total particle flux (Figure 2D and Supplementary Figure S2C). The absolute maximum of the P_{Si} component of the flux occurred in January 2012 reaching $149 \text{ mg m}^{-2} \text{ d}^{-1}$. High P_{Si} values above the long-term mean were observed in January 2010, February (2005, 2007, 2013), March (2000), April (2002, 2003, 2005, 2013), May (2006, 2010), June (2008, 2015), August 2003, November (2007, 2010, 2011) and December 2004. Overall, the monthly POC, PON and P_{Si} components of the total particle flux (Figures 2B–D) followed a similar pattern in most years with elevated values occurring around the same time period. The most striking difference appeared in the P_{Si} component of the flux, which pronounced maxima were missing since 2016 to the end of the time series. However, no clear trend could be derived for the P_{Si} component of the total particle flux, other components (POC and PON) or the total particle flux itself due to the high variability observed in the data over time.

The monthly C:N ratio showed a large variability (Figure 2E). Its long-term mean over the 22 year-period was 9. The C:N ratio was at its minimum in May 2001 and December 2017 with values close to 5. The maximum values were observed in January/February 2000, July 2004 and March/May 2019, in all of them with values around 15. There are some years in which the monthly C:N ratio was mostly below the long-term mean throughout the year as in 2007, 2008, 2013 and 2017, but in 2004 and 2019 it was the opposite. The stable isotope composition of organic carbon in the total particle flux varied on monthly basis between -32‰ and -19‰ , with a long-term mean over the studied period of -25‰ (Figure 2F). Sinking material with slightly heavier $\delta^{13}\text{C}$ values (around -23‰) was usually collected between June and September e.g., in 2002, 2004, 2006, 2008, 2010, 2011 and 2020, while sinking material with relatively light $\delta^{13}\text{C}$ values (around -26‰) sank between January and March in 2000, 2001, 2002, 2019. The isotope composition of organic carbon in the total particle flux was above the long-term mean throughout the year in 2004, 2008 and 2011, and below for the entire year between 2013 and 2015. The nitrogen

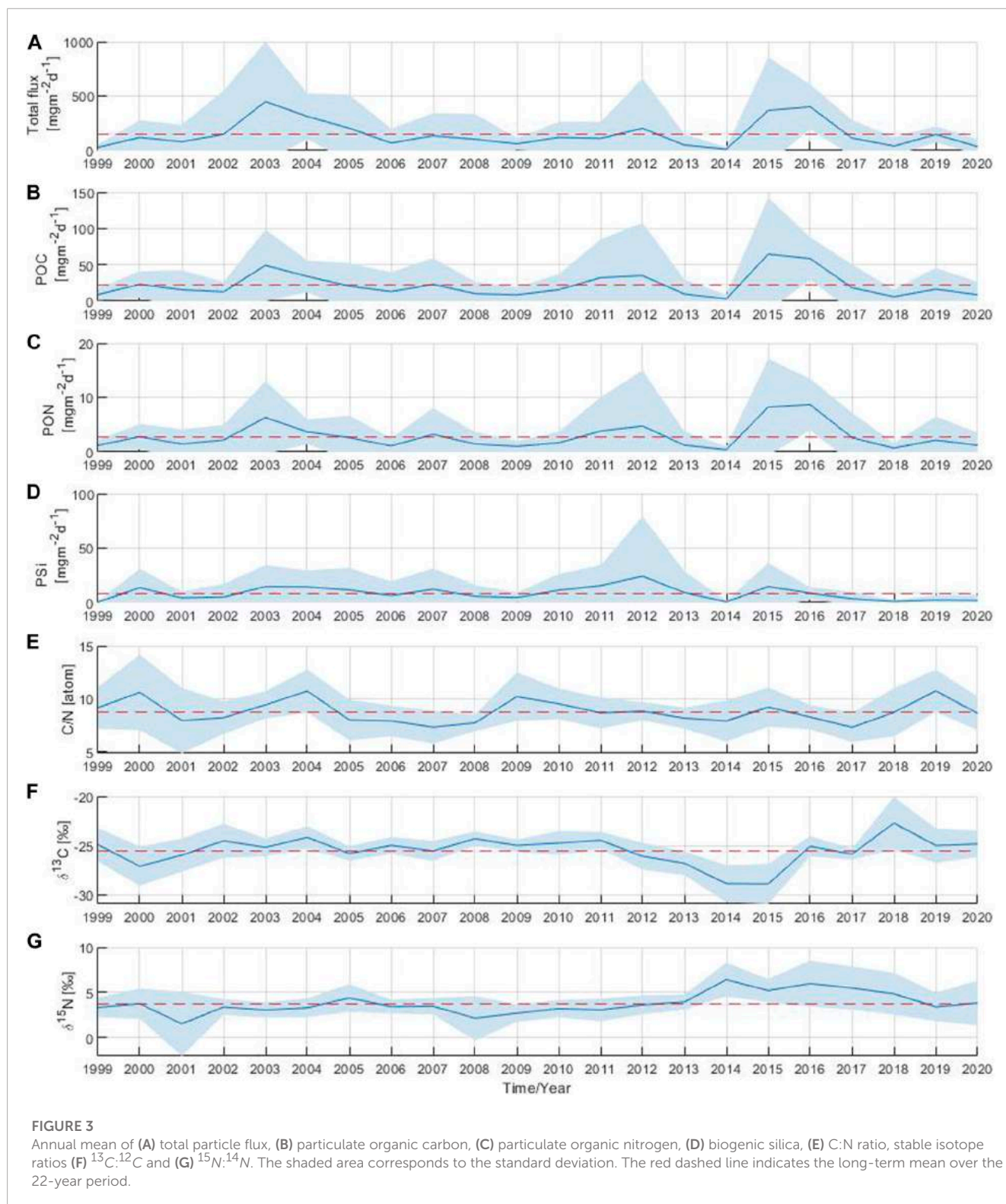


isotope composition of the total particle flux varied on monthly basis from -5‰ to 12‰ , with a long-term mean over the 22-year period of 4‰ (Figure 2G). The nitrogen isotope composition reached minimum values of -5 , -4 , -3 and -2‰ in May 2001, July 2001, November 2008 and December 2008, respectively. The monthly nitrogen isotopic composition mostly fluctuated around 4‰ , but in 2001 and 2003 the $\delta^{15}\text{N}$ became lighter for the whole year. Since 2014, the monthly nitrogen isotopic composition has increased slightly, reaching isotopically heavy values (above 10‰) in November 2014, April 2016, January 2017 and February 2018. In general, the particle flux and its components showed large

variability with values that stood out during certain periods without a recognizable pattern, indicating the need for further analysis at other time scales.

3.2 Inter-annual variability

The annual total particle flux showed significant inter-annual variability over the 22-year study period with three distinct periods of above-average flux. The first period occurred in 2003 with a moderate particle flux in March followed by the highest recorded



particle flux of the entire time series in July of that year (Figure 2A; Figure 3A). The second period occurred 9 years later, driven by the elevated particle flux observed in January 2012. The last period took place 3 years later with above-average particle flux in June 2015 and throughout 2016. The annual total particle flux varied widely,

ranging from 11 to $450 \text{ mg m}^{-2} \text{ d}^{-1}$, with the lowest and highest values observed in 2014 and 2003, respectively.

The annual POC and PON components of the flux showed similar periods of above-average flux as those observed in the annual total particle flux (Figures 3B,C). In years with high total particle flux such as 2003, 2012, 2015 and 2016, the annual POC component of

TABLE 2 Seasonal means of total particle flux, POC, PON, PSi, C:N, $\delta^{13}\text{C}$ and $\delta^{15}\text{N}$ from sediment traps moored at 180 m depth in the Gotland Basin between 1999 and 2020. The seasons were divided into spring (March–May), summer (June–August), autumn (September–November) and winter (December–February) (Supplementary Figure S4). Values in parentheses correspond to the percentage of the variable with respect to its total value over all seasons.

Variables	Winter	Spring	Summer	Autumn	Total
Total particle flux ($\text{mg m}^{-2} \text{d}^{-1}$)	169.2 (26.8)	150.4 (23.8)	193.1 (30.6)	118.1 (18.7)	630.8
POC ($\text{mg m}^{-2} \text{d}^{-1}$)	15.9 (17.7)	19.8 (22.1)	29.6 (33.0)	24.4 (27.2)	89.7
PON ($\text{mg m}^{-2} \text{d}^{-1}$)	2.2 (19.5)	2.2 (19.5)	3.5 (31.0)	3.4 (30.1)	11.3
PSi ($\text{mg m}^{-2} \text{d}^{-1}$)	11.0 (33.7)	8.8 (27.0)	6.1 (18.7)	6.7 (20.6)	32.6
C:N	9.5 (27.1)	8.9 (25.4)	8.0 (22.9)	8.6 (24.6)	35.0
$\delta^{13}\text{C}$ (‰)	−26.1 (25.6)	−26.0 (25.5)	−25.1 (24.6)	−24.9 (24.4)	−102.1
$\delta^{15}\text{N}$ (‰)	4.2 (27.6)	4.5 (29.6)	3.3 (21.7)	3.2 (21.1)	15.2

the flux reached maximum values ranging from 35 to 65 $\text{mg m}^{-2} \text{d}^{-1}$ (Figure 3B). The lowest annual POC value was observed in 2014 with a value of 3 $\text{mg m}^{-2} \text{d}^{-1}$. The maximum annual PON value was observed in 2016, followed by the annual PON component of the flux in 2015, 2003 and 2012 with values of 9, 8, 6 and 5 $\text{mg m}^{-2} \text{d}^{-1}$, respectively (Figure 3C). The minimum annual PON value occurred in 2014 (around 0.4 $\text{mg m}^{-2} \text{d}^{-1}$), as was also previously observed for the total particle flux and the POC component of the flux. The annual PSi component of the flux fluctuated between 1 and 24 $\text{mg m}^{-2} \text{d}^{-1}$ (Figure 3D). The absolute maximum of the annual PSi component of the flux was observed in 2012 reaching a value of 24 $\text{mg m}^{-2} \text{d}^{-1}$. Maximum annual PSi values were also observed in 2015 and 2003 with values around 15 $\text{mg m}^{-2} \text{d}^{-1}$. However, since 2016, the annual PSi component of the flux has decreased and remained at minimum values well below the average.

The annual C:N ratio fluctuated between 7 and 11 throughout the 22 year-period (Figure 3E). The maximum annual C:N ratios were observed in 2000, 2004, 2009 and 2019 close to 11, while the minimum annual values were found in 2007 and 2017 around 7. For the $\delta^{13}\text{C}$, a single annual maximum of −23‰ was identified in 2018, whereas annual minimum values of −29‰ were observed in 2014 and 2015 (Figure 3F). Minimum annual $\delta^{15}\text{N}$ values of 2‰ were observed in 2001 and 2008 (Figure 3G). A single $\delta^{15}\text{N}$ annual maximum of 6‰ was observed in 2014. An increase in $\delta^{15}\text{N}$ annual values above the long-term mean (4‰) was observed from 2014 to 2018.

3.3 Seasonal variability

Monthly means of the total particle flux and its components were grouped by season. The contribution of each component by season was calculated as a percentage of the total seasonal signals (Table 2). The summer season had the largest contribution to the total particle flux with about one-third (31%) of the sinking material, followed by winter (27%), spring (24%) and autumn (19%). The seasonal particle flux was between 118 and 193 $\text{mg m}^{-2} \text{d}^{-1}$. The seasonal variability of POC and PON followed a similar pattern, with higher POC and PON values in summer and autumn than in winter and spring. Seasonal means of POC and PON reached the highest values during summer, reflecting the contribution of the summer bloom

to the seasonal particle flux. The POC contribution to the seasonal particle flux ranged between 16 and 30 $\text{mg m}^{-2} \text{d}^{-1}$, whereas the PON component of the flux fluctuated between 2 and 4 $\text{mg m}^{-2} \text{d}^{-1}$. The minimum and maximum of the seasonal PSi were between 6 and 11 $\text{mg m}^{-2} \text{d}^{-1}$, with the maximum PSi values occurring in winter (December, January and February) and spring (March, April and May). The C:N ratio fluctuated between 8 and 9.5, with the highest value in winter and the lowest in summer. The seasonal PSi and C:N ratio showed an opposite pattern to the seasonal contributions of POC and PON in terms of the occurrence of maxima and minima, indicating the species succession from diatoms to cyanobacteria in the Gotland Basin (see Table 2). The seasonal mean of $\delta^{13}\text{C}$ varied slightly between seasons with values between −26‰ and −25‰, whereas the seasonal mean of $\delta^{15}\text{N}$ reached higher values in winter and spring rather than in summer and autumn. The maximum and minimum seasonal $\delta^{15}\text{N}$ values were observed in spring (4.5‰) and autumn (3.2‰), respectively.

3.4 Annual cycle

The annual cycle of the total particle flux revealed three discernible periods with high values in April, July and November, reaching up to 97 $\text{mg m}^{-2} \text{d}^{-1}$ in the Gotland Basin (Figure 4A). From December to March, there was a low particle flux with high variability. The annual cycle of the POC component of the flux reached maximum values in November (25 $\text{mg m}^{-2} \text{d}^{-1}$), followed by April and July with values of 16 and 9 $\text{mg m}^{-2} \text{d}^{-1}$, respectively (Figure 4B). The minimum POC in the flux (below 3 $\text{mg m}^{-2} \text{d}^{-1}$) was mostly observed between January and March. Maximum PON values of 2.1, 1.1 and 2.6 $\text{mg m}^{-2} \text{d}^{-1}$ occurred in April, July and November, respectively, with large variability observed throughout the year (Figure 4C). The POC and PON components of the flux showed similar patterns to the total particle flux (Figures 4A–C), coinciding the maximum values during the same months. The PSi in the flux had two maxima, the first one in April (4 $\text{mg m}^{-2} \text{d}^{-1}$) and the second one in November (6 $\text{mg m}^{-2} \text{d}^{-1}$) (Figure 4D). The PSi component of the flux was characterized by low values and variability in the remaining months, especially between June and September, with minimum PSi values occurring in July. The C:N ratio showed a bimodal cycle with values fluctuating between 7

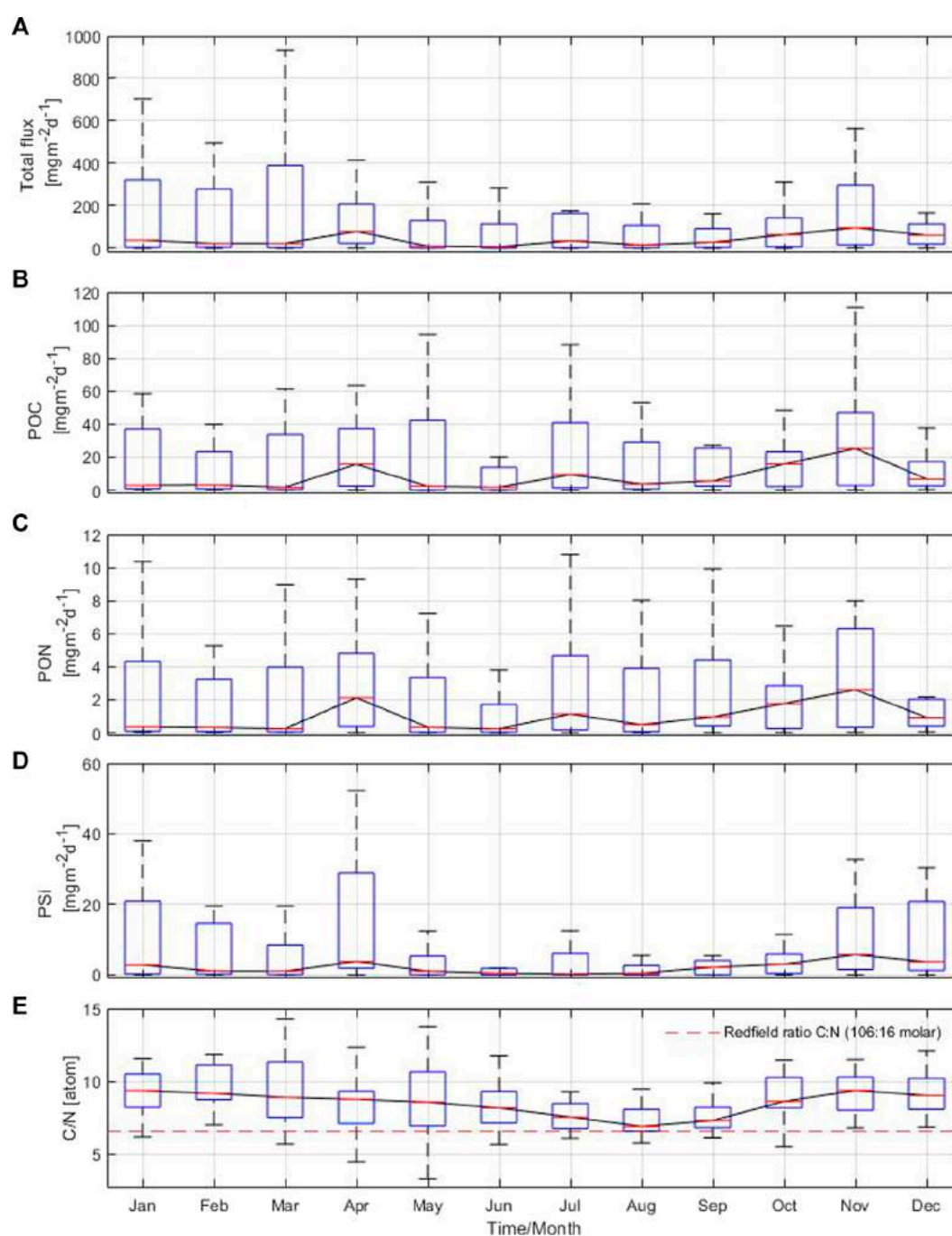


FIGURE 4

Annual cycle based on monthly means of (A) total particle flux, (B) particulate organic carbon, (C) particulate organic nitrogen, (D) biogenic silica and (E) C:N ratio from sediment traps moored at 180 m depth in the Gotland Basin between 1999 and 2020. The central red line in each box represents the median over 22 years. The bottom and top edges in each box indicate the 25th and 75th percentiles, respectively. The whiskers extend to the most extreme data points.

and 9. The highest C:N ratios were observed above the molar Redfield ratio (106:16) between November and February, while the lowest C:N ratios occurred in July, August and September (Figure 4E). The changes in the annual cycle of the total particle flux and POC marked the contribution of phytoplankton blooms to the sinking material in the Gotland Basin, while PON, PSi and C:N ratio reflected the species succession from silica-rich species like diatoms to species able to fix nitrogen from the

atmosphere such as cyanobacteria and *vice versa* (as in autumn), with the corresponding effects on the nutrient pool (Figure 4E and Supplementary Figure S3). Nitrate concentration showed high values prior to the onset of spring (March–April), summer (June) and autumn (October) blooms in the Gotland Basin with the additional contribution of nitrogen fixed by cyanobacteria observed in August (Supplementary Figure S3A). Phosphate showed a similar behavior with higher pre-bloom phosphate concentrations in April,

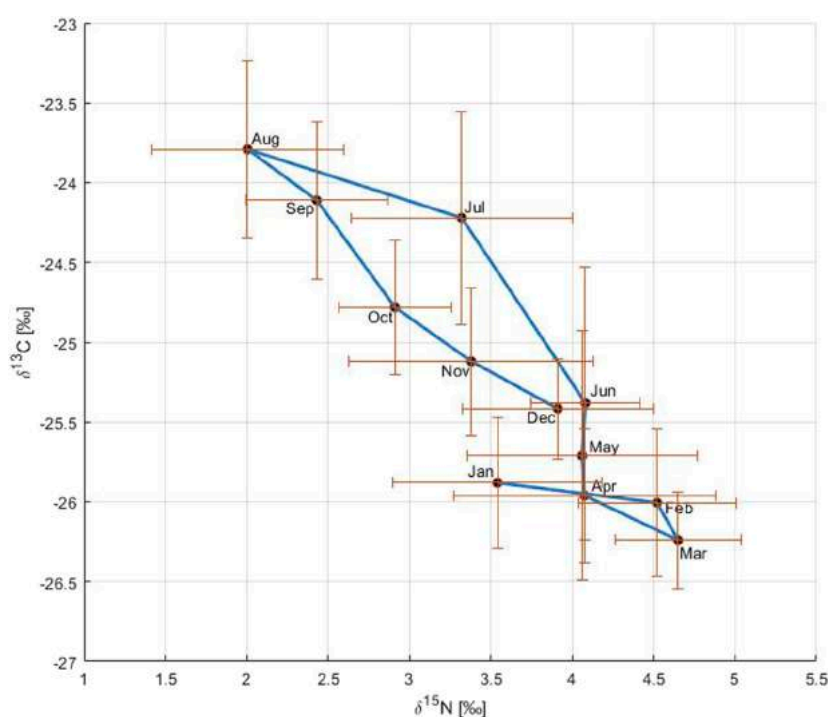


FIGURE 5

Relationship between $\delta^{13}\text{C}$ and $\delta^{15}\text{N}$ on an annual basis. The circles connected by a blue solid line correspond to monthly means of carbon and nitrogen stable isotopes over the period 1999 to 2020. The blue solid line shows the annual cycle of changes in both $\delta^{13}\text{C}$ and $\delta^{15}\text{N}$. The bars represent the standard deviation with respect to the variable on the axis.

June and September (Supplementary Figure S3B). Thus, periods of nutrient depletion and availability in the water column are driven by the development of blooms and species succession throughout the annual cycle.

3.5 Changes in the isotopic composition of organic carbon and nitrogen at 180 m depth

The relationship between $\delta^{13}\text{C}$ and $\delta^{15}\text{N}$ reflected the primary production cycle in the Gotland Basin (Figure 5). In January and February, both $\delta^{13}\text{C}$ and $\delta^{15}\text{N}$ remained uniform, likely related to low primary production resulting from the limited light and low temperature during winter. In March, primary production started as shown by the light $\delta^{13}\text{C}$ (CO_2 uptake) and heavy $\delta^{15}\text{N}$ values (nutrient consumption). During April and June, $\delta^{15}\text{N}$ values were similar reflecting the nitrate- $\delta^{15}\text{N}$ value as the nitrogen pool was fully consumed, but primary production continued with slightly heavier $\delta^{13}\text{C}$ values during this period. The gradual change to heavier $\delta^{13}\text{C}$ and lighter $\delta^{15}\text{N}$ values between June and August indicated the occurrence of the cyanobacteria bloom characterized by high nitrogen fixation and CO_2 uptake rates, the latter dominated initially more by the increase in temperature than by primary production (Montoya et al., 2002; Schneider et al., 2017). From September onwards, $\delta^{15}\text{N}$ started to return to heavier values and $\delta^{13}\text{C}$ to lighter values as a result of the change in the phytoplankton community from cyanobacteria to diatoms and the transport of deeper CO_2 -enriched water to the surface (Schneider et al., 2017).

4 Discussion

Primary production in the surface layer is reflected in the seasonality of the particle flux (Antia et al., 2001; Leipe et al., 2008). Diatoms dominate the export of organic particles in spring and autumn, whereas cyanobacteria do this in summer (Schneider et al., 2017). The total particle flux and its components showed a large variability in the long-term and inter-annual time scale as previously observed (Figures 2, 3). The main particle flux events were observed in 2003, 2012 and 2015, which coincided with the periods of Major Baltic Inflow events (MBIs) in the Baltic Sea (Mohrholz et al., 2015). The transport of large amounts of saline water into the Baltic Sea has an influence on the environmental conditions below the permanent halocline and therefore on the exported particles (Voss et al., 1997). A MBI occurred in January 2003, ending the stagnation period that had started in 1995. A moderate inflow event took place in 2011, followed by one of the strongest MBIs ever observed in December 2014. The MBIs are the sole source of deep water renewal and ventilation in the central Baltic basins, transporting water rich in oxygen, nutrients and salinity. The inflow pushes the anoxic water partly also across sills into the northern basins. Hence, phosphate-rich water is advected into shallower depths and leads to stronger cyanobacteria blooms after the inflow, which may contribute to the high particle flux observed with sediment traps in 2003, 2012 and 2015. The effects of the MBI in December 2014 were mainly observed in the Gotland Basin in June 2015, with the drastic increase in the total particle flux and its components in this year. In 2016, the inflow's effects were still noticed with above average flux throughout the year.

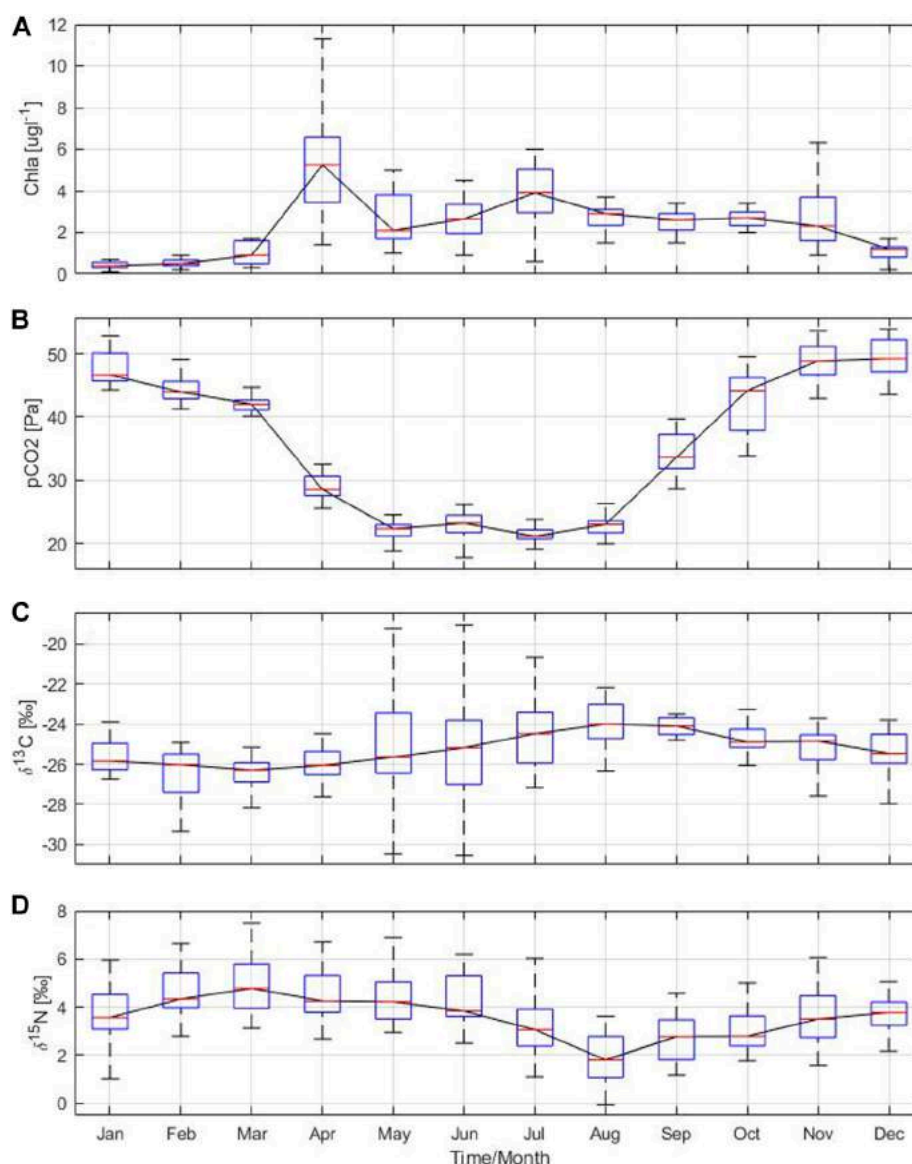


FIGURE 6

Annual cycle based on monthly means of (A) chlorophyll a and (B) partial pressure of carbon dioxide derived from water column measurements, stable isotope ratios (C) $^{13}\text{C}:^{12}\text{C}$ and (D) $^{15}\text{N}:^{14}\text{N}$ from sediment traps moored at 180 m depth in the Gotland Basin between 1999 and 2020. The central red line in each box represents the median over 22 years. The bottom and top edges in each box indicate the 25th and 75th percentiles, respectively. The whiskers extend to the most extreme data points.

According to [Struck et al. \(2004\)](#), lateral advection is the main source of particulate matter in the Gotland Basin. They compared the annual accumulation rates of organic carbon, nitrogen and phosphorus at 241-m depth with the vertical particle flux between summer of 1996 and 1997. [Schneider et al. \(2000\)](#) supports these results, suggesting that an additional source of carbon, e.g., via advection, is necessary to balance the carbon budget in the Gotland Basin. This might imply that the high particle flux observed in 2003, 2012 and 2015 in the Gotland Basin may have been generated by advection processes likely fueled by MBIs. However, [Cisternas-Novoa et al. \(2019\)](#) associate the high transfer efficiency of POC to aggregates of particulate organic matter and manganese oxide-like (MnOx-like) particles formed after the inflow of oxygen-rich water into the Gotland Basin in 2015. Thereby, aggregates containing

MnOx-like particles and organic matter may reach the sediments more quickly changing the biogeochemistry of the water column, the composition and vertical flux of particulate material. Further research is needed to confirm these hypotheses since they are beyond the scope of this study.

The seasonal and annual cycle of the particle flux in the Gotland Basin is led by primary production, which is reflected in the chlorophyll a concentration. Chlorophyll a, which serves as a proxy for primary production, exhibited a similar annual cycle to that of the particle flux and its components. The highest concentrations of chlorophyll a were observed in April and July with values of 6 and $4 \mu\text{g L}^{-1}$, respectively ([Figure 6A](#)). These elevated values in chlorophyll a coincided with the occurrence of spring and summer blooms as well as high particle flux in the Gotland

Basin (Supplementary Figure S1). The slow decline in chlorophyll a concentration after the summer bloom may be related to the occurrence of the diatom bloom in autumn (Wasmund and Uhlig, 2003), as shown by the increase in total particle flux, POC, PON and PSi in November. Chlorophyll a concentration was low with little variability between December and February, likely associated to light limitations and deep mixing during this period of the year. Sinking material produced by the spring and autumn blooms was enriched in PSi, indicating the presence of diatoms in the sinking particles. This observation was confirmed by the moderate chlorophyll a concentration and high POC and PSi in April and November (Figures 4B–D), as well as by microscopic analyses (Schneider et al., 2017).

Seasonal production was mainly dominated by carbon over-consumption, with a minor shift to nitrogen over-consumption in summer as observed in Figure 4E (Körtzinger et al., 2001). Thus, the C:N ratio allowed to identify three stages in the nutrient pool cycle where nitrate deficiency leads to a less nitrogen-rich organic matter (Körtzinger et al., 2001). First, a high concentration of inorganic nutrients was observed in March after winter-time mixing, followed by their consumption by the spring bloom in April (Spilling et al., 2019). Second, the contribution of isotopically light atmospheric nitrogen by cyanobacteria to the nutrient pool was observed in July. Lastly, there was a recharge of the nutrient pool due to remineralization and re-supply of nutrients by e.g., wind induced mixing in November. There is a correlation between the sinking material, its isotopic composition and nutrients. The total particle flux correlated positively and significantly with its components POC, PON and PSi. Therefore, a higher/lower total particle flux leads to a higher/lower POC, PON and PSi (see Table 3). The POC in the flux is most strongly correlated with PON and PSi because nitrogen and silicate are essential elements used by diatoms and other planktonic species for growth and cell wall formation, which also explains the strong correlation observed between PON and PSi. Chlorophyll a showed a positive and significant correlation with PON, indicating its relationship with the summer bloom containing mainly diazotrophic cyanobacteria. The negative but significant relationship between chlorophyll a and $\delta^{15}\text{N}$ confirmed that the summer bloom formed by cyanobacteria species like *Nodularia spumigena* and *Aphanizomenon flos-aquae* contributes light $\delta^{15}\text{N}$ values to the Gotland Basin, as also indicated by Struck et al. (2000) using sediment cores from the southern and central Baltic Sea. Overall, the total particle flux and its components POC, PON and PSi were weakly correlated with $\delta^{13}\text{C}$ and $\delta^{15}\text{N}$. Comparing the mean annual nitrogen isotope composition estimated by Struck et al. (2004) (3.7‰) and by Korth et al. (2014) (3.6‰ \pm 1‰) with the long-term mean over the 22-year period from this study (4‰), it seems that the source of nitrogen in the sediment traps remains unchanged. This implies, first, that most of the nitrogen comes from the surface particle flux (i.e., pelagic origin) rather than from nitrogen-enriched coastal waters, as suggested by Struck et al. (2004); Voss et al. (2005). Second, the depleted nitrogen signal is spreading through all marine organisms (from bacteria to fish) (Voss et al., 2005; Wannicke et al., 2013; Lesutiene et al., 2014; Karlson et al., 2015).

Changes in the isotopic composition of organic matter are driven by internal and external factors. Internal factors include cell size, growth, membrane permeability and enzymatic pathways for carbon

TABLE 3 Pearson correlation coefficients of monthly mean total particle flux, POC, PON, PSi, $\delta^{13}\text{C}$, $\delta^{15}\text{N}$ from sediment traps moored at 180 m depth, and chlorophyll a and partial pressure of carbon dioxide derived from water column measurements in the Gotland Basin between 1999 and 2020. Correlations that are statistically significant are shown in bold (p -value < 0.05).

	Total flux	POC	PON	PSi	$\delta^{13}\text{C}$	$\delta^{15}\text{N}$	Chla
POC ($\text{mg m}^{-2} \text{d}^{-1}$)	0.91						
PON ($\text{mg m}^{-2} \text{d}^{-1}$)	0.92	0.98					
PSi ($\text{mg m}^{-2} \text{d}^{-1}$)	0.92	0.79	0.79				
$\delta^{13}\text{C}$ (‰)	-0.05	0.18	0.19	-0.1			
$\delta^{15}\text{N}$ (‰)	0.01	-0.15	-0.15	0.07	-0.91		
Chla ($\mu\text{g L}^{-1}$)	0.29	0.45	0.55	0.05	0.36	-0.29	
$p\text{CO}_2$ (Pa)	0.53	0.3	0.24	0.66	-0.34	0.23	-0.62

uptake (Khim et al., 2018, and references therein), while external factors comprise the isotopic signature of dissolved inorganic carbon (DIC) and/or degradation routes of organic particles (Altabet, 1988; Altabet and Francois, 1994). Carbon isotopes indicate the content of dissolved CO_2 in the water column [$\text{CO}_2(\text{aq})$], as the dissolved CO_2 is the main source of carbon for most of phytoplankton species (Rau, 1994). Therefore, patterns of $\delta^{13}\text{C}$ may be attributed to the seasonal changes in $\text{CO}_2(\text{aq})$ as has also been observed in other ecosystems (Lehmann et al., 2004). The partial pressure of carbon dioxide showed a bimodal behavior with minimum values close to 20 Pa between May and August and maximum values around 50 Pa between November and January (Figure 6B). $\text{CO}_2(\text{aq})$ concentration in surface water is inversely related to $\delta^{13}\text{C}$ values in marine plankton because the carbon isotopic values reflect the increase in $\delta^{13}\text{C}$ -DIC (Lehmann et al., 2004) in response to CO_2 reduction by phytoplankton uptake (Figures 6B,C). There was no correlation found between $p\text{CO}_2$ and $\delta^{13}\text{C}$ and $\delta^{15}\text{N}$. However, $p\text{CO}_2$ had a moderate to strong correlation with the total particle flux, PSi and chlorophyll a, implying that more phytoplankton production results in more CO_2 uptake and therefore higher $\delta^{13}\text{C}$ - $\text{CO}_2(\text{aq})$ in surface water and higher particle flux (see Table 3). The low $\delta^{13}\text{C}$ values observed during spring (Figure 6C) may be related to cold, CO_2 -rich surface water due to the temperature-dependent fractionation between bicarbonate and dissolved CO_2 . $\delta^{13}\text{C}$ values during summer and autumn suggest low CO_2 -levels due to ongoing production, which was confirmed by direct measurements of CO_2 in the surface waters of the Gotland Sea (Thomas, 1997). $\delta^{13}\text{C}$ and $\delta^{15}\text{N}$ followed an opposite pattern (Figures 6C,D). While the $\delta^{13}\text{C}$ is at its minimum in March, the $\delta^{15}\text{N}$ is at its maximum, and *vice versa* in August.

$\delta^{15}\text{N}$ -PON at 180 m water depth reflects the pattern of pelagic production, as there is a shift from higher to lower $\delta^{15}\text{N}$ values between spring, summer and autumn (Leipe et al., 2008). $\delta^{15}\text{N}$ increased in February and March as a result of fractionation during nitrate uptake (Altabet, 1988). This may theoretically result in a fractionation of up to 12‰ - depending on the species - as described by Montoya and Mccarthy (1995). However, the euphotic zone is an open system in which such a fraction is not expressed, and therefore the fractionation is much lower as such reflected

in the sinking organic matter (Voss et al., 1996). Thus, the high $\delta^{15}\text{N}$ values in spring during the high production period may be related to the residual nitrate produced during nutrient utilization by phytoplankton (Altabet and Francois, 1994). In summer, decreasing $\delta^{15}\text{N}$ values in organic matter indicated nitrogen fixation, as nitrate contains more $\delta^{15}\text{N}$ than elemental nitrogen used by cyanobacteria (Leipe et al., 2008). Thereby, the variation in $\delta^{15}\text{N}$ values seems seasonal reflecting the transition from spring to summer driven by the species succession. During the transition from summer to autumn (August/September), the $\delta^{15}\text{N}$ reached its minimum value just after the maximum in cyanobacteria (Figure 6D). During late autumn and winter, degradation processes of organic matter and the resupply of nitrate to the surface waters re-establish a $\delta^{15}\text{N}$ value of nitrate that is around 3.7‰ and nicely reflect the $\delta^{15}\text{N}$ of the spring bloom sinking to the bottom. Additional factors that may contribute to changes in $\delta^{15}\text{N}$ include nitrogen contributions from terrestrial sources, phytoplankton growth and/or degradation, lateral transport of particles and particle residence times (Khim et al., 2018, and references therein). The $\delta^{15}\text{N}$ values in sinking material are mostly impacted by the signatures of nitrate reflected in phytoplankton and by nitrogen fixation.

Analyses of sediment traps from the Gotland Basin by Wasmund et al. (1998) and Cisternas-Novoa et al. (2019) revealed that the POC consisted of recently produced biogenic material. Therefore, the high POC flux observed in spring, summer and autumn may be related to the new production from the surface layer. Groetsch et al. (2016) and Beltran-Perez and Waniek (2022) confirmed based on *in-situ* observations and modeling results the occurrence of phytoplankton blooms during these periods of the year. The averaged climatology of phytoplankton biomass revealed explicit seasonality with spring blooms mostly composed of diatoms from March to April and summer blooms of cyanobacteria during June and August. An autumn diatom bloom also occurred, but of lesser magnitude compared to the spring and summer blooms. Additionally, Kahru et al. (2016) reported the spatial variability of primary production in terms of estimated chlorophyll a concentration using satellite images in the Baltic Sea. It was observed that the high summer POC in the flux corresponded to seasonal peaks in the estimated chlorophyll a concentration, indicating the seasonal presence of cyanobacteria blooms. The apparent increase in particle flux matches a general increasing trend in net sediment accumulation rates of carbon and nitrogen over the past 50 years in the Baltic Sea (Leipe et al., 2008). Based on sediment cores from the southern and central Baltic Sea, Struck et al. (2000) reported a clear shift to higher organic carbon concentrations and $\delta^{13}\text{C}$ values over the last 30 years in the Gotland Basin. Although high productivity in the Gotland Basin has been observed in the last decades, the tendency to heavier $\delta^{13}\text{C}$ values was not observed on either the long-term or inter-annual time scales analyzed in this study.

According to Leipe et al. (2008), the annual carbon flux between 1995 and 2003 was dominated by diazotrophic cyanobacteria in the Gotland Basin, which made up to two-thirds of the yearly flux. Nowadays, the export of carbon to the sea floor is still dominated by cyanobacteria, but its contribution to the total flux is close to one-third (Table 2). Several studies have reported earlier and longer cyanobacteria blooms in the Baltic Sea (Kahru and Elmgren, 2014; Kahru et al., 2016; Beltran-Perez and Waniek, 2022), which may partly explain the reduction observed in this

study. However, there is still no consensus about the increase or decrease of cyanobacteria blooms in the coming years, their future remains uncertain considering the continuous changes in the environment (Wasmund and Uhlig, 2003; Meier et al., 2019). Given the decrease in POC flux since 2016, there appears to be a shift from diatoms to dinoflagellates as the dominant bloom species. However, since both species may co-occur and therefore contribute to the particle flux, it is not possible to determine from the available sediment trap data whether the sinking material originates from diatoms or dinoflagellates to confirm this hypothesis. Using data on phytoplankton abundance and biomass (1979–1999) and chlorophyll a (1979–2000) from surface samples, Wasmund and Uhlig (2003) found a decrease in diatoms during spring blooms in the Gotland Sea and an upward trend in dinoflagellate abundance in all seasons in the Baltic Proper. Similarly, Klais et al. (2011) reported that the proportion of dinoflagellates relative to diatoms increased between 1995 and 2004, especially in the Gulf of Bothnia (from 0.1 to 0.4) and the Gulf of Finland (from 0.4 to 0.6). Shifts in the dominant bloom forming species have significant effects on the functioning of the Baltic Sea ecosystem. Changes in the food web may be expected as the efficiency of energy transfer to higher trophic levels might be reduced due to the timing of food availability (match-mismatch hypothesis, Smith and Hollibaugh, 1993; Winder and Schindler, 2004). A shift in phytoplankton may also inhibit the survival of zooplankton and fish, affecting the recruitment of larvae, as larval spawning continues to match the original timing of the bloom prior to changes (Cole, 2014; Gittings et al., 2018). Therefore, shifts in the phytoplankton community along with current environmental changes may have potentially large impacts on the Baltic Sea. Overall, the long-term sediment trap data used in this study allowed us to identify changes in sinking particles that would not otherwise be possible, given the difficulty of modeling and predicting the behavior of sinking particles with such high variability over time.

5 Conclusion

Sinking particles provide the major connection between processes in the upper part of the water column and sediments. In spite of the high temporal variability in the particle flux and its components, three distinct periods driven by primary production at the surface were identified in the Gotland Basin. Sinking material in spring and autumn is derived from the diatom bloom. The large particle export from the surface in summer is driven by the growth of nitrogen fixing cyanobacteria, mainly of the species *Aphanizomenon* and *Nodularia*, which take up and store phosphate for use when it is already depleted from the water column. The contribution of isotopically light atmospheric nitrogen by diazotrophic cyanobacteria to the sinking material is evidenced by the changes in the $\delta^{15}\text{N}$ values in summer, reflecting as well the succession between diatom and cyanobacteria species in the annual cycle. The succession in the phytoplankton community and the occurrence of phytoplankton blooms are important factors determining the seasonal pattern of sinking material in the Gotland Basin. Unusual high particle flux from surface blooms occurred in 2003, 2012 and 2015, showing the capability of sediment traps

to reflect changes in primary production that would otherwise be difficult to observe due to the patchiness of these events. There are some indications that MBIs lead to increased particle flux after their occurrence. However, a comprehensive analysis of the effects of MBIs throughout the water column is still needed.

The Baltic Sea has undergone significant changes, the reduction in carbon exported to the sediment in summer compared to past decades is a sign of these changes. Sinking particles may be influenced by factors not directly related to the surface, such as mixing or advection processes within the water column. In addition, the complete pathway of nutrient sources is unknown, as a low $\delta^{15}N$ signal in the sinking material may be related to multiple processes such as nitrogen fixation, N-release or ammonium uptake. Therefore, while the findings of this study provide valuable insights into the carbon exported at different seasons and years linked to the development of phytoplankton blooms in the Gotland Basin, they should be interpreted in the context of the broader changes that are occurring in the Baltic Sea. Furthermore, given the temporal variability exhibited by the particle flux and its components, this study demonstrates the importance of continued monitoring of the Baltic Sea and the challenges of modeling and making future predictions in such a highly variable system.

Data availability statement

The data sets analyzed in this study can be found in: the Global Ocean Surface Carbon product provided by the Copernicus Marine Service (<https://data.marine.copernicus.eu/products>), the oceanographic database of the Leibniz Institute for Baltic Sea Research Warnemünde (IOWDB and ODIN) (<https://odin2.iowarnemuende.de/>) and the SHARKweb database administered by the Swedish Meteorological and Hydrological Institute (SMHI) (<https://sharkweb.smhi.se/hamta-data/>).

Author contributions

FP was the scientist in charge of the sediment trap deployments for many years and provided the bulk parameters of the sediment trap data set. MV and IL provided the isotope data, MV also contributed to their interpretation and discussion. JW supervised all data analyses and interpretation of results for this study. OB-P explored, harmonized and analyzed the data, prepared the figures and wrote the manuscript. All authors contributed to the article and approved the submitted version.

References

- Almroth-Rosell, E., Eilola, K., Hordoir, R., Meier, H. E., and Hall, P. O. (2011). Transport of fresh and resuspended particulate organic material in the Baltic Sea - a model study. *J. Mar. Syst.* 87, 1–12. doi:10.1016/j.jmarsys.2011.02.005
- Altabet, M. A., and Francois, R. (1994). Sedimentary nitrogen isotopic ratio as a recorder for surface ocean nitrate utilization. *Glob. Biogeochem. Cycles* 8, 103–116. doi:10.1029/93GB03396
- Altabet, M. A. (1988). Variations in nitrogen isotopic composition between sinking and suspended particles: Implications for nitrogen cycling and particle transformation in the open ocean. *Deep Sea Res. Part A, Oceanogr. Res. Pap.* 35, 535–554. doi:10.1016/0198-0149(88)90130-6
- Antia, A. N., Koeve, W., Fischer, G., Blanz, T., Schulz-Bull, D., Scholten, J., et al. (2001). Basin-wide particulate carbon flux in the Atlantic Ocean: Regional export

Funding

The Funding was granted by the DAAD program: Research Grants—Doctoral Programmes in Germany 2018/19, as well as by the Leibniz Institute for Baltic Sea Research Warnemünde (IOW) and the Bundesamt für Seeschifffahrt und Hydrographie (BSH) as part of the long-term data collection and monitoring program of the Baltic Sea.

Acknowledgments

The authors would like to thank the DAAD and the IOW for the funding and support provided during the preparation of the manuscript. The authors thank the BSH for the funding provided during the collection of data over the past decades, the scientists and technicians involved in deploying the sediment trap during various cruises and the ship crews for their technical support. Special thanks to Uwe Hehl and Regina Hansen, without their effort over decades this data set would not exist. We would also like to thank the reviewers for their constructive comments, which helped us to improve the quality of the manuscript.

Conflict of interest

The authors declare that the research was conducted in the absence of any commercial or financial relationships that could be construed as a potential conflict of interest.

The handling editor GH declared a shared committee with the author MV at the time of review.

Publisher's note

All claims expressed in this article are solely those of the authors and do not necessarily represent those of their affiliated organizations, or those of the publisher, the editors and the reviewers. Any product that may be evaluated in this article, or claim that may be made by its manufacturer, is not guaranteed or endorsed by the publisher.

Supplementary material

The Supplementary Material for this article can be found online at: <https://www.frontiersin.org/articles/10.3389/feart.2023.1171917/full#supplementary-material>

- patterns and potential for atmospheric CO₂ sequestration. *Glob. Biogeochem. Cycles* 15, 845–862. doi:10.1029/2000GB001376
- Belkin, I. M. (2009). Rapid warming of large marine ecosystems. *Prog. Oceanogr.* 81, 207–213. doi:10.1016/j.pocean.2009.04.011
- Beltran-Perez, O. D., and Waniek, J. J. (2022). Inter-annual variability of spring and summer blooms in the eastern Baltic Sea. *Front. Mar. Sci.* 9. doi:10.3389/fmars.2022.928633
- Blomqvist, S., and Heiskanen, A. (2001). "A systems analysis of the Baltic Sea ecological studies," in *Chall. Sediment. Balt. Sea* Editors F. Wulff, L. Rahm, and P. Larsson (Berlin, Heidelberg: Springer).
- Blomqvist, S., and Larsson, U. (1994). Detrital bedrock elements as tracers of settling resuspended particulate matter in a coastal area of the Baltic Sea. *Limnol. Oceanogr.* 39, 880–896. doi:10.4319/lo.1994.39.4.0880
- Bodungen, B. V., Wunsch, M., and Fürderer, H. (1991). *Sampling and analysis of suspended and sinking particles in the northern North atlantic* Editors D. C. Hurd, and D. W. Spencer 63 edn. (Washington, DC: Geophysical Monograph Series, American Geophysical Union), 47–56. doi:10.1029/GM063P0047
- Carstensen, J., Conley, D. J., Bonsdorff, E., Gustafsson, B. G., Hietanen, S., Janas, U., et al. (2014). Hypoxia in the Baltic Sea: Biogeochemical cycles, benthic fauna, and management. *Ambio* 43, 26–36. doi:10.1007/s13280-013-0474-7
- Christensen, O. B., Kjellström, E., and Zorita, E. (2015). "Projected change — atmosphere," in *Second assess clim chang balt sea basin reg clim stud.* Editor T. B. I. A. Team (Cham: Springer), 217–233. doi:10.1007/978-3-319-16006-1
- Cisternas-Novoa, C., Le Moigne, F. A., and Engel, A. (2019). Composition and vertical flux of particulate organic matter to the oxygen minimum zone of the central Baltic Sea: Impact of a sporadic North Sea inflow. *Biogeosciences* 16, 927–947. doi:10.5194/bg-16-927-2019
- Cole, H. S. (2014). The natural variability and climate change response in phytoplankton. England: University of Southampton. Doctoral dissertation.
- Diaz, R. J., and Rosenberg, R. (2008). Spreading dead zones and consequences for marine ecosystems. *Sci.* (80-.) 321, 926–929. doi:10.1126/science.1156401
- Eilola, K., Mårtensson, S., and Meier, H. E. (2013). Modeling the impact of reduced sea ice cover in future climate on the Baltic Sea biogeochemistry. *Geophys. Res. Lett.* 40, 149–154. doi:10.1029/2012GL054375
- Elmgren, R. (1984). Trophic dynamics in the enclosed, brackish Baltic Sea. *Rapp. P.-v. Réun. - Cons. Int. Explor. Mer.* 1984, 152–169.
- Fleming-Lehtinen, V., Laamanen, M., Kuosa, H., Haahti, H., and Olsonen, R. (2008). Long-term development of inorganic nutrients and chlorophyll α in the open Northern Baltic Sea. *Ambio* 37, 86–92. doi:10.1579/0044-7447(2008)37[86:LDOINA]2.0.CO;2
- Gittings, J. A., Raitsos, D. E., Krokos, G., and Hoteit, I. (2018). Impacts of warming on phytoplankton abundance and phenology in a typical tropical marine ecosystem. *Sci. Rep.* 8, 2240. doi:10.1038/s41598-018-20560-5
- Groetsch, P. M., Simis, S. G., Eleveld, M. A., and Peters, S. W. (2016). Spring blooms in the Baltic Sea have weakened but lengthened from 2000 to 2014. *Biogeosciences* 13, 4959–4973. doi:10.5194/bg-13-4959-2016
- Gustafsson, Ö., Andersson, P., Roos, P., Kukulska, Z., Broman, D., Larsson, U., et al. (2004). Evaluation of the collection efficiency of upper ocean sub-photoc-layer sediment traps: A 24-month *in situ* calibration in the open Baltic Sea using ²³⁴Th. *Limnol. Oceanogr. Methods* 2, 62–74. doi:10.4319/lom.2004.2.62
- Gustafsson, Ö., Gelting, J., Andersson, P., Larsson, U., and Roos, P. (2013). An assessment of upper ocean carbon and nitrogen export fluxes on the boreal continental shelf: A 3-year study in the open Baltic Sea comparing sediment traps, ²³⁴Th proxy, nutrient, and oxygen budgets. *Limnol. Oceanogr. Methods* 11, 495–510. doi:10.4319/lom.2013.11
- Havenhand, J. N. (2012). How will ocean acidification affect Baltic Sea ecosystems? An assessment of plausible impacts on key functional groups. *Ambio* 41, 637–644. doi:10.1007/s13280-012-0326-x
- Heiskanen, A. S., and Kononen, K. (1994). Sedimentation of vernal and late summer phytoplankton communities in the coastal Baltic Sea. *Arch. fur Hydrobiol.* 131, 175–198. doi:10.1127/archiv-hydrobiol/131/1994/175
- HELCOM/Baltic Earth (2021). Climate change in the Baltic Sea 2021 fact sheet. Tech. rep. Helsinki, Finland: Helsinki Commission – HELCOM.
- Kahru, M., and Elmgren, R. (2014). Multidecadal time series of satellite-detected accumulations of cyanobacteria in the Baltic Sea. *Biogeosciences* 11, 3619–3633. doi:10.5194/bg-11-3619-2014
- Kahru, M., Elmgren, R., and Savchuk, O. P. (2016). Changing seasonality of the Baltic Sea. *Biogeosciences* 13, 1009–1018. doi:10.5194/bg-13-1009-2016
- Karlson, A. M., Duberg, J., Motwani, N. H., Hogfors, H., Klawonn, I., Ploug, H., et al. (2015). Nitrogen fixation by cyanobacteria stimulates production in Baltic food webs. *Ambio* 44, 413–426. doi:10.1007/s13280-015-0660-x
- Khim, B. K., Otsuka, S., Park, K. A., and Noriki, S. (2018). $\delta^{13}\text{C}$ and $\delta^{15}\text{N}$ values of sediment-trap particles in the Japan and Yamato basins and comparison with the core-top values in the east/Japan sea. *Ocean. Sci. J.* 53, 17–29. doi:10.1007/s12601-018-0003-5
- Klais, R., Tamminen, T., Kremp, A., Spilling, K., and Olli, K. (2011). Decadal-scale changes of dinoflagellates and diatoms in the anomalous Baltic Sea spring bloom. *PLoS One* 6, e21567. doi:10.1371/journal.pone.0021567
- Korth, F., Deutsch, B., Frey, C., Moros, C., and Voss, M. (2014). Nitrate source identification in the Baltic Sea using its isotopic ratios in combination with a Bayesian isotope mixing model. *Biogeosciences* 11, 4913–4924. doi:10.5194/bg-11-4913-2014
- Körtzinger, A., Koeve, W., Kähler, P., and Mintrop, L. (2001). C:N ratios in the mixed layer during the productive season in the northeast Atlantic ocean. *Deep. Res. Part I Oceanogr. Res. Pap.* 48, 661–688. doi:10.1016/S0967-0637(00)00051-0
- Kremling, K., Lentz, U., Zeitzschel, B., Schulz-Bull, D. E., and Duinker, J. C. (1996). New type of time-series sediment trap for the reliable collection of inorganic and organic trace chemical substances. *Rev. Sci. Instrum.* 67, 4360–4363. doi:10.1063/1.1147582
- Kudryavtseva, E. A., Pimenov, N. V., Aleksandrov, S. V., and Kudryavtsev, V. M. (2011). Primary production and chlorophyll content in the southeastern Baltic Sea in 2003–2007. *Oceanology* 51, 27–35. doi:10.1134/S0001437011010103
- Lehmann, M. F., Bernasconi, S. M., McKenzie, J. A., Barbieri, A., Simona, M., and Veronesi, M. (2004). Seasonal variation of the $\delta^{13}\text{C}$ and $\delta^{15}\text{N}$ of particulate and dissolved carbon and nitrogen in Lake Lugano: Constraints on biogeochemical cycling in a eutrophic lake. *Limnol. Oceanogr.* 49, 415–429. doi:10.4319/lo.2004.49.2.0415
- Lehtoranta, J., Ekholm, P., and Pitkänen, H. (2008). Eutrophication-driven sediment microbial processes can explain the regional variation in phosphorus concentrations between Baltic Sea sub-basins. *J. Mar. Syst.* 74, 495–504. doi:10.1016/j.jmarsys.2008.04.001
- Leipe, T., Harff, J., Meyer, M., Hille, S., Pollehn, F., Schneider, R., et al. (2008). "Sedimentary records of environmental changes and anthropogenic impacts during the past decades," in *State evol. Balt. Sea, 1952-2005 A detail. 50-Year surv. Meteorol. Clim. Physics, chem. Biol. Mar. Environ.* (New Jersey, United States: John Wiley and Sons, Ltd). chap 14 395–439. doi:10.1002/9780470283134.CH14
- Lesutiene, J., Bukaveckas, P. A., Gasuniute, Z. R., Pilkaityte, R., and Razinkovas-Baziukas, A. (2014). Tracing the isotopic signal of a cyanobacteria bloom through the food web of a Baltic Sea coastal lagoon. *Estuar. Coast. Shelf Sci.* 138, 47–56. doi:10.1016/j.ecss.2013.12.017
- Mariotti, A. (1983). Atmospheric nitrogen is a reliable standard for natural N abundance measurements. *Nature* 1983, 8–10.
- Meier, H. E., Andersson, H. C., Eilola, K., Gustafsson, B. G., Kuznetsov, I., Mller-Karulis, B., et al. (2011). Hypoxia in future climates: A model ensemble study for the Baltic Sea. *Geophys. Res. Lett.* 38, 1–6. doi:10.1029/2011GL049929
- Meier, H. E., Dieterich, C., Eilola, K., Gröger, M., Höglund, A., Radtke, H., et al. (2019). Future projections of record-breaking sea surface temperature and cyanobacteria bloom events in the Baltic Sea. *Ambio* 48, 1362–1376. doi:10.1007/s13280-019-01235-5
- Meier, H. E., Hordoir, R., Andersson, H. C., Dieterich, C., Eilola, K., Gustafsson, B. G., et al. (2012). Modeling the combined impact of changing climate and changing nutrient loads on the Baltic Sea environment in an ensemble of transient simulations for 1961–2099. *Clim. Dyn.* 39, 2421–2441. doi:10.1007/s00382-012-1339-7
- Mohrholz, V. (2018). Major Baltic inflow statistics - revised. *Front. Mar. Sci.* 5, 1–16. doi:10.3389/fmars.2018.00384
- Mohrholz, V., Naumann, M., Nausch, G., Krüger, S., and Gräwe, U. (2015). Fresh oxygen for the Baltic Sea - an exceptional saline inflow after a decade of stagnation. *J. Mar. Syst.* 148, 152–166. doi:10.1016/j.jmarsys.2015.03.005
- Montoya, J. P., Carpenter, E. J., and Capone, D. G. (2002). Nitrogen fixation and nitrogen isotope abundances in zooplankton of the oligotrophic North Atlantic. *Limnol. Oceanogr.* 47, 1617–1628. doi:10.4319/lo.2002.47.6.1617
- Montoya, J. P., and McCarthy, J. J. (1995). Isotopic fractionation during nitrate uptake by phytoplankton grown in continuous culture. *J. Plankton Res.* 17, 439–464. doi:10.1093/plankt/17.3.439
- Murray, C. J., Müller-Karulis, B., Carstensen, J., Conley, D. J., Gustafsson, B. G., and Andersen, J. H. (2019). Past, present and future eutrophication status of the Baltic Sea. *Front. Mar. Sci.* 6, 1–12. doi:10.3389/fmars.2019.00002
- Nieuwenhuize, J., Maas, Y., and Middelburg, J. (1994). Rapid analysis of organic carbon and nitrogen in particulate materials. *Mar. Chem.* 45, 217–224. doi:10.1016/0304-4203(94)90005-1
- Rau, G. (1994). "Variations in sedimentary organic $\delta^{13}\text{C}$ as a proxy for past changes in ocean and atmospheric CO₂ concentrations," in *Carbon cycl. glacial ocean constraints ocean role glob chang.* Editors R. Zahn, T. Pedersen, M. Kaminski, and L. Labeyrie (Berlin, Heidelberg: Springer).
- Reissmann, J. H., Burchard, H., Feistel, R., Hagen, E., Lass, H. U., Mohrholz, V., et al. (2009). Vertical mixing in the Baltic Sea and consequences for eutrophication - a review. *Prog. Oceanogr.* 82, 47–80. doi:10.1016/j.pocean.2007.10.004
- Schlitzer, R. (2023). *Ocean Data View*. Available at: odv.awi.de.
- Schneider, B., Dellwig, O., Kuliński, K., Omstedt, A., Pollehn, F., Rehder, G., et al. (2017). "Biogeochemical cycles," in *Biol. Oceanogr. Balt. Sea* Editors H. Schubert, and T. Radziejewska (Dordrecht: Springer). doi:10.1007/978-94-007-0668-2_3/COVER

- Schneider, B., and Müller, J. D. (2018). "The main hydrographic characteristics of the Baltic Sea," in *Biogeochem. Transform. Balt. Sea* (Cham: Springer Oceanography), 35–41. doi:10.1007/978-3-319-61699-5_3
- Schneider, B., Nagel, K., and Struck, U. (2000). Carbon fluxes across the halocline in the eastern Gotland Sea. *J. Mar. Syst.* 25, 261–268. doi:10.1016/S0924-7963(00)00020-8
- Smetacek, V., von Bodungen, B., Knoppers, B., Peinert, R., Pollehne, F., Stegmann, P., et al. (1984). Seasonal stages characterizing the annual cycle of an inshore pelagic system. *Rapp. P.-v. Réun. Cons. Int. Explor. Mer.* 183, 126–135.
- Smith, S. V., and Hollibaugh, J. T. (1993). Coastal metabolism and the oceanic organic carbon balance. *Rev. Geophys.* 31, 75–89. doi:10.1029/92RG02584
- Spilling, K., Fuentes-Lema, A., Quemaliños, D., Klais, R., and Sobrino, C. (2019). Primary production, carbon release, and respiration during spring bloom in the Baltic Sea. *Limnol. Oceanogr.* 64, 1779–1789. doi:10.1002/lno.11150
- Struck, U., Emeis, K. C., Voss, M., Christiansen, C., and Kunzendorf, H. (2000). Records of southern and central Baltic Sea eutrophication in $\delta^{13}\text{C}$ and $\delta^{15}\text{N}$ of sedimentary organic matter. *Mar. Geol.* 164, 157–171. doi:10.1016/S0025-3227(99)00135-8
- Struck, U., Pollehne, F., Bauerfeind, E., and Bodungen, B. V. (2004). Sources of nitrogen for the vertical particle flux in the Gotland Sea (Baltic Proper) - results from sediment trap studies. *J. Mar. Syst.* 45, 91–101. doi:10.1016/j.jmarsys.2003.11.012
- Tamelaender, T., and Heiskanen, A. S. (2004). Effects of spring bloom phytoplankton dynamics and hydrography on the composition of settling material in the coastal northern Baltic Sea. *J. Mar. Syst.* 52, 217–234. doi:10.1016/j.jmarsys.2004.02.001
- Tamelaender, T., Spilling, K., and Winder, M. (2017). Organic matter export to the seafloor in the Baltic Sea: Drivers of change and future projections. *Ambio* 46, 842–851. doi:10.1007/s13280-017-0930-x
- Thomas, H. (1997). Anorganischer Kohlenstoff im Oberflächenwasser der Ostsee. *Tech. Rep.* 23. Institut für Ostseeforschung Warnemünde.
- Vahtera, E., Conley, D. J., Gustafsson, B. G., Kuosa, H., Pitkänen, H., Savchuk, O. P., et al. (2007). Internal ecosystem feedbacks enhance nitrogen-fixing cyanobacteria blooms and complicate management in the Baltic Sea. *Ambio* 36, 186–194. doi:10.1579/0044-7447(2007)36[186:IEFENC]2.0.CO;2
- Voss, M., Altabet, M. A., and Bodungen, B. V. (1996). $\delta^{15}\text{N}$ in sedimenting particles as indicator of euphotic-zone processes. *Deep. Res. Part I Oceanogr. Res. Pap.* 43, 33–47. doi:10.1016/0967-0637(95)00099-2
- Voss, M., Emeis, K. C., Hille, S., Neumann, T., and Dippner, J. W. (2005). Nitrogen cycle of the Baltic Sea from an isotopic perspective. *Glob. Biogeochem. Cycles* 19, 1–15. doi:10.1029/2004GB002338
- Voss, M., Nausch, G., and Montoya, J. P. (1997). Nitrogen stable isotope dynamics in the central Baltic Sea: Influence of deep-water renewal on the N-cycle changes. *Mar. Ecol. Prog. Ser.* 158, 11–21. doi:10.3354/meps158011
- Wannicke, N., Korth, F., Liskow, I., and Voss, M. (2013). Incorporation of diazotrophic fixed N₂ by mesozooplankton - case studies in the southern Baltic Sea. *J. Mar. Syst.* 117–118, 1–13. doi:10.1016/j.jmarsys.2013.03.005
- Wasmund, N., Alheit, J., Pollehne, F., Siegel, H., and Zettler, M. L. (1998). Ergebnisse des Biologischen Monitorings der Ostsee im Jahre 1997 im Vergleich mit bisherigen Untersuchungen. *Tech. Rep.* 32. Institut für Ostseeforschung Warnemünde.
- Wasmund, N., Nausch, G., Postel, L., Witek, Z., Zalewski, M., Gromisz, S., et al. (2000). Trophic status of coastal and open areas of the south-eastern Baltic Sea based on nutrient and phytoplankton data from 1993–1997. *Tech. Rep.* 86.
- Wasmund, N., and Uhlig, S. (2003). Phytoplankton trends in the Baltic Sea. *ICES J. Mar. Sci.* 60, 177–186. doi:10.1016/S1054-3139(02)00280-1
- Winder, M., and Schindler, D. E. (2004). Climate change uncouples trophic interactions in an aquatic ecosystem. *Ecology* 85, 2100–2106. doi:10.1890/04-0151

Supplementary Material

Manuscript title: Temporal variability of particle flux and its components in the Gotland Basin, eastern Baltic Sea

Manuscript ID: 1171917

Authors: Oscar Dario Beltran-Perez, Maren Voss, Falk Pollehne, Iris Liskow and Joanna Jadwiga Waniek

Journal: Frontiers in Earth Science, section Marine Geoscience

Article type: Original Research

Submitted on: 22 Feb 2023

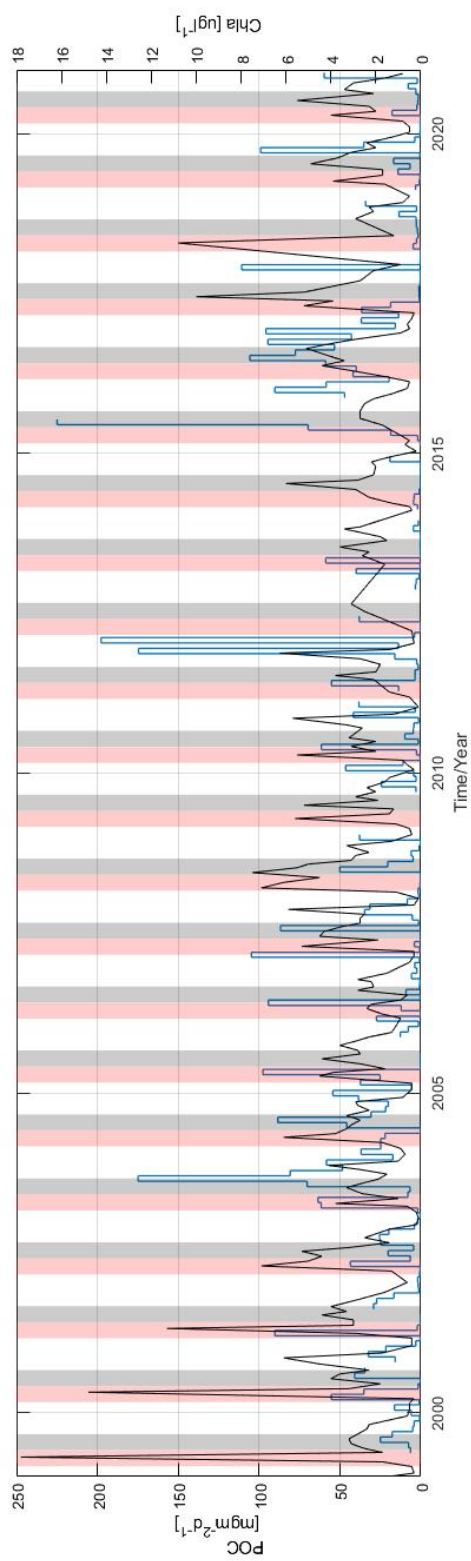


Figure S1. The POC component of the total particle flux (blue line) from sediment traps moored at 180 m depth and chlorophyll a (black line) measured at the surface in the Gotland Basin between 1999 and 2020. The red and gray stripes represent spring (March-May) and summer (June-August) seasons, respectively.

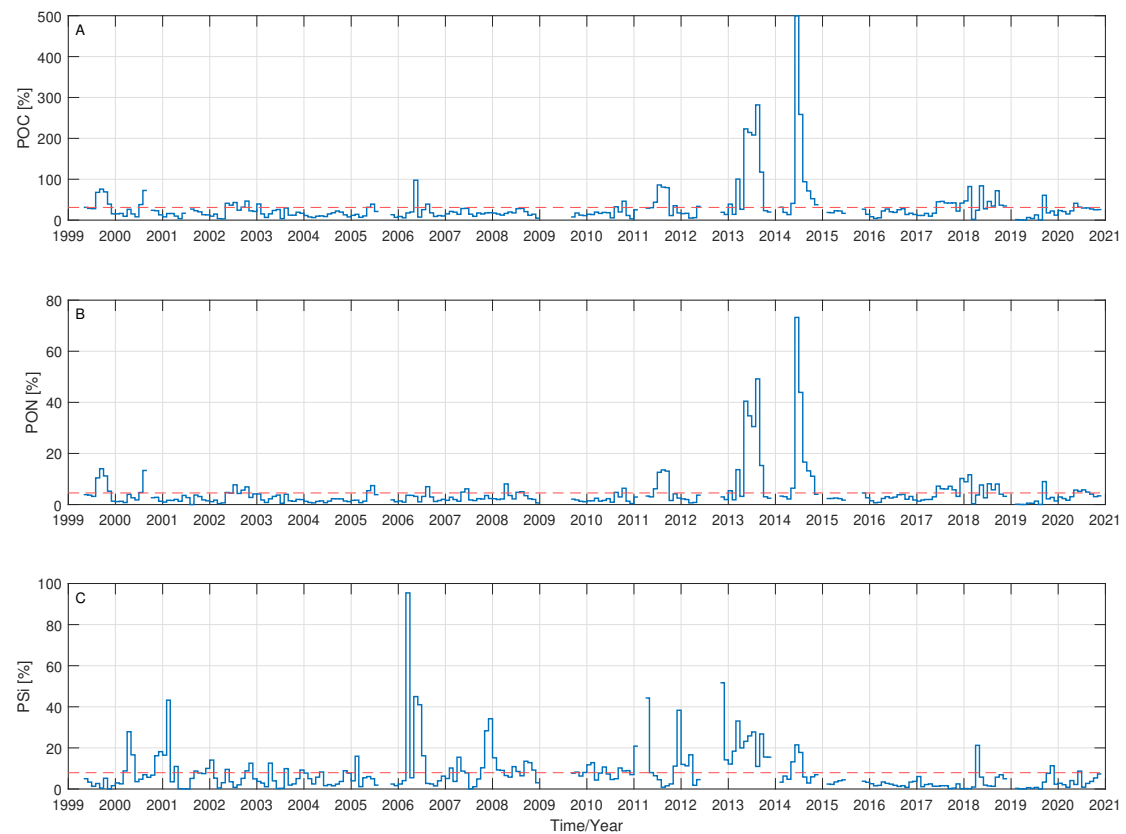


Figure S2. Monthly mean of the components of the flux expressed as a percentage of the total particle flux. A) particulate organic carbon, B) particulate organic nitrogen and C) biogenic silica. The red dashed line indicates the long-term mean over the 22-year period with values of 31, 5 and 8%, respectively.

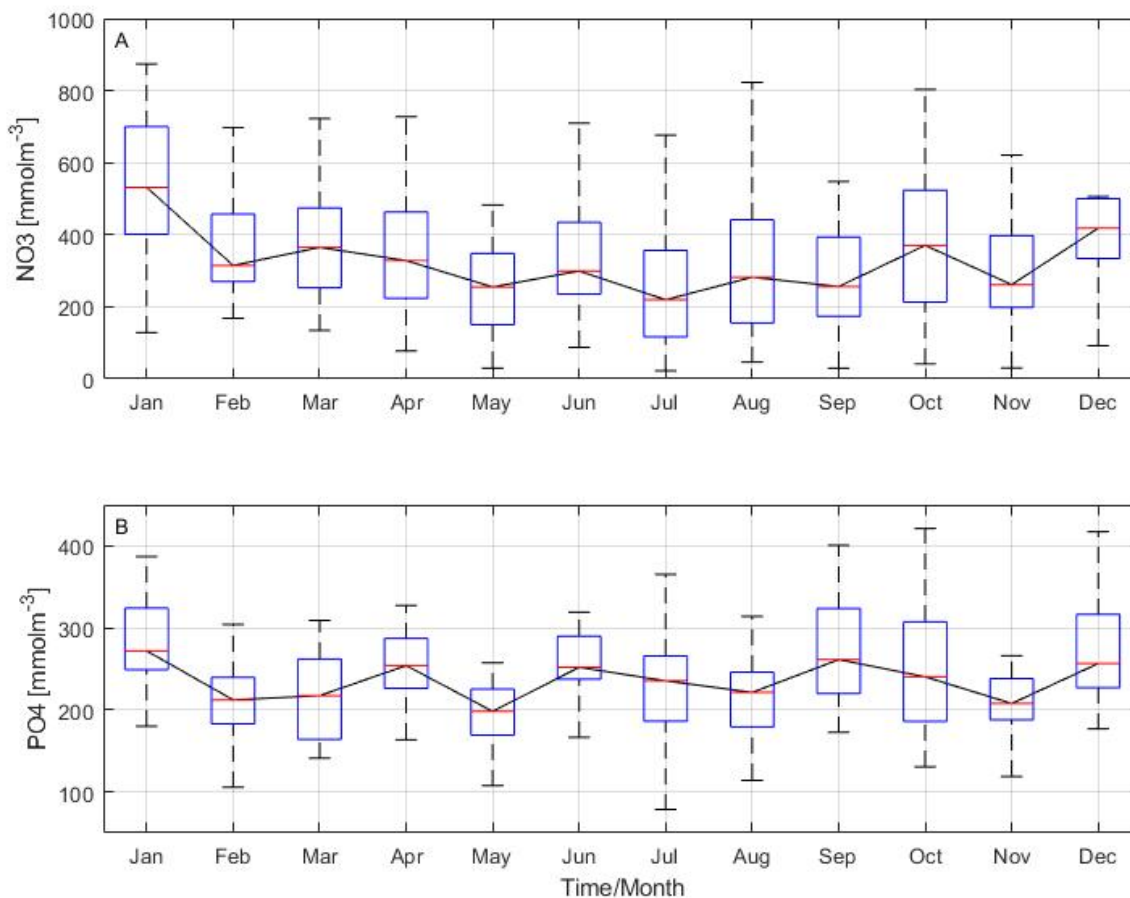


Figure S3. Annual cycle from monthly means of A) nitrate and B) phosphate concentrations integrated over the water column in the Gotland Basin between 1999 and 2020. The data were downloaded from ODIN and SHARKweb databases. The central red line in each box represents the median over 22 years. The bottom and top edges of the box indicate the 25th and 75th percentiles, respectively. The whiskers extend to the most extreme data points.

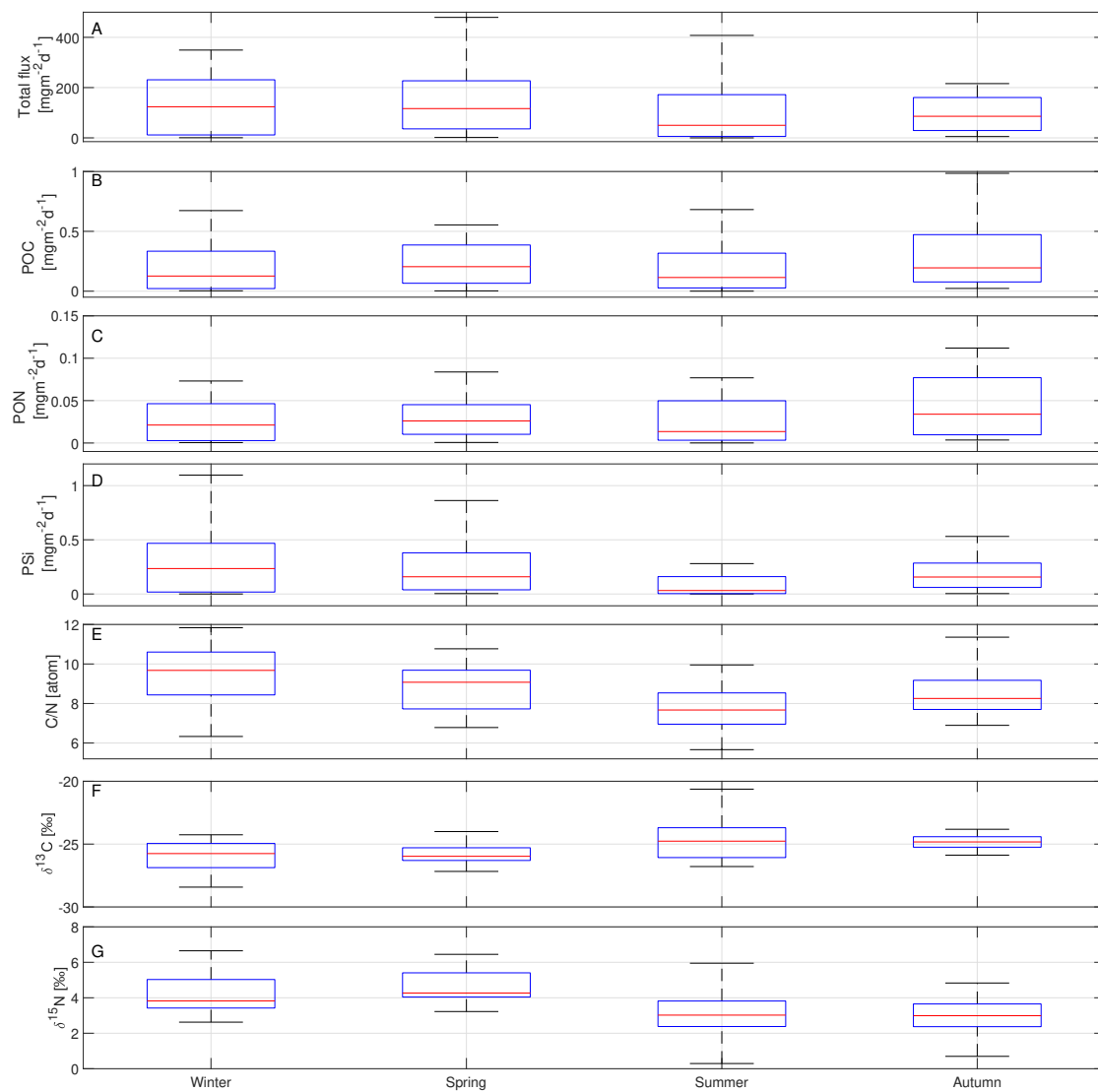


Figure S4. Seasonal means of total particle flux, POC, PON, PSi, C:N, $\delta^{13}C$ and $\delta^{15}N$ from sediment traps moored at 180 m depth in the Gotland Basin between 1999 and 2020. The seasons were divided into spring (March-May), summer (June- August), autumn (September-November) and winter (December-February). The central red line in each box represents the median over 22 years. The bottom and top edges of the box indicate the 25th and 75th percentiles, respectively. The whiskers extend to the most extreme data points.